



***p*-Carboxylatocalix[4]arenes: Versatile Building
Blocks for the Assembly of Novel Nanostructures**

Robyn Eleanor Fairbairn, *MChem*

Submitted for the degree of Master of Philosophy

Heriot-Watt University

Chemistry

Institute of Chemical Sciences

March 2016

The copyright in this thesis is owned by the author. Any quotation from the thesis or use of any of the information contained in it must acknowledge this thesis as the source of the quotation or information.

Abstract

This thesis focuses on the synthesis and characterisation of supramolecular structures containing *p*-carboxylatocalix[4]arenes with pyridine derivative guest molecules. X-ray diffraction was predominantly utilised to help with the characterisation of these molecules. This thesis contains five chapters dealing with the synthesis and applications of novel *p*-carboxylatocalix[4]arenes.

Chapter 1 gives a short overview of supramolecular chemistry, calixarene synthesis and their conformational properties. In addition, the supramolecular chemistry of several *p*-carboxylatocalix[4]arenes are also summarised.

Chapter 2 describes the synthesis and characterisation of a variety of lower-rim di-functionalised *p*-carboxylatocalix[4]arenes. The lower-rim groups include alkyl, polyethylene glycol and alkenyl chains. With only one crystal structure generated containing a pyridine derivative, it is difficult to say if the other molecules synthesised will display the same behaviour. In the solid state this system was found to assemble *via* both the CO₂H \cdots CO₂H homosynthon and the Py \cdots CO₂H heterosynthon and packed in a common bi-layer arrangement.

Chapter 3 describes the effects of pyridine on the formation of a non-covalent assembly based on *p*-carboxyethylcalix[4]arene, which was found to pack in bi-layer arrays. Tetra-*O*-propoxy-*p*-carboxylatocalix[4]arene was synthesised in a different manner and was found to give a partial-cone conformation and when crystallised from DMF, gave a hydrogen-bonded head-to-head dimer through function of CO₂H \cdots CO₂H interactions.

Chapter 4 deals with calix[4]arenes fixed in a rigid cone conformation by selective lower-rim functionalisation. The effects of pyridine templates on the formation of non-covalent assemblies based on di-*O*-propoxy-di-*p*-carboxylatocalix[4]arene-crown-4 and *p*-carboxylatocalix[4]arene-biscrown-3 are described. These structures assemble *via* the Py \cdots CO₂H heterosynthon and the CO₂H \cdots CO₂H homosynthon respectively. The latter compound was also used to form transition metal complexes/coordination polymers.

Chapter 5 describes the effects of pyridine templates (including 2-AP) on the formation of non-covalent assemblies based on Suzuki cross-coupled tetra(*p*-benzoic acid)-tetrapropoxycalix[4]arene and di(*p*-benzoic acid)-tetrapropoxycalix[4]arene (and derivatives). The majority of these structures assemble *via* the Py \cdots CO₂H heterosynthon.

DECLARATION STATEMENT

(Research Thesis Submission Form should be placed here)

Table of contents

Symbols and abbreviations	i-ii
---------------------------	------

Chapter 1: Introduction.

1.1. Supramolecular chemistry.	1
1.2. Introduction to calix[<i>n</i>]arenes.	2
1.3. Synthetic modifications of calix[<i>n</i>]arenes.	6
1.3.1. Calix[<i>n</i>]arene lower-rim functionalisation.	6
1.3.2. Calix[<i>n</i>]arene upper-rim functionalisation.	7
1.4. Calix[<i>n</i>]arenes as hosts.	8
1.5. Palladium-catalysed cross-coupling.	10
1.5.1. Suzuki cross-coupling.	11
1.5.2. Applications of cross-coupling to calix[4]arenes.	12
1.6. <i>p</i> -Carboxylatocalix[4]arene assemblies.	14
1.6.1. Non-covalent assemblies.	15
1.6.2. Metal-directed assemblies.	18
1.7. Aims.	23
1.8. References.	25

Chapter 2: Lower-rim functionalisation of *p*-carboxylatocalix[4]arenes.

2.1. Introduction.	30
2.2. Lower-rim functionalisation of calix[4]arenes.	30
2.2.1. Monopropoxycalix[4]arene.	32
2.2.2. 1,3-Dipropoxycalix[4]arene.	33
2.2.3. Syn-1,2-dipropoxycalix[4]arene.	33
2.2.3.1. Structure of syn-1,2-dipropoxycalix[4]arene, 5.	34
2.2.4. Tetrapropoxycalix[4]arene.	36
2.3. Synthesis of di(PEGylated)-di- <i>p</i> -carboxylatocalix[4]arenes and tetra(PEGylated)-tetra- <i>p</i> -carboxylatocalix[4]arenes.	37
2.4. X-ray crystal structures of compound 20 .	41
2.4.1. Structure of di(monomethyl diethylene glycol)-di- <i>p</i> -carboxylatocalix[4]arene, 20 .	41

2.4.2. Structure of di(monomethyl diethylene glycol)-di- <i>p</i> -carboxylatocalix[4]arene 3-picoline, 2.1 .	43
2.5. Synthesis of dialkenyl-dihydroxy-di- <i>p</i> -carboxylatocalix[4]arenes.	45
2.6. X-ray crystal structure of compound 29 .	47
2.6.1. Structure of di(4-chloropentane)-di- <i>p</i> -formylcalix[4]arene acetone, 2.2 .	47
2.7. Conclusion.	50
2.8. Experimental.	51
2.8.1. General comments.	51
2.8.2. General experimental.	51
2.8.3. Synthesis of compounds 1 - 32 .	52
2.8.4. X-ray details of data collection/structure refinement of compounds 5, 20, 2.1 - 2.2 .	73
2.9. References.	75

Chapter 3: Upper-rim *p*-carboxylatocalix[4]arene protection/deprotection.

3.1. Introduction.	78
3.2. Upper-rim functionalisation of calix[4]arene.	79
3.3. X-ray crystal structures of compounds 36 - 38 .	83
3.3.1. Structure of <i>p</i> -carboxyethylcalix[4]arene pyridine, 3.1 .	83
3.3.2. Structure of tetra- <i>O</i> -propoxy- <i>p</i> -carboxyethylcalix[4]arene, 37 .	86
3.3.3. Structure of tetra- <i>O</i> -propoxy- <i>p</i> -carboxylatocalix[4]arene DMF, 3.2 .	88
3.4. Conclusion.	91
3.5. Experimental.	92
3.5.1. General comments.	92
3.5.2. General experimental.	92
3.5.3. Synthesis of compounds 33 - 38 .	93
3.5.4. X-ray details of data collection/structure refinement for compounds 37, 3.1 - 3.2 .	97
3.6. References.	98

Chapter 4: Calix[4]arenes fixed in a rigid cone conformation by selective lower-rim functionalisation.

4.1. Introduction.	99
4.2. Calix[4]arene-crown ethers.	99
4.3. X-ray crystal structures of compounds 42b , 43a and 47 .	103
4.3.1. Structure of di- <i>O</i> -butoxy-di- <i>p</i> -formylcalix[4]arene-crown-4, 42b .	104
4.3.2. Structure of di- <i>O</i> -propoxy-di- <i>p</i> -carboxylatocalix[4]arene-crown-4·DMF, 4.1 .	105
4.3.3. Structure of di- <i>O</i> -propoxy-di- <i>p</i> -carboxylatocalix[4]arene-crown-4·pyridine, 4.2 .	107
4.3.4. Structure of <i>p</i> -carboxylatocalix[4]arene-biscrown-3·4-picoline, 4.3 .	109
4.3.5. Structure of [(47 -4H)(2-AP+H) ₄].(H ₂ O) ₄ , 4.4 .	111
4.4. Metal-organic assemblies of <i>p</i> -carboxylatocalix[4]arene-biscrown-3.	114
4.4.1. Structure of <i>p</i> -carboxylatocalix[4]arene-biscrown-3 metal-organic coordination polymer: [Cu ^{II} PyC(47-2H)(Py) ₂], 4.5 .	114
4.4.2. Structure of <i>p</i> -carboxylatocalix[4]arene-biscrown-3 metal-organic coordination polymer: [Mn ^{II} (47-2H)(Py) ₂ (OMe)]·Py(H ₂ O) ₂ , 4.6 .	116
4.5. Conclusion.	118
4.6. Experimental.	119
4.6.1. General comments.	119
4.6.2. General experimental.	119
4.6.3. Synthesis of compounds 39 - 47 and complexes 4.5 - 4.7 .	120
4.6.4. X-ray details of data collection/structure refinement of compounds 42b , 4.1 - 4.6 .	129
4.7. References.	132

Chapter 5: Suzuki cross-coupling reactions of calix[4]arenes.

5.1. Introduction.	134
5.2. Synthesis of cross-coupled calix[4]arenes.	134
5.3. X-ray crystal structures of compounds 51 , 54 , 56 , 58 and 59 .	140
5.3.1. Structure of tetra(<i>p</i> -benzoic acid)tetrapropoxycalix[4]arene·pyridine, 5.1 .	140
5.3.2. Structure of tetra(<i>p</i> -benzoic acid)tetrapropoxycalix[4]arene·4-picoline, 5.2 .	142
5.3.3. Structure of [(51 -2H)(2-AP+H) ₂].(MeOH) ₂ (H ₂ O) ₂ , 5.3 .	145
5.3.4. Structure of di(<i>p</i> -benzoic acid)tetrapropoxycalix[4]arene·3-picoline, 5.4 .	147
5.3.5. Structure of di(<i>p</i> -benzoic acid)tetrapropoxycalix[4]arene·4-picoline, 5.5 .	149

5.3.6. Structure of di(<i>p</i> -benzoic acid)dipropoxycalix[4]arene-crown-4·DMF, 5.6 .	151
5.3.7. Structure of di(4-formylphenyl)-dibenzyloxy-dipropoxycalix[4]arene, 58 .	154
5.3.8. Structure of di(<i>p</i> -benzoic acid)-dibenzyloxy-dipropoxycalix[4]arene·2-picoline, 5.7 .	157
5.3.9. Structure of di(<i>p</i> -benzoic acid)-dibenzyloxy-dipropoxycalix[4]arene·4-picoline, 5.8 .	160
5.4. Conclusion.	164
5.5. Experimental.	165
5.5.1. General comments.	165
5.5.2. General experimental.	165
5.5.3. Synthesis of compounds 48 - 59 .	166
5.5.4. X-ray details of data collection/structure refinement of compounds 5.1 - 5.8 , 58 .	175
5.6. References.	178

Symbols and abbreviations

Å	Angstrom (0.1 nm)
Ar	Aryl
Bn	Benzyl
Bu	Butyl
°C	Degrees Celsius
Et	Ethyl
FT	Fourier transform
g	Gram
Hz	Hertz
IR	Infrared
br	Broad (IR)
m	Medium (IR)
s	Strong (IR)
str.	Stretching vibration (IR)
w	Weak (IR)
J	Coupling constant
L	Litre
M	Molar
mg	Milligram
mins	Minutes
mol	Mole
MS	Mass spectrometry
MW	Molecular weight
m/z	Ratio between mass and electric charge
M ⁺	Molecule ion peak
NMR	Nuclear Magnetic Resonance
¹ H	Proton (NMR)
¹³ C	Carbon (NMR)
br s	Broad singlet
d	Doublet
m	Multiplet
s	Singlet
t	Triplet

OTs	Tosylate group
Ph	Phenyl
ppm	Parts per million
Pr	Propyl
R _f	Retention factor
RT	Room temperature
TLC	Thin Layer Chromatography
TM	Transition metal
π	Pi
ν	Wavelength (cm ⁻¹)
C[4]	Calix[4]arene
CDCl ₃	Deuterated chloroform
DCM	Dichloromethane
DMF	N,N-Dimethylformamide
DMSO	Dimethyl sulfoxide
DMSO-d ⁶	Deuterated dimethyl sulfoxide
EtOH	Ethanol
HCHO	Formaldehyde
HCl	Hydrochloric acid
H ₂ O	Water
HMTA	Hexamethylenetetramine
K ₂ CO ₃	Potassium carbonate
KOH	Potassium hydroxide
MeCN	Acetonitrile
MeOH	Methanol
NaH	Sodium hydride
NaOH	Sodium hydroxide
PE	Petroleum ether
PEG	Poly(ethylene glycol)
SnCl ₄	Tin tetrachloride
TBC[4]	<i>p</i> - <i>tert</i> -butyl-calix[4]arene
TFA	Trifluoroacetic acid
THF	Tetrahydrofuran
TsOH	Toluenesulfonic acid

Chapter 1: Introduction.

1.1. Supramolecular chemistry.

Over the past decades, supramolecular chemistry has advanced as a scientific field among biology, chemistry and physics. In the 1970s Lehn defined the term supramolecular chemistry as “chemistry beyond the molecule.”¹ The main theory of supramolecular chemistry involves the molecular recognition and the self-assembly of molecules. The supramolecular architecture is constructed from organised structures of higher complexity resulting from the association of two or more chemical species that are held together by non-covalent interactions. These non-covalent interactions are the driving force in supramolecular chemistry and are significantly weaker than covalent bonds. Some typical intermolecular interactions include hydrogen bonding, metal coordination and π - π interactions.² Molecular chemistry is concerned with molecules, whereas supramolecular chemistry is associated with supramolecular species. These species are usually referred to as a “molecular receptor” and “substrate” as shown in Figure 1.1. The development of supramolecular chemistry to date includes complexes that contain complementary binding sites (“molecular recognition”) and multi-component complexes (“supramolecular assemblies”) between molecules.³

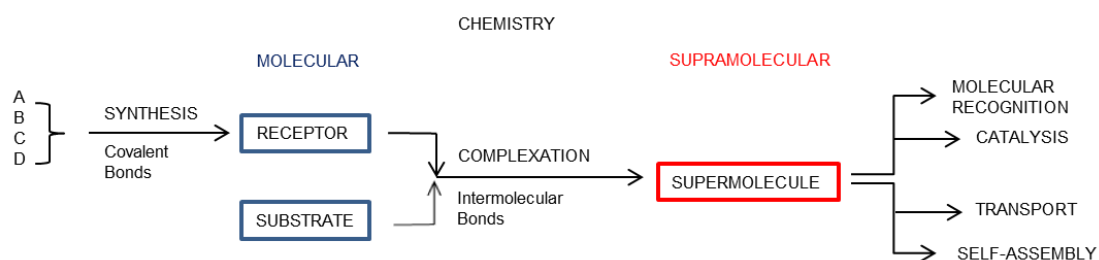


Figure 1.1. From molecular to supramolecular chemistry.

In 1894, Emil Fischer compared the selectivity of hosts and guests to the “lock and key” principle of the specific interaction of an enzyme with a single substrate.⁴ Supramolecular chemistry can be divided into two extensive categories: host-guest chemistry and self-assembly. Host-guest systems involve large 'host' molecules (often a macrocycle) that are capable of encapsulating smaller 'guest' molecules (including metal ions) *via* non-covalent interactions. In addition to the binding of one molecule by another, supramolecular chemistry examines self-assembly which occurs from non-

covalent interactions joining two or more complementary species to afford a supramolecular system.

In the 1960s Charles Pedersen discovered crown ethers which are a type of macrocyclic compound.⁵ They are derived from ethylene glycol and are composed of $\text{-OCH}_2\text{CH}_2\text{-}$ repeating units. In order to compile a variety of different sized crown ethers, the number of these repeating units can be varied. They have been shown to selectively bind to metal cations, such as Li^+ , Na^+ and K^+ and is a distinguished example of molecular recognition in the field of host-guest chemistry.⁶ Examples of other macrocyclic host compounds investigated to date include cryptands, cyclodextrins and calixarenes.⁷

Advancements in supramolecular chemistry have led to an increased interest in the design and synthesis of macrocyclic molecules embodying intramolecular cavities.⁷ Calixarenes, along with related compounds such as resorcinarenes, pyrogallolarenes and pillararenes have been employed as building blocks for host architectures such as capsules^{8,9} and nanotubes^{10,11} that possess diverse supramolecular functions.

1.2. Introduction to calix[n]arenes.

Calix[n]arenes¹²⁻¹⁴ have emerged as very attractive building blocks in supramolecular chemistry due to their ease of synthesis and versatility. Their distinctive concave molecular framework plays an important role for its function in host-guest chemistry. While the synthesis is moderately undemanding to produce these complexes, expansion in this area is fairly recent.

Initial work on calixarenes dates back to 1872 when Adolf von Bayer exhibited an interest in the reaction of various phenols and formaldehyde.¹⁵ He reported that a 'cement-like' substance was observed when aqueous formaldehyde was heated with phenol in the presence of a strong acid. Owing to the lack of advanced analytical techniques, the first crystal structure of a calixarene was not confirmed until 1942.¹⁶ Three decades later in 1907 Leo Baekeland profited from these phenol-formaldehyde products by patenting what is now well established as the Bakelite process.¹⁷ Further development came when this research generated interest from Zinke and his co-worker Zeigler, who discovered the formation of a cyclic tetrameric structure for the products yielded from the base-induced reaction of *p*-*tert*-butylphenol and formaldehyde in

1944.¹⁸ Regardless of this, it was not until the revolutionary work of Carl David Gutsche in the 1970s that revealed, on further examination of the Zinke mixture, that it contained three species identified as cyclic tetramers, hexamers and octamers.^{12,14}

Calixarenes are cyclic oligomers that are easily prepared from the condensation of phenols with formaldehyde.¹⁹ It was Gutsche that led to the naming of these products as calixarenes in 1978.²⁰ The term calixarene is derived from the Greek word *calyx* meaning vase, because of the compound's likeness to the Greek calix crater. The suffix *arene* indicates the presence of aromatic rings in the macrocycle.²¹ Calixarenes have been synthesised in a variety of different sizes by selecting appropriate reaction conditions.²² The bracketed number [*n*] (usually *n* = 4, 5, 6, 8)^{13,23} equals the number of aryl groups present in the macrocycle. The nature and the positions of substituents are given by consecutive numeration of the atoms and the term is placed in front of calix[*n*]arene. Hydroxyl substituents follow the same procedure as previous but are placed after the term calix[*n*]arene. When the values of *n* = 4, 6, 8 ("major") the calixarenes can be prepared relatively easy in high yields, while other values of *n* ("minor") are difficult to prepare as they are not as stable and which results in low yields. Calixarenes with as few as 3 and as many as 20 repeating units have been reported.²

Previous work has been conducted using calix[4]arenes as molecular frameworks and building blocks for extensive use in the formation of supramolecular structures and across a wide-range of both organic and inorganic chemistry.²⁴ Their characteristic cyclic (typically bowl-shape) structure consists of repeating phenolic units linked by methylene groups (-CH₂-), generating a cavity in the centre of the molecular skeleton. In this class of molecular structure there are two distinct regions present; the hydrophobic wide upper-rim defined by the *para*-positions of the aromatic nuclei and a hydrophilic narrow lower-rim, where the phenolic oxygens are situated (Figure 1.2).²⁵ These four phenolic oxygens form strong hydrogen bonds that "close" the macrocycle into a stable basket-like shape.

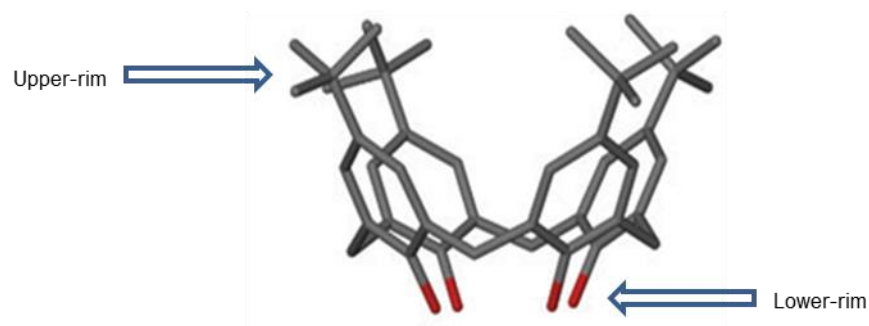


Figure 1.2. Illustration of the two synthetically useful regions known as the upper- and lower-rims.

It was the work conducted by Cornforth²⁶ that revealed these molecules can exist in four conformations, which were later designated names by Gutsche in 1983.²⁷ The four main different conformers adopted by these macrocycles are established as the cone, partial-cone, 1,2-alternative and the 1,3-alternative as shown in Figure 1.3. The conformation of a calixarene can be easily determined through the analysis and interpretation of ^1H and ^{13}C NMR spectral data.¹³ These conformations are generated through ring inversion of Ar-CH₂-Ar bonds. In the majority of cases the cone conformation is the favoured choice in both solution and the solid state. This is where all the phenolic units are orientated in the same direction forming a well-defined π -rich aromatic cavity. Hydrogen bonding is eliminated at the lower-rim upon alkylation, which allows for the molecular framework to become more flexible. However, the macrocycle can be restricted to one of their four conformations depending on the reaction conditions employed and the bulkiness of the *O*-substituents (propyl or larger)^{12,13} attached to the lower-rim of the macrocycle. It should also be noted that the conformation adopted once the macrocycle has been alkylated can be altered subject to the solvent of choice, alkylating agent and the base utilised for deprotecting the hydroxyl groups (metal template effect).²⁸

Calixarenes adopting the cone conformation are advantageous with regard to their ability to accommodate guest molecules within the cavity. There have been numerous studies that have explored the inclusion properties^{29,30} of calixarenes as hosts and found that functionalised calixarene derivatives can self-assemble in the presence of guest molecules.³¹

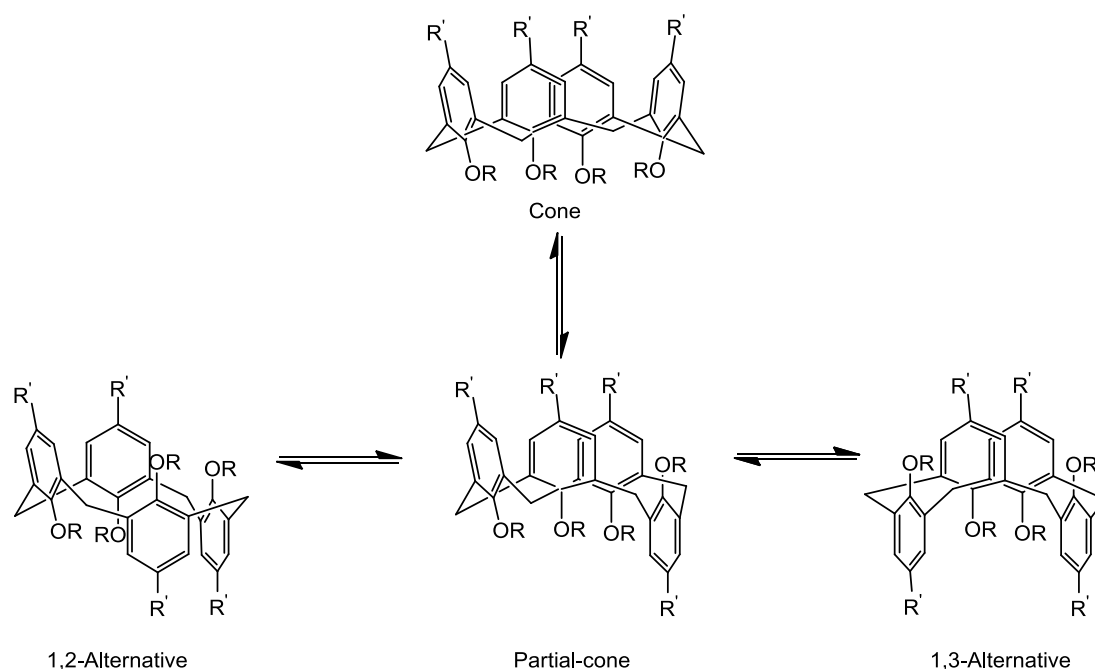


Figure 1.3. Conformational isomerism of calix[4]arenes.

Although both ^1H and ^{13}C NMR spectroscopy³² can be used to aid determination of conformation, X-ray crystallography is the conclusive method employed. In 1979 an X-ray structure of a phenol-derived calixarene³³ was reported by Pochini *et al.*³⁴ revealing a toluene guest molecule within the calixarene cavity. The lead to the theory that calixarenes could therefore be used in the formation of inclusion complexes. It has been reported that tetra-*O*-alkylated calix[4]arenes do not adopt the cone conformation. X-ray crystal structure determination in addition to temperature-dependant NMR experiments in solution³⁵ has demonstrated that the pinched-cone is favoured as shown in Figure 1.4.

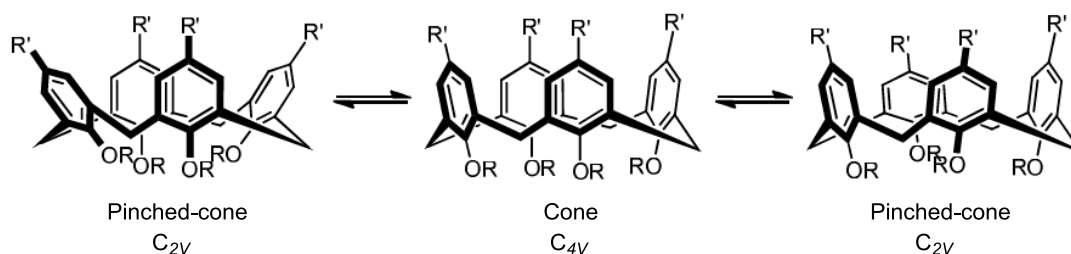


Figure 1.4. Inversion of calix[4]arenes in the cone conformation.

1.3. Synthetic modification of calix[*n*]arenes.

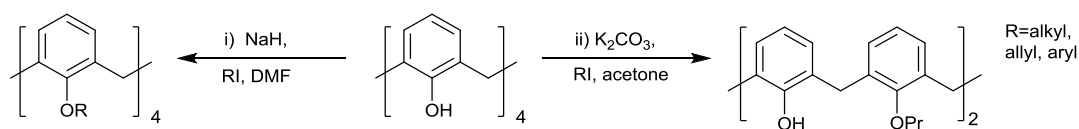
The insertion of new functional groups on both the upper- and lower-rims of the macrocycle can be easily accomplished using common reactions in organic chemistry.¹⁴ This allows for the preparation of a variety of calixarene derivatives, making them one of the most versatile class of supramolecular hosts. The *p*-*tert*-butyl group frequently observed on the upper-rim (as seen in Figure 1.2) can be removed using aluminium trichloride, leaving the upper-rim free for functionalisation.

The introduction of amide, ester or ketone functionalisation at the lower-rim has generated a plethora of efficient and selective receptors for cation binding.^{13,14} This synthetic versatility of calix[*n*]arenes is the reason they can be considered as useful building blocks for the synthesis of novel supramolecular architectures. In addition to the upper- and lower-rims, the bridging group that connects the aromatic rings of the macrocycle can be modified and oxidation/reduction of the calixarene phenolic ring can also be achieved.¹⁴

1.3.1. Calix[*n*]arene lower-rim functionalisation.

One of the easiest reactions in calixarene chemistry is the alkylation of the phenolic hydroxyl groups. This enables a wide variety of functional groups to be introduced *via* alkylation with appropriate reagents. One of the first reactions tested on calixarenes involved the esterification of the hydroxyl groups on the lower-rim.¹²

Altering the base employed during synthesis can result in either partial or full alkylation at the lower-rim. When sodium hydride is selected, all four sites on the tetrahydroxycalix[4]arene become deprotonated and hence alkylated with the use of an alkyl halide.²⁷ In contrast, using a weaker base such as sodium or potassium carbonate results in the 1 and 3 positions being deprotonated, leading to the formation of a 1,3-disubstituted calixarene (Scheme 1.1). In order to dictate the overall conformation of the calixarene, bulky substituents are added which prevent the interconversion between the four main conformers.³⁶



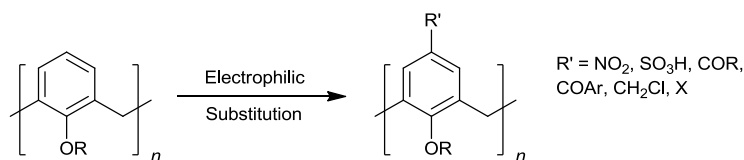
Scheme 1.1. Alkylation of calix[4]arene to afford i) tetra-substituted and ii) 1,3-disubstituted calix[4]arene.

Dialkylation of the parent calixarene can occur in different regiochemistries to give either the distal 1,3-dialkylated compound (most common) or the proximal 1,2-dialkylated product.³⁷ As previously stated distal alkylation is more frequently observed due to its easier synthesis compared to that of proximal alkylation. Proximal dialkylation can be accomplished by using a strong base such as sodium hydride, with a stoichiometric amount of alkylating agent.³⁸

Another important functionalisation of calix[4]arenes on the lower-rim is the introduction of crown ether tethers.³⁹ Calixarenes are generally insoluble in water and many organic solvents,⁴⁰ but it has been shown that esterification and etherification on the lower-rim, or the addition of carboxylate or sulfonate groups to the upper-rim can improve their solubility.⁴⁰ The addition of these rigidifying ethylene glycol units ensures the compound is held in the cone conformation, enforcing the cavity while keeping the upper-rim available for further modification. The crown ether tether has the ability to bridge by either the 1,3- or 1,2-positions (distal and proximal phenol units respectively).^{41,42} Research on the 1,3-bridged calix[4]arene-crowns is further advanced than that of their 1,2-bridged counterparts, primarily due to the challenging synthesis of the latter.

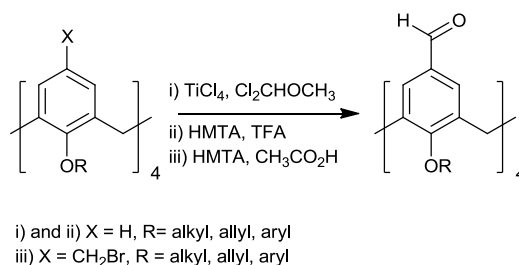
1.3.2. Calix[n]arene upper-rim functionalisation.

In order to be able to functionalise at the upper-rim it is first necessary to remove any substituents, these usually being *tert*-butyl groups. This is executed by a retro Friedel-Craft alkylation reaction which unmarks the *para* positions, leaving this ready for functionalisation.⁴³ Some of the most common alterations that can be implemented using electrophilic substitution include halogenation,^{44,45} nitration⁴⁶ and formylation,⁴⁷ most of which allow for additional conversion to introduce further functionality (Scheme 1.2).



Scheme 1.2. Electrophilic substitution to modify the calix[*n*]arenes upper-rim.

The efficient and selective introduction of desired functional groups is of great interest, as demonstrated by recent reports directed at the formylation of the upper-rim.^{36,47,48} Selective Gross formylation^{36,48f} has been employed for many of these and results in a variety of regioselective formylated calix[4]arenes depending on the reagents and conditions employed during synthesis. Hexamethylenetetraamine (HMTA) in glacial acetic acid has been used to convert bromomethylcalix[4]arene to its corresponding tetraformyl derivative.⁴⁷ Tetraformylation can also be implemented directly from tetraalkoxycalix[4]arenes using HMTA and trifluoroacetic acid (TFA) (Scheme 1.3).^{36,48d-f}



Scheme 1.3. Tetraformylation of calix[4]arene using either i) TiCl₄ and dichloromethyl methyl ether, ii) HMTA and glacial acetic acid, iii) HMTA and TFA.

Additionally *meta* functionalisation is possible on the macrocycle framework. This is generally achieved by prior modification at the *para* position along with an *ortho*-directing group as reported by Reinhoudt *et al.*⁴⁹ Shinkai and co-workers also demonstrated this was conceivable by employing intramolecular ring closure.⁵⁰

1.4. Calix[*n*]arenes as hosts.

The three-dimensional structure of calixarenes and related derivatives makes them attractive building blocks for supramolecular chemistry. Furthermore, they are readily available from cheap starting materials and can be functionalised as desired. In order to generate larger architectures non-covalent interactions such as dipole-dipole and

hydrogen bonding are required. There are a multitude of examples in Nature that are dependent on hydrogen bonding for their self-assembly.⁵¹ To date there are numerous papers on the self-assembly of various functionalised calix[4]arenes which undergo different types of dimerization.³¹ Calixarenes can serve as molecular baskets for neutral molecules and as a result of this have been involved in the construction of cavitands,⁵² (hemi)carcerands⁵³ and self-assembling capsules.⁵⁴ One of the first examples was reported by Shimizu and Rebek that involved the use of tetrakis(phenyl urea)-tetrabenzylcalix[4]arene, resulting in a self-assembled dimeric capsule with an encapsulated guest molecule (toluene or chloroform).⁵⁵ The formation of the dimeric capsule was obtained by taking advantage of the urea group's ability to both donate and accept hydrogen bonds. The capsule was found to self-assemble *via* an unusual circular array of eight urea groups, all of which hydrogen bond to their neighbours, forming 16 hydrogen bonds in total. This work was the foundation on which Böhmer *et al.*⁵⁶ were able to grow single crystals of a similar dimeric capsule (Figure 1.5). It was seen again that there were a total of 16 hydrogen bonds that occur between the urea groups; two hydrogen bonds are donated by the NH groups and on the other side two hydrogen bonds are accepted by the C=O group.

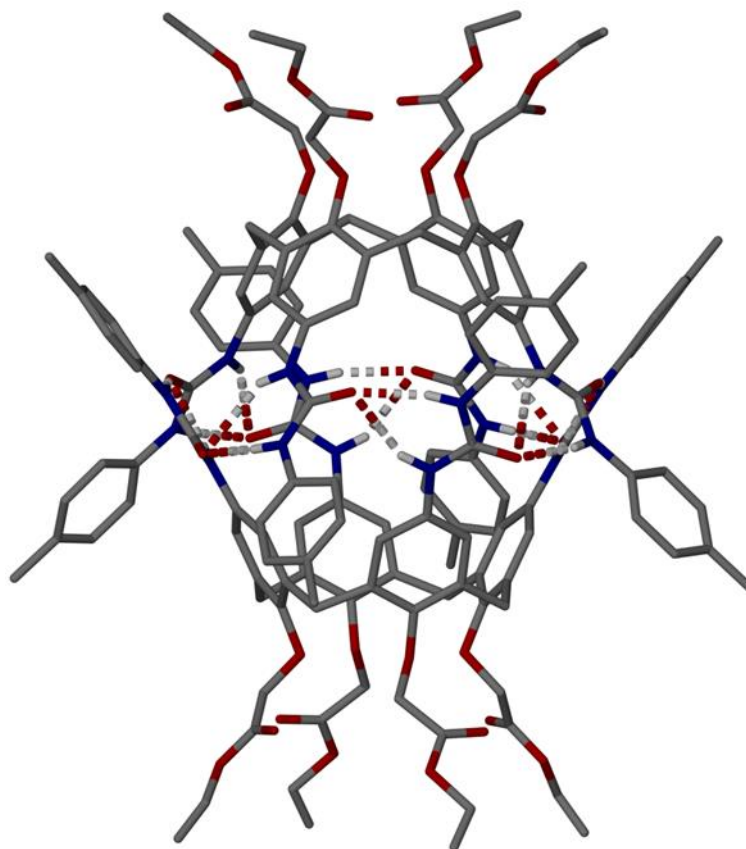


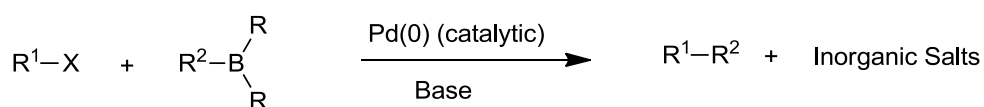
Figure 1.5. X-ray crystal structure of dimeric tetraurea calix[4]arene capsule self-assembled due to hydrogen bonds between urea moieties.^{56,57} Guest molecule and hydrogen atoms not involved in hydrogen bonding have been omitted for clarity. Hydrogen bonds are shown as split-colour dashed lines.

1.5. Palladium-catalysed cross-coupling.

The formation of carbon-carbon and carbon-heteroatom bonds through transition metal-catalysed cross-coupling reactions⁵⁸ is one of the most significant contributions in organic synthesis over the last half-century. It has developed into a powerful tool for the preparation of small and macromolecular architectures in both industrial and synthetic chemistry. In most cases, cross-coupling reactions are based on palladium(0) catalysts, but nickel(0) catalysis is known.⁵⁹ Examples of palladium-catalysed cross-coupling reactions that are used today include the Suzuki-Miyaura, Stille, Negishi and Sonogashira reactions.⁶⁰

1.5.1. Suzuki cross-coupling.

Since first being published in 1979,⁶¹ the Suzuki coupling of alkyl halides (and their equivalents) with organoboron reagents has become an efficient method for the preparation of functionalised biaryls.⁶² The organoboron reagent typically comes in the form of a boronic acid that requires activation by base to enable it to undergo transmetallation. This generates the nucleophilic ‘ate’ complex *in situ*, allowing cross-coupling to occur. Suzuki coupling can be catalysed with all forms of palladium with tetrakis(triphenylphosphine)palladium(0) (Pd(PPh₃)₄) being the most commonly used catalyst.^{62b} However, bis(triphenylphosphine)palladium(II) dichloride (PdCl₂(PPh₃)₂) and palladium(II) acetate (Pd(OAc)₂) with phosphine ligands were also frequently used owing to their stability in air.⁶³ The generic reaction scheme for Suzuki cross-coupling reactions is shown in Scheme 1.4.



R¹ = alkenyl, aryl, alkyl; R² = alkyl, alkenyl, alkynyl, aryl; R = alkyl, OH, O-alkyl; X = Cl, Br, I, OTf
Base = Sodium carbonate, sodium hydroxide

Scheme 1.4. General reaction scheme for Suzuki cross-coupling reactions.

The general catalytic cycle for the Suzuki cross-coupling reaction is shown in Figure 1.6. In most cases the catalytic cycle begins with a palladium(0) species, but the catalytic species can also be formed *in situ* utilising a palladium source. The second step involves the oxidative addition of the aryl halide to give a palladium(II) intermediate species. This palladium(II) intermediate then goes through transmetallation with the alkenyl borate leading to the removal of the desired product, while regenerating the palladium(0) catalyst in the process.

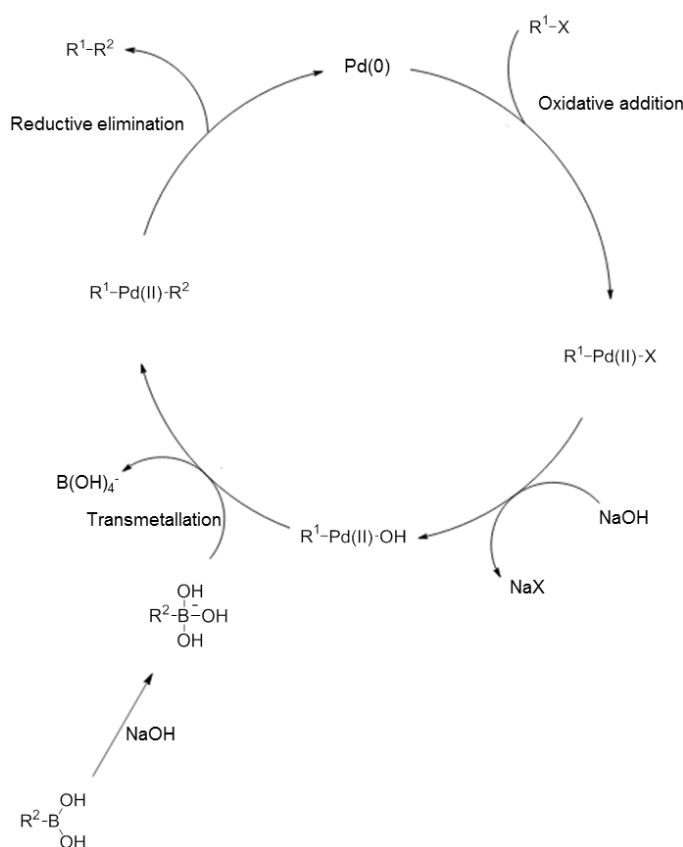
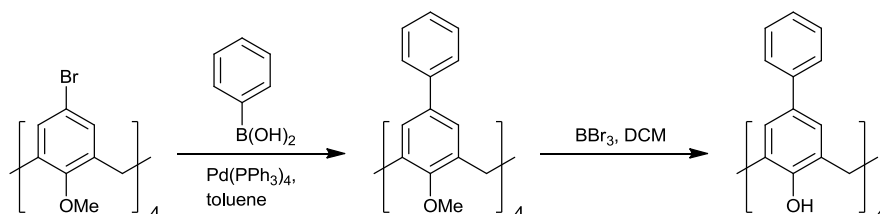


Figure 1.6. Catalytic cycle for Suzuki cross-coupling of organic halides and organoboranes in the presence of NaOH.

1.5.2. Applications of cross-coupling to calix[4]arenes.

The calix[4]arene platform can be further extended at the *para*-position by coupling planar aromatic moieties to the phenolic units at the upper-rim. It also has the added benefit of increasing the cavity size and the potential for functionalisation of the cross-coupled units. Interest in this area has recently surged for the construction of supramolecular systems that takes advantage of the calix[4]arenes expanded preorganised rigid platforms.⁶⁴ It is hoped that these molecules will have desirable host-guest and metal directed chemistry properties. Although these compounds are of great interest, the progress in synthesising novel deep-cavity calixarenes has been delayed as a result of low yielding synthetic procedures. *p*-phenylcalix[4]arene was one of the first compounds synthesised with a rigid extended hydrophobic cavity by Gutsche and No.⁶⁵ A stepwise procedure was employed with the idea that it could have the potential to bind large organic guest molecules. This low yield was increased slightly when Arduini *et al.* utilised either mercury or thallium containing calix[4]arenes.⁶⁶ Palladium-

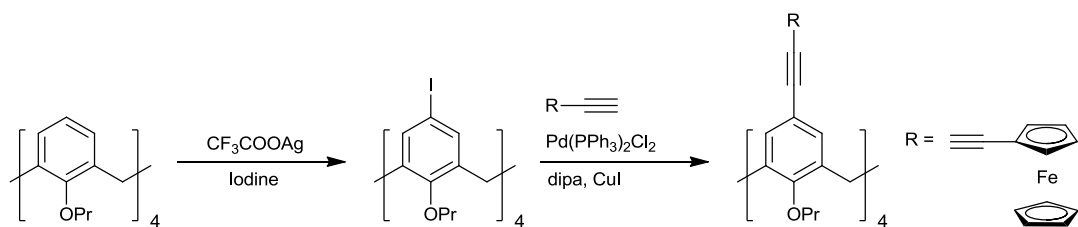
catalysed Suzuki cross-coupling procedures for the modification of calixarenes have also been described using *p*-bromo substituents on the upper-rim of the calixarene framework by Atwood *et al.*⁶⁷ This author also reported a general synthetic route for the synthesis of *p*-phenylcalix[4]arene tetramethyl ether in high yield by a palladium(0)-catalysed reaction (Scheme 1.5). However, the methyl ether R group was conformationally mobile and resulted in the partial-cone conformation being primarily exhibited in the solution state.



Scheme 1.5. Palladium-catalysed reaction of phenylboronic acid with *p*-bromocalix[4]arene tetramethyl ether.

More recently the palladium catalysed coupling of aryl boronic acids with bromocalixarene derivatives to give carboxylphenylcalix[4]arenes has been reported.⁶⁸ They take advantage of the preorganised rigid calix[4]arene platform for studying the binding properties with cytochrome *c*. These carboxylphenylcalix[4]arenes are discussed further in Chapter 5.

Deep cavity calixarenes have also been synthesised using the palladium-catalysed Sonogashira cross-coupling of halogenated calixarene precursors with terminal alkynes.⁶⁹ There have been various reports demonstrating the application of alkynyl calixarenes as molecular receptors,⁷⁰ building blocks for supramolecular assemblies⁷¹ and ligand-coordination compounds.⁷² One such example, reported by Misra *et al.*,⁷³ utilised palladium-catalysed Sonogashira cross-coupling reaction of tetraiodocalix[4]arene with ethynyl ferrocene to synthesise the substituted calix[4]arene shown in Scheme 1.6. The authors obtained a crystal structure of the compound by a slow diffusion of methanol into a chloroform solution at room temperature (Figure 1.7).



Scheme 1.6. Synthesis of a ferrocenyl substituted calix[4]arene using Sonogashira cross-coupling.

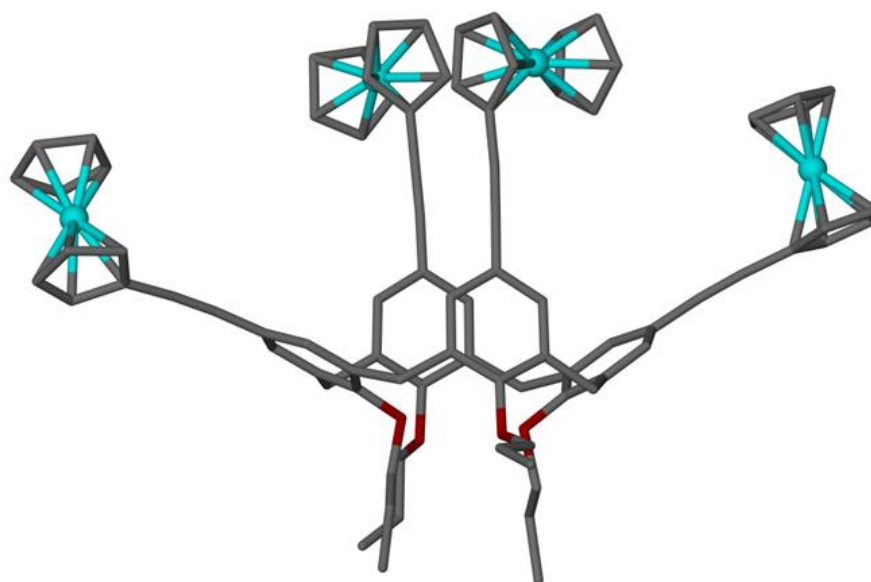


Figure 1.7. Single crystal X-ray structure of ferrocenyl substituted calix[4]arene by Sonogashira cross-coupling. Hydrogen atoms have been omitted for clarity.

1.6. *p*-Carboxylatocalix[4]arene assemblies.

p-Carboxylatocalix[4]arenes (general notation *p*CO₂[4]) are a relatively unexplored class of building block, which is surprising as they have the potential to display some interesting coordination chemistry and host-guest properties. Regardless of this, they present a new challenge in the construction of novel materials from cavity containing sub-units. There have been reports of self-assembly of these molecules that are driven by well-established supramolecular synthons (Figure 1.8).⁷⁴

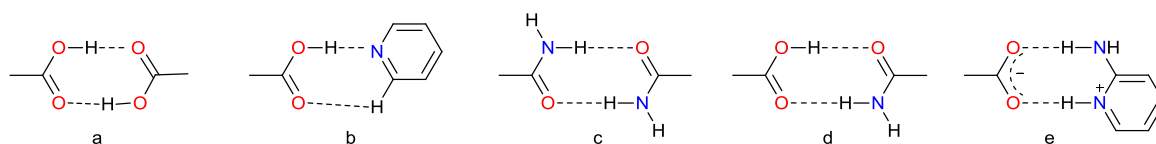


Figure 1.8. Most common synthons observed in supramolecular chemistry for self-assembly.

The types of supramolecular synthons can be divided into two categories; homosynthons or heterosynthons. Figure 1.8 above gives examples of supramolecular synthons which are commonly seen and include: a – homosynthon formed between carboxylic acid dimer; b – heterosynthon formed between carboxylic acid group and pyridine; c – homosynthon formed between amide dimer; d – heterosynthon formed between carboxylic acid group and amide group; e – organic salt heterosynthon.⁷⁵

The formation of large capsule based assemblies with large internal cavities has proven to be a major challenge in supramolecular chemistry. Attempts in this area have been made by either introducing chemical complementarity to the molecular architecture, or by covalent/metal directed assembly.⁷⁶

1.6.1. Non-covalent assemblies.

Exploration of the self-assembly of $p\text{CO}_2[4]$ s that are readily accessible in either the cone or pinched-cone conformation, (dependant on lower-rim alteration) has recently been conducted.⁷⁴ The presence of the carboxylic acid groups can lead to the formation of a pyridine-carboxylic acid heterosynthon ($\text{Py} \cdots \text{CO}_2\text{H}$), which has been utilised extensively in the area of non-covalent self-assembly. Dalgarno and co-workers first reported the spontaneous self-assembly of $p\text{CO}_2[4]$ when crystallised from pyridine, which resulted in the formation of non-covalent organic nanotubes.^{74a} The X-ray crystal structure reveals the presence of a single guest molecule of pyridine in the cavity of each $p\text{CO}_2[4]$. Furthermore, an uncommon hexameric back-to-back assembly is seen in the extended structure (Figure 1.9).

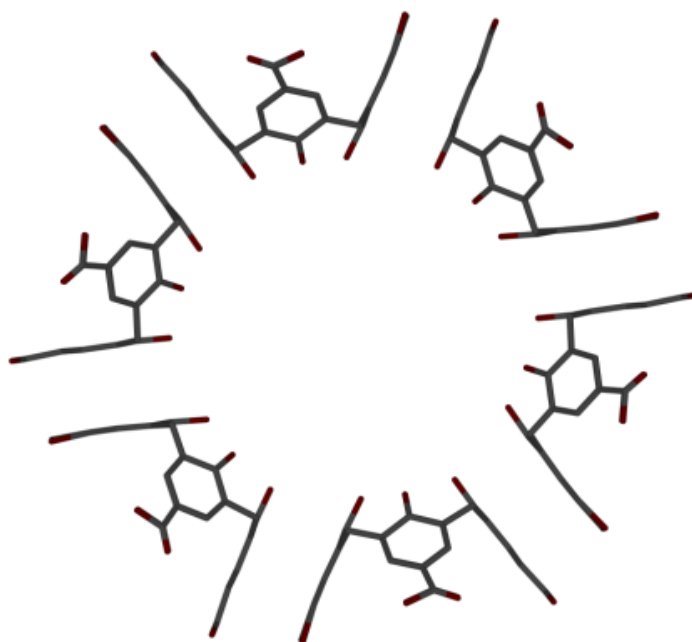


Figure 1.9. Single crystal X-ray structure showing the hexameric back-to-back packing of $p\text{CO}_2[4]$. Hydrogen atoms and solvent molecules have been omitted for clarity.

The same complementary interactions can be seen when synthetic alteration is carried out at the lower-rim to afford di-*O*-alkyl *p*-carboxylatocalix[4]arenes. These molecules adopt a cone conformation due to the hydrogen bonding which occurs at the lower-rim. It was found that di-*O*-propoxycalix[4]arene self-assembles to form triply helical non-covalent nanotubes that pack together in a cog-like fashion. Introduction of upper-rim CO_2H groups to three *para* positions, followed by crystallisation in pyridine, resulted in a related triply-helical modulation of nanotube spacing in the solid state.^{74b} The structural tolerance of this assembly was tested further by altering the pyridine template to 2-picoline. This resulted in only nanotube formations being produced. However, when the length of the carbon chain is increased the nanotube does not form, but rather results in the formation of a distorted bi-layer array.

This nanotube motif was found to be very sensitive to minor adjustments in the solvent used after an investigation into the effect of pyridine derivatives as templates was concluded.^{74d} Along with pyridine, it was found that 2-methylpyridine were suitable templates to allow for the formation of the targeted nanotube structure. However, the introduction of 2-ethylpyridine and other spatially demanding pyridine derivatives were found to disrupt nanotube formation. Although the nanotube packing was modulated through utilising the $\text{Py} \cdots \text{CO}_2\text{H}$ heterosynthon, disorder was present for the CO_2H

groups due to the two possible orientations of the calix[4]arene. In order to remove this crystallographic disorder, the tetra-*p*CO₂[4] analogue was synthesised by a novel procedure.^{74g} Crystallisation from pyridine resulted in an analogous nanotube structure for that obtained for the *tris-p*CO₂[4] (Figure 1.10), but one that is free from disorder.

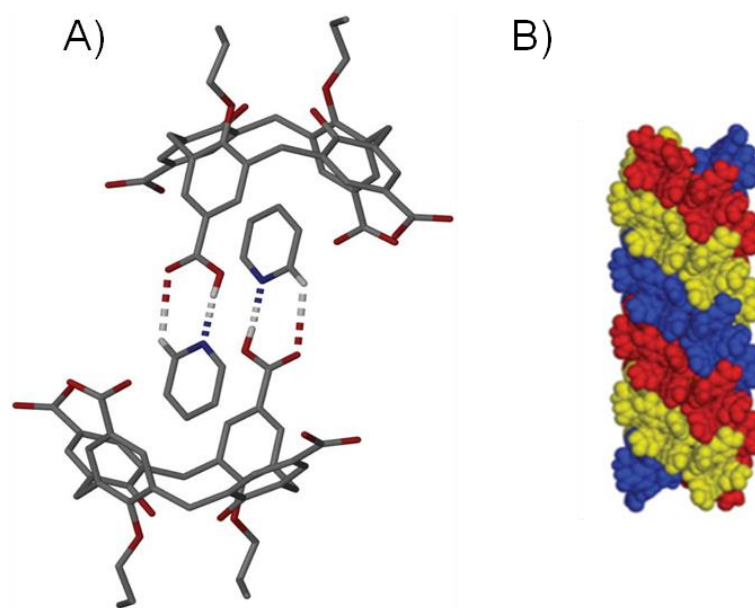


Figure 1.10. A) Hydrogen-bonded dimeric capsule formed from *p*CO₂[4], and pyridine. Hydrogen atoms (except those involved in synthon formation) are omitted for clarity. B) Space filling side view of the triply helical nanotubular array.^{74g}

As mentioned above the assembly of a variety of *p*CO₂[4]s containing two^{74b,d,f,g} or four^{74c,e} lower-rim alkyl chains have been explored in the presence of pyridine derivatives. In the series discussed above the *p*CO₂[4]s commonly formed the expected Py^{···}CO₂ heterosynthon as shown in Figure 1.10 A, with a guest molecule residing in the cavity. In a similar approach the conformational properties of a range of tetra-*O*-alkylated *p*CO₂[4]s were studied alongside their preferred assembly once salt formation had been executed.⁷⁷ This was achieved by introducing 2-aminopyridine as the template. This differs from pyridine by the introduction of an amino group and was designed to structurally compare the two common synthons as depicted in Figure 1.8. It was found that this more basic pyridine template was able to fully deprotonate the *p*CO₂[4]s studied. In these cases it was found that the 2-aminopyridinium cation guest was still located inside the cavity of the calixarenes, giving rise to the formation of

hydrogen-bonded head-to-head dimers (Figure 1.11) *via* the targeted heterosynthon in Figure 1.8.

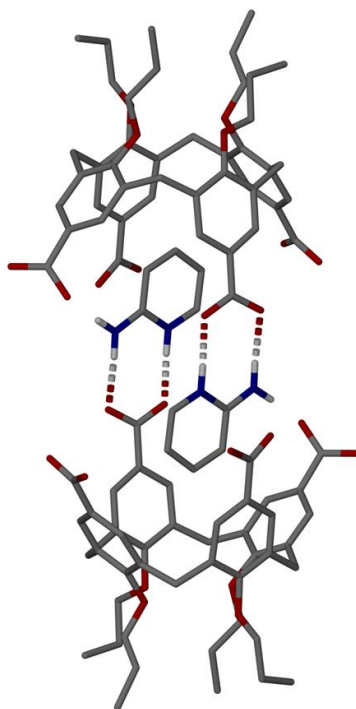


Figure 1.11. X-ray crystal structure of a hydrogen-bonded head-to-head capsule with 2-aminopyridinium cations. Hydrogen bonding is shown as split-colour dashed lines. Hydrogen atoms (apart from those involved in hydrogen bonding) have been omitted for clarity.

1.6.2. Metal-directed assemblies.

Moving on from the non-covalent assemblies which have been shown to have a high degree of control over nanotube formation, greater interest now lies in the formation of metal-organic structures as they could potentially offer enhanced stability within the resulting architectures and controlled bridging in nanometre-scale assemblies. It is thought that the proximal nature of the CO₂H groups in the *p*CO₂[4] could be utilised in the formation of discrete structures (linked by two transition metal centres) that would possess a degree of curvature to disturb the bi-layer formation. Transition metal ions such as Ni²⁺, Mn²⁺ and Co²⁺ are known to form binuclear aqua-bridged complexes (general formula [TM₂(μ-H₂O)(μ-C₆H₅CO₂)₂(Py)₄(C₆H₅CO₂)₂]) in the presence of benzoic acids and *N*-donor ligands, and have been investigated as potential directing

centres, enabling control over the assembly.⁷⁸ Results based on similar research showed the formation of a $[\text{Co}_2(\mu\text{-H}_2\text{O})(\text{Bu}_4[\text{CO}_2]_4(\text{Py})_4)]$ complex with addition of methanolic cobalt nitrate in the presence of pyridine (Figure 1.12 A). It was found to show a distorted curvature that yielded nanotubes with two discrete channels when these complexes packed (Figure 1.12 B).⁷⁸ The supermolecule synthesised is from the pinched-cone tetra-*O*-butoxy-tetracarboxylatocalix[4]arene, where two of the phenyl rings come into the centre of the molecular cleft and two splay open.

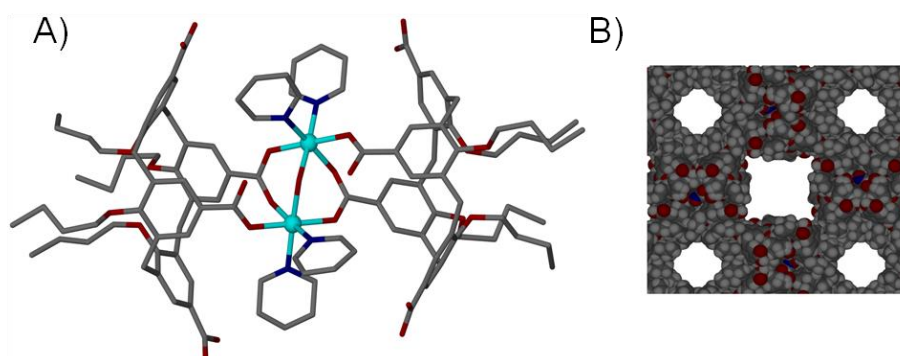


Figure 1.12. A) Binuclear aqua-bridged complex containing sufficient tilt to promote nanotube formation; B) Space filling representation of the extended nanotube. Hydrogen atoms and solvent molecules of crystallisation are omitted for clarity.

One dimensional (1-D) coordination polymers have also been synthesised from targeted transition metal/ $p\text{CO}_2[4]$ panels linked by various 4,4'-bipyridyl components. These were obtained from the reaction of tetra-*O*-propoxy-monocarboxylatocalix[4]arene, cobalt nitrate and methanolic solutions of either 4,4'-bipyridine, 4,4'-bipyridylethane or 4,4'-bipyridylethylene.⁷⁹ It was reported that the presence of solvent-filled channels or pockets can be subsequently altered by varying the length of the linker used in the synthetic procedure. In addition, the metal-directed assembly of di-*O*-alkyl-dicarboxylatocalix[4]arenes has been investigated. The research was focussed on placing the upper-rim functional groups at different distal positions in order to establish if they affected the end outcome of assembly (Figure 1.13). As predicted the original diacid motif (Type I) was found to assemble into interwoven coordination polymer chains with cadmium nitrate and 1,10-phenanthroline (Phen) as a co-ligand (Figure 1.14).⁸⁰ In contrast the Type II diacid design resulted in the formation of discrete, tilted metal-organic capsules from analogous conditions (Figure 1.15).

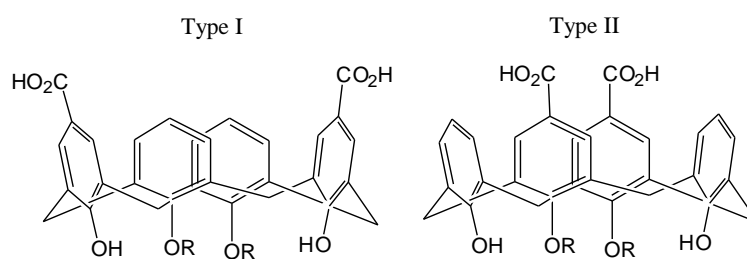


Figure 1.13. Type I and II di-*O*-alkyldicarboxylatocalix[4]arenes.

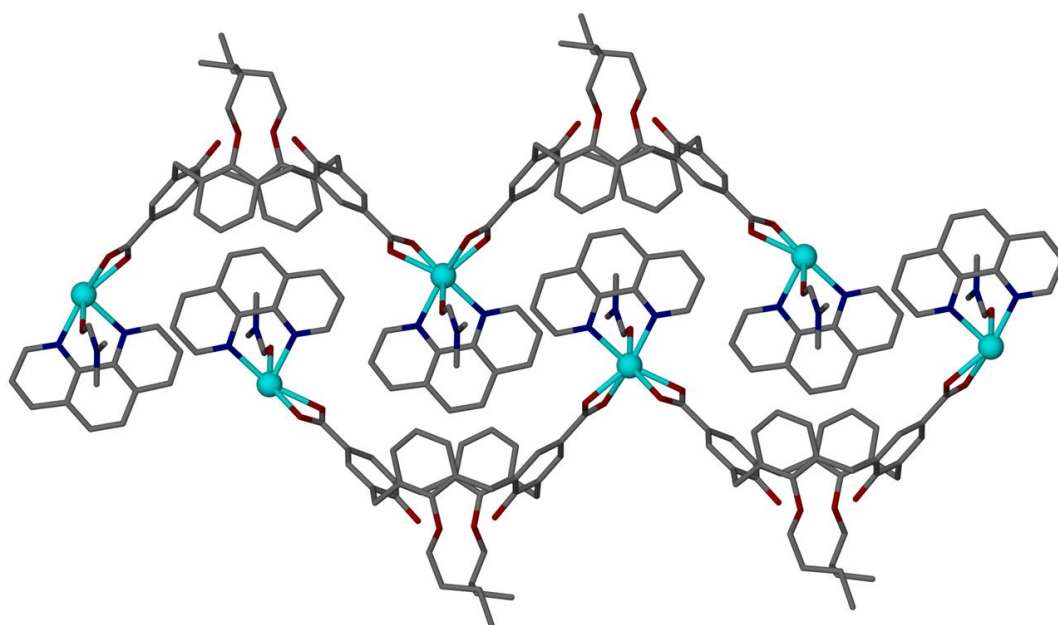


Figure 1.14. Partial extended structure of the metal-organic coordination polymer using type I diacid with cadmium nitrate and Phen. Hydrogen atoms and solvent molecules omitted for clarity.

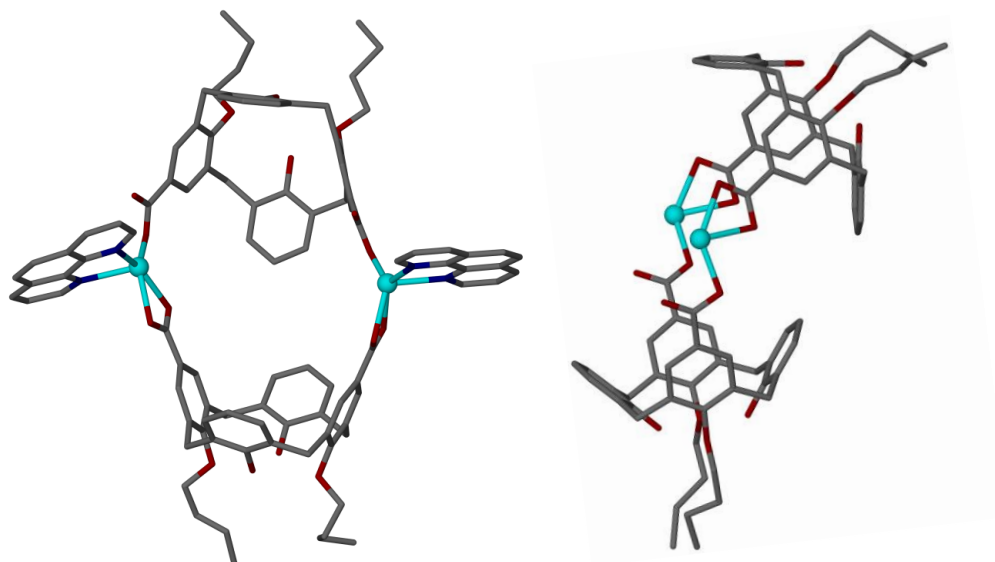


Figure 1.15. Two views of the skewed metal-organic capsule showing the offset nature of the calixarenes and the tilted nature of the capsule. Hydrogen atoms and ligated/guest DMF molecules removed.

Subsequent work found that alteration of the ligand used in the crystallisation process can have a marked effect on the cluster motif formed. Exchanging Phen for a bulkier substituent such as 3,4,7,8-tetramethyl-1,10-phenanthroline (TMePhen) results in a complex three dimensional (3-D) coordination polymer.⁸¹ Furthermore, reaction of the Type II diacid-dibutoxycalix[4]arene with cadmium nitrate in the presence of either 2-methyl-1,10-phenanthroline (2-MePhen) (Figure 1.16 A) or TMePhen (Figure 1.16 B) showed the components assemble to form a new head-to-head metal-organic capsule.⁸¹

There are few other examples of importance in this area. The first example was the synthesis of a series of $p\text{CO}_2[4]$ metal-organic frameworks (MOFs) generated from a tetra-*O*-alkylcalix[4]arene dicarboxylic acid.⁸² It should also be mentioned that the authors experienced difficulty when trying to remove the ligated solvent in order to activate the MOFs. Finally, de Mendoza and co-workers published the formation of giant regular polyhedra by utilising the metal-directed assembly of $p\text{CO}_2[4]$ s and $p\text{CO}_2[5]$ s with the uranyl ion.⁸³

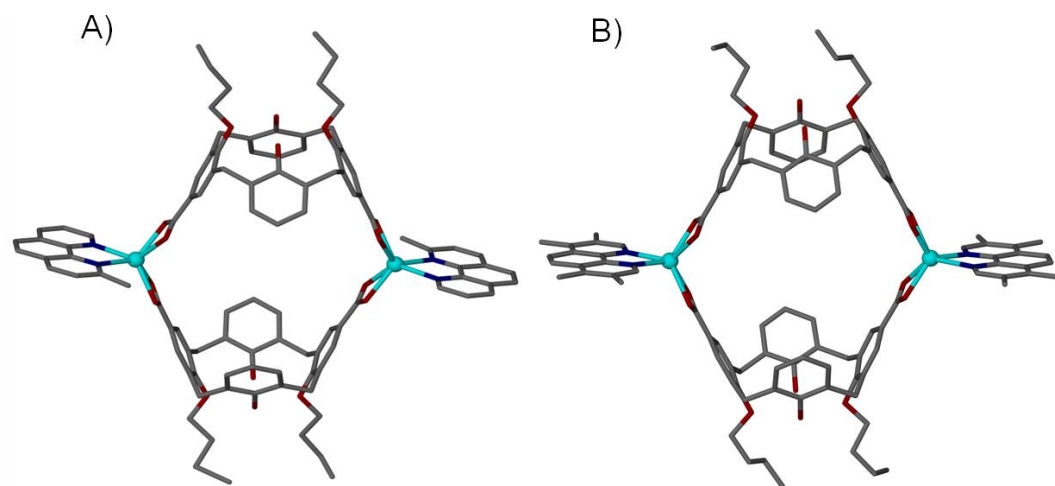


Figure 1.16. A) Head-to-head metal-organic capsule with 2-MePhen; B) Head-to-head metal-organic capsule with TMePhen.

For the most part, reported cases of large calixarene based assemblies have involved these macrocycles being in the favourable cone conformation which leads to the formation of discrete architectures.²⁴ One example where this is not the case is the interpenetrated nano-capsule formed from the reaction between *p*-carboxylatocalix[4]arene-*O*-methyl ether and rubidium or caesium hydroxide.⁸⁴ The calixarene was found to adopt a 1,3-alternate conformation where the resulting *pseudo*-cavity is occupied by a rubidium atom (Figure 1.17), and is the first example of a three-dimensional construction with directly bound capsule assemblies. This alongside the formation of *p*CO₂[4]s nanotubes is encouraging in their use for the assembly of novel supramolecular systems.

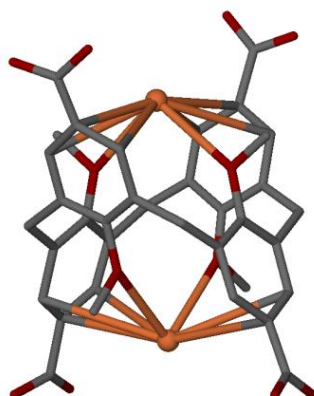


Figure 1.17. Binding of two rubidium centres within the 1,3-alternate tetra-*O*-methyl-*p*-tetracarboxylatocalix[4]arene. Hydrogen atoms are omitted for clarity.

1.7. Aims.

This project will primarily focus on the design of new molecular building blocks in order to study their self- and metal-directed assemblies. This will be achieved by the combination of calix[4]arene building blocks with useful chemical functionality and pyridine derivatives or metal-organic fragments in the hope of affording interesting supramolecular architectures.

In this project the main area of interest lies within the synthesis of new $p\text{CO}_2[4]\text{s}$ containing various degrees of functionality introduced to both the upper- and lower-rims. In the case of $p\text{CO}_2[4]\text{s}$, the macrocycles investigated will be di- or tetra-carboxylated, with either di- or tetra- R groups attached at the lower-rim. Variation in functionalisation at the lower-rim in the literature is vast, and examples of some target compounds are illustrated in Figure 1.18. It is thought that the introduction of a variety of different lower-rim substituents will have marked effects on the chemical environment generated within the supramolecular structures. Their applications as molecular building blocks in self- and metal-directed assembly will be studied. The examples of $p\text{CO}_2[4]\text{s}$ to be synthesised below will be reacted with a series of pyridine-derivatives in the hope to study their pyridine-templated assembly. In addition, a study of a series of transition metals as potential directing centres will be undertaken.

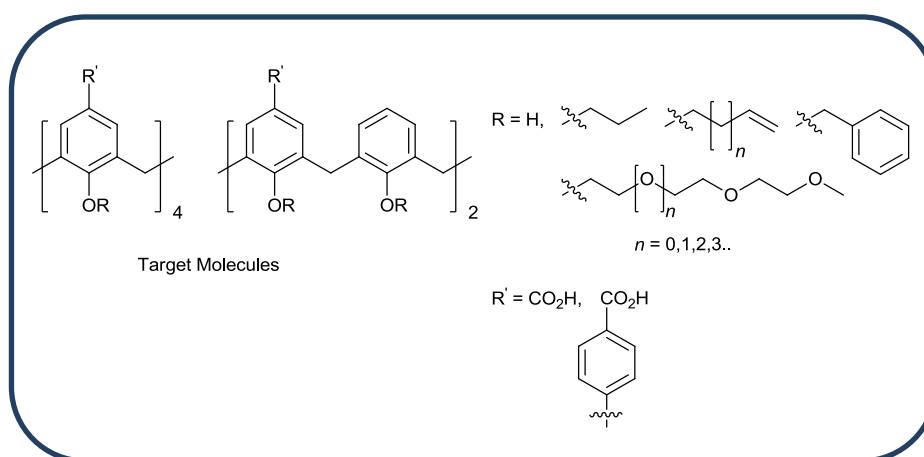


Figure 1.18. Some examples of $p\text{CO}_2[4]\text{s}$ to be synthesised.

The second major aspect of the project involves the locking of the calix[4]arene framework into the cone conformation. Addition of lower-rim selective functionalisation to afford conformationally rigid molecules such as calix[4]arene-

biscrown-3 (Figure 1.19) were carried out. The proximal biscrown is now locked in a cone *pseudo-C*₄ conformation, leaving the upper-rim susceptible to modification.

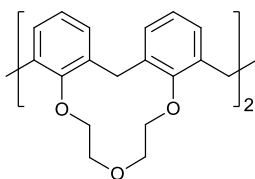


Figure 1.19. Calix[4]arene-biscrown-3 with diethylene glycol bridges.

The final goal of the project is to investigate extending the calix[4]arene molecular framework to form preorganised rigid platforms on the upper-rim. This will be attempted using Suzuki palladium-catalysed cross-coupling reactions to generate a series of calix[4]arene carboxyphenyl derivatives. They will be designed and constructed by a calix[4]arene scaffold stabilised in the cone conformation with di- or tetra-carboxyphenyl groups present at the upper-rim. Once generated, the desired compounds will be used as building blocks for supramolecular assemblies. Results from each of these aims are discussed in individual chapters.

1.8. References.

1. J. M. Lehn, *Pure Appl. Chem.*, 1978, **50**, 871.
2. J. W. Steed, D. R. Turner and K. J. Wallace, *Core Concepts in Supramolecular Chemistry and Nanochemistry*, John Wiley & Sons, 2001.
3. F. Vögtle, *Supramolecular Chemistry*, Wiley, Chichester, 1991.
4. E. Fischer, *Chem. Ber.* 1894, **27**, 2985.
5. C. J. Pedersen, *J. Am. Chem. Soc.* 1967, **89**, 7017.
6. J. W. Steed and J. L. Atwood, *Supramolecular Chemistry*, Wiley, Chichester, 2000.
7. J. M. Lehn, J. L. Atwood, J. E. D. Davies, D. D. McNicol and F. Vogtle, *Comprehensive Supramolecular Chemistry*, Pergamon, Elsevier Science, Oxford, 1996.
8. S. M. Biroš and J. Rebek, Jr., *Chem. Soc. Rev.*, 2007, **36**, 93.
9. S. Xu, G. Podoprygorina, V. Böhmer, Z. Ding, P. Rooney, C. Rangan and S. Mittler, *Org. Biomol. Chem.*, 2007, **5**, 558.
10. V. G. Organo and D. M. Rudkevich, *Chem. Commun.*, 2007, 3891.
11. S. J. Dalgarno, G. W. V. Cave and J. L. Atwood, *Angew. Chem. Int. Ed.* 2006, **45**, 570.
12. C. D Gutsche, *Calixarenes*, The Royal Society of Chemistry, Cambridge, 1989; and references therein.
13. L. Mandolini and R. Ungaro, *Calixarenes in Action*, Imperial College Press, London, 2000; and references therein.
14. Z. Asfari, V. Böhmer, J. Harrowfield and J. Vicens, *Calixarenes 2001*, Kluwer Academic Publishers, 2001.
15. A. Baeyer, *Ber.*, 1872, **5**, 25.
16. N. J. L. Megson, *Phenolic Resin Chemistry*, Butterworths, London, 1958.
17. L. H. Baekeland, *US Patent*, 1908, **942**, 699.
18. A. Zinke, E. Ziegler, *Ber.*, 1944, **77**, 26.
19. K. H. No and C. D. Gutsche, *J. Org. Chem.* 1982, **47**, 2713-2719.
20. C. D. Gutsche and R. Muthukrishnan, *J. Org. Chem.* 1978, **43**, 4905.
21. C. D. Gutsche, *Acc. Chem. Res.* 1983, **16**, 161.
22. C. D. Gutsche, B. Dhawan, M. Leonis and D. Stewart, *Org. Synth.* 1990, **68**, 238.

23. W. Sliwa and C. Kozlowski, *Calixarenes and Resorcinarenes*, Wiley-VCH, 2009.
24. a) L. R. MacGillivray and J. L. Atwood, *Nature* 1997, **389**, 469; b) S. J. Dalgarno, S. A. Tucker, D. B. Bassil and J. L. Atwood, *Science* 2005, **309**, 2037; c) E. S. Barrett, T. J. Dale and J. Rebek, Jr., *J. Am. Chem. Soc.* 2007, **129**, 3818.
25. D. Parker, L. M. Harwood and C. J. Moody, *Macrocyclic Synthesis*, Oxford University Press, 1996.
26. J. W. Cornforth, P. D'Arcy Hart, G. A. Nicholls, R. J. W. Rees and J. A. Stock, *Br. J. Pharmacol.*, 1955, **10**, 73.
27. C. D. Gutsche, B. Dhawan, J. A. Levine, K. H. No and L. J. Bauer, *Tetrahedron* 1983, **39**, 409.
28. a) K. Iwamoto, K. Araki and S. Shinkai, *J. Org. Chem.* 1991, **56**, 4955; b) K. Iwamoto, K. Fujimoto, T. Matsuda and S. Shinkai, *Tetrahedron Lett.* 1990, **31**, 7169; c) L. C. Groenen, J-D. van Loon, W. Verboom, S. Harkema, A. Casnati, R. Ungaro, A. Pochini, F. Ugozzoli and D. N. Reinhoudt, *J. Am. Chem. Soc.* 1991, **113**, 2385.
29. M. M. Conn and J. Rebek, *Chem. Rev.*, 1997, **97**, 1647.
30. A. Ikeda and S. Shinkai, *Chem. Rev.*, 1997, **97**, 1713.
31. a) A. Casnati, G. Cavallo, P. Metrangolo, G. Resnati, F. Ugozzoli and R. Ungaro, *Chem. Eur. J.*, 2009, **15**, 7903; b) O. Mogck, E. F. Paulus, V. Böhmer, I. Thondorfc and W. Vogt, *Chem. Commun.*, 1996, 2533; and references therein.
32. C. Jaime, J. de Mendoza, P. Prados, P. M. Nieto and C. Sanchez, *J. Org. Chem.* 1991, **56**, 3372.
33. S. Högberg, S. Abrahamsson and B. Nilsson, *Tetrahedron Lett.*, 1968, 1679.
34. G. D. Andreetti, R. Ungaro and A. Pochini, *J. Chem. Soc., Chem. Commun.*, 1979, 1005.
35. A. Arduini, M. Fabbi, M. Mantovani, L. Mirone, A. Pochini, A. Secchi and R. Ungaro, *J. Org. Chem.* 1995, **60**, 1454.
36. A. Arduini, S. Fanni, G. Manfredi, A. Pochini, R. Ungaro, A. R. Sicuri and F. Ugozzoli, *J. Org. Chem.* 1995, **60**, 1448.
37. C. D. Gutsche, *Calixarenes Revisited*, Royal Society of Chemistry, Cambridge, 1998.
38. J. A. J. Brunink, W. Verboom, J. F. J. Engbersen, S. Harkema and D. N. Reinhoudt, *Recl. Trav. Chim. Pays-Bas* 1992, **111**, 511.

39. C. D. Gutsche, *Calixarenes: Synthesis and Historical Perspectives*, In *Encyclopedia of Supramolecular Chemistry*, J. L. Atwood, J. W. Steed (eds.), Marcel Dekker, Inc, New York, 2004.
40. C. D. Gutsche, *Calixarenes: An Introduction in Monographs in Supramolecular Chemistry*, 2nd Ed, The Royal Society of Chemistry, Cambridge, 2008.
41. C. Alfieri, E. Dradi, A. Pochini, R. Ungaro and G. D. Andreetti, *J. Chem. Soc., Chem. Commun.*, 1983, 1075.
42. a) A. Arduini, A. Casnati, L. Dodi, A. Pochini and R. Ungaro, *J. Chem. Soc., Chem. Commun.*, 1990, 1597; b) A. Arduini, L. Domiano, A. Pochini, A. Secchi, R. Ungaro, F. Ugozzoli, O. Struck, W. Verboom and D. N. Reinhoudt, *Tetrahedron* 1997, **53**, 3767; c) S. Caccmese, A. Notti, S. Pappalardo, M. F. Parisi and G. Principato, *Tetrahedron* 1999, **55**, 5505.
43. C. D. Gutsche, J. A. Levine and P. K. Sujeeth, *J. Org. Chem.* 1985, **50**, 5802.
44. M. Conner, V. Janout and S. L. Regen, *J. Org. Chem.* 1992, **57**, 3744.
45. A. Arduini, A. Pochini, A. R. Sicuri, A. Secchi and R. Ungaro, *Gazz. Chim. Ital.* 1994, **124**, 129.
46. W. Verboom, A. Durie, R. J. M. Egberink, Z. Asfari and D. N. Reinhoudt, *J. Org. Chem.* 1992, **57**, 1313.
47. T. D. Guo, Q. Y. Zheng, L. M. Yang and Z. T. Huang, *J. Incl. Phen. Macro. Chem.* 2000, **36**, 327.
48. a) A. Decken, P. D. Harvey and J. Douville, *Acta Cryst., Sect. E: Struct. Rep. Online* 2004, **60**, 1170. b) O. Ediz, M. Tabakci, S. Memon, M. Yilmaz and D. M. Roundhill, *Supramol. Chem.* 2004, **16**, 199. c) V. Arora, H. M. Chawla and A. Santra, *Tetrahedron* 2002, **58**, 5591. d) H. M. Chawla and A. Santra, *Synth. Commun.* 2001, **31**, 2605. e) T. Komori and S. Shinkai, *Chem. Lett. Chem. Soc. Japan.* 1992, 901. f) A. Arduini, G. Manfredi, A. Pochini, A. R. Sicuri and R. Ungaro, *J. Chem. Soc., Chem. Commun.* 1991, 936.
49. W. Verboom, P. J. Bodewes, G. van Essen, P. Timmerman, G. J. van Hummel, S. Harkema and D. N. Reinhoudt, *Tetrahedron* 1995, **51**, 499.
50. A. Ikeda, M. Yoshimura, P. Lhotak and S. Shinkai, *J. Chem. Soc., Perkin Trans.1* 1996, 1945.
51. Y. Rudzevich, V. Rudzevich and V. Böhmer, *Chem. Eur. J.*, 2010, **16**, 4541.
52. a) S. D. Starnes, D. M. Rudkevich and J. Rebek Jr, *J. Am. Chem. Soc.* 2001, **123**, 4659; b) D. M. Rudkevich and J. Rebek Jr, *Eur. J. Org. Chem.* 1999, 1991.

53. D. J. Cram and J. M. Cram, *Container Molecules and their Guests*; The Royal Society of Chemistry, Cambridge, 1994.
54. F. Hof, S. L. Craig, C. Nuckolls and J. Rebek Jr, *Angew. Chem. Int. Ed.* 2002, **41**, 1488.
55. K. D. Shimizu and J. Rebek, Jr, *Proc. Natl. Acad. Sci. USA*, 1995, **92**, 12403.
56. O. Mogck, V. Böhmer and W. Vogt, *Tetrahedron* 1996, **52**, 8489.
57. L. Adriaenssens and P. Ballester, *Chem. Soc. Rev.*, 2013, **42**, 3261.
58. a) A. O. King and N. Yasuda, In *Organometallics in Process Chemistry*, Springer, 2004; b) K. C. Nicolaou, P. G. Bulger and D. Sarlah, *Angew. Chem. Int. Ed.* 2005, **44**, 4442; c) C. Tsukana and M. Sasaki, *J. Am. Chem. Soc.* 2003, **125**, 14294.
59. K. Tmao, K. Sumitani and M. Kumada, *J. Am. Chem. Soc.* 1972, **94**, 4373.
60. F. Diedrich and P. J. Stang, ed. *Metal-Catalyzed Cross-Coupling Reactions*, Wiley-VCH, New York, 1998.
61. N. Miyaura and A. Suzuki, *Chem. Commun.*, 1979, 886.
62. a) N. Miyaura, T. Yanagi and A. Suzuki, *Synth. Commun.* 1981, **11**, 513. b) N. Miyaura and A. Suzuki, *Chem. Rev.* 1995, **95**, 2457.
63. C. Amatore, A. Jutand and A. Suarez, *J. Am. Chem. Soc.* 1993, **115**, 9531.
64. Y. L. Cho, D. M. Rudkevich and J. Rebek Jr, *J. Am. Chem. Soc.* 2000, **122**, 9868.
65. a) C. D. Gutsche and K. H. No, *J. Org. Chem.* 1982, **47**, 2708; b) K. H. No and C. D. Gutsche, *J. Org. Chem.* 1982, **47**, 2713.
66. A. Arduini, A. Pochini, A. Rizzi, A. R. Sicuri and R. Ungaro, *Tetrahedron Lett.* 1990, **31**, 4653.
67. R. K. Juneja, K. D. Robinson, C. P. Johnson and J. L. Atwood, *J. Am. Chem. Soc.* 1993, **115**, 3818.
68. W. T. An, Y. Jiao, X. H. Sun, X. L. Zhang, C. Dong, S. M. Shuang, P. F. Xia and M. S. Wong, *Talanta* 2009, 54.
69. R. Chinchilla and C. Nájera, *Chem. Rev.* 2007, **107**, 874.
70. a) E. Pinkhassik, V. Sidorov and I. Stibor, *J. Org. Chem.* 1998, **63**, 9644; b) T. Haino, M. Yanase and Y. Fukazawa, *Tetrahedron Lett.* 2005, **46**, 1411.
71. M. Yamanaka, Y. Yamada, Y. sei, K. Yamaguchi and K. Kobayashi, *J. Am. Chem. Soc.* 2006, **128**, 1531.
72. G. Dyker, M. Mastalerz and I. M. Müller, *Eur. J. Org. Chem.* 2005, 3801.
73. R. Sharma, R. Margani, S. M. Mobin and R. Misra, *RSC Adv.*, 2013, **3**, 5785.

74. a) S. J. Dalgarno, J. E. Warren, J. Antesberger, T. E. Glass and J. L. Atwood, *New. J. Chem.* 2007, **31**, 1891; b) S. Kennedy and S. J. Dalgarno, *Chem. Commun.*, 2009, 5275; c) S. Kennedy, S. J. Teat and S. J. Dalgarno, *Dalton Trans.*, 2010, **39**, 384; d) S. Kennedy, C. M. Beavers, S. J. Teat and S. J. Dalgarno, *New. J. Chem.* 2011, **35**, 28; e) S. Kennedy, C. M. Beavers, S. J. Teat and S. J. Dalgarno, *Cryst. Growth Des.* 2012, **12**, 679; f) S. Kennedy, I. E. Dodgson, C. M. Beavers, S. J. Teat and S. J. Dalgarno, *Cryst. Growth Des.* 2012, **12**, 688; g) S. Kennedy, P. Cholewa, R. D. McIntosh and S. J. Dalgarno, *CrystEngComm.*, 2013, **15**, 1520.
75. S. R. Fukte, M. P. Wagh and S. Rawat, *Int. J. Pharm. Pharm Sci*, 2014, **6**, 9.
76. P. P. Cholewa and S. J. Dalgarno, *CrystEngComm.*, 2014, **16**, 3655.
77. S. Kennedy, C. M. Beavers, S. J. Teat and S. J. Dalgarno, *CrystEngComm.*, 2014, **16**, 3712.
78. S. Kennedy, G. Karotsis, C. M. Beavers, S. J. Teat, E. K. Brechin and S. J. Dalgarno, *Angew. Chem. Int. Ed.* 2010, **49**, 4205.
79. P. P. Cholewa, C. M. Beavers, S. J. Teat and S. J. Dalgarno, *Cryst. Growth Des.* 2013, **13**, 2703.
80. P. P. Cholewa, C. M. Beavers, S. J. Teat and S. J. Dalgarno, *Chem. Commun.*, 2013, **49**, 3203.
81. P. P. Cholewa, C. M. Beavers, S. J. Teat and S. J. Dalgarno, *Cryst. Growth Des.* 2013, **13**, 5165.
82. S. P. Bew, A. D. Burrows, T. Duren, M. F. Mahon, P. Z. Moghadam, V. M. Sebestyen and S. Thurston, *Chem. Commun.*, 2012, **48**, 4824.
83. S. Pasquale, S. Sattin, E. C. Escudero-Adan, M. Martinez-Belmonte and J. de Mendoza, *Nat. Commun.*, 2012, **3**, 785.
84. S. J. Dalgarno, K. M. Claudio-Bosque, J. E. Warren, T. E. Glass, J. L. Atwood, *Chem. Commun.*, 2008, 1410.

Chapter 2: Lower-rim functionalisation of *p*-carboxylatocalix[4]arenes.

2.1. Introduction.

This chapter is concerned with lower-rim modification of calix[4]arenes with various functional groups in order to generate a library of novel *p*CO₂[4] building blocks. Some of these new molecules have been successfully crystallised and single crystal X-ray structures are discussed below. In addition to this, pyridine was used as a template for directed self-assembly of these compounds in the solid state.

As discussed in Chapter 1, there is a vast array of calixarenes that may serve as building blocks for the formation of large supramolecular architectures.¹ The *p*-sulfonato- and *p*-carboxylatocalix[4]arenes, where the upper-rim *para* positions have been functionalised with SO₃H or CO₂H groups, have been used extensively for this purpose.²⁻⁸ An area of calix[4]arene synthesis that has received little attention is lower-rim modification, followed by alteration of the upper-rim to afford the desired carboxylic acid derivative.

2.2. Lower-rim functionalisation of calix[4]arene.

Calix[4]arenes are becoming the subject of increasing interest in the field of supramolecular chemistry due to their unique basket-like shape and the versatility of both the upper- and lower-rim(s) of the molecular framework with respect to functionalisation.^{9,10} Amongst the many chemical modifications that calix[4]arenes can undergo, alkylation of the lower-rim phenolic groups is of great importance.

This section will involve the synthesis of a library of *p*CO₂[4]s that will be used as building blocks, possessing various lower- and upper-rim functionality. There is huge scope for variation in lower-rim functionalisation but this chapter is concerned with the introduction of alkyl, polyethylene glycol and alkenyl chains onto the lower-rim of the calix[4]arene framework in order to generate a variety of novel calixarene derivatives. The number of upper-rim CO₂H groups will be explored when employing self- and metal-directed assembly (Figure 2.1).

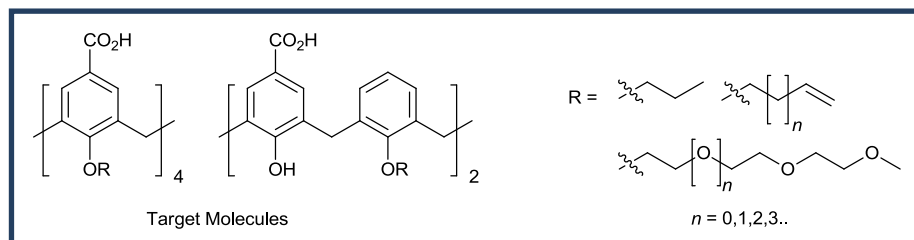
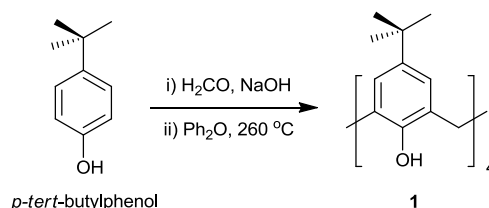


Figure 2.1. Examples of $p\text{CO}_2[4]$ s to be synthesised.

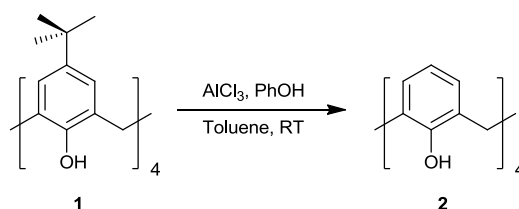
The first reaction undertaken was the modified Zincke-Cornforth base-catalysed condensation of *p*-*tert*-butylphenol and formaldehyde, followed by 'curing' in diphenyl ether to give *p*-*tert*-butylcalix[4]arene (TBC[4]) **1** as white crystals (Scheme 2.1).¹¹ TBC[4] is the most common member of the calixarene family, providing an invaluable molecular framework for the synthesis of more elaborate compounds.



Scheme 2.1. Schematic representation of the base-catalysed synthesis of TBC[4] **1** from *p*-*tert*-butylphenol.

Strong intramolecular hydrogen bonding between the lower-rim hydroxyl groups locks TBC[4] **1** in a bowl-like conformation with a specific geometry, C_4 ,¹² as confirmed by ^1H NMR. The ^1H NMR spectrum of TBC[4] **1**, shows a singlet at 10.37 ppm for the phenolic protons and a characteristic set of doublets at 4.28 and 3.50 ppm for the methylene bridging units.

TBC[4] **1**, was subsequently subjected to a reverse Friedel-Crafts reaction in order to remove the bulky *t*-butyl groups using a procedure reported by Ungaro *et al.*¹³ De-*tert*-butylation of compound **1** resulted in the formation of calix[4]arene (C[4]) **2** (Scheme 2.2), leaving the upper-rim free for chemical modification. Upon analysis compound **2** was found to contain similar peaks to the parent compound **1**. The most obvious difference was the loss of the *t*-butly peak at 1.24 ppm and the appearance of a triplet at 6.76 ppm corresponding to the *para* protons on the upper-rim of the C[4] framework.

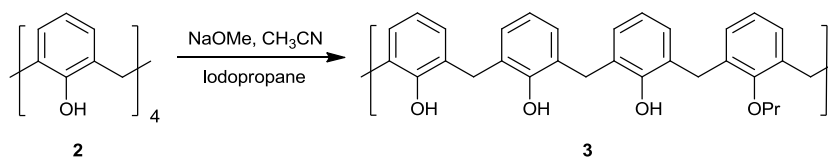


Scheme 2.2. Schematic representation of the synthesis of C[4] **2** from TBC[4] **1**.

With the upper-rim free for modification it is possible to alkylate the lower-rim hydroxyl groups in order to introduce a variety of different functional groups. Depending on the base employed during synthesis it is possible to selectively obtain mono-, bis-, tris- and tetra functional groups as described previously.¹⁴

2.2.1. Monopropoxycalix[4]arene.

Previously recorded in literature, monoalkoxycalix[4]arenes have been synthesised by two different procedures. The first method employs a multistep process¹⁵ whilst the second is a one-step protocol, in which the desired product is obtained through chromatographic separation techniques.¹⁶ More recently it was discovered that the use of sodium methoxide (NaOMe) in acetonitrile (CH₃CN) could generate the monoalkylated calix[4]arene product in good yield (Scheme 2.3).¹⁷

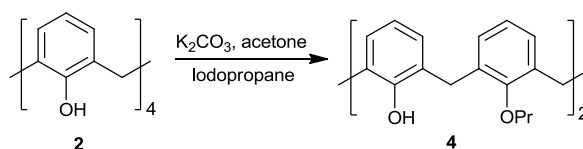


Scheme 2.3. Synthesis of monopropoxycalix[4]arene **3** from C[4] **2**.

For the monopropoxy product, compound **3**, this procedure was followed utilising NaOMe as the base with C[4] **2** in CH₃CN. After 30 minutes, iodopropane was added to the mixture of the monodeprotonated C[4] **2** and the reaction was heated at reflux for one day. This compound has previously been synthesised by Shu *et al.*¹⁷ It has not yet been possible to grow single crystals suitable for X-ray diffraction studies.

2.2.2. 1,3-Dipropoxycalix[4]arene.

In order to generate the dipropoxycalix[4]arene, compound **4**, with the propyl groups being distal to each other, potassium carbonate (K_2CO_3) was employed as a relatively mild base with the addition of iodopropane. The mixture was heated at reflux in acetone for one day and subsequent crystallisation from acetone yielded di-*O*-propoxycalix[4]arene **4** in good yield (Scheme 2.4).¹⁸ Compound **4** is employed and discussed further in Chapter 5.

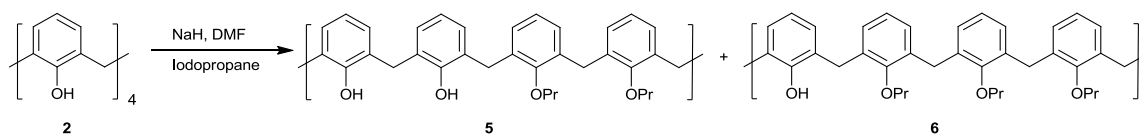


Scheme 2.4. Synthesis of 1,3-dipropoxycalix[4]arene **4** from C[4] **2**.

2.2.3. Syn-1,2-dipropoxycalix[4]arene.

In comparison to the previously described formation of the distal compound **4**, the alkylation of two hydroxyl groups which are proximal to each other is less favoured. This is surprising given that 1,2-hetero-alkylated C[4]s are of particular interest as chemically and/or biologically chiral guest molecules.¹⁹ Owing to the asymmetrical arrangement of the propyl chains on the lower-rim, this results in inherent chirality of the compound.

Synthesis of the syn-1,2-dipropoxycalix[4]arene **5** from C[4] **2** is relatively straightforward. In order to achieve the deprotonation of a pair of proximal hydroxyl groups, a stronger base was used. Sodium hydride (NaH) was employed before addition of iodopropane. The reaction was left to stir at room temperature for three hours before work-up.^{20,21} In order to obtain compound **5**, the crude product was subjected to chromatographic separation. When this technique was implemented the dipropoxycalix[4]arene **5** was eluted last, following after an unexpected trispropoxycalix[4]arene **6** by-product (Scheme 2.5). As compound **6** was unanticipated, it was not used in any further reactions, but was fully characterised.



Scheme 2.5. Synthesis of compounds **5** and **6** using NaH and iodopropane.

2.2.3.1 Structure of syn-1,2-dipropoxycalix[4]arene, **5**.

In the previous section it was discussed that compound **5** had been previously synthesised but that its crystal structure was yet to be reported. The crystal structure of **5** was determined in the course of this study. Recrystallisation of compound **5** from DCM/MeOH yielded suitable block-shaped crystals for X-ray diffraction studies. Crystals of syn-1,2-dipropoxycalix[4]arene, **5** are in the hexagonal cell and the structure solution was performed in the space group $P6_5$ with a complete molecule in the asymmetric unit making up one quarter of the unit cell (Figure 2.2). Details of data collection and structure refinement are given in Table 2.4 at the end of this chapter.

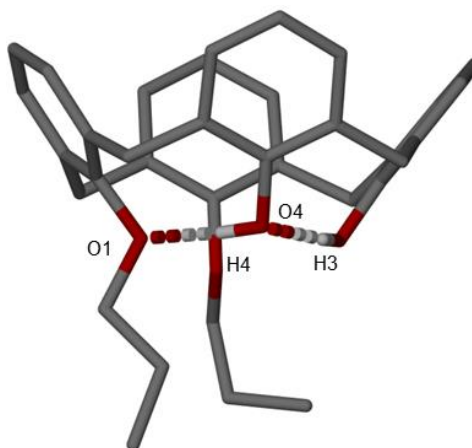


Figure 2.2. Asymmetric unit found in the single crystal X-ray structure of compound **5**. Hydrogen atoms (apart from those involved in hydrogen bonding) have been omitted for clarity. Selected atoms have been labelled according to discussion.

Prior to data collection it was predicted that compound **5** would adopt a near perfect cone conformation in the solid state. This arises as a direct result of there being two hydroxyl groups at the lower-rim, which form hydrogen bonding interactions to neighbouring ethereal oxygens. There are a total of 2 OH \cdots O hydrogen bonding interactions in the asymmetric unit, with [H3] \cdots [O4] and [H4] \cdots [O1] distances of 1.845 and 1.888 Å respectively.

Symmetry expansion shows there is one molecule above the other with one of the propoxy chains pointing directly into the cavity of another. There was found to be three CH $\cdots\pi$ interactions between the alkyl chain and three aromatic rings of the molecule, ranging from 2.855 – 3.750 Å (full details in Table 2.1). There was also found to be one CH $\cdots\pi$ interaction between the last aromatic ring of one molecule and the para hydrogen atom of another molecules phenol ring (Figure 2.3). This has a distance of 2.757 Å between H[10] \cdots aromatic centroid.

H[31A] \cdots aromatic centroid	3.168
H[31B] \cdots aromatic centroid	2.855
H[31C] \cdots aromatic centroid	3.750

Table 2.1. CH $\cdots\pi$ interaction distances (in Å) in the symmetry expansion of compound 5.

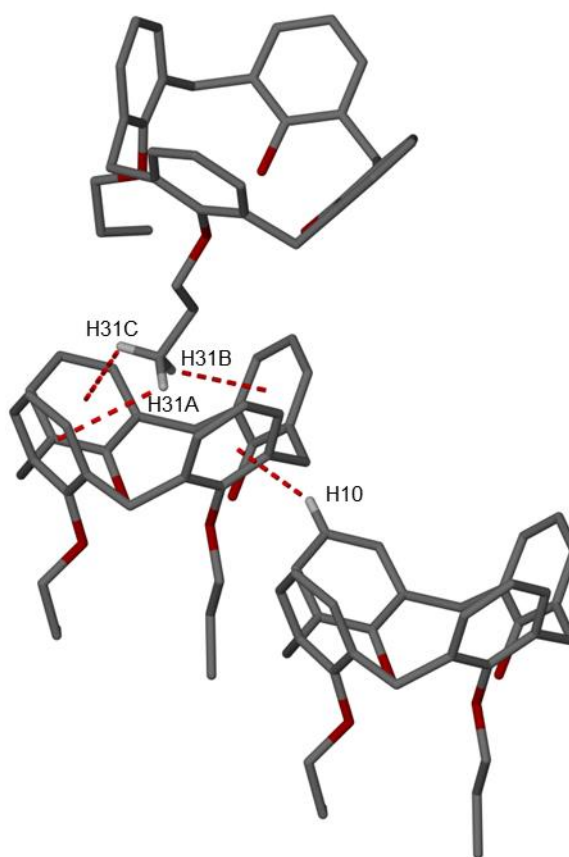
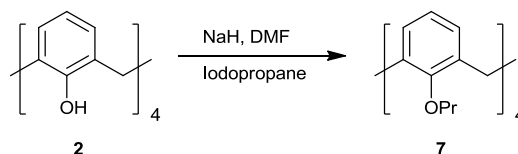


Figure 2.3. Symmetry expansion of the X-ray crystal structure showing CH $\cdots\pi$ interactions between molecules of **5** as dashed red lines. Hydrogen atoms (apart from those involved in CH $\cdots\pi$ interactions) have been omitted for clarity. Selected atoms have been labelled according to discussion.

2.2.4. Tetrapropoxycalix[4]arene.

Unlike the two dialkylated products discussed previously which adopt near perfect cone conformations, tetra-alkylation of the lower-rim can lead to a number of different conformers being formed. The length of the alkyl chain attached to the lower-rim of the macrocycle dictates which conformation the calixarene will be retained in. It has been shown that in solution shorter chain lengths with either methoxy or ethoxy chains will adopt various conformations. This is attributed to the fact that the chain lengths are short enough to allow flipping through the annulus of the macrocycle.^{1,3} The macrocycle can be locked in the cone conformation, or in this case a pinched-cone conformation with C_{2v} symmetry, by employing longer alkyl chains. Tetra-alkylation of **C[4] 2**, to obtain tetrapropoxycalix[4]arene **7**, is achieved by using NaH with iodopropane under reflux for one hour (Scheme 2.6).¹⁸ After purification from acetone,

white crystals of compound **7** were isolated. Compound **7** will be employed and discussed further in Chapters 3 and 5.

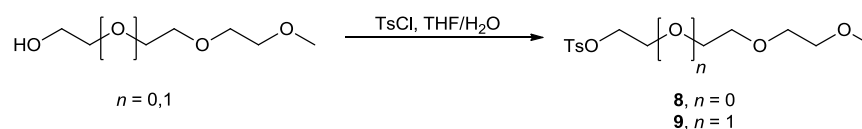


Scheme 2.6. Schematic representation of tetra-alkylation of C[4] **2** using NaH and iodopropane to yield compound **7**.

2.3. Synthesis of di(PEGylated)-di-*p*-carboxylatocalix[4]arenes and tetra(PEGylated)-tetra-*p*-carboxylatocalix[4]arenes.

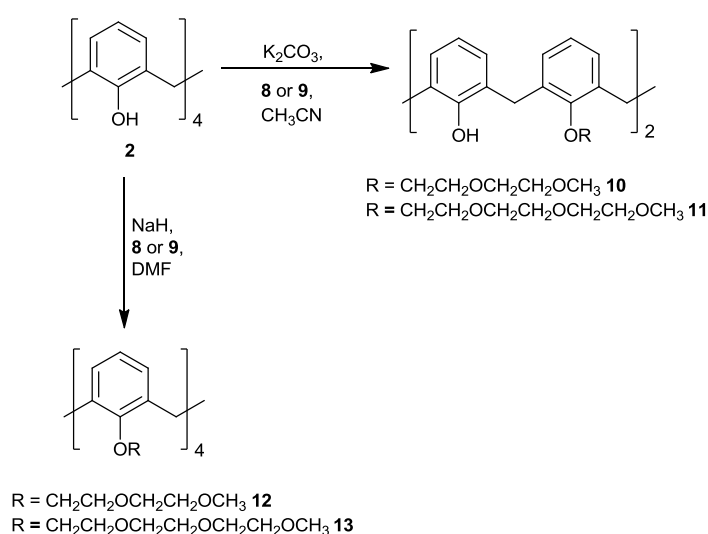
Calix[*n*]arenes are generally insoluble in water and are found to be only partially soluble in many organic solvents. This limits the ability to explore their substrate binding abilities and consequently the derivatisation of water soluble calix[*n*]arenes is beneficial in order to overcome this. There are many methods in which this can be implemented but the most common is to introduce different functionalities to the calix[*n*]arene framework that will help increase its solubility properties. Examples of such groups can contain either positive or negative charges or neutral molecules with highly hydrophilic groups. Functions such as carboxylates, sulfonates, phosphates or ammonium groups can be used for such modifications.

Another means of increasing the calixarenes solubility in water or organic solvents was to attach polyethylene glycol (PEG) chains to the lower-rim of the macrocycle. The PEG chain precursors to be attached to the lower-rim as either di- or tetra-substituents, were prepared in a straightforward procedure (Scheme 2.7).^{22,23} This involved the reaction of the given tosylate with NaOH in THF before the slow addition of tosyl chloride. Once the reaction was complete (two hours) it produced compounds **8** and **9** as viscous liquids in almost quantitative yields (96% and 90% respectively). The ¹H NMR spectra were in agreement with literature values so compounds **8** and **9** were used in subsequent reactions without further purification.



Scheme 2.7. Schematic representation of the synthesis of 2-(2-methoxyethoxy) ethyl tosylate ($n = 0$), or triethylene glycol monomethyl ether tosylate ($n = 1$).

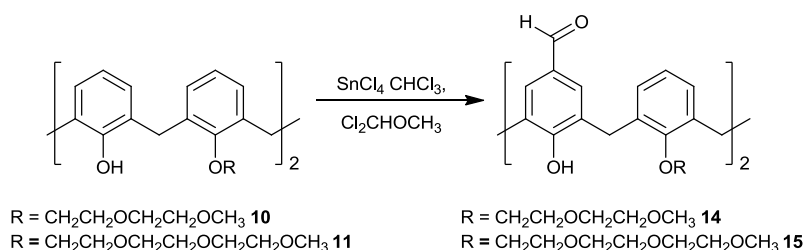
To produce the di-substituted compounds **10** and **11**, it was first 1,3-*O*-dialkylated with 2 equivalents of the respective tosylate (either compound **8** or **9**) in the presence of 1 equivalent of K_2CO_3 in CH_3CN for one week (Scheme 2.8).²⁴ This resulted in a complex crude ^1H NMR spectrum. Chromatography separation was carried out using a silica column, and recrystallisation from methanol yielded compound **10** as a white solid (43%), or compound **11** as a yellow oil (34%).



Scheme 2.8. Schematic representation of di-alkylation using K_2CO_3 and tetra-alkylation using NaH.

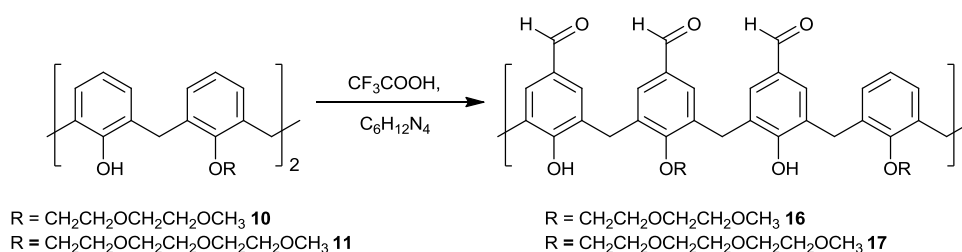
In order to generate the tetra-substituted calixarene derivatives **12** and **13**, C[4] **2** was first reacted with 5 equivalents of the respective tosylate in the presence of 6 equivalents of NaH in DMF over three days.²⁵ Again, the ^1H NMR spectra obtained were impure and column chromatography was performed to yield compounds **12** (20%) or **13** (25%) as yellow oils. The yields obtained for the tetra-substituted products was lower than that obtained for the di-alkylated compounds, which is in agreement with the reported literature.^{24,25}

Once pure, these alkylated compounds were reacted further in an attempt to vary the number of CO₂H groups present on the upper-rim. Formylation of compounds **10** and **11** was carried out *via* reaction with SnCl₄ and 1,1-dichloromethyl methyl ether at lower temperature.¹⁸ Once the reaction work-up was complete the diformylated-dialkylated compounds **14** and **15** were obtained as orange oils (Scheme 2.9).



Scheme 2.9. Schematic of the formylation of compounds **10** and **11** using SnCl₄ and 1,1-dichloromethyl methyl ether.

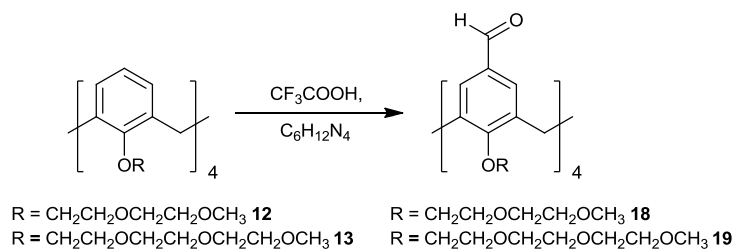
Compounds **12** and **13** were also subject to formylation using different reaction conditions. This included reacting the calixarene macrocycles **10** and **11** in trifluoroacetic acid (TFA) along with hexamethylene tetramine (HMTA) over a period of three days (Scheme 2.10).^{26c} This produced the dialkylated-*tris-p*-formylcalix[4]arenes **16** and **17** as white solids after purification from column chromatography. The yields obtained for both compounds was low (< 15%) and due to time constraints they were not used in any further reactions, but were fully characterised as they are novel calixarene products.



Scheme 2.10. Schematic of the formylation of compounds **10** and **11** using TFA and HMTA.

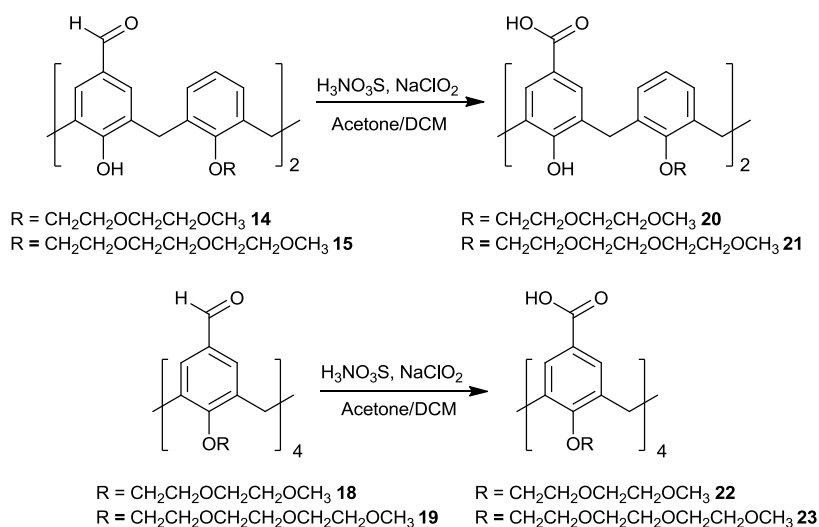
Synthesis of compounds **18** and **19** by the respective formylation of compounds **12** and **13** is easily achieved under the previously described harsh conditions involving heating

the obtained compound at reflux in TFA, with HMTA over a period of three days (Scheme 2.11).^{26c}



Scheme 2.11. Schematic of the formylation of compounds **12** and **13** using TFA and HMTA.

Oxidation of compounds **14**, **15**, **18** and **19** to yield the corresponding series of di-*O*-alkoxy-di-*p*-carboxylatocalix[4]arenes **20**, **21** and tetra-*O*-alkoxy-tetra-*p*-carboxylatocalix[4]arenes **22** and **23** respectively, is carried out using a slightly modified literature procedure.²⁷ The standard procedure executed involved dissolving the given formylated calixarene in a 3:1 mixture of acetone:DCM and reacting it with an aqueous solution of sulfamic acid (H₃NO₃S) and sodium chlorite (NaClO₂) at room temperature over a period of one day. The products are isolated following the addition of 1 M HCl (Scheme 2.12).



Scheme 2.12. Schematic of the synthesis of desired *p*-carboxylatocalix[4]arenes **20** - **23** using H₃NO₃S and NaClO₂.

Compounds **20** - **23** were dissolved in a series of commercially available pyridine containing solvents which were pyridine (Py), 2-picoline (2-Pic), 3-picoline (3-Pic) and 4-picoline (4-Pic). DMF was also used in an attempt to form single crystals that could be examined using single crystal X-ray diffraction. This resulted in the formation of single crystals for three of the sample which will be discussed in detail in the sections below.

2.4. X- ray crystal structures of compound 20.

2.4.1. Structure of di(monomethyl diethylene glycol)-di-*p*-carboxylatocalix[4]arene, 20.

Suitable block-shaped crystals of compound **20** were grown by crystallisation from DMF and X-ray diffraction studies were performed. Single crystals of compound **20** are in the triclinic cell and the structure solution was performed in the space group *P*-1 with a complete molecule of compound **20** in the asymmetric unit making up one quarter of the unit cell (Figure 2.4). Even though the crystallisation was carried out in DMF solution, the crystal lattice included no solvent molecules. Details of data collection and structure refinement are given in Table 2.4 at the end of this chapter.

Compound **20** adopts a near perfect cone conformation due to the hydrogen bonding interactions present between the two hydroxyl groups at the lower-rim with the ethereal oxygens of the propyl chains. There are a total of 2 OH \cdots O hydrogen bonding interactions in the asymmetric unit, [H3O] \cdots [O2] and [H1O] \cdots [O4] with distances of 1.847 and 1.884 Å (Figure 2.4).

Symmetry expansion around compound **20** shows there is one molecule above the other with one of the monomethyl diethylene glycol chains pointing directly into the cavity of another. There was found to be three CH \cdots π interactions between the end of the PEG chain and three of the aromatic rings of the molecule ranging from 2.703 – 3.316 Å (full details in Table 2.2).

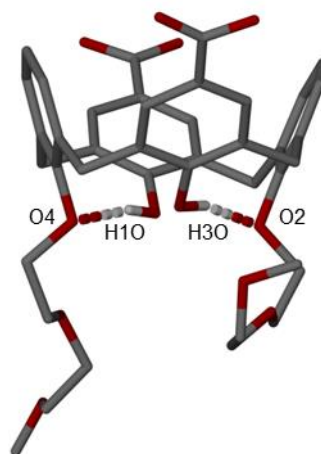


Figure 2.4. X-ray crystal structure of the asymmetric unit of compound **20**. Hydrogen bonding is shown as split-colour lines. Hydrogen atoms (apart from those involved in hydrogen bonding) have been omitted for clarity. Selected atoms have been labelled according to discussion.

H[40A]...aromatic centroid	2.703
H[40B]...aromatic centroid	3.316
H[40C]...aromatic centroid	2.913

Table 2.2. CH... π interaction distances (in Å) in the symmetry expansion of compound **20**.

There are also two symmetry unique OCOH...OCO₂H interactions between compound **20** and symmetry equivalent molecules with a H[5O]...O[6] and H[7O]...O[8] distances of 1.748 and 1.749 Å respectively. Expansion of compound **20** also results in a common bi-layer arrangement of molecules owing to the CO₂H...CO₂H synthon that occurs between both carboxylic acid groups of one molecule to that of another (Figure 2.5).

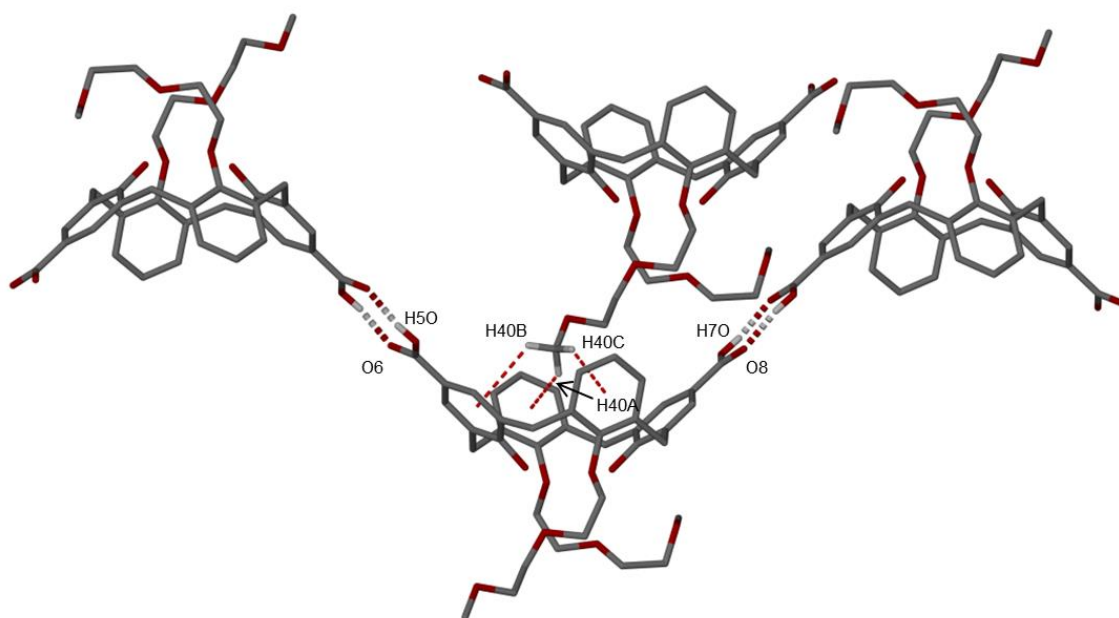


Figure 2.5. Symmetry expansion around compound **20**. Hydrogen bonding is shown as split-colour lines and $\text{CH}\cdots\pi$ interactions as dashed red lines. Hydrogen atoms (apart from those involved in hydrogen bonding and $\text{CH}\cdots\pi$ interactions) have been omitted for clarity. Selected atoms have been labelled according to discussion.

2.4.2. Structure of di(monomethyl diethylene glycol)-di-*p*-carboxylatocalix[4]arene-3-picoline, **2.1**.

Crystals of di(monomethyl diethylene glycol)-di-*p*-carboxylatocalix[4]arene-3-Pic, **2.1**, were obtained as a result of the addition of 2 mL 3-Pic to compound **20**. Slow evaporation of the solvent over several weeks yielded small-block shaped crystals which were suitable for X-ray diffraction studies. Single crystals of **2.1** are in the triclinic cell and structure solution was performed in the space group *P*-1. Details of data collection and structure refinement are given in Table 2.4 of this chapter. The asymmetric unit of **2.1** consists of one molecule of **20** and one molecule of 3-Pic (Figure 2.6).

Compound **20** adopts a near perfect cone conformation due to the hydrogen bonding interactions present between the two hydroxyl groups at the lower-rim with the ethereal oxygens of the propyl chains. There are a total of 2 $\text{OH}\cdots\text{O}$ hydrogen bonding interactions in the asymmetric unit, $[\text{H1O}]\cdots[\text{O2}]$ and $[\text{H3O}]\cdots[\text{O4}]$ with distances of 1.868 and 1.889 Å (Figure 2.6).

The cavity of **2.1** is occupied by one molecule of 3-Pic. There are two CH $\cdots\pi$ interactions located between one *ortho* hydrogen atom and one *para* hydrogen atom on the 3-Pic guest and the aromatic rings on the host. The two interactions are located with H[45] \cdots aromatic centroid and H[47] \cdots aromatic centroid distances of 2.513 and 2.755 Å.

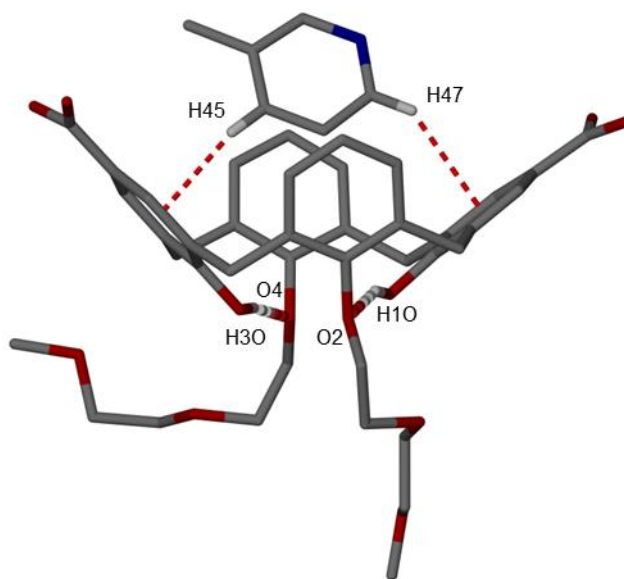


Figure 2.6. X-ray crystal structure of the asymmetric unit observed in **2.1**. Hydrogen bonding is shown as split-colour lines and CH $\cdots\pi$ interactions are shown as red dashed lines. Hydrogen atoms (apart from those involved in hydrogen bonding and CH $\cdots\pi$ interactions) have been omitted for clarity. Selected atoms have been labelled according to discussion.

Symmetry expansion of the asymmetric unit around **2.1** results in the formation of a common bi-layer arrangement of the molecules where the familiar CO₂H \cdots CO₂H synthon is observed between one carboxylic acid group of one molecule to that of another. The second carboxylic acid group on the molecule can be seen to hydrogen bond to the 3-Pic guest as shown in Figure 2.7. There is one N \cdots HOCO and one OCOH \cdots OCOH hydrogen bonding interaction present with respective H[50] \cdots N[1] and H[80] \cdots O[6] distances of 1.804 and 1.744 Å.

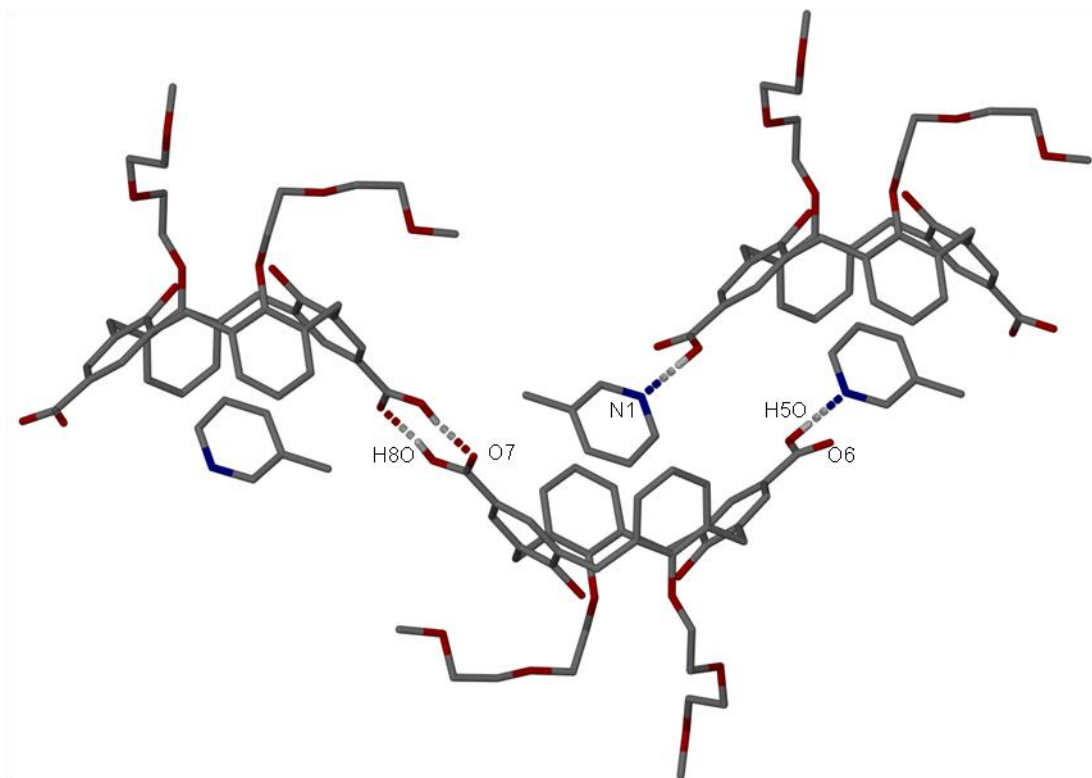


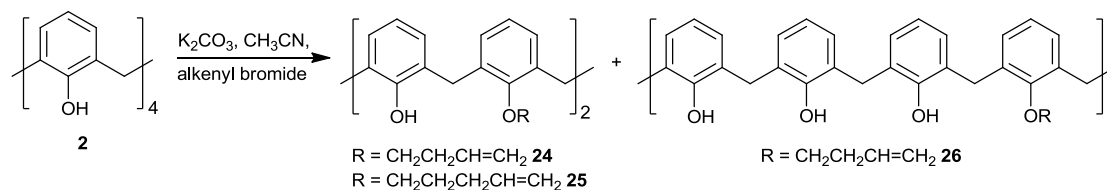
Figure 2.7. Symmetry expansion of molecule **2.1**. Hydrogen bonding is shown as split-colour lines. Hydrogen atoms (apart from those involved in hydrogen bonding) have been omitted for clarity. Selected atoms have been labelled according to discussion.

2.5. Synthesis of dialkenyl-dihydroxy-di-*p*-carboxylatocalix[4]arenes.

The Claisen rearrangement of allyloxycalixarenes to the corresponding *p*-allylcalixarenes is a well-established practiced procedure.²⁸ These calixarene derivatives have great potential as they possess double bonds which can be easily modified for host-guest complexation studies.^{29,30}

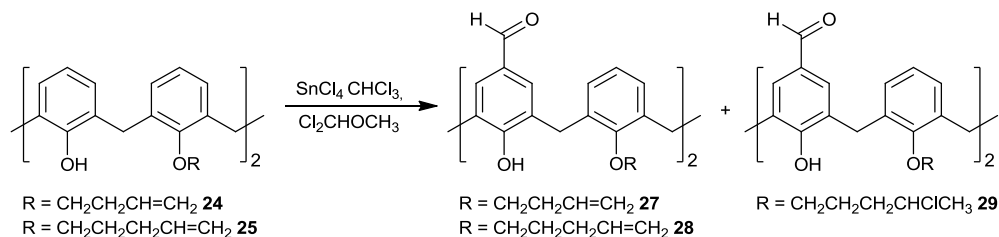
As previously said, there is a huge scope for variation in lower-rim functionalisation and it is thought that the introduction of alkenyl chains will have a marked effect on the supramolecular structures that could be generated from these modified *p*CO₂[4]s. When C[4] **2** was reacted with the appropriate alkenyl bromide in the presence of 5.5 equivalents of K₂CO₃ in refluxing CH₃CN, reasonable yields of the corresponding compounds **24** and **25** could be isolated. This reaction results in the disubstituted products adopting the cone conformation, as indicated by the ¹H NMR spectra.³¹ In addition to the synthesis of these molecules the monosubstituted product **26** was also obtained (Scheme 2.13). An average yield was obtained for compound **26**, which was

fully characterised as it is a novel calixarene derivative, but was not employed in subsequent reactions.



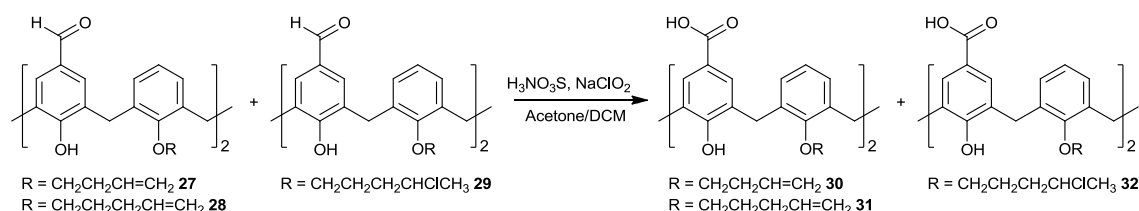
Scheme 2.13. Mono- and di-substituted allylation of C[4] **2**.

The Gross formylation was then employed in order to diformylate the positions *para* to the hydroxyl groups. This is an electrophilic reaction, where dichloromethyl methyl ether is promoted by a Lewis acid (SnCl_4) to give compounds **27** and **28** in reasonable yields (Scheme 2.14).¹⁸ Compound **29** was also obtained by this method, where the reaction was not quenched thoroughly enough and the excess Cl^- added across the more substituted carbon of the double bond. This mode of addition is regioselective in the direction predicted by Markovnikov's rule.



Scheme 2.14. Gross formylation of compounds **24** and **25**.

Oxidation of compounds **27**, **28** and **29** to yield the corresponding series of di-*p*-carboxylatocalix[4]arenes **30**, **31** and **32** was executed. The procedure was accomplished by dissolving the given formylated calix[4]arene in a 3:1 mixture of acetone:DCM and reacting it with an aqueous solution of sulfamic acid and sodium chlorite at room temperature for one day. The products are isolated following the addition of 1 M HCl (Scheme 2.15).²⁷



Scheme 2.15. Schematic of the synthesis of desired *p*-carboxylatocalix[4]arenes **30** – **32** using $\text{H}_3\text{NO}_3\text{S}$ and NaClO_2 .

Although tetra-*O*-allylation of C[4] **2** can be carried out,³² it was pointless to synthesise owing to the use of TFA in the formylation step. The TFA is found to attack the double bonds on the lower-rim *via* Markovnikov's rule, under relatively mild conditions.³³

Recrystallisation of compound **29** from acetone generated crystals that were suitable for X-ray diffraction studies and will be discussed below. Compounds **30** – **32** were dissolved in a series of commercially available pyridine containing solvents which were pyridine (Py), 2-picoline (2-Pic), 3-picoline (3-Pic) and 4-picoline (4-Pic) along with DMF in an attempt to form single crystals that could be examined using single crystal X-ray diffraction. This has been unsuccessful to date.

2.6. X-ray crystal structure of compound **29**.

2.6.1 Structure of di(4-chloropentane)-di-*p*-formylcalix[4]arene:acetone, **2.2**.

Crystals of di(4-chloropentane)-di-*p*-formylcalix[4]arene:acetone, **2.2** were obtained from the slow evaporation of acetone overnight to yield small lath-shaped colourless crystals. Single crystals of **2.2** are in the monoclinic cell and the structure solution was performed in the space group $P2_1$. Details of the collection and structure refinement are given in Table 2.5 of this chapter. The asymmetric unit of **2.2** consists of one molecule of **29** and one solvent molecule of acetone (Figure 2.8).

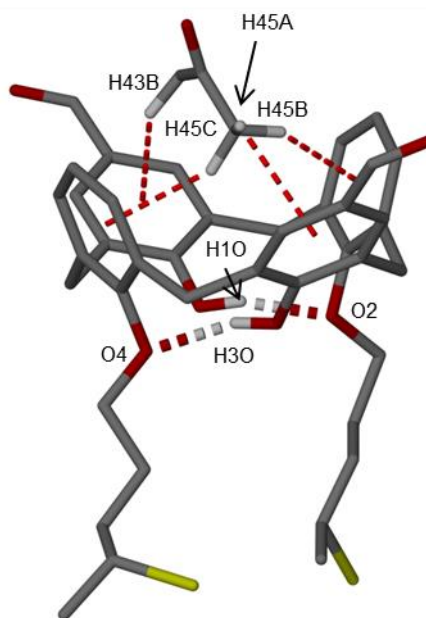


Figure 2.8. Asymmetric unit found in the single crystal X-ray structure of **2.2**. Hydrogen atoms (apart from those involved in hydrogen bonding and CH $\cdots\pi$ interactions) have been omitted for clarity. Hydrogen bonding is shown as split-colour lines and CH $\cdots\pi$ interactions as red dashed lines. Selected atoms have been labelled according to discussion.

With hydrogen bonding interactions present at the lower-rim between the two hydroxyl groups with the ethereal oxygens of the chains allows the calixarene to adopt a near perfect cone conformation. There are a total of 2 OH \cdots O hydrogen bonding interactions within the asymmetric unit between [H1O] \cdots [O2] and [H3O] \cdots [O4] with distances of 1.866 and 1.894 Å respectively. There was found to be four CH $\cdots\pi$ interactions between the methyl groups of the acetone and the aromatic rings of the molecule ranging from 2.707 – 3.137 Å (full details in Table 2.3).

Symmetry expansion of the asymmetric unit around **2.2** reveals the presence of a CH $\cdots\pi$ interaction located between one of the *meta* hydrogen atoms on the aromatic ring of the asymmetric unit and one of the aromatic rings of a symmetry equivalent molecule (Figure 2.9). This has a H[9] \cdots aromatic centroid distance of 2.573 Å. There is also a CH \cdots Cl(C) interaction between the other *meta* hydrogen atom on the same ring with one of the chlorine atoms from one of the pentane chains, with a H[11] \cdots Cl[2] distance of 2.681 Å.

H[43B]...aromatic centroid	2.768
H[45A]...aromatic centroid	3.137
H[45B]...aromatic centroid	2.751
H[45C]...aromatic centroid	2.707

Table 2.3. CH... π interaction distances (in Å) in the symmetry expansion of compound 2.2.

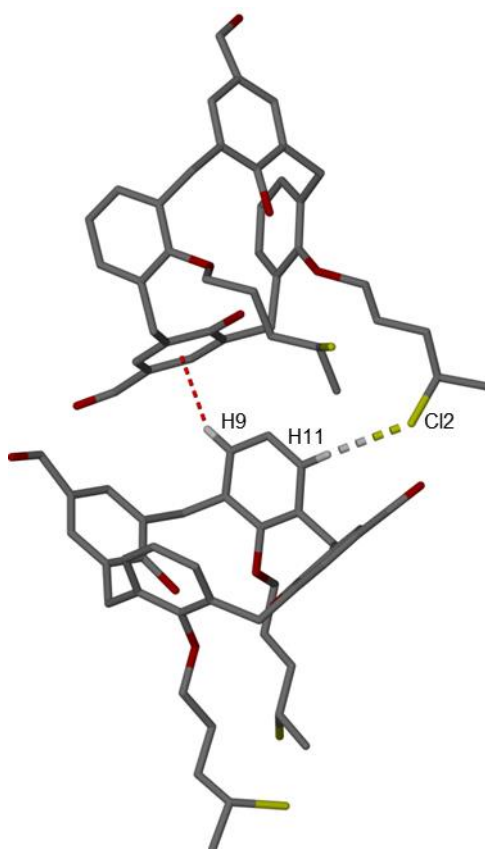


Figure 2.9. Symmetry expansion of 2.2. CH... π interaction is shown as red dashed lines and the CH...Cl interaction is shown as split-colour lines. Hydrogen atoms (apart from those involved in hydrogen bonding) have been omitted for clarity. Selected atoms have been labelled according to discussion.

2.7. Conclusion.

To conclude, alteration of the C[4] lower-rim with a selection of different substituents was successful. This was undertaken with a view to examining any changes in the packing behaviour for these synthesised compounds. The study of the effect of pyridine-templates over the control of the assembly of cone shaped and pinched-cone $p\text{CO}_2[4]\text{s}$ has been ongoing in the literature.³ With only one crystal structure generated containing a pyridine derivative template (**2.1**), it is difficult to conclude if compounds **21** - **23**, **30** - **32** will display the same structural preferences. Compound **20** was found to act as a host molecule, with the 3-Pic guest residing in the cavity. Owing to the near perfect cone shape of the host a guest molecule can be permitted access into the cavity, which is stabilised by $\text{CH}\cdots\pi$ interactions. The common bilayer arrangement that is seen in complex **20** is still observed in **2.1**, through one $\text{N}\cdots\text{HOCO}$ and one $\text{OCOH}\cdots\text{OCOH}$ hydrogen bonding interaction.

Further work with these systems could focus on optimising conditions in which to grow suitable crystals for *X*-ray diffraction studies. This would allow for full structural comparison and determination of the effect of different lower-rim substituents on self-assembly.

2.8. Experimental.

2.8.1. General comments.

The majority of work that has been conducted so far has been ligand synthesis, with a view to exploring the self- and metal-directed assembly of all the compounds synthesised.

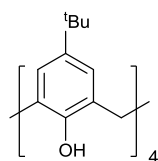
2.8.2. General experimental.

Unless stated, all reagents employed were purchased from chemical suppliers (Alfa Aesar, Fisher Scientific and Sigma Aldrich) and used as received. If required solvents were dried over molecular sieves (pore size 4 Å). Unless stated all experiments were carried out in air. When performed under a nitrogen atmosphere, this was dried over two columns of Drierite® gas purifier connected in series. Analytical thin layer chromatography was performed on precoated silica gel plates (Merck, 60 F254) and column chromatography was performed with silica gel (Merck, particle size 40-60 µm).

Electrospray ionisation and fourier transform mass spectra (ESI-FTMS) were obtained on a LTQ Orbitrap XL spectrometer at Swansea University. ¹H NMR and ¹³C NMR spectra were recorded on Bruker AC 300 and Bruker AC 400 spectrometers, with chemical shifts reported in ppm with respect to TMS as an internal standard. IR spectra were acquired on a Perkin Elmer Spectrum 100 FT-IR Spectrometer, with wavenumber (ν) of absorption reported in cm⁻¹. Single crystals were analysed on either a Bruker Apex II CCD diffractometer operating at 100(2) K with Mo-K α radiation (λ = 0.71073 Å) with a graphite monochromator or a Bruker D8 diffractometer with PHOTON 100 detector operating at 100(2) K with synchrotron radiation (λ = 0.77490 Å). Microanalysis results were obtained using an Exeter Analytical CE440 Elemental Analyser.

2.8.3. Synthesis of compounds 1 - 32.

5,11,17,23-tetra(*tert*-butyl)-25,26,27,28-tetrahydroxycalix[4]arene, **1**¹¹



p-*tert*-butylphenol (500.90 g, 3.33 mol) was added to a 10 L reactor vessel, equipped with a mechanical stirrer, thermometer and Dean-Stark water trap. Formaldehyde solution (37%, 305 mL) and NaOH (2.80 g, 0.07 mol) dissolved in water (10 mL) was then added to the flask. The reaction mixture was heated to 120 °C under nitrogen flow. Heating and stirring were stopped rapidly as the mixture became viscous and toluene (500 mL) was added to the solid mass and the mixture cooled to RT. Diphenyl ether (2.5 L) was added and the reaction mixture was heated to 120 °C where toluene and water were removed. The reaction was heated at reflux at 260 °C for 4 hours. When the mixture had cooled to 60 °C ethyl acetate (3 L) was added and the solution was stirred as it cooled to RT. The pale brown crystals were filtered by suction filtration using a Buchner funnel and washed with ethyl acetate (500 mL) to yield compound **1** as glistening white crystals (334.60 g, 62%).

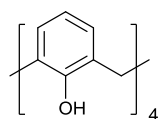
¹H NMR (300 MHz, 25 °C, CDCl₃): δ = 10.37 (s, 4H, OH), 7.08 (s, 8H, ArH), 4.28 (d, J = 12.2 Hz, 4H, ArCH₂Ar), 3.50 (d, J = 12.2 Hz, 4H, ArCH₂Ar), 1.24 (s, 36H, C(CH₃)₃).

¹³C NMR (300 MHz, 25 °C, CDCl₃): δ = 146.52, 144.41, 127.70, 125.95, 77.2, 34.24, 32.22, 31.41.

IR (solid phase, ν cm⁻¹) = 3165m, 2953s, 1738m, 1481s, 1461s, 1240s.

MS m/z observed 649.4258, theoretical 649.4251 [M + H]⁺.

25,26,27,28-Tetrahydroxycalix[4]arene, **2**^{28b}



To a 1 L 3-necked round-bottomed flask (rbf) was added compound **1** (100 g, 235.7 mmol), AlCl₃ (202.70 g, 1.5 mol), PhOH (15.1g, 160.8 mmol) and toluene (1 L) were added and the solution left to stir under nitrogen at RT for 3 hours. The solution was quenched with ice and DCM (750 mL) was added to extract the product. The organic layer was washed with 1M HCl (300 mL), water (300 mL) and dried over MgSO₄. After removing MgSO₄ by filtration, the solvent

was then removed under reduced pressure to yield compound **2** (44.60 g, 68%) as pale yellow crystals.

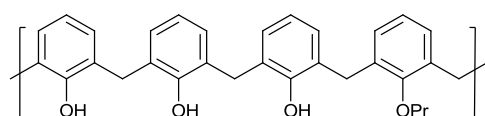
¹H NMR (300 MHz, 25 °C, CDCl₃): δ = 10.23 (s, 4H, OH), 7.09 (d, *J* = 12.1 Hz, 8H, ArH), 6.76 (t, *J* = 8.8 Hz, 4H, ArH), 4.29 (broad s, 4H, ArCH₂Ar), 3.59 (broad s, 4H, ArCH₂Ar).

¹³C NMR (300 MHz, 25 °C, CDCl₃): δ = 148.81, 129.02, 128.28, 122.28, 31.74.

IR (solid phase, ν cm⁻¹) = 3155w, 2972m, 1594m, 1463s, 1447s.

MS *m/z* observed 425.1748, theoretical 425.1747 [M + H]⁺.

25-Propoxy-26,27,28-trihydroxycalix[4]arene, **3**¹⁷



A sample of C[4] **2** (2.12 g, 5.00 mmol) and sodium methoxide (0.32 g, 5.90 mmol) was heated at reflux in 150 mL of CH₃CN for 30 min to monodeprotonate compound **2**. An excess amount of iodopropane (1.20 mL, 12.3 mmol) was added and the mixture was heated at reflux for 24 hours. The reaction mixture was neutralised with 1M HCl and left to stir for an hour. The product was extracted with CHCl₃, washed with water (2 X 100 mL) and dried over MgSO₄. The solvent was removed under reduced pressure to afford a yellow oil, which was purified by chromatography on silica (petrol/DCM 3:1) to afford compound **3** as an off-white solid (0.91 g, 39%).

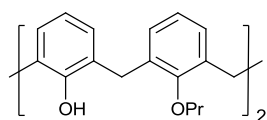
¹H NMR (300 MHz, 25 °C, CDCl₃): δ = 9.65 (s, 1H, OH), 9.34 (s, 2H, OH), 6.98 (m, 8H, ArH), 6.79 (t, *J* = 4.5, 1H, ArH), 6.61 (m, 3H, ArH), 4.30 (d, *J* = 13.2, 2H, ArCH₂Ar), 4.18 (d, *J* = 13.2, 2H, ArCH₂Ar), 4.06 (t, *J* = 6.4, 2H, CH₂CH₂), 3.39 (d, *J* = 13.4, 4H, ArCH₂Ar), 2.12 (m, 2H, CH₂CH₂), 1.24 (t, *J* = 6.6, 3H, CH₂CH₃).

¹³C NMR (300 MHz, 25 °C, CDCl₃): δ = 151.47, 150.84, 149.25, 134.28, 129.35, 128.87, 128.83, 128.77, 128.49, 128.44, 126.11, 121.98, 120.94, 79.06, 77.24, 31.94, 31.48, 23.31, 10.70.

IR (solid phase, ν cm⁻¹) = 3318w, 2966m, 2873m, 1593w, 1462s, 1250s, 1077m.

MS *m/z* observed 466.6098, theoretical 466.6103 [M + H]⁺.

25,27-Dipropoxy-26,28-dihydroxycalix[4]arene, **4**^{18,34}



To a suspension of C[4] **2** (6.14 g, 14.45 mmol) in CH₃CN (300 mL) was added iodopropane (0.06 mol) and K₂CO₃ (0.06 mol) and the reaction mixture was stirred under reflux for 24 hours. Once cooled the solvent was removed under reduced pressure and the residue quenched with 100 mL HCl (10%) and 100 mL DCM. The organic phase was separated and washed twice with water before being dried over MgSO₄. The solvent was evaporated to afford a crude solid which was recrystallised from DCM/methanol to yield compound **4** as an off-white solid (5.34 g, 73%).

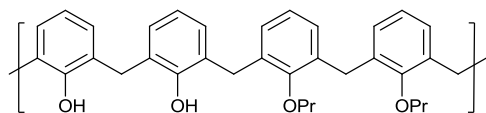
¹H NMR (300 MHz, 25 °C, CDCl₃): δ = 8.32 (s, 2H, OH), 7.10 (d, *J* = 7.5 Hz, 4H, ArH), 6.95 (d, *J* = 7.5 Hz, 4H, ArH), 6.78 (t, *J* = 7.5 Hz, 2H, ArH), 6.70 (t, *J* = 7.5 Hz, 2H, ArH), 4.38 (d, *J* = 12.9 Hz, 4H, ArCH₂Ar), 4.02 (t, *J* = 6.2 Hz, 4H, OCH₂CH₂CH₃), 3.43 (d, *J* = 12.9 Hz, 4H, ArCH₂Ar), 2.13 (m, 4H, OCH₂CH₂CH₃), 1.36 (t, *J* = 7.3 Hz, OCH₂CH₂CH₃).

¹³C NMR (300 MHz, 25 °C, CDCl₃): δ = 153.39, 151.92, 133.52, 128.93, 128.43, 128.18, 125.30, 118.97, 78.34, 31.45, 23.52, 10.95.

IR (solid phase, ν cm⁻¹) = 3286w, 2957m, 2923m, 1592w, 1465s, 1107s, 1067s.

MS *m/z* observed 509.2679, 526.2940, theoretical 509.2686 [M + H]⁺, 526.2952 [M + NH₄]⁺.

25,26-Dipropoxy-27,28-dihydroxycalix[4]arene, **5**^{20,21}



C[4] **2** (5.00 g, 11.78 mmol), DMF (40 mL) and NaH (60%, 1.70 g, 42.5 mmol) were added to an rbf and stirred at RT for 15 mins. Iodopropane (2.30 mL, 24.0 mmol) was then added and the solution was stirred for 2 hours at RT. MeOH was added to quench the reaction and the solvent was removed under reduced pressure. The residue was dissolved in 75 mL DCM, washed with 1M HCl (25 mL), water and dried over MgSO₄. The solvent was removed under reduced pressure to afford a yellow oil which was purified by chromatography on silica (petrol/DCM 3:2) to afford compound **5** (rf 0.6) as colourless crystals (2.63 g, 44%).

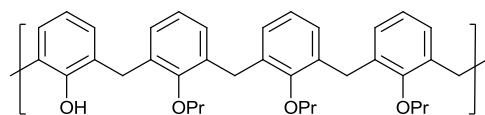
¹H NMR (300 MHz, 25 °C, CDCl₃): δ = 8.90 (s, 2H, OH), 6.98 (d, *J* = 7.8, 2H, ArH), 6.91 (d, *J* = 7.8, 6H, ArH), 6.72 (t, *J* = 6.8, 2H, ArH), 6.58 (t, *J* = 6.8, 2H, ArH), 4.49 (d, *J* = 13.4, 1H, ArCH₂Ar), 4.28 (d, *J* = 13.4, 3H, ArCH₂Ar), 4.03 (q, *J* = 4.4, 2H, CH₂CH₂), 3.87 (q, *J* = 4.4, 2H, CH₂CH₂), 3.34 (d, *J* = 12.8, 4H, ArCH₂Ar), 2.08 (m, 4H, CH₂CH₂), 1.05 (t, *J* = 5.8, 6H, CH₂CH₃).

¹³C NMR (300 MHz, 25 °C, CDCl₃): δ = 153.52, 151.24, 134.70, 134.17, 129.47, 129.16, 129.10, 128.83, 128.81, 128.07, 124.75, 120.58, 78.33, 31.96, 31.83, 30.03, 23.31, 10.38.

IR (solid phase, ν cm⁻¹) = 3318w, 2966m, 2873m, 1591w, 1454s, 1065s.

MS *m/z* observed 509.2674, 526.2936, theoretical 509.2686 [M + H]⁺, 526.2952 [M + NH₄]⁺.

25-Hydroxy-26,27,28-tripropoxycalix[4]arene, **6**



This was prepared by the same route to form compound **5**. The crude product was purified by chromatography on silica (petrol/DCM 3:2) to afford compound **6** (rf 0.7) as an off-white solid (1.23 g, 22%).

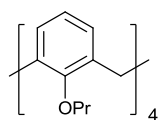
¹H NMR (300 MHz, 25 °C, CDCl₃): δ = 7.08 (d, *J* = 6.8 Hz, 2H, ArH), 7.04 (d, *J* = 6.8 Hz, 2H, ArH), 6.82 (t, *J* = 7.0 Hz, 1H, ArH), 6.68 (t, *J* = 7.0 Hz, 1H, ArH), 6.29 (m, 6H, ArH), 4.60 (s, 1H, OH), 4.32 (dd, *J* = 13.0 Hz, 4H, ArCH₂Ar), 3.72 (m, 2H, CH₂CH₂), 3.62 (t, *J* = 5.8 Hz, 4H, CH₂CH₂), 3.16 (dd, *J* = 13.0 Hz, 4H, ArCH₂Ar), 2.20 (m, 2H, CH₂CH₂), 1.81 (m, 4H, CH₂CH₂), 1.03 (t, *J* = 6.2 Hz, 3H, CH₂CH₃), 0.80 (m, 6H, CH₂CH₃).

¹³C NMR (300 MHz, 25 °C, CDCl₃): δ = 156.91, 154.43, 153.33, 137.22, 133.44, 132.68, 131.26, 129.20, 128.42, 127.90, 127.79, 123.02, 122.98, 119.30, 30.79, 23.48, 22.37, 10.87, 9.63.

IR (solid phase, ν cm⁻¹) = 3540w, 2960w, 2922m, 2872m, 1590w, 1456s, 1200s.

MS *m/z* observed 551.3150, theoretical 551.3156 [M + H]⁺.

25,26,27,28-Tetrapropoxycalix[4]arene, **7**¹⁸



C[4] **2** (4.00 g, 9.40 mmol) was added to a solution of NaH (60%, 3.20 g, 80.0 mmol) in DMF (80 mL) and the mixture was stirred for 30 mins. Next the iodopropane (80.0 mmol) was added and the stirred solution was heated at 80 °C for one hour. The solution was quenched with MeOH and the solvents removed under reduced pressure. The residue was washed with water and left to dry. The crude product were recrystallised from hot acetone to afford compound **7** as a white solid (3.64 g, 66%).

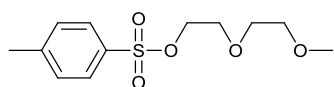
¹H NMR (300 MHz, 25 °C, CDCl₃): δ = 6.59 (m, 12H, ArH), 4.48 (d, *J* = 12.9 Hz, 4H, ArCH₂Ar), 3.86 (t, *J* = 6.2 Hz, 8H, OCH₂CH₂CH₃), 3.16 (d, *J* = 12.9 Hz, 4H, ArCH₂Ar), 1.92 (m, 8H, OCH₂CH₂CH₃), 1.01 (t, *J* = 7.3 Hz, 12H, OCH₂CH₂CH₃).

¹³C NMR (300 MHz, 25 °C, CDCl₃): δ = 156.61, 135.17, 128.13, 121.88, 31.01, 23.28, 10.36.

IR (solid phase, ν cm⁻¹) = 2965m, 2921m, 2874m, 1454s, 1383m, 1192s.

MS *m/z* observed 610.3883, theoretical 610.3891 [M + NH₄]⁺.

2-(2-Methoxyethoxy)ethyl tosylate, **8**²²



To a solution of diethylene glycol monomethyl ether (100.05 g, 0.83 mol) in 345 mL THF, cooled to 0 °C, was added NaOH (56.70 g, 1.42 mol) dissolved in water (345 mL) with vigorous stirring. To this mixture was added drop-wise a solution of tosyl chloride (190.44 g, 0.99 mol) in THF (345 mL) over an hour at this temperature. Once complete the reaction was raised to RT and stirred under nitrogen overnight. The aqueous layer was extracted twice with diethyl ether (250 mL) and the combined organic phase was washed with 1 N aqueous NaOH and dried over MgSO₄. The solvent was removed under reduced pressure to afford compound **8** as a viscous liquid (192.60 g, 84%).

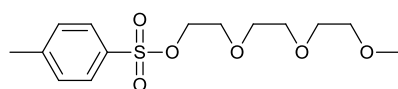
¹H NMR (300 MHz, 25 °C, CDCl₃): δ = 7.79 (d, *J* = 8.3 Hz, 2H, ArH), 7.33 (d, *J* = 8.3 Hz, 2H, ArH), 4.17 (m, 2H, CH₂OSO₂), 3.69 (m, 2H, OCH₂CH₂O), 3.58 (m, 6H, OCH₂CH₂O), 3.48 (m, 2H, OCH₂CH₂O), 3.35 (s, 3H, OCH₃), 2.45 (s, 3H, CH₃).

^{13}C NMR (300 MHz, 25 °C, CDCl_3): δ = 144.84, 132.85, 129.82, 127.82, 71.65, 70.42, 69.31, 68.52, 58.80, 21.46.

IR (solid phase, $\nu \text{ cm}^{-1}$) = 2895m, 1598m, 1354s, 1172s, 1096s.

MS m/z observed 275.0948, theoretical 275.0948 $[\text{M} + \text{H}]^+$.

Triethylene glycol monomethyl ether tosylate, **9**²³



Triethylene glycol monomethyl ether (100.00 g, 0.61 mol) was taken in 350 mL THF and the contents

cooled in an ice bath. To the cooled solution, NaOH (73.00 g, 1.83 mol) in 350 mL water was added. Tosyl chloride (150 g, 0.77 mol) in THF (250 mL) was added slowly using a dropping funnel over 2 hours, after which time the reaction mixture was allowed to warm to RT and stirred overnight. The organic layer was collected and the aqueous layer was washed with diethyl ether (2 X 250 mL). The combined organic layer was washed with 10% NaOH solution, followed by brine and water. The solution was dried over Na_2SO_4 , filtered and concentrated to obtain the pure product **9** as a viscous liquid (187.1 g, 96%).

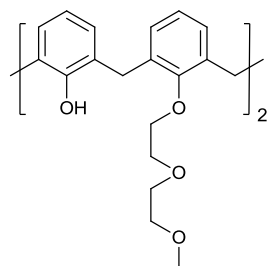
^1H NMR (300 MHz, 25 °C, CDCl_3): δ = 7.80 (d, J = 8.2 Hz, 2H, ArH), 7.45 (d, J = 8.4 Hz, 2H, ArH), 4.16 (t, 2H, CH_2OSO_2), 3.70-3.50 (m, 10H, $\text{OCH}_2\text{CH}_2\text{O}$), 3.37 (s, 3H, OCH_3), 2.45 (s, 3H, CH_3).

^{13}C NMR (300 MHz, 25 °C, CDCl_3): δ = 144.82, 132.91, 129.82, 127.88, 71.81, 70.61, 70.41, 69.28, 68.57, 58.89, 21.55.

IR (solid phase, $\nu \text{ cm}^{-1}$) = 2898m, 2873m, 1598m, 1350s, 1173s, 1094s.

MS m/z observed 336.1471, theoretical 336.1475 $[\text{M} + \text{NH}_4]^+$.

25,27-Di(monomethyl diethylene glycol)-dihydroxy-26,28-dihydroxycalix[4]arene, **10**²⁴



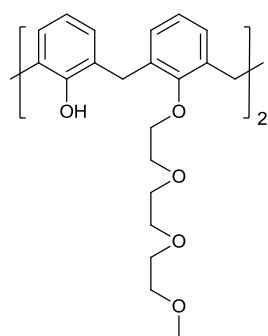
C[4] 2 (2.01 g, 4.73 mmol) and K_2CO_3 (0.66 g, 4.71 mmol) were dissolved in 100 mL CH_3CN and stirred at RT for one day. A solution of the tosylate of 2-(2-methoxyethoxy)-ethanol **8** (2.59 g, 9.42 mmol) in 50 mL CH_3CN was added drop-wise and the solution was heated at reflux for 7 days. After evaporation of the

solvent the residue was dissolved in DCM, and the solution neutralised with 1N HCl. The organic phase was separated and dried over Na_2SO_4 . The filtrate was evaporated to

¹H NMR (300 MHz, 25 °C, CDCl₃): δ = 7.74 (s, 2H, OH), 7.05 (d, *J* = 7.4 Hz, 4H, ArH), 6.88 (d, *J* = 7.3 Hz, 4H, ArH), 6.68 (m, 4H, ArH), 4.44 (d, *J* = 13.0 Hz, 4H, ArCH₂Ar), 4.45 (t, *J* = 4.6 Hz, 4H, ArOCH₂CH₂O), 4.20 (t, *J* = 4.6 Hz, 4H, ArOCH₂CH₂O), 4.46 (t, *J* = 4.6 Hz, 4H, ArOCH₂CH₂O), 4.01 (t, *J* = 4.6 Hz, 4H, ArOCH₂CH₂O), 3.85 (t, *J* = 4.6 Hz, 4H, OCH₂CH₂OCH₃), 3.62 (t, *J* = 4.6 Hz, 4H, OCH₂CH₂OCH₃), 3.37 (s, 6H, OCH₃), 3.36 (d, *J* = 13.0 Hz, 4H, ArCH₂Ar).

IR (solid phase, ν cm^{-1}) = 3349w, 2917w, 2225w, 1605w, 1464s, 1454s, 1201m.

25,27-Di(monomethyl triethylene glycol)-dihydroxy-26,28-dihydroxycalix[4]arene, **11**²⁴

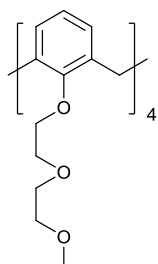


¹H NMR (300 MHz, 25 °C, CDCl₃): δ = 7.68 (s, 2H, OH), 6.99 (d, *J* = 7.3 Hz, 4H, ArH), 6.78 (d, *J* = 7.2 Hz, 4H, ArH), 6.56 (m, 4H, ArH), 4.34 (d, *J* = 13.0 Hz, 4H, ArCH₂Ar), 4.10 (t, *J* = 4.6 Hz, 4H, ArOCH₂CH₂O), 3.90 (t, *J* = 4.6 Hz, 4H, ArOCH₂CH₂O), 3.75 (t, *J* = 4.6 Hz, 4H, OCH₂CH₂O), 3.63 (t, *J* = 4.6 Hz, 4H, OCH₂CH₂O), 3.58 (t, *J* = 4.6 Hz, 4H, OCH₂CH₂OCH₃), 3.40 (t, *J* = 4.6 Hz, 4H, OCH₂CH₂OCH₃), 3.21 (s, 6H, OCH₃), 3.25 (d, *J* = 13.0 Hz, 4H, ArCH₂Ar).

IR (solid phase, v cm^{-1}) = 3318w, 2866m, 2225w, 1592w, 1467s, 1453s, 1081s.

MS m/z observed 734.3896, theoretical 734.3899 $[M + NH_4]^+$.

Tetrakis(monomethyl diethylene glycol)calix[4]arene, **12**²⁵



To a suspension of C[4] **2** (2.00 g, 4.71 mmol) in DMF (100 mL) was added NaH (60%, 1.51 g, 0.04 mol) and the solution stirred for 20 mins before tosylate **8** (15.51 g, 0.06 mol) dissolved in DMF (10 mL) was added drop-wise. Once addition was complete the reaction was heated at reflux for 3 days. MeOH was added to kill any excess NaH and the solvent was removed under reduced pressure to afford an orange solid. The oil was extracted into $CHCl_3$ and washed with water three times. The organic layer was separated, dried over $MgSO_4$ and the solvent evaporated to give the crude product, which was purified by gradient elution chromatography on silica (chloroform/acetone 5:1) to afford compound **12** as a yellow oil (0.59 g, 20%).

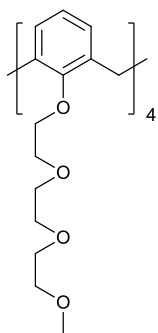
1H NMR (300 MHz, 25 °C, $CDCl_3$): δ = 6.50 (m, 12H, ArH), 4.38 (d, J = 12.9 Hz, 4H, ArCH₂Ar), 4.08 (t, J = 5.4 Hz, 8H, ArOCH₂CH₂O), 3.80 (t, J = 5.4 Hz, 8H, ArOCH₂CH₂O), 3.55 (t, J = 4.2 Hz, 8H, OCH₂CH₂O), 3.47 (t, J = 4.2 Hz, 8H, OCH₂CH₂O), 3.31 (s, 12H, OCH₃), 3.15 (d, J = 13.0 Hz, 4H, ArCH₂Ar).

^{13}C NMR (300 MHz, 25 °C, $CDCl_3$): δ = 156.25, 135.01, 128.19, 122.23, 72.87, 72.04, 70.39, 59.05, 30.90.

IR (solid phase, ν cm^{-1}) = 2870m, 2817w, 1585w, 1449s, 1196s, 1107s, 1088s.

MS m/z observed 850.4716, theoretical 850.4736 $[M + NH_4]^+$.

Tetrakis(monomethyl triethylene glycol)calix[4]arene, **13**²⁵



This was prepared by a route similar to compound **12** using triethylene glycol monomethyl ether tosylate, **9**. The crude product was purified by gradient elution chromatography on silica (chloroform/acetone 5:1) to afford compound **13** as a yellow oil (1.18 g, 25%).

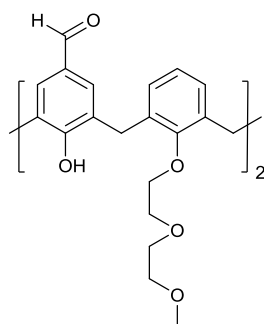
¹H NMR (300 MHz, 25 °C, CDCl₃): δ = 6.51 (m, 12H, ArH), 4.42 (d, *J* = 13.0 Hz, 4H, ArCH₂Ar), 4.15 (t, *J* = 5.2 Hz, 8H, OCH₂CH₂O), 3.81 (t, *J* = 5.2 Hz, 8H, OCH₂CH₂O), 3.55 (t, *J* = 4.6 Hz, 8H, OCH₂CH₂O), 3.47 (t, *J* = 4.6 Hz, 8H, OCH₂CH₂O), 3.56 (m, 24H, OCH₂CH₂O), 3.49 (t, *J* = 4.8 Hz, 8H, OCH₂CH₂O), 3.29 (s, 12H, OCH₃), 3.14 (d, *J* = 13.0 Hz, 4H, ArCH₂Ar).

¹³C NMR (300 MHz, 25 °C, CDCl₃): δ = 156.30, 135.00, 128.17, 122.19, 72.92, 72.49, 71.96, 70.67, 70.58, 70.51, 70.45, 70.34, 61.76, 59.02, 30.92.

IR (solid phase, ν cm⁻¹) = 2868m, 1585w, 1449m, 1198m, 1103s, 1088s.

MS *m/z* observed 1026.4801, theoretical 1026.4824 [M + NH₄]⁺.

Di(monomethyl diethylene glycol)-di-*p*-formylcalix[4]arene, **14**



Compound **10** (1.00 g, 1.59 mmol) was dissolved in 20 mL CHCl₃ and the flask was flushed with nitrogen. The solution was cooled to -15 °C before the rapid addition of SnCl₄ (1.92 mL, 0.02 mol) and 1,1-dichloromethyl methyl ether (0.38 mL, 4.14 mmol), and the reaction was allowed to stir for 30 mins warming to RT. The solution was quenched with water and left to stir overnight. The organic layer was separated, washed with water (3 X 100 mL) and dried over MgSO₄. The solvents were removed under reduced pressure to afford compound **14** as an orange oil (1.00 g, 92%).

¹H NMR (300 MHz, 25 °C, CDCl₃): δ = 9.72 (s, 2H, CHO), 8.78 (s, 2H, OH), 7.59 (s, 4H, ArH), 6.88 (d, *J* = 7.2 Hz, 4H, ArH), 6.71 (t, *J* = 7.0 Hz, 2H, ArH), 4.38 (d, *J* = 13.0 Hz, 4H, ArCH₂Ar), 4.16 (t, *J* = 4.4 Hz, 4H, OCH₂CH₂O), 3.92 (t, *J* = 4.4 Hz, 4H, OCH₂CH₂O), 3.74 (t, *J* = 4.6 Hz, 4H, OCH₂CH₂O), 3.51 (t, *J* = 4.6 Hz, 4H, OCH₂CH₂O), 3.40 (d, *J* = 13.0 Hz, 4H, ArCH₂Ar), 3.28 (s, 6H, OCH₃).

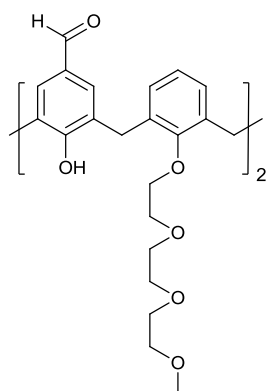
¹³C NMR (300 MHz, 25 °C, CDCl₃): δ = 190.91, 159.57, 151.68, 132.49, 132.39, 132.08, 130.92, 129.43, 128.73, 128.63, 128.52, 125.71, 76.62, 75.59, 72.03, 70.95, 69.97, 59.09, 31.03.

IR (solid phase, ν cm⁻¹) = 3288w, 3014w, 2930w, 1680s, 1588m, 1249s.

Anal. Calcd. For C₄₀H₄₄O₁₀: C, 70.16; H, 6.48. *Found*: C, 41.01; H, 3.62; loses weight on balance quickly.

MS *m/z* observed 685.3020, 702.3274, theoretical 685.3007 [M + H]⁺, 702.3273 [M + NH₄]⁺.

Di(monomethyl triethylene glycol)-*tris-p*-formylcalix[4]arene, **15**



This was prepared by a route similar to compound **14** using compound **11**. Compound **15** was formed as an orange oil (0.92 g, 85%).

¹H NMR (300 MHz, 25 °C, CDCl₃): δ = 9.70 (s, 2H, CHO), 8.75 (s, 2H, OH), 7.56 (s, 4H, ArH), 6.84 (d, *J* = 7.2 Hz, 4H, ArH), 6.70 (t, *J* = 7.5 Hz, 2H, ArH), 4.39 (d, *J* = 13.0 Hz, 4H, ArCH₂Ar), 4.18 (t, *J* = 4.6 Hz, 4H, OCH₂CH₂O), 3.90 (t, *J* = 4.6 Hz, 4H, OCH₂CH₂O), 3.78 (t, *J* = 4.4 Hz, 4H, OCH₂CH₂O), 3.65 (t, *J* = 4.4 Hz, 4H, OCH₂CH₂O), 3.48 (t, *J* = 4.6 Hz, 4H, OCH₂CH₂O), 3.37 (m, 8H, overlap ArCH₂Ar and OCH₂CH₂O), 3.25 (s, 6H, OCH₃).

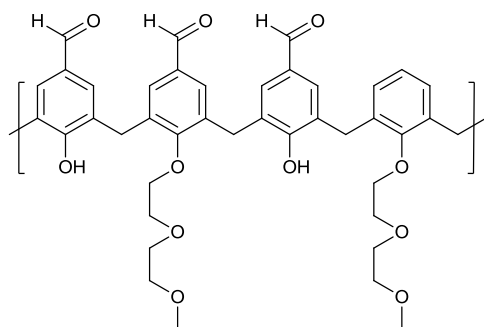
¹³C NMR (300 MHz, 25 °C, CDCl₃): δ = 189.84, 158.54, 150.63, 131.47, 129.89, 128.38, 127.60, 127.48, 124.67, 76.24, 74.58, 70.85, 70.04, 69.69, 69.60, 68.94, 57.96, 29.98.

IR (solid phase, ν cm⁻¹) = 3289w, 3009w, 2876m, 1680s, 1588s, 1131s, 1099s.

Anal. Calcd. For C₄₄H₅₂O₁₂: C, 68.38; H, 6.78. *Found*: C, 54.61; H, 5.35; loses weight on balance quickly.

MS *m/z* observed 773.3540, 790.3796, theoretical 773.3532 [M + H]⁺, 790.3797 [M + NH₄]⁺.

Di(monomethyl diethylene glycol)-*tris-p*-formylcalix[4]arene, **16**



Compound **10** (0.75 g, 1.19 mmol) and HMTA (6.02 g, 0.04 mol) were dissolved in TFA (40 mL) and the solution was heated at reflux for 3 days. After cooling to RT, the solution was poured into 100 mL ice water. The aqueous solution was extracted into 100 mL DCM and

left to stir for 1 hour. The organic layer was separated, washed with water (3 X 100 mL) and dried over MgSO₄. The solvents were removed under reduced pressure to afford an orange oil. This was subject to column chromatography on silica (EtOAc/PE 3:1) to afford compound **16** as an orange oil (0.14 g, 14%).

¹H NMR (300 MHz, 25 °C, CDCl₃): δ = 9.84 (s, 2H, CHO), 9.69 (s, 1H, CHO), 8.66 (s, 2H, OH), 7.70 (d, J = 4.2 Hz, 4H, ArH), 7.48 (s, 2H, ArH), 6.97 (d, J = 7.2 Hz, 2H, ArH), 6.80 (t, J = 7.3 Hz, 1H, ArH), 4.55 (d, J = 12.8 Hz, 2H, ArCH₂Ar), 4.46 (d, J = 12.8 Hz, 2H, ArCH₂Ar), 4.27 (m, 4H, OCH₂CH₂O), 4.04 (m, 4H, OCH₂CH₂O), 3.84 (m, 4H, OCH₂CH₂O), 3.61 (m, 4H, OCH₂CH₂O), 3.51 (d, J = 13.0 Hz, 4H, ArCH₂Ar), 3.33 (s, 6H, OCH₃).

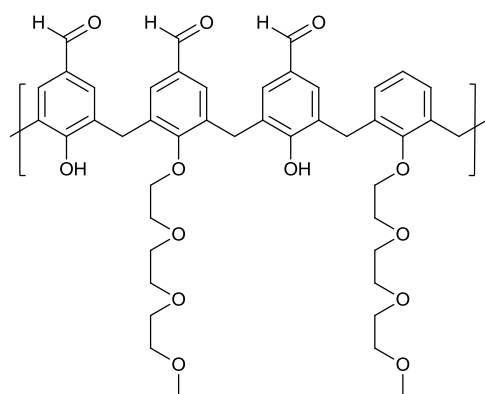
¹³C NMR (300 MHz, 25 °C, CDCl₃): δ = 190.06, 189.81, 158.32, 150.46, 132.77, 132.56, 131.28, 130.19, 130.09, 129.93, 128.53, 127.70, 127.51, 126.86, 124.82, 74.80, 74.64, 70.98, 69.90, 68.86, 58.03, 30.01.

IR (solid phase, ν cm⁻¹) = 3291w, 2989w, 2876m, 1680s, 1654s, 1580s, 1128s, 1087s.

Anal. Calcd. For C₄₁H₄₄O₁₁: C, 69.09; H, 6.22. **Found:** C, 55.74; H, 5.21; loses weight on balance quickly.

MS m/z observed 713.8698, theoretical 713.8695 [M + H]⁺.

Di(monomethyl triethylene glycol)-*tris-p*-formylcalix[4]arene, **17**



This was prepared by a route similar to compound **16** using compound **11**. The crude product was purified by gradient elution chromatography on silica (EtOAc/PE 3:1) to afford compound **17** as an orange oil (0.17 g, 15%).

¹H NMR (300 MHz, 25 °C, CDCl₃): δ = 9.82 (s, 2H, CHO), 9.67 (s, 1H, CHO), 8.68 (s, 2H, OH), 7.68 (d, J = 4.0 Hz, 4H, ArH), 7.47 (s, 2H, ArH), 6.95 (d, J = 7.2 Hz, 2H, ArH), 6.78 (t, J = 7.3 Hz, 1H, ArH), 4.55 (d, J = 12.8 Hz, 2H, ArCH₂Ar), 4.46 (d, J = 12.8 Hz, 2H, ArCH₂Ar), 4.24 (m, 4H, OCH₂CH₂O), 4.02 (m, 4H, OCH₂CH₂O), 3.83

(m, 4H, OCH₂CH₂O), 3.72 (m, 4H, OCH₂CH₂O), 3.59 (m, 4H, OCH₂CH₂O), 3.50 (d, J = 13.0 Hz, 4H, ArCH₂Ar), 3.44 (m, 4H, OCH₂CH₂O), 3.32 (s, 6H, OCH₃).

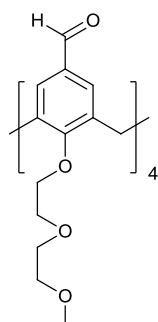
¹³C NMR (300 MHz, 25 °C, CDCl₃): δ = 190.04, 189.74, 158.46, 158.33, 156.15, 150.46, 132.81, 132.56, 132.34, 131.40, 131.31, 130.17, 130.07, 129.92, 128.50, 127.70, 127.61, 127.57, 127.53, 127.11, 126.88, 124.79, 74.86, 74.68, 70.84, 70.03, 70.01, 69.68, 69.59, 68.88, 57.95, 29.99, 29.95, 29.88.

IR (solid phase, ν cm⁻¹) = 3290w, 2992w, 2880m, 1678s, 1652s, 1583s, 1134s, 1082s.

Anal. Calcd. For C₄₅H₅₂O₁₃: C, 67.49; H, 6.54. *Found*: C, 54.34; H, 5.38; loses weight on balance quickly.

MS m/z observed 801.9701, theoretical 801.9687 [M + H]⁺.

Tetrakis(monomethyl diethylene glycol)-tetra-*p*-formylcalix[4]arene, **18**²⁵



A solution of compound **12** (0.59 g, 0.71 mmol), HMTA (3.60 g, 0.03 mol) in 30 mL TFA was heated at reflux for three days. After cooling to RT, the solution was poured into 100 mL ice water. The aqueous solution was extracted with DCM. The organic layer was separated, washed with water (3 X 100 mL) and dried over MgSO₄. The solvents were removed under reduced pressure to afford a yellow oil. This was subject to gradient column chromatography on silica (up to CHCl₃/acetone 5:1) to afford compound **18** as a yellow solid (0.25 g, 38%).

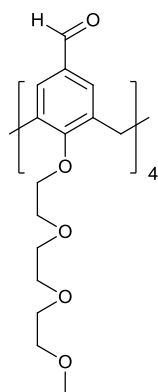
¹H NMR (300 MHz, 25 °C, CDCl₃): δ = 9.51 (s, 4H, CHO), 7.09 (s, 8H, ArH), 4.52 (d, J = 12.9 Hz, 4H, ArCH₂Ar), 4.17 (t, J = 4.8 Hz, 8H, OCH₂CH₂O), 3.72 (t, J = 4.8 Hz, 8H, OCH₂CH₂O), 3.54 (t, J = 4.6 Hz, 8H, OCH₂CH₂O), 3.46 (t, J = 4.6 Hz, 8H, OCH₂CH₂O), 3.28 (d, J = 12.9 Hz, 4H, ArCH₂Ar), 3.22 (s, 12H, OCH₃).

¹³C NMR (300 MHz, 25 °C, CDCl₃): δ = 190.29, 160.77, 134.70, 130.49, 129.17, 72.68, 70.95, 69.40, 69.33, 58.01, 29.91, 29.86.

IR (solid phase, ν cm⁻¹) = 2873m, 2726w, 1684s, 1596m, 1289m, 1106s, 1040s.

MS m/z observed 962.4523, theoretical 962.4533 [M + NH₄]⁺.

Tetrakis(monomethyl triethylene glycol)-tetra-*p*-formylcalix[4]arene, **19**²⁵



This was prepared by a route similar to compound **18** using compound **13**. The crude product was purified by gradient elution chromatography on silica (up to CHCl₃/acetone 5:1) to afford compound **19** as a yellow solid (0.56 g, 50%).

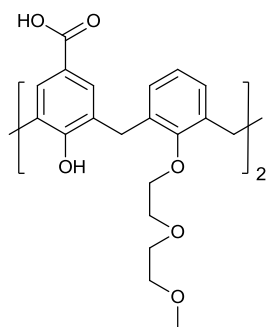
¹H NMR (300 MHz, 25 °C, CDCl₃): δ = 9.49 (s, 4H, CHO), 7.02 (s, 8H, ArH), 4.50 (d, *J* = 13.0 Hz, 4H, ArCH₂Ar), 4.11 (t, *J* = 4.8 Hz, 8H, OCH₂CH₂O), 3.78 (t, *J* = 4.8 Hz, 8H, OCH₂CH₂O), 3.54 (m, 24H, OCH₂CH₂O), 3.44 (m, 8H, OCH₂CH₂O), 3.30 (s, 12H, OCH₃), 3.27 (d, *J* = 13.0 Hz, 4H, ArCH₂Ar).

¹³C NMR (300 MHz, 25 °C, CDCl₃): δ = 190.26, 160.80, 134.68, 130.49, 129.17, 72.74, 70.91, 69.61, 69.56, 69.45, 69.41, 57.99, 29.87.

IR (solid phase, ν cm⁻¹) = 2870m, 2730w, 1686s, 1600m, 1289m, 1244m, 1110s, 1054s.

MS *m/z* observed 1138.6923, theoretical 1138.6934 [M + NH₄]⁺.

Di(monomethyl diethylene glycol)-tetra-*p*-carboxylatocalix[4]arene, **20**



To a solution of compound **14** (1.00 g, 1.47 mmol) in DCM (10 mL) and acetone (30 mL) was added a solution of NaClO₂ (0.53 g, 5.86 mmol) in water (3 mL) and sulfamic acid (0.57 g, 5.86 mmol) in water (3 mL). The solution was stirred at RT for one day. The solvents were removed under reduced pressure to afford a yellow solid, which was taken-up in 1 M HCl, filtered and

dried to yield compound **20** as a yellow solid (0.40 g, 38%).

¹H NMR (300 MHz, 25 °C, DMSO-*d*⁶): δ = 12.44 (bs, 2H, COOH), 8.89 (s, 2H, CHO), 7.82 (s, 4H, ArH), 7.10 (d, *J* = 7.2 Hz, 4H, ArH), 6.86 (t, *J* = 7.5 Hz, 2H, ArH), 4.36 (d, *J* = 13.2 Hz, 4H, ArCH₂Ar), 4.21 (m, 4H, OCH₂CH₂O), 3.98 (m, 4H, OCH₂CH₂O), 3.81 (m, 4H, OCH₂CH₂O), 3.62 (m, 8H, overlap of OCH₂CH₂O and ArCH₂Ar), 3.29 (s, 6H, OCH₃).

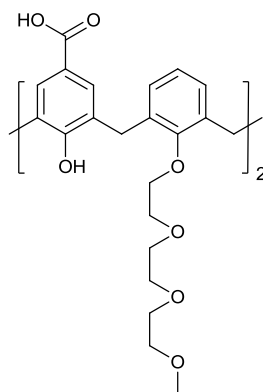
^{13}C NMR (300 MHz, 25 °C, DMSO- d_6): δ = 167.31, 157.18, 151.71, 133.20, 130.23, 129.05, 127.65, 121.05, 71.24, 69.91, 69.24, 58.03, 30.09.

IR (solid phase, ν cm^{-1}) = 3235w, 2925m, 2360w, 1660s, 1602s, 1451m, 1075s.

Anal. Calcd. For $\text{C}_{40}\text{H}_{44}\text{O}_{12}$: C, 67.03; H, 6.19. *Found*: C, 66.75; H, 6.04.

MS m/z observed 734.3169, theoretical 734.3171 $[\text{M} + \text{NH}_4]^+$.

Di(monomethyl triethylene glycol)-tetra-*p*-carboxylatocalix[4]arene, **21**



This was prepared by a route similar to compound **20** using compound **15**. Compound **21** was obtained as a yellow solid (0.56 g, 58%).

^1H NMR (300 MHz, 25 °C, DMSO- d_6): δ = 12.42 (bs, 2H, COOH), 8.92 (s, 2H, CHO), 7.86 (s, 4H, ArH), 7.11 (d, J = 7.4 Hz, 4H, ArH), 6.88 (t, J = 7.4 Hz, 2H, ArH), 4.38 (d, J = 13.0 Hz, 4H, ArCH_2Ar), 4.22 (m, 4H, $\text{OCH}_2\text{CH}_2\text{O}$), 3.99 (m, 4H, $\text{OCH}_2\text{CH}_2\text{O}$), 3.82 (m, 4H, $\text{OCH}_2\text{CH}_2\text{O}$), 3.68 (m, 4H, $\text{OCH}_2\text{CH}_2\text{O}$), 3.60 (m, 12H, overlap of 2 X $\text{OCH}_2\text{CH}_2\text{O}$ and ArCH_2Ar), 3.25 (s, 6H, OCH_3).

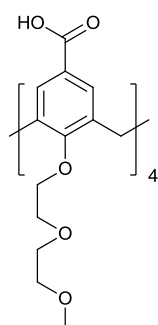
^{13}C NMR (300 MHz, 25 °C, DMSO- d_6): δ = 167.27, 157.17, 151.71, 133.21, 130.23, 129.05, 127.63, 121.08, 71.12, 70.23, 69.76, 69.56, 69.29, 57.92, 30.09.

IR (solid phase, ν cm^{-1}) = 3231w, 2879m, 2360w, 1664s, 1590m, 1453m, 1074s.

Anal. Calcd. For $\text{C}_{44}\text{H}_{52}\text{O}_{14}$: C, 65.66; H, 6.51. *Found*: C, 65.04; H, 6.37.

MS m/z observed 822.3693, theoretical 822.3695 $[\text{M} + \text{NH}_4]^+$.

Tetrakis(monomethyl diethylene glycol)-tetra-*p*-carboxylatocalix[4]arene, **22**²⁵



To a solution of compound **18** (0.48 g, 0.50 mmol) in DCM (5 mL) and acetone (15 mL) was added a solution of sulfamic acid (0.39 g, 4.04 mmol) in 3 mL water and a solution of NaClO_2 (0.37 g, 4.04 mmol) in 3 mL water and the mixture was stirred at RT overnight. The solvents were removed under reduced pressure and the residue taken-up with 1M HCl.

The resulting precipitate was collected and dried to give the title compound **22** (0.42 g, 82%).

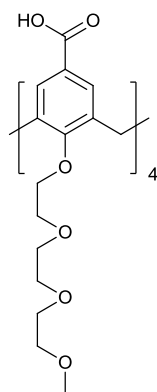
¹H NMR (300 MHz, 25 °C, DMSO-*d*⁶): δ = 12.44 (s, 4H, COOH), 7.38 (s, 8H, ArH) 4.52 (d, *J* = 13.0 Hz, 4H, ArCH₂Ar), 4.21 (t, *J* = 4.9 Hz, 8H, OCH₂CH₂O), 3.92 (t, *J* = 4.9 Hz, 8H, OCH₂CH₂O), 3.62 (m, 8H, OCH₂CH₂O), 3.48 (m, 8H, OCH₂CH₂O), 3.44 (d, *J* = 13.0 Hz, 4H, ArCH₂Ar), 3.28 (s, 12H, OCH₃).

¹³C NMR (300 MHz, 25 °C, DMSO-*d*⁶): δ = 166.87, 160.0, 134.48, 129.52, 124.50, 73.40, 71.24, 69.76, 69.43, 58.02, 30.03.

IR (solid phase, ν cm⁻¹) = 2922m, 2877m, 1693s, 1600m, 1423m, 1295s, 1199s, 1105s.

MS *m/z* observed 1009.4086, 1026.4329, 1031.3873, theoretical 1009.4064 [M + H]⁺, 1026.4329 [M + NH₄]⁺, 1031.3883 [M + Na]⁺.

Tetrakis(monomethyl triethylene glycol)-tetra-*p*-carboxylatocalix[4]arene, **23**²⁵



This was prepared by a route similar to compound **22** using compound **19**. Compound **23** was obtained as a yellow solid (0.45 g, 80%).

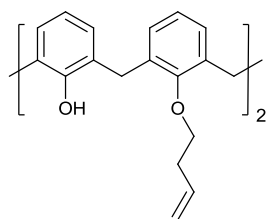
¹H NMR (300 MHz, 25 °C, DMSO-*d*⁶): δ = 12.48 (s, 4H, COOH), 7.42 (s, 8H, ArH) 4.54 (d, *J* = 13.0 Hz, 4H, ArCH₂Ar), 4.24 (t, *J* = 4.6 Hz, 8H, OCH₂CH₂O), 3.89 (t, *J* = 4.6 Hz, 8H, OCH₂CH₂O), 3.58 (m, 24H, OCH₂CH₂O), 3.46 (m, 8H, OCH₂CH₂O), 3.42 (d, *J* = 13.0 Hz, 4H, ArCH₂Ar), 3.26 (s, 12H, OCH₃).

¹³C NMR (300 MHz, 25 °C, DMSO-*d*⁶): δ = 166.87, 160.01, 134.48, 129.54, 124.52, 73.43, 71.20, 69.76, 69.72, 69.56, 57.96, 30.01.

IR (solid phase, ν cm⁻¹) = 2873m, 2593w, 1678s, 1599m, 1422m, 1297s, 1201s, 1104s, 1046s.

MS *m/z* observed 1202.5370, theoretical 1202.5378 [M + NH₄]⁺.

Dibutenyl-dihydroxycalix[4]arene, **24**³¹



In a 250 mL rbf, C[4] **2** (2.00 g, 4.71 mmol) was dissolved in 80 mL CH₃CN and K₂CO₃ (3.58 g, 0.03 mol) added. The suspension was treated with 4-bromobutene (2.63 mL, 0.03 mol) and the mixture was heated at reflux under nitrogen for one day. After evaporation of the solvent, the mixture was taken up in CHCl₃ (100 mL) and washed with 1 N HCl (2 X 25 mL). The organic layer was dried with MgSO₄ and evaporated to give a crude orange oil that was recrystallised from DCM/MeOH to obtain the corresponding dialkenyl substituted calixarene **24** as a white solid (1.55 g, 62%).

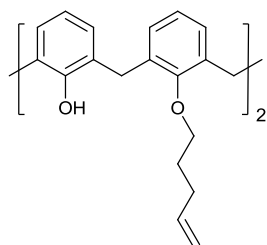
¹H NMR (300 MHz, 25 °C, CDCl₃): δ = 7.98 (s, 2H, OH), 7.01 (d, *J* = 7.2 Hz, 4H, ArH), 6.86 (d, *J* = 7.2 Hz, 4H, ArH), 6.69 (t, *J* = 6.9 Hz, 2H, ArH), 6.58 (t, *J* = 6.9 Hz, 2H, ArH), 6.15 (m, 2H, HC=), 5.22 (d, *J* = 7.8 Hz, 2H, H₂C=), 5.12 (d, *J* = 7.8 Hz, 2H, H₂C=), 4.23 (d, *J* = 13.4 Hz, 4H, ArCH₂Ar), 3.99 (t, *J* = 6.6 Hz, 4H, OCH₂), 3.31 (d, *J* = 13.4 Hz, 4H, ArCH₂Ar), 2.74 (m, 4H, CH₂CH₂).

¹³C NMR (300 MHz, 25 °C, CDCl₃): δ = 153.36, 151.88, 134.53, 133.35, 128.95, 128.47, 128.12, 125.35, 118.99, 117.55, 76.11, 34.55, 31.47.

IR (solid phase, ν cm⁻¹) = 3240m, 3072w, 2924m, 1642m, 1592m, 1456s, 1430m, 1196s, 1013s.

MS *m/z* observed 550.2943, theoretical 550.2952 [M + NH₄]⁺.

Dipentenyl-dihydroxycalix[4]arene, **25**³¹



This was prepared by a route similar to compound **24** using 5-bromopentene. Compound **25** was obtained as a white solid (0.82 g, 31%).

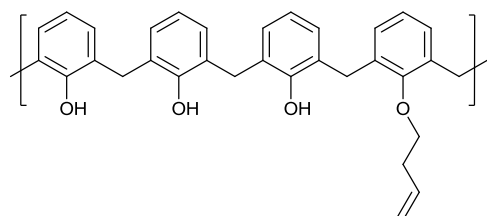
¹H NMR (300 MHz, 25 °C, CDCl₃): δ = 8.15 (s, 2H, OH), 6.99 (d, *J* = 7.4 Hz, 4H, ArH), 6.85 (d, *J* = 7.4 Hz, 4H, ArH), 6.67 (t, *J* = 7.2 Hz, 2H, ArH), 6.61 (t, *J* = 7.2 Hz, 2H, ArH), 5.93 (m, 2H, HC=), 5.12 (d, *J* = 8.0 Hz, 2H, H₂C=), 4.98 (d, *J* = 8.0 Hz, 2H, H₂C=), 4.25 (d, *J* = 13.4 Hz, 4H, ArCH₂Ar), 3.96 (t, *J* = 6.8 Hz, 4H, OCH₂), 3.30 (d, *J* = 13.4 Hz, 4H, ArCH₂Ar), 2.48 (m, 4H, CH₂CH₂), 2.09 (m, 4H, CH₂CH₂).

^{13}C NMR (300 MHz, 25 °C, CDCl_3): δ = 153.37, 151.91, 137.93, 133.45, 128.96, 128.48, 128.15, 125.37, 119.02, 115.53, 75.84, 31.48, 30.13, 29.28.

IR (solid phase, ν cm^{-1}) = 3266m, 3025w, 2923m, 2872w, 1640m, 1591m, 1456s, 1249m, 1195s, 1087s, 1042s.

MS m/z observed 578.3256, theoretical 578.3265 $[\text{M} + \text{NH}_4]^+$.

Monobutenyl-trihydroxycalix[4]arene, 26



This was prepared by the same synthetic route to form compound **24**. The crude product was purified by chromatography on silica (PE/DCM 3:2) to afford compound **26** (rf 0.3) as an off-

white solid (0.24 g, 6%).

^1H NMR (300 MHz, 25 °C, CDCl_3): δ = 9.61 (s, 1H, OH), 9.23 (s, 2H, OH), 6.96 (m, 8H, ArH), 6.80 (t, J = 6.2 Hz, 1H, ArH), 6.62 (m, 3H, ArH), 6.08 (m, 1H, HC=), 5.27 (dd, 2H, H₂C=), 4.30 (d, J = 13.2 Hz, 2H, ArCH₂Ar), 4.18 (d, J = 13.2 Hz, 2H, ArCH₂Ar), 4.14 (t, J = 7.6 Hz, 2H, OCH₂), 3.41 (d, J = 13.4 Hz, 4H, ArCH₂Ar), 2.84 (q, J = 6.2, 4H, CH₂CH₂).

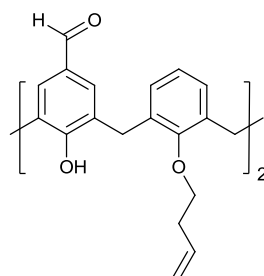
^{13}C NMR (300 MHz, 25 °C, CDCl_3): δ = 151.39, 150.83, 149.24, 134.21, 133.93, 129.38, 128.84, 128.77, 128.44, 128.42, 126.19, 121.96, 120.93, 118.31, 76.21, 34.48, 31.92, 31.50.

IR (solid phase, ν cm^{-1}) = 3287m, 2934m, 2875w, 1644w, 1594w, 1453s, 1379m, 1266m, 1149m, 1081m.

Anal. Calcd. For $\text{C}_{32}\text{H}_{30}\text{O}_4$: C, 80.31; H, 6.32. *Found*: C, 79.77; H, 6.34.

MS m/z observed 479.2212, 496.2474, theoretical 479.2217 $[\text{M} + \text{H}]^+$, 496.2482 $[\text{M} + \text{NH}_4]^+$.

Diformyl-dibutenyl-dihydroxycalix[4]arene, 27



Compound **24** (1.00 g, 1.88 mmol) was dissolved in 15 mL CHCl_3 in a 100 mL 3-necked flask that had been flushed with nitrogen. SnCl_4 (2.26 mL, 0.02 mol) and dichloromethyl methyl ether (0.44 mL, 4.88 mmol) were rapidly added once the solution

had been cooled to -15°C . The mixture was left to stir for 30 mins, before water was added to quench the reaction. The organic layer was separated, washed with water (3 X 100 mL), dried over MgSO_4 and the solvents removed under reduced pressure to afford a crude orange solid. This was dissolved in CHCl_3 and MeOH was added to crystallise out compound **27** as colourless crystals (0.45 g, 41%).

^1H NMR (300 MHz, 25°C , CDCl_3): δ = 9.75 (s, 2H, CHO), 8.88 (s, 2H, OH), 7.59 (s, 4H, ArH), 6.88 (d, J = 6.8 Hz, 4H, ArH), 6.74 (t, J = 6.6 Hz, 2H, ArH), 6.12 (m, 2H, HC=), 5.28 (d, J = 13.4 Hz, 2H, $\text{H}_2\text{C=}$), 5.15 (d, J = 7.8 Hz, 2H, $\text{H}_2\text{C=}$), 4.24 (d, J = 13.2 Hz, 4H, ArCH_2Ar), 4.01 (t, J = 6.8 Hz, 4H, OCH_2), 3.46 (d, J = 13.2 Hz, 4H, ArCH_2Ar), 2.75 (m, 4H, CH_2CH_2).

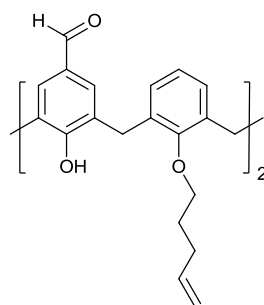
^{13}C NMR (300 MHz, 25°C , CDCl_3): δ = 189.85, 158.54, 150.69, 133.03, 131.22, 129.92, 128.41, 127.57, 127.54, 124.70, 117.02, 75.32, 33.46, 30.27.

IR (solid phase, v cm^{-1}) = 3164m, 2927m, 2728w, 1666s, 1584s, 1439m, 1131s.

Anal. Calcd. For $\text{C}_{38}\text{H}_{36}\text{O}_6$: C, 77.53; H, 6.16. *Found*: C, 69.22; H, 5.69.

MS m/z observed 589.2571, theoretical 589.2585 $[\text{M} + \text{H}]^+$.

Diformyl-dipentenyl-dihydroxycalix[4]arene, **28**



This was prepared by a route similar to compound **27** using compound **25**. Compound **28** was obtained from recrystallisation from $\text{CHCl}_3/\text{MeOH}$ as colourless crystals (0.31 g, 34%).

^1H NMR (300 MHz, 25°C , CDCl_3): δ = 9.71 (s, 2H, CHO), 9.08 (s, 2H, OH), 7.58 (s, 4H, ArH), 6.90 (d, J = 6.6 Hz, 4H, ArH), 6.71 (t, J = 7.0 Hz, 2H, ArH), 5.88 (m, 2H, HC=), 5.12 (d, J = 13.4 Hz, 2H, $\text{H}_2\text{C=}$), 5.01 (d, J = 7.8 Hz, 2H, $\text{H}_2\text{C=}$), 4.20 (d, J = 13.2 Hz, 4H, ArCH_2Ar), 3.97 (t, J = 6.2 Hz, 4H, OCH_2), 3.42 (d, J = 13.2 Hz, 4H, ArCH_2Ar), 2.46 (m, 4H, CH_2CH_2), 2.12 (m, 4H, CH_2CH_2).

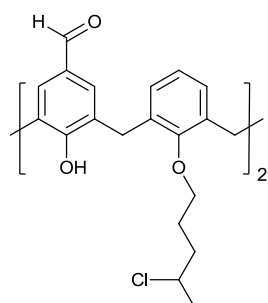
^{13}C NMR (300 MHz, 25°C , CDCl_3): δ = 190.87, 159.57, 151.72, 137.54, 132.35, 130.96, 129.46, 128.65, 128.60, 125.75, 115.82, 77.23, 76.11, 31.31, 30.03, 29.22.

IR (solid phase, v cm^{-1}) = 3179m, 2925m, 2360w, 1668s, 1584s, 1480m, 1439m, 1272s, 1131s.

Anal. Calcd. For $\text{C}_{40}\text{H}_{40}\text{O}_6$: C, 77.90; H, 6.54. *Found*: C, 73.99; H, 6.42.

MS m/z observed 617.2896, 634.3159, 639.2710, theoretical 617.2898 $[M + H]^+$, 634.3163 $[M + NH_4]^+$, 639.2717 $[M + Na]^+$.

Diformyl-di(4-chloropentyl)-dihydroxycalix[4]arene, **29**



This was prepared by the same synthetic route as compound **28**. Compound **29** was obtained as colourless blocks from recrystallisation from acetone (0.08 g, 26%).

1H NMR (300 MHz, 25 °C, $CDCl_3$): δ = 9.76 (s, 2H, CHO), 8.84 (s, 2H, OH), 7.60 (s, 4H, ArH), 6.88 (d, J = 7.4 Hz, 4H, ArH), 6.72 (t, J = 6.8 Hz, 2H, ArH), 4.26 (d, J = 4.2 Hz, 2H, CH_2CH_2) 4.18 (d, J = 4.8 Hz, 4H, $ArCH_2Ar$), 3.99 (m, 4H, CH_2CH_2), 3.46 (d, J = 12.9 Hz, 4H, $ArCH_2Ar$), 2.46 (m, 2H, CH_2CH_2), 2.11 (m, 6H, CH_2CH_2), 1.05 (d, J = 7.0 Hz, 6H, CH_2CH_2).

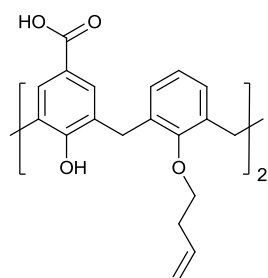
^{13}C NMR (300 MHz, 25 °C, $CDCl_3$): δ = 191.02, 158.62, 155.45, 134.34, 130.51, 128.23, 124.02, 123.53, 77.24, 68.85, 58.72, 38.60, 32.12, 25.42, 24.24.

IR (solid phase, $\nu\text{ cm}^{-1}$) = 3224m, 2927m, 1676s, 1587s, 1458m, 1440m, 1272s, 1211s, 1131s, 763s.

Anal. Calcd. For $C_{40}H_{42}Cl_2O_6$: C, 73.44; H, 6.47. *Found*: C, 70.30; H, 6.10.

MS m/z observed 689.2435, 706.2692, theoretical 689.2431 $[M + H]^+$, 706.2697 $[M + NH_4]^+$.

Dibutenyl-dihydroxy-di-*p*-carboxylatocalix[4]arene, **30**



To a solution of compound **27** (0.33g, 0.56 mmol) in DCM (5 mL) and acetone (15 mL) was added a solution of sulfamic acid (0.22 g, 2.24 mmol) in 3 mL water and a solution of $NaClO_2$ (0.20 g, 2.24 mmol) in 3 mL water and the mixture was stirred at RT overnight. The solvents were removed under reduced

pressure and the residue taken-up with 1M HCl. The resulting precipitate was collected and dried to give the title compound **30** as an off-white solid (0.32 g, 91%).

^1H NMR (300 MHz, 25 °C, DMSO- d^6): δ = 12.42 (s, 2H, COOH), 8.94 (s, 2H, OH), 7.83 (s, 4H, ArH), 7.05 (d, J = 8.0 Hz, 4H, ArH), 6.83 (m, 2H, ArH), 6.28 (m, 2H, CH=), 5.34 (d, J = 13.2 Hz, 2H, H₂C=), 5.22 (d, J = 8.6 Hz, 2H, H₂C=), 4.16 (d, J = 13.0 Hz, 4H, ArCH₂Ar), 4.04 (t, J = 6.8 Hz, 4H, CH₂CH₂), 3.59 (d, J = 13.0 Hz, 4H, ArCH₂Ar), 2.72 (m, 4H, CH₂CH₂).

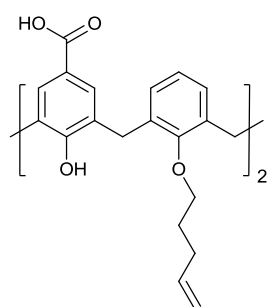
^{13}C NMR (300 MHz, 25 °C, DMSO- d^6): δ = 167.22, 157.05, 151.59, 134.77, 132.99, 130.32, 129.13, 127.62, 121.35, 117.61, 33.99, 30.28.

IR (solid phase, ν cm⁻¹) = 3166m, 2930m, 2732w, 1665s, 1580s, 1444m, 1128s.

Anal. Calcd. For C₃₈H₃₆O₈: C, 73.53; H, 5.85. *Found*: C, 69.20; H, 5.59.

MS m/z observed 638.2747, theoretical 638.2748 [M + H]⁺.

Dipentenyl-dihydroxy-di-*p*-carboxylatocalix[4]arene, **31**



This was prepared by a route similar to compound **30** using compound **28**. Compound **31** was obtained from as colourless crystals (0.14 g, 43%).

^1H NMR (300 MHz, 25 °C, DMSO- d^6): δ = 12.50 (s, 2H, COOH), 8.98 (s, 2H, OH), 7.88 (s, 4H, ArH), 7.12 (d, J = 8.0 Hz, 4H, ArH), 6.88 (m, 2H, ArH), 6.32 (m, 2H, CH=), 5.40 (d, J = 13.4 Hz, 2H, H₂C=), 5.30 (d, J = 8.6 Hz, 2H, H₂C=), 4.22 (d, J = 13.2 Hz, 4H, ArCH₂Ar), 4.14 (t, J = 6.8 Hz, 4H, CH₂CH₂), 4.08 (t, J = 6.8 Hz, 4H, CH₂CH₂), 3.61 (d, J = 13.2 Hz, 4H, ArCH₂Ar), 2.78 (m, 4H, CH₂CH₂).

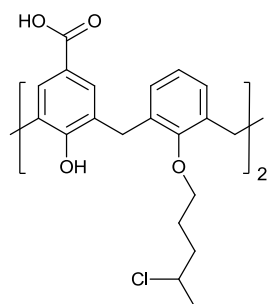
^{13}C NMR (300 MHz, 25 °C, DMSO- d^6): δ = 169.32, 158.00, 155.42, 151.59, 136.54, 134.34, 129.93, 128.64, 126.52, 124.04, 123.53, 115.82, 69.45, 30.21, 28.90.

IR (solid phase, ν cm⁻¹) = 3170m, 2927m, 2736w, 1662s, 1579s, 1440m, 1134s.

Anal. Calcd. For C₄₀H₄₀O₈: C, 74.06; H, 6.21. *Found*: C, 70.54; H, 6.58.

MS m/z observed 666.2974, theoretical 666.2976 [M + H]⁺.

Di(4-chloropentyl)-dihydroxy-di-*p*-carboxylatocalix[4]arene, **32**



This was prepared by a route similar to compound **30** using compound **29**. Compound **32** was obtained from as colourless crystals (0.08 g, 95%).

¹H NMR (300 MHz, 25 °C, DMSO-*d*⁶): δ 12.46 (s, 2H, COOH), 8.98 (s, 2H, OH), 7.81 (s, 4H, ArH), 7.06 (d, *J* = 7.8 Hz, 4H, ArH), 6.81 (t, *J* = 7.6 Hz, 2H, ArH), 4.38 (m, 2H, CH₂CH₂), 4.16 (d, *J* = 13.2 Hz, ArCH₂Ar), 4.02 (m, 4H, CH₂CH₂), 3.59 (d, *J* = 13.0 Hz, ArCH₂Ar), 2.12 (m, 8H, CH₂CH₂), 1.58 (d, *J* = 6.8 Hz, 6H, CH₂CH₂).

¹³C NMR (300 MHz, 25 °C, DMSO-*d*⁶): δ = 167.20, 151.60, 133.01, 130.31, 129.16, 127.69, 125.58, 121.47, 59.14, 35.92, 25.29.

IR (solid phase, ν cm⁻¹) = 3230m, 2930m, 1672s, 1585s, 1450m, 1444m, 1270s, 1216s, 1134s, 765s.

Anal. Calcd. For C₄₀H₄₂Cl₂O₈: C, 66.57; H, 5.87. *Found*: C, 66.52; H, 5.98.

MS *m/z* observed 738.2600, 743.2151, theoretical 738.2595 [M + NH₄]⁺, 743.2149 [M + Na]⁺.

2.8.4. X-ray details of data collection/structure refinement of compounds 5, 20, 2.1 - 2.2.

Complex number	5	20	2.1
Formula	C ₃₄ H ₃₆ O ₄	C ₄₀ H ₄₄ O ₁₂	C ₄₆ H ₅₁ NO ₁₂
<i>Mr</i>	508.70	716.75	809.88
Crystal system	Hexagonal	Triclinic	Triclinic
Space group	<i>P</i> 6 ₅	<i>P</i> -1	<i>P</i> -1
<i>T</i> /K	100(2)	100(2)	100(2)
<i>a</i> /Å	11.1313(6)	11.1638(4)	12.1354(6)
<i>b</i> /Å	11.1313(6)	11.8310(5)	13.5147(6)
<i>c</i> /Å	38.317(2)	15.0801(6)	13.5736(6)
α /°	90	87.952(3)	83.563(2)
β /°	90	88.135(3)	71.665(2)
γ /°	120	63.000(2)	73.938(3)
<i>U</i> Å ³	4111.6(4)	1773.24(12)	2029.88(16)
<i>Z</i>	6	2	2
<i>F</i> (000)	1560	760	860
<i>D_c</i> /g cm ⁻³	1.181	1.342	1.325
μ /mm ⁻¹	0.075	0.119	0.096
<i>2</i> θ_{max} /°	63.6	50.5	49.4
Data collected	32376	19526	10273
Unique data	7775	4933	6312
<i>R_{int}</i>	0.0418	0.0558	0.0337
Obs data (<i>I</i> >2 σ (<i>I</i>))	7141	3599	3872
Parameters	347	471	535
Restraints	1	0	6
<i>R</i> ₁ (observed data)	0.0557	0.0661	0.0678
ωR_2 (all data)	0.1536	0.1674	0.1592
<i>GooF</i>	1.170	1.044	0.999
Max/min residuals [e.Å ⁻³]	0.31/-0.26	0.89/-0.56	0.36/-0.43

Table 2.4. Details of data collection and structure refinement for complexes **5**, **20** and **2.1**.

Complex number	2.2
Formula	$\text{C}_{43}\text{H}_{48}\text{Cl}_2\text{O}_7$
<i>Mr</i>	747.71
Crystal system	Monoclinic
Space group	$P2_1$
<i>T</i> /K	100(2)
<i>a</i> /Å	10.0573(5)
<i>b</i> /Å	15.8782(8)
<i>c</i> /Å	12.9313(6)
α /°	90
β /°	112.651(3)
γ /°	90
<i>U</i> Å ³	1905.74(16)
<i>Z</i>	2
<i>F</i> (000)	792
<i>D_c</i> /g cm ⁻³	1.303
μ /mm ⁻¹	0.275
$2\theta_{\text{max}}$ /°	49.3
Data collected	19867
Unique data	4947
<i>R_{int}</i>	0.0540
Obs data (<i>I</i> >2 $\sigma(I)$)	4368
Parameters	449
Restraints	20
<i>R</i> ₁ (observed data)	0.0809
ωR_2 (all data)	0.2111
<i>GooF</i>	1.036
Max/min residuals	1.09/-1.02
[e.Å ⁻³]	

Table 2.5. Details of data collection and structure refinement for complex **2.2**.

2.9. References.

1. For examples see a) A. Shivanyuk, J. C. Friesse, S. Döring and J. Rebek Jr., *J. Org. Chem.*, 2003, **68**, 6489. b) L. R. MacGillivray and J. L. Atwood, *Nature*, 1997, **389**, 469. c) N. P. Power, S. J. Dalgarno and J. L. Atwood, *New J. Chem.*, 2007, **31**, 17. d) S. J. Dalgarno, S. A. Tucker, D. B. Bassil and J. L. Atwood, *Science*, 2005, **309**, 2037 and references therein.
2. a) G. W. Orr, L. J. Barbour and J. L. Atwood, *Science*, 1999, **285**, 1049. b) J. L. Atwood, L. J. Barbour, S. J. Dalgarno, M. J. Hardie, C. L. Raston and H. R. Webb, *J. Am. Chem. Soc.*, 2004, **126**, 13170. c) S. J. Dalgarno, J. L. Atwood and C. L. Raston, *Chem. Commun.*, 2006, 4567. d) S. J. Dalgarno, N. P. Power and J. L. Atwood, *Coord. Chem. Rev.*, 2008, **252**, 825.
3. a) S. J. Dalgarno, J. E. Warren, J. Antesberger, T. E. Glass and J. L. Atwood, *New. J. Chem.* 2007, **31**, 1891. b) S. Kennedy and S. J. Dalgarno, *Chem. Commun.*, 2009, 5275. c) S. Kennedy, S. J. Teat and S. J. Dalgarno, *Dalton Trans.*, 2010, **39**, 384. d) S. Kennedy, C. M. Beavers, S. J. Teat and S. J. Dalgarno, *New. J. Chem.* 2011, **35**, 28. e) S. Kennedy, C. M. Beavers, S. J. Teat and S. J. Dalgarno, *Cryst. Growth Des.* 2012, **12**, 679. f) S. Kennedy, I. E. Dodgson, C. M. Beavers, S. J. Teat and S. J. Dalgarno, *Cryst. Growth Des.* 2012, **12**, 688. g) S. Kennedy, P. Cholewa, R. D. McIntosh and S. J. Dalgarno, *CrystEngComm.*, 2013, **15**, 1520.
4. P. P. Cholewa and S. J. Dalgarno, *CrystEngComm.*, 2014, **16**, 3655.
5. S. Kennedy, G. Karotsis, C. M. Beavers, S. J. Teat, E. K. Brechin and S. J. Dalgarno, *Angew. Chem. Int. Ed.* 2010, **49**, 4205.
6. P. P. Cholewa, C. M. Beavers, S. J. Teat and S. J. Dalgarno, *Cryst. Growth Des.* 2013, **13**, 2703.
7. P. P. Cholewa, C. M. Beavers, S. J. Teat and S. J. Dalgarno, *Chem. Commun.*, 2013, **49**, 3203.
8. P. P. Cholewa, C. M. Beavers, S. J. Teat and S. J. Dalgarno, *Cryst. Growth Des.* 2013, **13**, 5165.
9. Z. Asfari, V. Böhmer, J. Harrowfield and J. Vicens, *Calixarenes 2001*, Kluwer Academic Publishers, 2001.
10. C. D. Gutsche, Calixarenes Revisited. In *Supramolecular Chemistry*; J. F. Stoddart, Ed.; The Royal Society of Chemistry: Cambridge, 1998.
11. C. D. Gutsche and M. Iqbal, *Org. Synth.* 1990, **68**, 234.

12. a) K. Iwamoto, H. Shimizu, K. Araki and S. Shinkai, *J. Am. Chem. Soc.* 1993, **115**, 12228. b) K. Iwamoto, H. Shimizu, K. Araki and S. Shinkai, *J. Am. Chem. Soc.* 1993, **115**, 3997.
13. A. Arduini, A. Pochini, S. Reverberi and R. Ungaro, *J. Chem. Soc. Chem. Commun.* 1984, 981.
14. K. Iwamoto, K. Araki and S. Shinkai, *Tetrahedron* 1991, **47**, 4325.
15. a) C. D. Gutsche and L-G. Lin, *Tetrahedron* 1986, **42**, 1633. b) A. Casnati, A. Arduini, E. Ghidini, A. Pochini and R. Ungaro, *Tetrahedron* 1991, **47**, 2221.
16. a) L. C. Groenen, B. H. M. Ruël, A. Casnati, W. Verboom, A. Pochini, R. Ungaro and D. N. Reinhoudt, *Tetrahedron* 1991, **47**, 8379. b) K. Araki, K. Iwamoto, S. Shinkai and T. Matsuda, *Bull. Chem. Soc. Jpn.* 1990, **63**, 3480. c) F. Bottino, L. Giunta and S. Pappalardo, *J. Org. Chem.* 1989, **54**, 5407.
17. C-M. Shu and W-S. Chung, *J. Org. Chem.* 1999, **64**, 2673.
18. A. Arduini, S. Fanni, G. Manfredi, A. Pochini, R. Ungaro, A. R. Sicuri and F. Ugozzoli, *J. Org. Chem.* 1995, **60**, 1448.
19. V. I. Boyko, Yu. I. Matvieiev, M. A. Klyachina, O. A. Yesypenko, S. V. Shishkina, O. V. Shishkin and V. I. Kalchenko, *Tetrahedron*, 2009, **65**, 4220.
20. J-D. van Loon, A. Arduini, L. Coppi, W. Verboom, A. Pochini, R. Ungaro, S. Harkema and D. N. Reinhoudt, *J. Org. Chem.*, 1990, **55**, 5639.
21. M. Awada, C. Jeunesse, D. Matt, L. Toupet and R. Welter, *Dalton Trans.*, 2011, **40**, 10063.
22. N. Mizoshita, T. Tani, H. Shinokubo, S. Inagaki, *Angew. Chem. Int. Ed.*, 2012, **51**, 1156.
23. S. G. Ramkumar, S. Ramakrishnan, *Macromolecules.*, 2010, **42**, 2307.
24. M. Saadioui, N. Reynier, J. F. Dozol, Z. Asfari, J. Vicens, *J. Inclusion Phenom. Mol. Recognit. Chem.*, 1997, **29**, 153.
25. Q. Lin, H. S. Park, Y. Hamuro, C. S. Lee and A. D. Hamilton, *Biopolymers (Peptide Science)*, 1998, **47**, 258.
26. a) A. Decken, P. D. Harvey and J. Douville, *Acta Cryst., Sect. E: Struct. Rep. Online* 2004, **60**, 1170. b) O. Ediz, M. Tabakci, S. Memon, M. Yilmaz and D. M. Roundhill, *Supramol. Chem.* 2004, **16**, 199. c) V. Arora, H. M. Chawla and A. Santra, *Tetrahedron* 2002, **58**, 5591. d) H. M. Chawla and A. Santra, *Synth. Commun.* 2001, **31**, 2605. e) T. Komori and S. Shinkai, *Chem. Lett. Chem. Soc. Japan.* 1992, 901. f) A. Arduini, G. Manfredi, A. Pochini, A. R. Sicuri and R. Ungaro, *J. Chem. Soc., Chem. Commun.* 1991, 936.

27. Q. Lin and A. D. Hamilton, *C. R. Chim.*, **5**, 2002, 441.
28. a) C. D. Gutsche and J. A. Levine, *J. Am. Chem. Soc.* 1982, **104**, 2652. b) C. D. Gutsche, J. A. Levine and P. K. Sujeeth, *J. Org. Chem.* 1985, **50**, 5802.
29. C. D. Gutsche, *Calixarenes. Monographs in Supramolecular Chemistry*, Vol. 1; Stoddart, F. J., Ed.; The Royal Society of Chemistry: Cambridge, 1989.
30. J. Vicens and V. Böhmer, *Calixarenes: A Versatile Classes of Macrocyclic Compounds*; Kluwer Academic Publishers: Dordrecht, 1991.
31. J-D. van Loon, A. Arduini, L. Coppi, W. Verboom, A. Pochini, R. Ungaro, S. Harkema and D. N. Reinhoudt, *J. Org. Chem.*, 1990, **55**, 5639.
32. M. Kimura, M. Yokokawa, S. Sato, T. Fukawa and T. Mihara, *Chem. Lett.*, 2011, 1402.
33. P. E. Peterson, R. J. Bopp, D. M. Chevli, E. L. Curran, D. E. Dillard and R. J. Kamat, *J. Am. Chem. Soc.*, 1967, **89**, 5902.
34. C. D. Gutsche, B. Dhawan, J. A. Levine, K. H. No and L. J. Bauer, *Tetrahedron* 183, **39**, 409.

Chapter 3: Upper-rim *p*-carboxylatocalix[4]arene protection/deprotection.

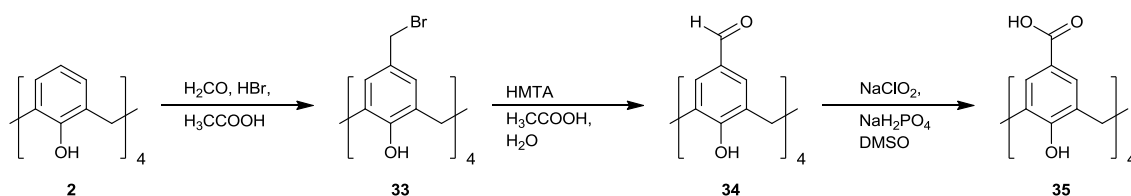
3.1. Introduction.

This chapter is concerned with the upper-rim protection of *p*CO₂[4], followed by alkylation of the lower-rim. Subsequent deprotection of the ester protecting group was implemented to yield the tetra-*O*-alkyl *p*-carboxylatocalix[4]arene product. Single crystal X-ray structures of the macrocycles synthesised here have been obtained and are discussed. In addition, the pyridine-templated assembly of these compounds was studied and results for all structural studies are presented.

As previously discussed in Chapter 2, di-*O*-alkoxy-di-*p*-carboxylatocalix[4]arenes adopt near perfect cone conformations owing to the hydrogen bonding interactions that occur at the lower-rim of the macrocycle. A number of different conformations can be obtained when tetra-*O*-alkylation is undertaken at the lower-rim. This is due to the fact that there is no longer hydrogen bonding present at the lower-rim, so the calix[4]arene is no longer fixed in the cone conformation. To date, the majority of *p*CO₂[4] assemblies reported have been based on cone conformers, thereby allowing for the formation of architectures.¹ There has been little published in respect to the exploration of conformational changes for *p*CO₂[4]s. One example that has previously been investigated involved the crystallisation of rubidium or caesium salts of tetra-*O*-methoxy-tetra-*p*-carboxylatocalix[4]arene.² The results obtained from these crystallisations revealed that the calix[4]arene adopted the 1,3-alternate conformation and assembled so as to form interpenetrated networks of nano-capsules. Another involves the pyridine-directed assembly of tetra-*O*-alkyl *p*-carboxylatocalix[4]arenes.³ The presence of shorter alkyl chains on the lower-rim (e.g. methyl and ethyl) allows for rapid conformational interconversion by rotation through the annulus of the macrocycle. Crystallisation from pyridine and 4-picoline resulted in the *p*CO₂[4]s adopting the partial-cone conformation due to this conformational flexibility, generating new *p*CO₂[4] building blocks.

3.2. Upper-rim functionalisation of calix[4]arene.

With the synthesis of C[4] **2** previously discussed in Chapter 2 further modifications were carried out at the upper-rim of the macrocycle. The introduction of CO₂H functionality to C[4] **2** was executed *via* a multi-step synthetic pathway as shown in Scheme 3.1.^{4,5}

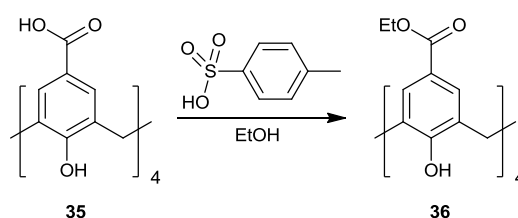


Scheme 3.1. Multi-step synthesis of *p*CO₂[4] **35**.

With the successful synthesis of C[4] **2**, formylation of the upper-rim is required in order to oxidise it to the corresponding carboxylic acid. The formylation of calixarenes can be achieved in a variety of ways,^{4,6,7} but the reaction usually results in low yields and uncertain conformations. In this case, formylation of the upper-rim was achieved *via* a bromomethyl intermediate, the synthesis of which involved the reaction of C[4] **2** with paraformaldehyde and hydrogen bromide in acetic acid at room temperature; this afforded compound **33** in quantitative yield.⁴ The next step involved the conversion of *p*-bromomethylcalix[4]arene **33** to the *p*-formylcalix[4]arene derivative *via* the Sommelet reaction, generating compound **34** in 85% yield.⁷ The reaction uses HMTA and acetic acid, with the sequential addition of water. The ¹H NMR spectrum compound **34** shows the existence of the aldehydic proton at 9.68 ppm as well as a pair of characteristic broad singlets at 4.22 and 3.71 ppm, indicating that compound **34** is in the cone conformation. Formylated calix[*n*]arenes are valuable precursors for the formation of a plethora of derivatives depending on subsequent synthetic modification carried out. An important reaction involves the oxidation of the aldehyde to produce *p*CO₂[4] **35**. The synthesis is accomplished by dissolving compound **34** in DMSO along with an aqueous solution of NaH₂PO₄, followed by the slow addition of an aqueous solution of NaClO₂ at room temperature over a 24 hour period to afford compound **35** in 80% yield.⁵ Although the synthesis was straightforward, a problem emerged concerning the solubility of compound **35**, resulting in an unsatisfactory ¹H NMR spectrum being generated. A broad peak masks the region of the spectrum that contains important characteristic peaks needed to identify the conformational properties of compound **35**.

However, it should be noted that the signal associated with the formyl group in compound **34** is no longer present, a feature suggesting successful conversion to compound **35**.

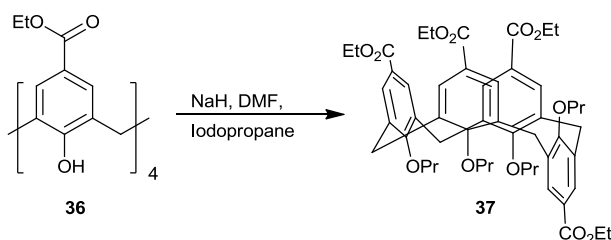
As mentioned in Chapter 2, strongly acidic and vigorous conditions are required for the formylation step. This synthetic route is therefore only applicable to molecules that have no acid-sensitive substituents present at the lower-rim. Compound **35** was synthesised in the hope of introducing a variety of acid-sensitive groups to the lower-rim. However, as the addition of base can result in the deprotonation of the acidic protons, the acid group must first be protected. This was achieved by protecting the group with an ester function by means of an acid-catalysed esterification through reaction of compound **35** with ethanol (EtOH) and *p*-toluenesulfonic acid to afford *p*-carboxyethylcalix[4]arene **36** (Scheme 3.2).



Scheme 3.2. Synthesis of *p*-carboxyethylcalix[4]arene **36** from compound **35**.

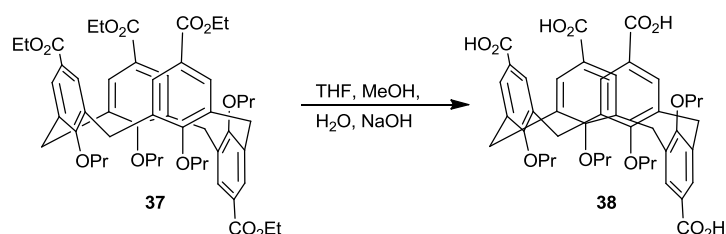
As the esterification process is both slow and reversible the reaction mixture was left to reflux over the period of a week and was monitored by TLC. The ¹H NMR spectrum is consistent with the molecule being in the cone conformation with the presence of a single peak at 10.17 ppm, corresponding to the four lower-rim hydroxyl groups. After work-up the final product was obtained in 72% yield. It was anticipated that compound **36** could be used as a potential precursor for functionalisation to be executed on the lower-rim with a range of R-groups that are sensitive to the formylation procedure described above. It is hoped that once the various substituents are introduced to the lower-rim, the ester moiety can subsequently be cleaved with saponification to produce a library of new *p*-CO₂[4] building blocks. Compound **36** was fully characterised using ¹H NMR, ¹³C NMR, MS, IR spectroscopy and CHN analysis. In addition to the compound being fully characterised, single crystals of compound **36** that were suitable for diffraction studies were obtained by slow evaporation from a pyridine solution. Structural analysis is discussed in detail in section **3.3.1** below.

Having successfully synthesised compound **36**, the next step required was the introduction of different R-groups on the lower-rim. Tetra-alkylation was first tested by reaction with 1-iodopropane in the presence of a strong base in order to establish whether this is a viable synthetic route (Scheme 3.3).⁸



Scheme 3.3. Synthetic route to *p*-carboxyethyl-tetra-*O*-propoxycalix[4]arene **37**.

It was expected that this would result in the formation of *p*-carboxyethyl-tetra-*O*-propoxycalix[4]arene **37** in the cone conformation, but this was not what resulted. The ¹H NMR spectrum shows a pair of doublets at 4.08 and 3.15 ppm and a singlet at 3.75 ppm for the bridging methylene protons, which is indicative for the partial-cone conformation of calix[4]arenes and supports the successful formation of compound **37**. The ¹³C NMR spectrum also gave crucial information about the calixarene conformation since the shift of the methylene carbons is little influenced by functionalisation at the *para* position or at the hydroxyl groups.⁹ There are two signals at 30.4 ppm and 35.7 ppm seen for the methylene protons that are in accordance with the partial-cone conformation. Single crystals of compound **37** that were suitable for diffraction studies were obtained upon recrystallisation from acetone. Structural analysis is discussed in detail in section 3.3.2 below, but did confirm the isolation of compound **37** as a partial-cone conformer. Following successful lower-rim alkylation the ester protecting group was then hydrolysed to the parent carboxylic acid under basic conditions; aqueous NaOH was employed and the reaction was heated overnight. An acid work-up afforded compound **38** (Scheme 3.4) in 24% yield.



Scheme 3.4. Saponification of compound **37**.

Although the ^1H NMR spectrum of compound **38** was difficult to analyse due to the overlap of several peaks, the molecule was still found to adopt the partial-cone conformation. Conclusive proof was provided by structural analysis of single crystals of compound **38** that were obtained by slow evaporation of DMF. This is discussed in detail in section **3.3.3** below.

In order to produce a library of novel *p*-CO₂[4] building blocks, it is of importance that the calix[4]arene is fixed in the cone conformation (or pinched-cone) as it will predetermine the shape of the cavity, and to a great extent, restrict conformational mobility of the molecule. As compound **38** was found to adopt the partial-cone conformation it was not suitable for achieving the aims of this study. Although this is the case, it is suitable for the use in the potential generation of new metal-organic systems (e.g. coordination polymers) due to its unusual topologically directing character.

Given the literature based on pyridine-templated assembly of *p*-CO₂[4]s, compounds **36** - **38** were dissolved in a series of commercially available pyridine containing solvents as well as acetone and DMF in a bid to grow single crystals suitable for X-ray diffraction studies; the pyridine-based solvents are pyridine (Py), 2-picoline (2-Pic), 3-picoline (3-Pic) and 4-picoline (4-Pic). Suitable single crystals grew in three cases and these are discussed in detail below.

3.3. X-ray crystal structures of compounds **36** - **38**.

As discussed above, three new calix[4]arene derivatives **36**, **37** and **38** have been synthesised and fully characterised. The NMR spectra recorded for each compound indicated that compound **36** is in a cone conformation, while compounds **37** and **38** are partial-cones. The structure of each of these molecules was determined by X-ray crystallography. The different conformational behaviour seen for compounds **36** - **38** is governed by the addition of *O*-propyl chains attached to the lower-rim of the calixarene framework. It is believed that the unusual formation of a partial-cone conformation is brought about by a metal templating effect with the Na⁺ ion used in the reaction (NaH as a base). Specific control of conformation for calix[4]arenes is imperative in designing a range of different calixarene derivatives and this is an unexpected yet convenient route to partial-cone conformers that have unique topologically directing properties.¹⁰

3.3.1. Structure of *p*-carboxyethylcalix[4]arene·pyridine, **3.1**.

Crystals of *p*-carboxyethylcalix[4]arene·Py, **3.1**, were obtained as a result of the addition of 2 mL of Py to compound **36**. Slow evaporation of the solvent over a week yielded small block-shaped crystals which were suitable for X-ray diffraction studies by synchrotron radiation in order to obtain satisfactory structure solution. Crystals of **3.1** are in a monoclinic cell and the structure solution was performed in the space group *P2₁/n*. Details of data collection and structure refinement are given in Table 3.4 at the end of this chapter. The asymmetric unit of **3.1** consists of a mono-anion of **36** and one pyridinium cation (Figure 3.1). The state of deprotection at the lower-rim hydroxyl groups is evident from peaks in the difference map, as is the protonation of Py.

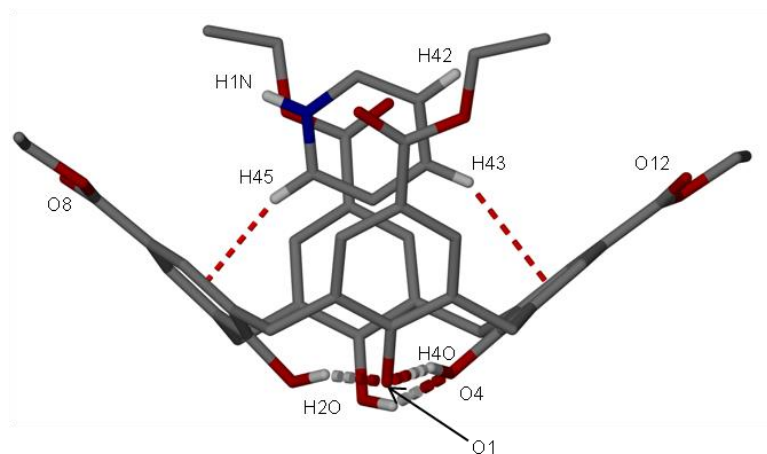


Figure 3.1. The asymmetric unit observed in the X-ray crystal structure of **3.1**. Hydrogen bonding interactions are shown as split-colour dashed lines and CH $\cdots\pi$ interactions are shown as red dashed lines. Hydrogen atoms (apart from those involved in hydrogen bonding and CH $\cdots\pi$ interactions) have been omitted for clarity. Selected atoms have been labelled according to discussion.

Prior to collection it was predicted that compound **36** would adopt a cone conformation in the solid state. ^1H NMR data for this compound reveals the presence of a pair of broad singlets at 4.26 and 3.75 ppm which is indicative of a calix[4]arene in the cone conformation. The typical cone conformer arises as a direct result of there being four hydroxyl groups at the lower-rim, which hydrogen bond to neighbouring ethereal oxygen atoms to give the macrocycle conformational rigidity. In this case there are three OH \cdots O hydrogen bonding interactions in the asymmetric unit, with distances ranging from 1.667 – 1.980 Å (full details in Table 3.1).

H[2O] \cdots O[1]	1.667
H[3O] \cdots O[4]	1.980
H[4O] \cdots O[1]	1.694

Table 3.1. OH \cdots O hydrogen bonding interaction distances (in Å) in the asymmetric unit of **3.1**.

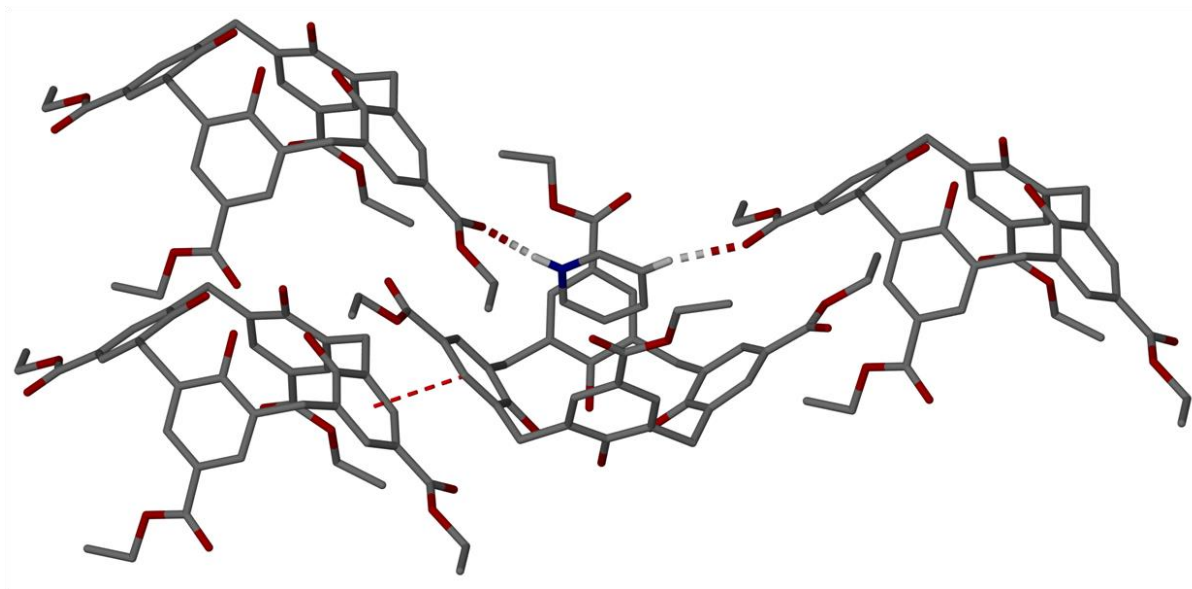


Figure 3.2. Symmetry expansion of the X-ray crystal structure of **3.1**. Hydrogen bonding interactions are shown as split-colour dashed lines and $\pi\cdots\pi$ interactions are shown as red dashed lines. Hydrogen atoms (apart from those involved in hydrogen bonding and $\pi\cdots\pi$ interactions) have been omitted for clarity.

The cavity of compound **36** is occupied by the pyridinium cation and this occurs with two $\text{CH}\cdots\pi$ interactions between the *meta* hydrogen atoms on the $[\text{PyH}]^+$ guest and the aromatic rings on the host. The two symmetry unique interactions are located with H[43] \cdots aromatic centroid and H[45] \cdots aromatic centroid distances of 2.901 and 2.494 Å as shown in Figure 3.1. In addition there is a $\pi\cdots\pi$ stacking interaction located between one of the aromatic rings of the host molecule with another aromatic ring from a symmetry equivalent molecule with an aromatic centroid \cdots aromatic centroid distance of 3.761 Å. Furthermore, there is one $\text{NH}\cdots\text{OCOH}$ hydrogen bonding interaction with a H[1N] \cdots O[12] distance of 1.864 Å between the $[\text{PyH}]^+$ guest and the C=O from the ester functionality of another host (one $\text{CH}\cdots\text{OCOH}$ hydrogen bonding interaction with a H[42] \cdots O[8] distance of 2.307 Å). Symmetry expansion of the asymmetric unit around **3.1** results in the formation of an antiparallel bi-layer arrangement (Figure 3.2) that has been previously seen in literature.³

3.3.2. Structure of tetra-*O*-propoxy-*p*-carboxyethylcalix[4]arene, **37**.

Crystals of tetra-*O*-propoxy-*p*-carboxyethylcalix[4]arene, compound **37**, were obtained from recrystallisation of compound **37** from acetone. Slow evaporation of the solvent overnight yielded small block-shaped crystals which were suitable for *X*-ray diffraction studies. Crystals of compound **37** are in an orthorhombic cell and structure solution was performed in the space group *Pnma*. Details of data collection and structure refinement are given in Table 3.4 at the end of this chapter. The asymmetric unit of compound **37** consists of one half molecule of compound **37** and symmetry expansion reveals the molecule adopts the partial-cone conformation (Figure 3.3).

Tetra-alkylation of the lower-rim leads to the elimination of hydrogen bonding interactions between these groups and subsequent loss of conformational rigidity. However, rather than it being based on previous results where the rotation of an aromatic ring through the annulus of the macrocycle occurs by the addition of relatively short *O*-methoxy and *O*-ethoxy chains,³ it is thought to occur *via* a template effect (Na^+). The shorter the chains the more flexible the molecular scaffold, making it difficult to be able to determine in solution what conformer is present. The inverted propoxy group in compound **37** reduces the size of the cavity, the result of which is that there is no solvent of crystallisation present. There is one symmetry equivalent $\text{CO}\cdots\text{HC}$ bonding between $\text{O}[8]\cdots\text{H}[30\text{B}]$ with a distance of 2.610 Å. The remaining interactions found in the molecule upon symmetry expansion are those between the propoxy hydrogen atoms and the oxygen atoms of the *p*-carboxyethylcalix[4]arene (Figure 3.4). These are shown below in Table 3.2.

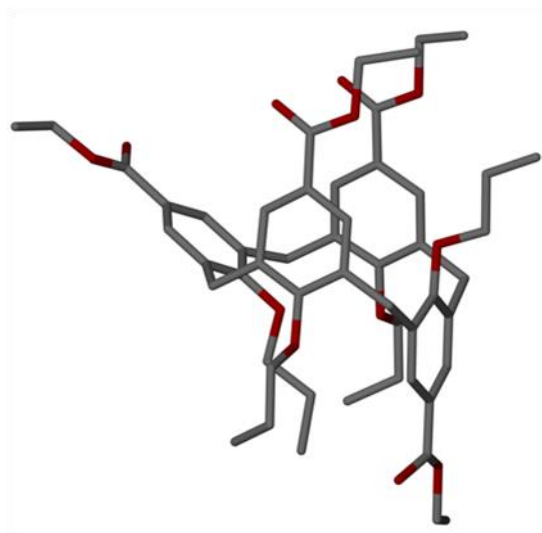


Figure 3.3. X-ray crystal structure of tetra-*O*-propoxy-*p*-carboxyethylcalix[4]arene **37** in the partial-cone conformation.

O[4A]...H[28B]	3.020
O[5]...H[26A]	2.503
O[6]...H[27A]	3.033

Table 3.2. CH...O hydrogen bonding interaction distances (in Å) in the asymmetric unit of compound **37**.

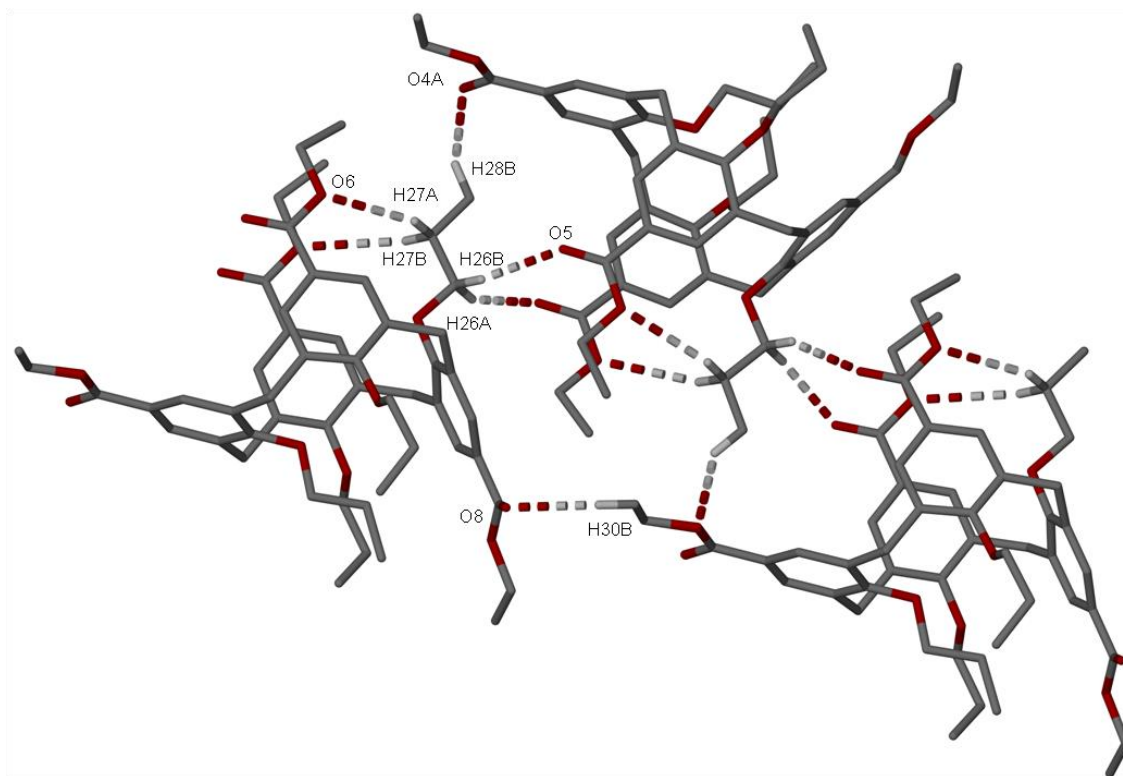


Figure 3.4. Symmetry expansion of the X-ray crystal structure of **3.2**. Hydrogen bonding interactions are shown as split-colour dashed lines. Hydrogen atoms (apart from those involved in hydrogen bonding interactions) have been omitted for clarity. Selected atoms have been labelled according to discussion.

3.3.3. Structure of tetra-*O*-propoxy-*p*-carboxylatocalix[4]arene·DMF, **3.2**.

Crystals of tetra-*O*-propoxy-*p*-carboxylatocalix[4]arene·DMF, **3.2**, were obtained as a result of the addition of 3 mL of DMF to compound **38**. Slow evaporation of the solvent over several weeks yielded small block-shaped crystals which were suitable for X-ray diffraction studies using synchrotron radiation. Crystals of **3.2** are in a monoclinic cell and the structure solution was performed in the space group *C2/c*. Details of data collection and structure refinement are given in Table 3.4 at the end of this chapter. The asymmetric unit of **3.2** consists of one molecule of compound **38** and two co-crystallised molecules of DMF (Figure 3.5).

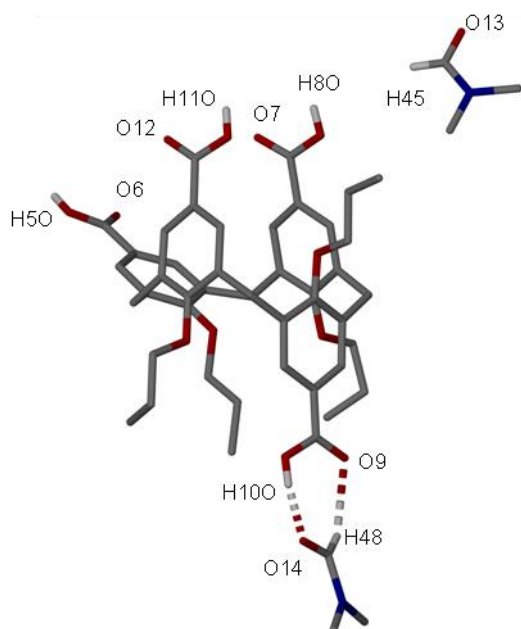


Figure 3.5. The asymmetric unit found in the X-ray crystal structure of **3.2**. Hydrogen bonding interactions are shown as split-colour lines. Hydrogen atoms (apart from those involved in hydrogen bonding) have been omitted for clarity. Selected atoms have been labelled according to discussion.

Based on the structural analysis of compound **37**, compound **38** in **3.2** is observed in the expected partial-cone conformation, where one aromatic ring has inverted through the annulus of the calix[4]arene, resulting in three aromatic rings oriented in a similar direction and one rotated by approximately 180° . One of the crystallographically unique DMF molecules forms hydrogen bonding interactions with the CO_2H group of the rotated aromatic ring ($\text{O}[14]\cdots\text{H}[100]$ and $\text{O}[9]\cdots\text{H}[48]$ distances of 1.777 and 2.423 Å respectively). Symmetry expansion of the asymmetric unit around **3.2** results in the formation of a hydrogen-bonded head-to-head dimer with a symmetry equivalent molecule *via* $\text{OCOH}\cdots\text{OCOH}$ interactions (Figure 3.6). Similar arrangements in the formation of type I carboxylic acid homosynthons have been observed throughout the literature.³ The remaining DMF molecule present in the asymmetric unit is disordered over two positions and was modelled at 50% occupancy in each position. The disordered DMF molecule forms hydrogen bonding interactions with the CO_2H group of the splayed aromatic ring with $\text{O}[13]\cdots\text{H}[50]$ and $\text{O}[6]\cdots\text{H}[45]$ distances of 1.787 and 3.230 Å respectively.

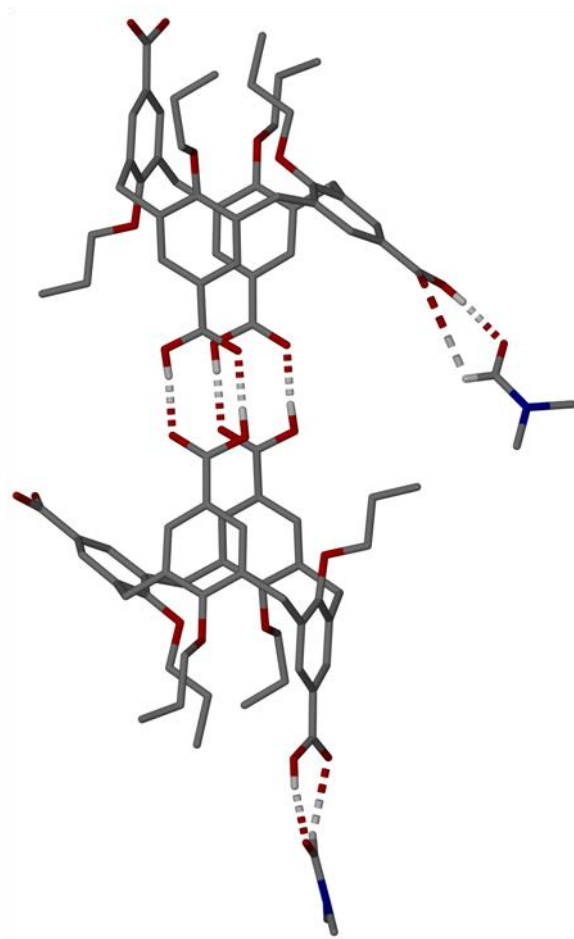


Figure 3.6. Hydrogen-bonded head-to-head dimer assembly observed in the *X*-ray crystal structure of **3.2**. Hydrogen bonding interactions are shown as split-colour dashed lines. Hydrogen atoms (apart from those involved in hydrogen bonding) are omitted for clarity.

Furthermore, there are two OCOH \cdots OCOH hydrogen bonding interactions present with respective H[8O] \cdots O[12] and H[11O] \cdots O[7] distances of 1.820 and 1.805 Å. Examination of the extended structure in **3.2** reveals that molecules pack in an anti-parallel bi-layer array.

3.4. Conclusion.

In conclusion, the synthesis of an unexpected partial-cone $p\text{CO}_2[4]$ (compound **38**) has been presented in this chapter. Single crystal *X*-ray diffraction studies were used in order to follow and confirm the structural changes that occur throughout the synthetic pathway. The assembly of tetra-*O*-alkoxy-*p*-carboxylatocalix[4]arenes in the presence of pyridine-based templates has previously been studied,^{3,11} and it is evident that the presence of the upper-rim ester functionality has a powerful effect on the conformation generated. Alkylation at the lower-rim of all four positions leads to a variety of different conformations. Unlike in the series of di-*O*-alkoxy-di-*p*-carboxylatocalix[4]arenes discussed in Chapter 2 (compounds **20** and **29**), where lower-rim hydrogen bonding interactions lead to the calix[4]arenes adopting the cone conformation, tetra-alkylation gave rise to different conformers due to the loss of this conformational rigidity. Compound **36** adopts the cone conformation when crystallised from Py, attributed to the three hydroxyl groups present at the lower-rim of the macrocycle. Calixarene derivatives **37** and **38** were found to adopt partial-cone conformations when crystallised from acetone and DMF respectively, with the latter forming a hydrogen-bonded head-to-head dimer assembly through complementary interactions.

Future work on the use of partial-cone $p\text{CO}_2[4]$ s could focus on their self- and metal-directed assembly with a view to analyse the effects of this unusual conformation associated with topological directionality.

3.5. Experimental.

3.5.1. General comments.

The majority of work that has been conducted so far has been ligand synthesis, with a view to exploring the self- and metal-directed assembly of all the compounds synthesised.

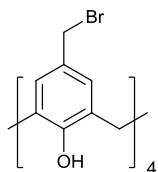
3.5.2. General experimental.

Unless stated, all reagents employed were purchased from chemical suppliers (Alfa Aesar, Fisher Scientific and Sigma Aldrich) and used as received. If required solvents were dried over molecular sieves (pore size 4 Å). Unless stated all experiments were carried out in air. When performed under a nitrogen atmosphere, this was dried over two columns of Drierite® gas purifier connected in series. Analytical thin layer chromatography was performed on precoated silica gel plates (Merck, 60 F254) and column chromatography was performed with silica gel (Merck, particle size 40-60 µm).

Electrospray ionisation and fourier transform mass spectra (ESI-FTMS) were obtained on a LTQ Orbitrap XL spectrometer at Swansea University. ¹H NMR and ¹³C NMR spectra were recorded on Bruker AC 300 and Bruker AC 400 spectrometers, with chemical shifts reported in ppm with respect to TMS as an internal standard. IR spectra were acquired on a Perkin Elmer Spectrum 100 FT-IR Spectrometer, with wavenumber (ν) of absorption reported in cm⁻¹. Single crystals were analysed on either a Bruker Apex II CCD diffractometer operating at 100(2) K with Mo-Kα radiation (λ = 0.71073 Å) with a graphite monochromator or a Bruker D8 diffractometer with PHOTON 100 detector operating at 100(2) K with synchrotron radiation (λ = 0.77490 Å). Microanalysis results were obtained using an Exeter Analytical CE440 Elemental Analyser.

3.5.3. Synthesis of compounds 33 - 38.

5,11,17,23-Tetrakis(bromomethyl)-25,26,27,28-tetrahydroxycalix[4]arene, **33**⁴



A suspension of compound **2** (5.25 g, 0.01 mol) and paraformaldehyde (3.0 g, 0.10 mol) in HBr solution (50 mL, 33% acetic acid) was heated to 50 °C in a 100 mL rbf for 18 hours. After cooling to RT the mixture was poured into a beaker of ice (200 mL) and stirred for a further 30 mins. The product was collected by filtration, washed with water (500 mL) and dried in a desiccator to yield compound **33** (9.5 g, 99%) as a light orange solid.

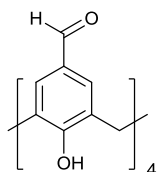
¹H NMR (300 MHz, 25 °C, CDCl₃): δ = 10.10 (s, 4H, OH), 7.12 (s, 8H, ArH), 4.38 (s, 8H, CH₂Br), 4.22 (broad s, 4H, ArCH₂Ar), 3.59 (broad s, 4H, ArCH₂Ar).

¹³C NMR (300 MHz, 25 °C, CDCl₃): δ = 149.00, 148.93, 131.70, 129.96, 129.81, 129.18, 128.76, 128.37, 128.28, 128.19, 127.79, 33.45, 33.32, 31.58.

IR (solid phase, ν cm⁻¹) = 3166m, 2970m, 1704m, 1478m, 1462s, 1204s, 632s.

MS *m/z* observed 797.2002, theoretical 797.1998 [M + H]⁺.

5,11,27,23-Tetraformyl-25,26,27,28-tetrahydroxycalix[4]arene, **34**⁷



A suspension of compound **33** (8.00 g, 10.0 mmol) and HMTA (11.2 g, 80.0 mmol) in glacial acetic acid (50 mL) was added to a 250 mL rbf and stirred at RT for 30 mins. Water (50 mL) was added and the solution was stirred for another 30 mins and heated at reflux for 2 hours before the addition of aqueous HCl (10 mL) and the solution heated for a further 2 hours. The mixture was cooled to RT and the precipitate was collected by filtration and washed sequentially with water (300 mL) before being dried in a desiccator to yield compound **34** (4.60 g, 85%) as a yellow solid.

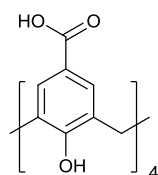
¹H NMR (300 MHz, 25 °C, CDCl₃): δ = 10.10 (s, 4H, OH), 9.68 (s, 4H, CHO), 7.60 (s, 8H, ArH), 4.22 (broad s, 4H, ArCH₂Ar), 3.71 (broad s, 4H, ArCH₂Ar).

¹³C NMR (300 MHz, 25 °C, CDCl₃): δ = 190.16, 153.91, 131.58, 131.43, 128.15, 31.36.

IR (solid phase, ν cm⁻¹) = 3160m, 2988s, 2901s, 1752m, 1681s, 1597s, 1455m, 1293s.

MS *m/z* observed 554.1798, theoretical 554.1809 [M + NH₄]⁺, 559.1363 [M + Na]⁺.

p-Carboxylato-25,26,27,28-tetrahydroxycalix[4]arene, **35**⁵



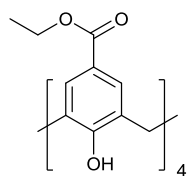
In a 250 mL rbf a suspension of compound **34** (3.83 g, 7.14 mmol), and NaH₂PO₄ (0.85 g, 6.18 mmol, in 10 mL water) were dissolved in 70 mL DMSO. A solution of NaClO₂ (6.42 g, 0.07 mol) in 60 mL water was added drop-wise over an hour. The reaction mixture was left to stir at RT for 24 hours. The solution was acidified with HCl (10 mL) and the yellow precipitate was collected by filtration to yield compound **35** (3.44 g, 80%).

Attempts to obtain ¹H NMR and ¹³C NMR spectroscopic data on compound **35** were thwarted by poor solubility, but subsequent reaction shows its formation.

IR (solid phase, ν cm⁻¹) = 3149m, 2987m, 2876m, 1676s, 1604s, 1434m, 1280s, 1192s.

MS m/z observed 601.5405, theoretical 601.5403 [M + H]⁺.

p-Carboxyethyl-25,26,27,28-tetrahydroxycalix[4]arene, **36**



A suspension of compound **35** (4.00 g, 6.66 mmol) and *p*-toluenesulfonic acid (12.70 g, 0.07 mol) in EtOH (250 mL) was added to a 500 mL rbf and the solution was heated at reflux for one week. The solvent was removed under reduced pressure, and the residue dissolved in DCM (300 mL) and washed twice with saturated NaHCO₃ (150 mL) and water (150 mL). The organic layer was dried over MgSO₄, and the solvent was removed under reduced pressure to afford compound **36** as a brown solid (3.44 g, 72%).

¹H NMR (300 MHz, 25 °C, CDCl₃): δ = 10.17 (s, 4H, OH), 7.85 (s, 8H, ArH), 4.34 (q, 8H, OCH₂CH₃), 4.26 (broad s, 4H, ArCH₂Ar), 3.75 (broad s, 4H, ArCH₂Ar), 1.38 (t, J = 4.2 Hz, 12H, OCH₂CH₃).

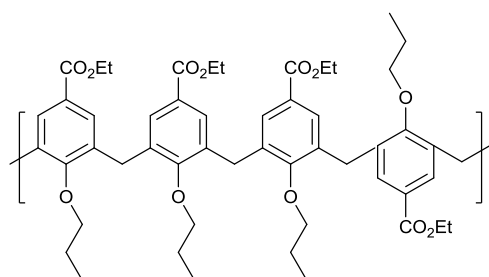
¹³C NMR (300 MHz, 25 °C, CDCl₃): δ = 165.70, 152.57, 131.16, 127.48, 124.89, 60.88, 31.42, 14.37.

IR (solid phase, ν cm⁻¹) = 3192m, 2978m, 2928m, 2360w, 1711s, 1607m, 1307s, 1281s, 1187s.

Anal. Calcd. For C₄₀H₄₀O₁₂: C, 67.41; H, 5.66. *Found*: C, 66.84; H, 5.63.

MS m/z observed 730.2859, theoretical 730.2858 [M + NH₄]⁺.

Tetra-*O*-propoxy-*p*-carboxyethylcalix[4]arene, **37**



To a 250 mL rbf was added compound **36** (1.00 g, 1.40 mmol) dissolved in 50 mL DMF before NaH (60%, 0.48 g, 11.90 mmol) was added and the mixture was allowed to stir at RT for 30 mins. After this time 1-iodopropane (1.16 mL, 0.01 mol) was added and the solution

was heated at 80 °C for an hour. Excess NaH was quenched by the addition of MeOH and the solvents removed under reduced pressure to afford a yellow solid. The yellow crude was washed with water and filtered before being dissolved in hot acetone and compound **37** crystallised out as colourless block crystals (0.84 g, 68 %).

¹H NMR (300 MHz, 25 °C, CDCl₃): δ = 8.0 (s, 2H, ArH), 7.88 (s, 2H, ArH), 7.67 (s, 2H, ArH), 7.01 (s, 2H, ArH), 4.42 (m, 4H, OCH₂CH₃), 4.23 (m, 6H, OCH₂CH₃), 4.08 (d, *J* = 12.0 Hz, 2H, ArCH₂Ar), 3.81 (q, *J* = 6.8 Hz, 4H, OCH₂CH₂CH₃), 3.75 (s, 4H, ArCH₂Ar), 3.59 (q, *J* = 6.8 Hz, 2H, OCH₂CH₃), 3.24 (q, *J* = 7.0 Hz, 2H, OCH₂CH₃), 3.15 (d, *J* = 12.0 Hz, 2H, ArCH₂Ar), 2.12 (q, *J* = 7.0 Hz, 2H, OCH₂CH₂CH₃), 1.93 (q, *J* = 6.8 Hz, 2H, OCH₂CH₂CH₃), 1.41 (m, 5H, overlap of OCH₂CH₃ and OCH₂CH₂CH₃), 1.29 (t, *J* = 7.4 Hz, 6H, OCH₂CH₂CH₃), 1.13 (m, 10H, overlap of 3 X OCH₂CH₂CH₃ and OCH₂CH₃), 0.64 (t, *J* = 7.4 Hz, 3H, OCH₂CH₂CH₃).

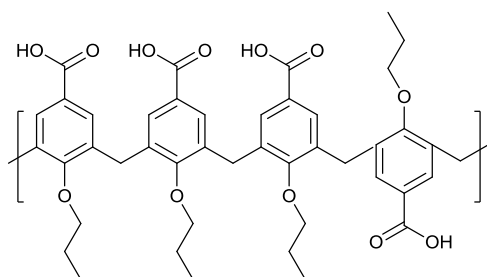
¹³C NMR (300 MHz, 25 °C, CDCl₃): δ = 166.78, 166.65, 166.07, 161.56, 160.90, 159.47, 136.34, 133.77, 133.32, 132.37, 131.47, 131.30, 130.91, 130.25, 124.82, 123.97, 123.92, 76.42, 75.72, 74.84, 60.78, 60.49, 60.21, 35.73, 30.93, 30.37, 23.71, 21.86, 14.45, 14.38, 14.20, 10.90, 10.73, 9.05.

IR (solid phase, ν cm⁻¹) = 3663w, 2969m, 1714s, 1600m, 1283s, 1187s.

Anal. Calcd. For C₅₂H₆₄O₁₂: C, 70.89; H, 7.32. *Found*: C, 69.56; H, 7.28.

MS *m/z* observed 898.4740, theoretical 898.4736 [M + NH₄]⁺.

Tetra-*O*-propoxy-*p*-carboxylatocalix[4]arene, **38**



A mixture of compound **37** (0.31 g, 0.35 mmol) and NaOH (0.17 g, 4.18 mmol) were dissolved in a mixture of THF, MeOH and water (2:1:1, 5 mL) and the reaction heated at 50 °C for 3 days. The solution was acidified with 1M HCl, diluted with EtOAc and washed with water (2 X 50 mL) followed by brine (2 X 50 mL). The solution was dried over MgSO₄ and the solvents evaporated to give compound **38** as a yellow solid (63.0 mg, 24%).

¹H NMR (300 MHz, 25 °C, DMSO-*d*⁶): δ = 12.23 (bs, 4H, COOH), 7.92 (s, 2H, ArH), 7.87 (s, 2H, ArH), 7.59 (s, 2H, ArH), 6.96 (s, 2H, ArH), 4.01 (m, 2H, OCH₂CH₂CH₃), 3.94 (d, *J* = 12.0 Hz, 2H, ArCH₂Ar), 3.74 (m, 10H, overlap of OCH₂CH₂CH₃ and ArCH₂Ar), 3.42 (m, 2H, OCH₂CH₂CH₃), 3.20 (d, *J* = 12.0 Hz, 2H, ArCH₂Ar), 1.91 (m, 2H, OCH₂CH₂CH₃), 1.74 (m, 4H, OCH₂CH₂CH₃), 1.08 (t, *J* = 7.4 Hz, 6H, OCH₂CH₂CH₃), 0.92 (t, *J* = 7.2 Hz, 3H, OCH₂CH₂CH₃), 0.55 (t, *J* = 7.2 Hz, 3H, OCH₂CH₂CH₃).

¹³C NMR (300 MHz, 25 °C, DMSO-*d*⁶): δ = 167.46, 166.78, 160.99, 159.09, 136.17, 133.27, 132.81, 132.52, 131.60, 131.16, 130.43, 23.04, 22.88, 10.67, 10.22, 8.90.

IR (solid phase, ν cm⁻¹) = 2961m, 2931m, 2875m, 1711s, 1676s, 1599m, 1424m, 1308s, 1283s, 1186s.

Anal. Calcd. For C₄₄H₄₈O₁₂: C, 68.74; H, 6.29. *Found*: C, 68.16; H, 6.08.

MS *m/z* observed 769.8901, theoretical 769.8896 [M + H]⁺.

3.5.4. X-ray details of data collection/structure refinement for compounds 37, 3.1 - 3.2.

Complex number	3.1	37	3.2
Formula	C ₄₅ H ₄₅ NO ₁₂	C ₅₂ H ₆₄ O ₁₂	C ₅₀ H ₆₂ N ₂ O ₁₄
<i>Mr</i>	791.82	881.03	915.02
Crystal system	Monoclinic	Orthorhombic	Monoclinic
Space group	<i>P</i> 2 ₁ / <i>n</i>	<i>Pnma</i>	<i>C</i> 2/ <i>c</i>
<i>T</i> /K	100(2)	100(2)	100(2)
<i>a</i> /Å	9.3836(3)	17.0322(13)	37.3004(15)
<i>b</i> /Å	20.4700(7)	16.7264(11)	14.2873(6)
<i>c</i> /Å	20.3370(7)	17.3355(13)	18.2486(8)
α /°	90	90	90
β /°	98.885(2)	90	93.557(2)
γ /°	90	90	90
<i>U</i> Å ³	3859.5(2)	4938.7(6)	9706.3(7)
<i>Z</i>	4	4	8
<i>F</i> (000)	1672	1888	3904
<i>D_c</i> /g cm ⁻³	1.363	1.185	1.252
μ /mm ⁻¹	0.119	0.083	0.110
2 θ_{max} /°	62.3	49.5	52.4
Data collected	58367	26905	54147
Unique data	9613	4394	7495
<i>R_{int}</i>	0.0490	0.0818	0.0512
Obs data (<i>I</i> >2 σ (<i>I</i>))	7285	3429	5993
Parameters	527	307	569
Restraints	0	8	29
<i>R</i> ₁ (observed data)	0.0618	0.1277	0.1240
ωR_2 (all data)	0.1546	0.2703	0.3633
<i>GooF</i>	1.101	1.630	2.978
Max/min residuals [e.Å ⁻³]	0.87/-0.31	1.77/-0.99	1.40/-0.94

Table 3.3. Details of data collection and structure refinement for complexes **37**, **3.1** - **3.2**.

3.6. References.

1. For examples of large assemblies see a) L. R. MacGillivray and J. L. Atwood, *Nature*, 1997, **389**, 469. b) G. W. Orr, L. J. Barbour and J. L. Atwood, *Science*, 1999, **285**, 1049. c) J. L. Atwood, L. J. Barbour, S. J. Dalgarno, M. J. Hardie, C. L. Raston and H. R. Webb, *J. Am. Chem. Soc.*, 2004, **126**, 13170. d) S. J. Dalgarno, S. A. Tucker, D. B. Bassil and J. L. Atwood, *Science*, 2005, **309**, 2037. e) X. Liu and R. Warmuth, *J. Am. Chem. Soc.*, 2006, **128**, 14120 and references therein.
2. S. J. Dalgarno, K. M. Claudio-Bosque, J. E. Warren, T. E. Glass and J. L. Atwood, *Chem. Commun.*, 2008, 1410.
3. S. Kennedy, C. M. Beavers, S. J. Teat and S. J. Dalgarno, *Cryst. Growth Des.*, 2012, **12**, 679.
4. T. D. Guo, Q. Y. Zheng, L. M. Yang and Z. T. Huang, *J. Incl. Phen. Macro. Chem.* 2000, **36**, 327.
5. Q. Lin and A. D. Hamilton, *C. R. Chimie* 2002, **5**, 441.
6. A. Arduini, S. Fanni, G. Manfredi, A. Pochini, R. Ungaro, A. R. Sicuri and F. Uguzzoli, *J. Org. Chem.* 1995, **60**, 1448.
7. a) A. Decken, P. D. Harvey and J. Douville, *Acta Cryst., Sect. E: Struct. Rep. Online* 2004, **60**, 1170. b) O. Ediz, M. Tabakci, S. Memon, M. Yilmaz and D. M. Roundhill, *Supramol. Chem.* 2004, **16**, 199. c) V. Arora, H. M. Chawla and A. Santra, *Tetrahedron* 2002, **58**, 5591. d) H. M. Chawla and A. Santra, *Synth. Commun.* 2001, **31**, 2605. e) T. Komori and S. Shinkai, *Chem. Lett. Chem. Soc. Japan.* 1992, 901. f) A. Arduini, G. Manfredi, A. Pochini, A. R. Sicuri and R. Ungaro, *J. Chem. Soc., Chem. Commun.* 1991, 936.
8. C. D. Gutsche, B. Dhawan, J. A. Levine, K. H. No and L. J. Bauer, *Tetrahedron* 183, **39**, 409.
9. C. Jaime, J. de Mendoza, P. Prados, P. M. Nieto and C. Sánchez, *J. Org. Chem.* 1991, **56**, 3372.
10. G. Yang, C. Jin, Y. Li, J. Hong, R. Miao, C. Zhao, Z. Guo and L. Zhu, *J. Incl. Phen. Macro. Chem.* 2005, **52**, 119.
11. S. Kennedy, C. M. Beavers, S. J. Teat and S. J. Dalgarno, *CrystEngComm.*, 2014, **16**, 3655.

Chapter 4: Calix[4]arenes fixed in a rigid cone conformation by selective lower-rim functionalisation.

4.1. Introduction.

This chapter is concerned with the lower-rim modification of calix[4]arenes with ethylene glycol ditosylate bridges in order to prevent interconversion between conformers and keep the calixarene held in the cone conformation, generating a library of novel $p\text{CO}_2[4]\text{s}$. The X-ray crystal structures for some of the different macrocycles synthesised have been obtained and will be discussed. Furthermore, the pyridine-templated assembly of the compounds synthesised was studied and results are presented in all cases that single crystals were obtained.

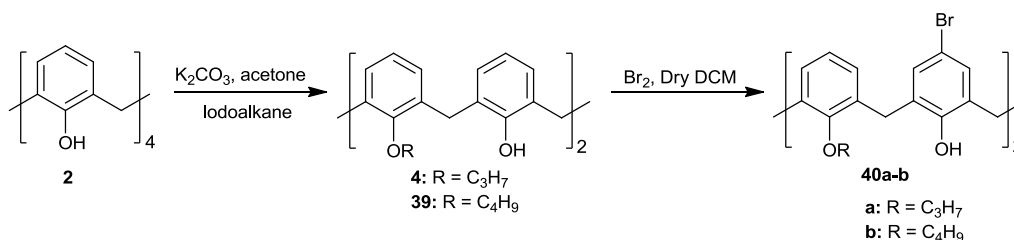
As stated previously, the introduction of bulky substituents onto the lower-rim of the calixarene can prevent the molecular framework from interconverting between its four possible conformers. Stereochemistry can be controlled depending on the reaction conditions employed during synthesis, as have been successful for lower-rim alkylation reactions.¹ As discussed in Chapter 2, di-*O*-alkoxy-di-*p*-carboxylatocalix[4]arenes adopt the cone conformation as a result of hydrogen bonding interactions at the lower-rim of the macrocycle. However, when tetra-alkylation is implemented at the lower-rim, a number of different conformations can be obtained owing to the flexibility of the macrocycle.

In order to increase the rigidity of C[4] **2**, the introduction of lower-rim tethering bridges has been explored. One family of molecules looked at were calix[4]arene-crown-4 and calix[4]arene-*bis*-crowns, which can be synthesised by reacting compound **2** with ethylene glycol ditosylates of varying length. This modification prevents it from interconverting between the four possible C[4] conformers, keeping it locked in the cone conformation as a result.

4.2 Calix[4]arene-crown ethers.

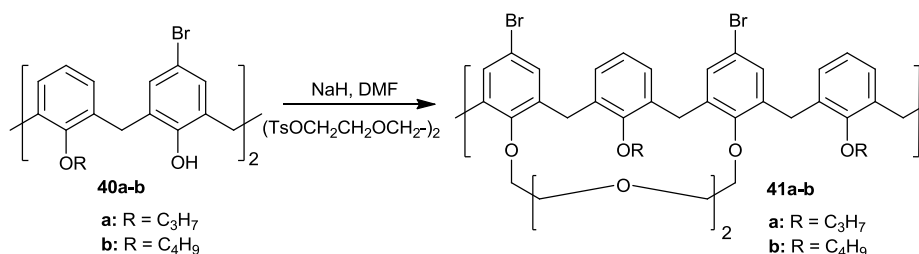
Calix[4]arene-crown ethers (or calix[4]crowns) are C[4]s that contain polyether chains on the lower-rim that bridge two of the aryl units. They have been shown to exhibit an affinity for alkali metal ions and can be easily modified by changing the size of the

crown ether loop.²⁻⁵ There are two groups into which the calix[4]crowns can be split, namely monocrowns and biscrowns. For the monocrown, bridging on the lower-rim can be between either the 1,3-⁶ or the 1,2-positions⁷ (distal and proximal phenol units respectively). The 1,3-bridged calix[4]-crowns have generally attracted more attention than their 1,2-bridged analogues due to the more difficult synthesis of the latter. Biscrowns can also bridge in different ways depending on the particular C[4] conformation: these can be 1,3;2,4 (1,3-alternate C[4]); or 1,2;3,4 (cone C[4]). The work in this section began by first looking at introducing one glycol chain onto the lower-rim of the C[4] framework. To allow the introduction of only one linking tether bridge, it was necessary to di-alkylate the remaining two hydroxyl sites using K_2CO_3 and an iodoalkane,⁸ as discussed in Chapter 2, to form di-*O*-propoxycalix[4]arene **4** and di-*O*-butoxycalix[4]arene **39**. Bromine solution was then used to selectively brominate the *para*-position of the phenyl group to give the halogenated calixarenes **40a-b** (Scheme 4.1).⁹



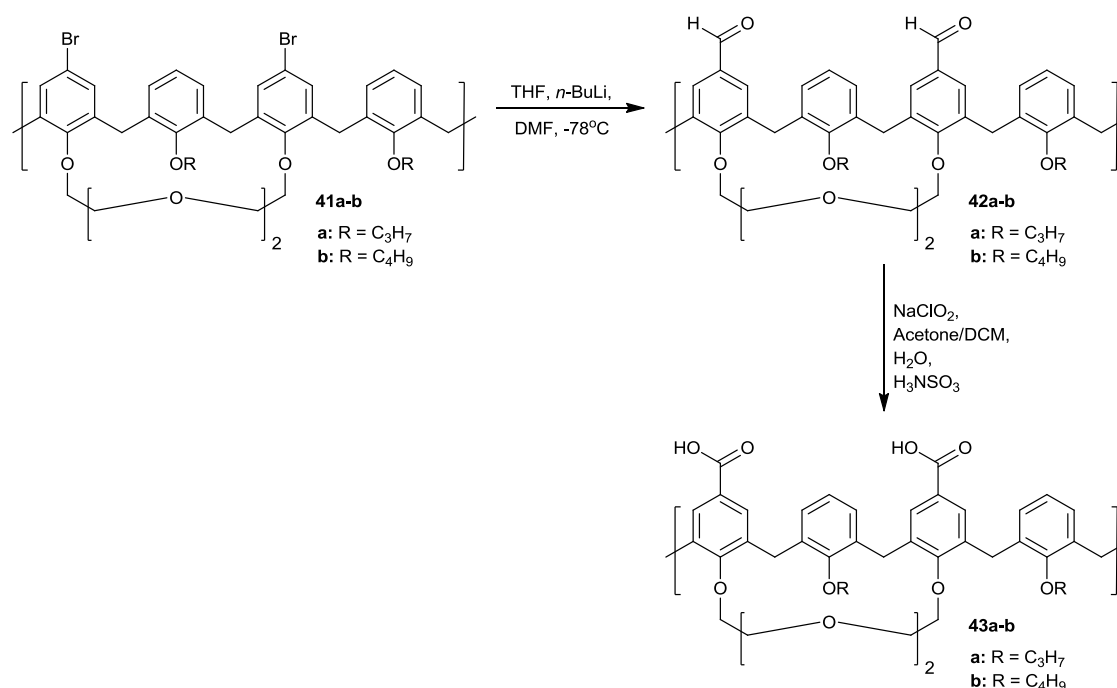
Scheme 4.1. Synthesis of di-*O*-alkoxycalix[4]arenes and subsequent dibromination.

The dibromocalix[4]arene-crown-4 derivatives **41a-b** were obtained by stirring a mixture of **40a-b** in DMF with NaH, followed by the drop-wise addition of triethylene glycol ditosylate.¹⁰ An intramolecular cyclisation reaction of the dibromo-dialkoxycalix[4]arenes with triethylene glycol ditosylate occurs to give the favoured product (Scheme 4.2) over oligomerisation due to high dilution conditions and more importantly, the template effect promoted by the presence of Na^+ .



Scheme 4.2. Synthesis of dibromocalix[4]arene-crown-4 derivatives **41a-b**.

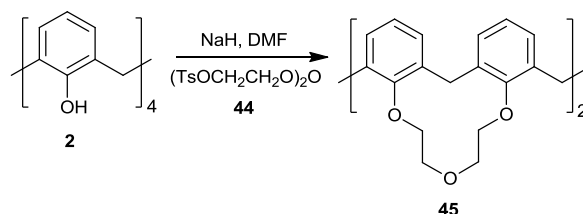
Following this, compounds **41a-b** were dilithiated by reaction with *n*-BuLi in THF at -78°C and quenched with dry DMF¹¹ to give the dialdehydes **42a-b** shown in Scheme 4.3. These were then oxidised with aqueous solutions of sodium chlorite and sulfamic acid¹² to yield calix[4]arenedicarboxylic acids **43a-b** in good yields.



Scheme 4.3. Dilithiation of compounds **41a-b** followed by subsequent oxidation to yield compounds **43a-b**.

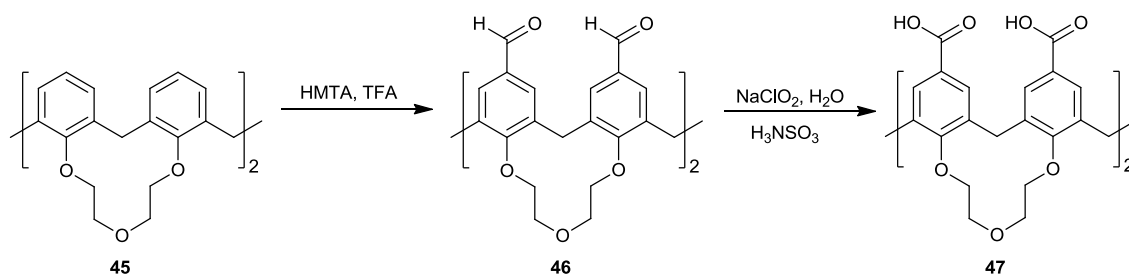
With the synthesis of monocrown derivatives **43a-b** achieved, the focus shifted to introducing two glycol bridges at the C[4] lower-rim. The di(ethylene glycol)di-*p*-tosylate precursor to be attached to the lower-rim was prepared according to a straightforward literature procedure.¹³ Diethylene glycol was reacted with NaOH in water before tosyl chloride was added drop-wise at 0 °C. Once the reaction was complete (3 hours) the crude product was filtered and purified by recrystallisation in

EtOH to give diethylene glycol ditosylate **44** as white crystalline needles. The next step in the synthetic route followed a procedure reported by Ungaro *et al.*¹⁴ which involved reacting a DMF solution of compounds **2** and **44** in the presence of an excess of NaH. This afforded a proximal biscrown that is now held in a cone *pseudo*- C_{4v} conformation, leaving the upper-rim free for further modification/functionalisation (Scheme 4.4). The crude product of this reaction was purified by column chromatography to afford compound **45** as a fine white powder.



Scheme 4.4. Schematic representation of the formation of calix[4]arene-biscrown-3, **45**.

As stated above, restricting the compound with these relatively rigid chains prevents conformational interconversion and leaves the upper-rim amenable to further functionalisation. Compound **45** was reacted with TFA and an excess of HMTA over a 24 hour period¹⁵ to produce the tetraformyl-calix[4]arene-biscrown-3 **46** (Scheme 4.5). The reaction mixture was neutralised with sodium carbonate, extracted and dried, to afford an off-white crude product. ^1H NMR reveals the presence of the target compound and a small amount of the *tris*-formylated biscrown-C[4]. Column chromatography was therefore carried out to separate these two products; it was found that the yield of the *tris*-formylated product was minimal in comparison to that of compound **46**. Subsequent reactions were carried out for longer periods at reflux and this was found to give full conversion from compound **45** to compound **46**. Although this is the case it is also worth noting that, should one wish to isolate the *tris*-functionalised biscrown-C[4], shorter reaction times offer a relatively convenient route to that particular compound. A Pinnick-type oxidation was the final step required to oxidise the aldehydic groups to the desired acids (compound **47**, Scheme 4.5), and this was carried out in water with sodium chlorite and sulfamic acid.¹²



Scheme 4.5. Formylation reaction of compound **45** followed by oxidation.

As discussed in Chapter 1, there is already an expanding series of *p*-CO₂[4]s that utilise Py templates in the formation of non-covalent assemblies.¹⁶ An area of greater interest lies in the metal-directed assembly of these calixarenes; there has been much activity in the use of metal-ligand interactions to programme the assembly of a diverse range of metallocsupramolecular architectures.¹⁷⁻¹⁹ In this regard it is well known that benzoates have proven useful in the formation of discrete polynuclear metal clusters^{20,21} and metal-organic frameworks.^{22,23} Transition metal ions such as Ni²⁺, Mn²⁺ and Co²⁺ are known to form binuclear aqua-bridged complexes in the presence of benzoic acids and *N*-donor ligands, and have been investigated as potential directing centres, enabling control over *p*-CO₂[4] assembly.²⁴

With the synthesis of compounds **43a-b** and **47** achieved their potential to undergo self-assembly was explored by attempted crystallisation from a series of commercially available (predominantly) pyridine containing solvents; these were pyridine (Py), 2-picoline (2-Pic), 3-picoline (3-Pic) and 4-picoline (4-Pic). Acetone and DMF were also used in the hope of generating suitable crystals. In addition to this, an investigation into the use of 2-aminopyridine (2-AP) as a pyridine-based template was executed. Finally the metal-directed assembly of compound **47** was examined. All of these crystallisations and reactions resulted in the formation of seven sets of single crystals, the structural analyses of which are discussed in detail below.

4.3. X-ray crystal structures of compounds **42b**, **43a** and **47**.

Calix[4]arene derivatives **43a-b**, and **47** were synthesised as outline above and ¹H NMR spectra recorded for each compound indicated that the dominant conformers for compounds **43a-b** and **47** were pinched-cone and cone respectively. The structure of compounds **42b**, **43a** and **47** were determined by X-ray crystallography. The slight

difference in conformation for compounds **42b**, **43a** and **47** is governed by the addition of a second glycol bridge in place of *O*-alkyl chains attached to the lower-rim, further restricting conformational flexibility.

4.3.1. Structure of di-*O*-butoxy-di-*p*-formylcalix[4]arene-crown-4, **42b**.

Crystals of di-*O*-butoxy-di-*p*-formylcalix[4]arene-crown-4 **42b**, were obtained by recrystallisation of compound **42b** from acetone. Slow evaporation overnight afforded small colourless lath-shaped crystals and these were found to be weakly diffracting. As a result of this they required synchrotron radiation in order to obtain data of sufficient resolution to afford a satisfactory structure solution. Single crystals of compound **42b** were found to be in an orthorhombic cell and structure solution was performed in the space group *Pna*2₁. Details of the collection and structure refinement are given in Table 4.4 at the end of this chapter. The asymmetric unit consists of one molecule of **42b** as shown in Figure 4.1.

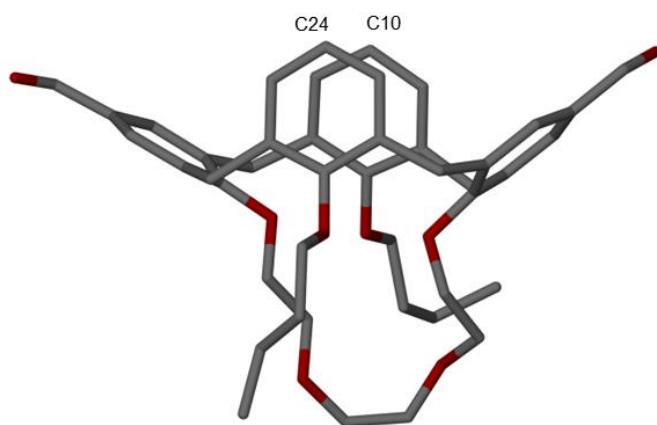


Figure 4.1. The asymmetric unit found in the crystal structure of compound **42b**. Selected atoms have been labelled according to discussion.

The ¹H NMR spectrum for compound **42b** reveals the presence of a pair of doublets at 3.21 and 4.37 ppm which is indicative of a calix[4]arene in a cone conformation. The cone conformer arises as a direct result of both the length of the *O*-butoxy chains and the triethylene glycol bridge at the lower-rim of the macrocycle. Structural studies showed that this was in fact a pinched-cone conformer in which two of the aromatic rings splay outward and two point inwards, effectively blocking the cavity to guest

molecules; proximal carbon atoms in the pinched upper-rim groups are separated by a C[10]...C[24] distance of 3.960 Å (Figure 4.1). Expansion of the asymmetric unit showed two crystallographically unique CH...O interactions. This hydrogen bonding occurs on both sides of **42b**, with one CH...OCH and one HCO...HCO interaction. The first is between one aldehydic oxygen and a *meta* hydrogen atom from the aromatic ring of a symmetry equivalent molecule of **42b**, with an O[7]...H[16] distance of 2.540 Å. The second is from the other aldehydic oxygen with the aldehydic proton from a symmetry equivalent molecule of **42b**, with an O[8]...H[29] distance of 2.814 Å (Figure 4.2).

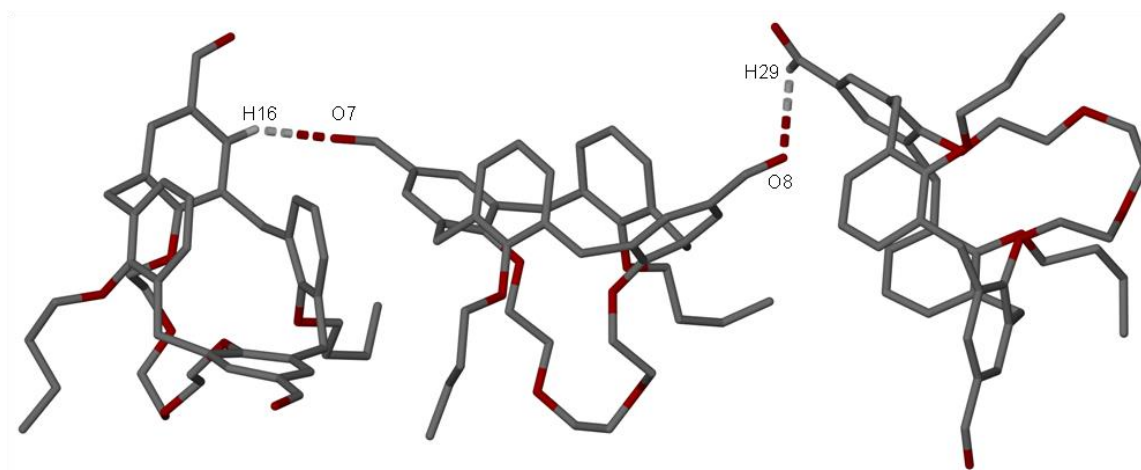


Figure 4.2. Symmetry expansion of the *X*-ray crystal structure of **42b**. Hydrogen bonding interactions are shown as split-colour dashed lines. Hydrogen atoms (apart from those involved in hydrogen bonding interactions) have been omitted for clarity. Selected atoms have been labelled according to discussion.

4.3.2. Structure of di-*O*-propoxy-di-*p*-carboxylatocalix[4]arene-crown-4·DMF, **4.1**.

Crystals of di-*O*-propoxy-di-*p*-carboxylatocalix[4]arene-crown-4·DMF, **4.1**, were obtained by recrystallisation of compound **43a** from DMF. Slow evaporation of the solvent over several days yielded colourless tablets that were suitable for *X*-ray diffraction studies. These crystals were also found to be weakly diffracting, so were studied using synchrotron radiation in order to obtain data of sufficient quality for structure solution. Single crystals of **4.1** were found to be in a triclinic cell and the structure solution was performed in the space group *P*-1. Details of data collection and structure refinement are given in Table 4.4 at the end of this chapter. The asymmetric unit in **4.1** consists of one molecule of **43a** and one DMF (Figure 4.3). Compound **43a**

was also found to adopt a pinched cone conformation, a feature also attributable to the two propyl chains present at the lower-rim of the macrocycle. The proximal carbon atoms in the pinched upper-rim groups are separated by a C[10]...C[24] distance of 3.837 Å, preventing guest molecules from accessing the cavity. The DMF molecule in the asymmetric unit forms hydrogen bonding interactions with one of the CO₂H groups with O[11]...H[70] and O[8]...H[43] distances of 1.777 and 2.773 Å respectively (Figure 4.3). One of the propoxy chains present in the asymmetric unit is disordered over two positions and was modelled at 50% occupancy in each position.

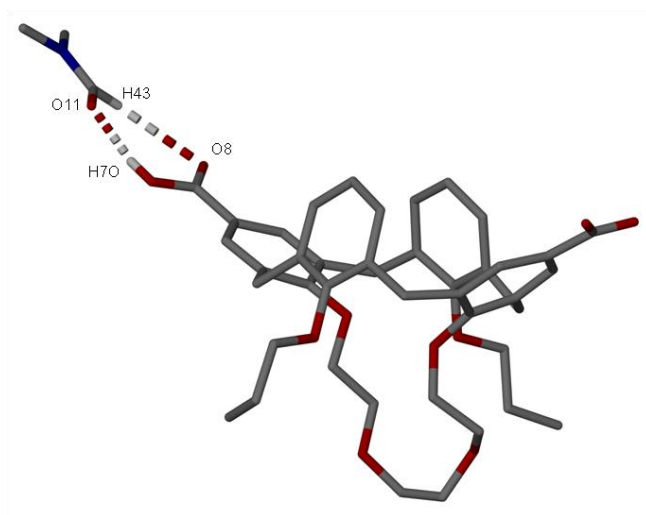


Figure 4.3. The asymmetric unit in the X-ray crystal structure of **4.1**. Hydrogen bonding interactions are shown as split-colour dashed lines. Hydrogen atoms (apart from those involved in hydrogen bonding interactions) have been omitted for clarity. Selected atoms have been labelled according to discussion.

The remaining interactions of note found in **4.1** are revealed upon symmetry expansion of the asymmetric unit (Figure 4.4). The first of these is a CH... π interaction located between a hydrogen atom from the DMF of crystallisation and an aromatic ring of compound **43a**; this occurs with a H[44A]...aromatic centroid distance of 3.090 Å. The second is an OCOH...O interaction between the proton of one carboxylic acid group and an oxygen in a symmetry equivalent triethylene glycol chain with an H[100]...O[5] distance of 1.811 Å. Finally there is an HOCO...H interaction between the oxygen atom of the same carboxylic acid and a hydrogen atom from the ether bridge with an O[9]...H[31A] distance of 3.026 Å.

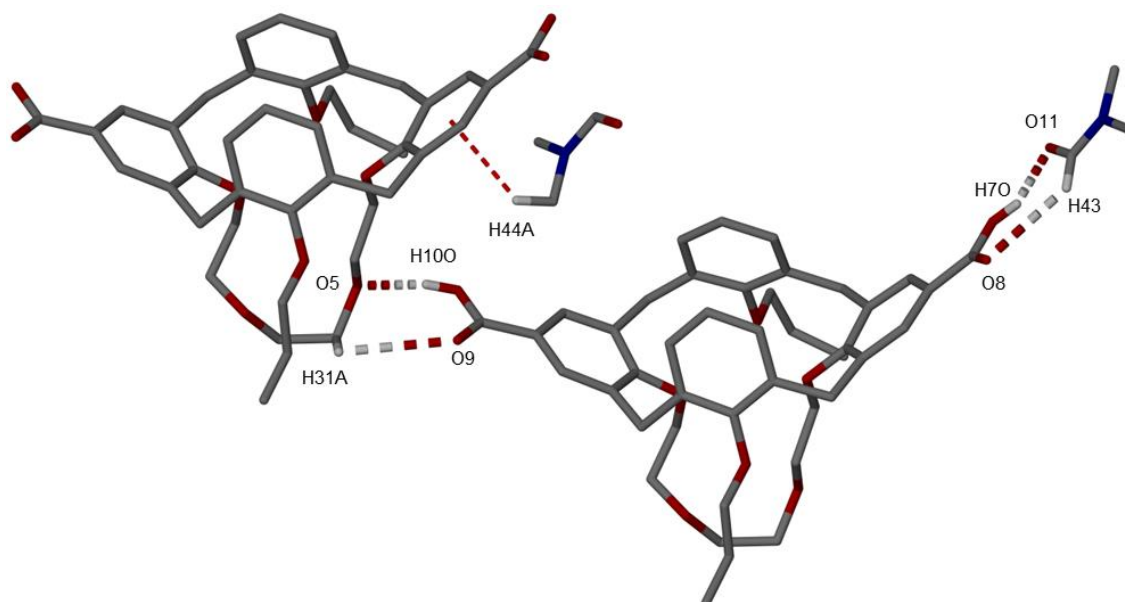


Figure 4.4. Symmetry expansion around complex **4.1**. Hydrogen bonding and CH $\cdots\pi$ interactions are shown as split-colour and red dashed lines respectively. Hydrogen atoms (apart from those involved in hydrogen bonding and CH $\cdots\pi$ interactions) have been omitted for clarity. Selected atoms have been labelled according to discussion.

4.3.3. Structure of di-*O*-propoxy-di-*p*-carboxylatocalix[4]arene-crown-4pyridine, **4.2**.

Crystals of di-*O*-propoxy-di-*p*-carboxylatocalix[4]arene-crown-4Py, **4.2**, were obtained as a result of the addition of 2 mL of Py to compound **43a**. Slow evaporation of the solvent over a period of several days yielded small colourless blocks that were suitable for X-ray diffraction studies by synchrotron radiation in order to obtain an adequate structure solution. Single crystals of **4.2** were found to be in a monoclinic cell and the structure solution was performed in the space group *P2/c*. Details of the collection and structure refinement are given in Table 4.4 at the end of this chapter. The asymmetric unit in **4.2** consists of one molecule of **43a** and two Py of crystallisation. Inspection showed that compound **43a** adopts a pinched cone conformation, as seen previously in Figure 4.3.

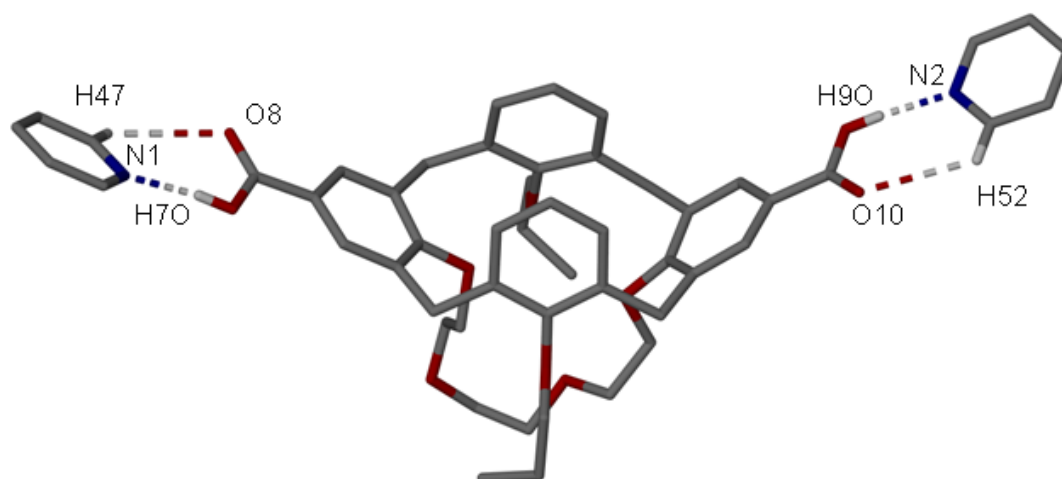


Figure 4.5. The asymmetric unit in the X-ray crystal structure of **4.2**. Hydrogen bonding interactions are shown as split-colour dashed lines. Hydrogen atoms (apart from those involved in hydrogen bonding interactions) have been omitted for clarity. Selected atoms have been labelled according to discussion.

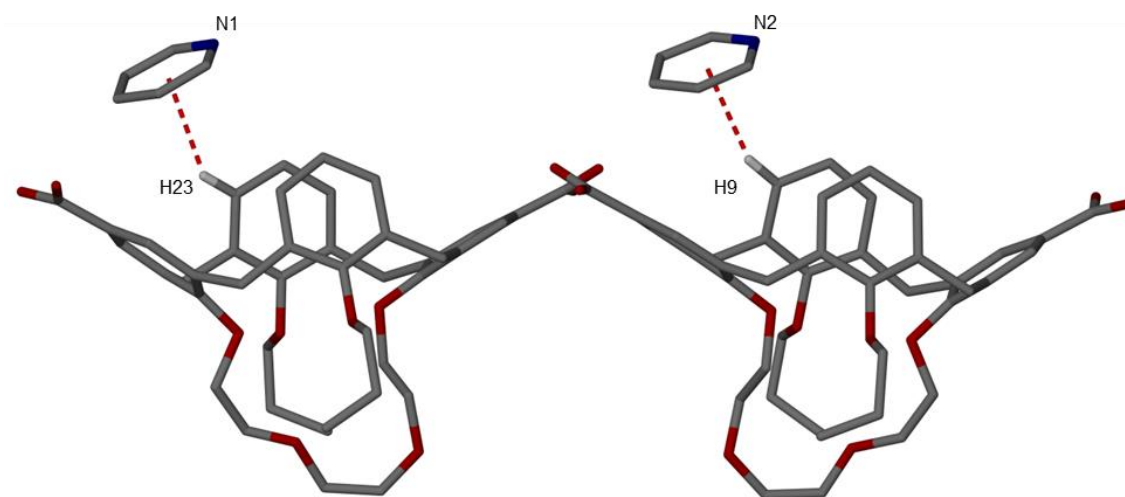


Figure 4.6. Symmetry expansion around molecule **4.2**. $\text{CH}\cdots\pi$ interactions are shown as red dashed lines. Hydrogen atoms (apart from those involved in $\text{CH}\cdots\pi$ interactions) have been omitted for clarity. Selected atoms have been labelled according to discussion.

The two Py molecules in the asymmetric unit interact with the upper-rim CO_2H groups *via* the common $\text{Py}\cdots\text{CO}_2\text{H}$ heterosynthon. There are two symmetry unique $\text{N}\cdots\text{HOCO}$ hydrogen bonding interactions between $\text{N}[1]\cdots[\text{H7O}]$ and $\text{N}[2]\cdots[\text{H9O}]$ with distances of 1.804 and 1.772 Å respectively. There are also two unique $\text{CH}\cdots\text{OCOH}$ interactions separating $\text{O}[8]\cdots\text{H}[47]$ and $\text{O}[10]\cdots\text{H}[52]$ by distances of 2.790 and 2.739 Å

respectively. Examination of the extended structure in **4.2** reveals that the molecules pack in a commonly seen bi-layer fashion. There are two CH $\cdots\pi$ interactions located between *meta* hydrogen atoms on the unsubstituted aromatic rings of the host and the aromatic rings of the Py guest. The two symmetry unique interactions are located with H[9] \cdots aromatic centroid and H[23] \cdots aromatic centroid distances of 2.728 and 2.789 Å as shown in Figure 4.6.

4.3.4. Structure of *p*-carboxylatocalix[4]arene-biscrown-3'4-picoline, **4.3**.

Crystals of *p*-carboxylatocalix[4]arene-biscrown-3'4-Pic, **4.3**, were obtained as a result of the addition of 2 mL of 4-Pic to a sample of compound **47**. Slow evaporation of the solvent over a period of several days yielded small colourless blocks which were suitable for X-ray diffraction studies by synchrotron radiation in order to obtain a complete structure solution. Single crystals of **4.3** were found to be in an orthorhombic cell and the structure solution was performed in the space group *Pna*2₁. Details of the collection and structure refinement are given in Table 4.5 at the end of this chapter. The asymmetric unit consists of one molecule of **47** and four molecules of 4-Pic (Figure 4.7). Compound **47** was found to adopt the cone rather than pinched-cone conformation as expected given the presence of a second rigid ether chain at the lower-rim. All four 4-Pic molecules in the asymmetric unit interact with the upper-rim CO₂H groups *via* formation of the common Py \cdots CO₂H heterosynthon. There are four symmetry unique N \cdots HOCO hydrogen bonding interactions with distances ranging from 1.736 – 1.852 Å, and four CH \cdots OCOH interactions with distances ranging from 2.606 – 2.720 Å (full details in Table 4.1).

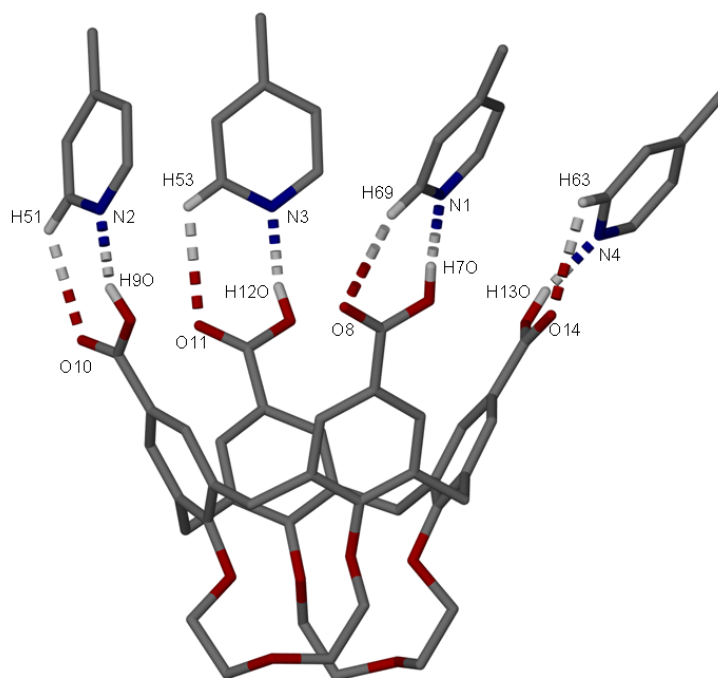


Figure 4.7. The X-ray crystal structure of the asymmetric unit in **4.3**. Hydrogen bonding interactions are shown as split-colour dashed lines. Hydrogen atoms (apart from those involved in the hydrogen bonding interactions) are omitted for clarity. Selected atoms have been labelled according to discussion.

H[70]···N[1]	1.736	H[51]···O[10]	2.606
H[90]···N[2]	1.852	H[53]···O[11]	2.720
H[120]···N[3]	1.827	H[63]···O[14]	2.702
H[130]···N[4]	1.769	H[69]···O[8]	2.710

Table 4.1. Hydrogen bonding distances (in Å) between 4-Pic molecules and the upper-rim CO₂H groups of compound **47**.

Symmetry expansion of **4.3** shows that the cavity of the molecule is filled with a symmetry equivalent 4-Pic, leading to two 4-Pic molecules interacting with one another *via* a π -stacking interaction (Figure 4.8); this occurs with an aromatic centroid···aromatic centroid distance of 3.564 Å. This also reveals the presence of three CH··· π interactions located between the hydrogen atoms on the methyl group of the 4-Pic molecule, and the aromatic ring with a H[70A]···aromatic centroid distance of 2.609 Å, a H[70B]···aromatic centroid distance of 3.077 Å and a H[70C]···aromatic centroid distance of 2.938 Å (Figure 4.8).

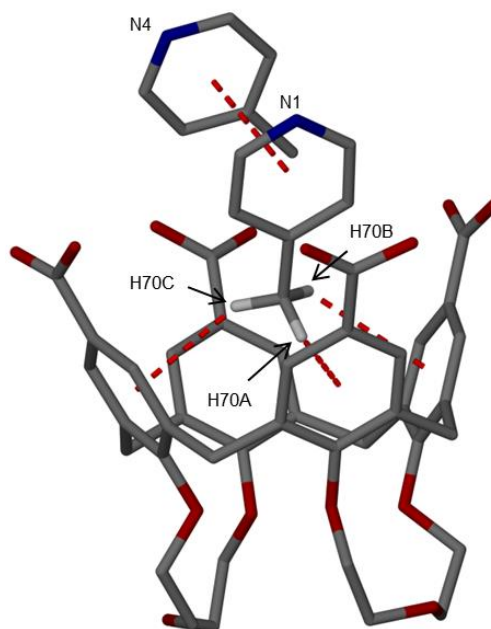


Figure 4.8. Symmetry expansion around molecule **4.3**. CH $\cdots\pi$ and $\pi\cdots\pi$ interactions are shown as red dashed lines. Hydrogen atoms (apart from those involved in CH $\cdots\pi$ interactions) have been omitted for clarity. Selected atoms have been labelled according to discussion.

4.3.5. Structure of [(**47-4H**)(2-AP+H)₄].(H₂O)₄, **4.4**.

Single crystals of the salt [(**47-4H**)(2-AP+H)₄].(H₂O)₄, **4.4** were obtained as the result of the addition of compound **47** to 3 mL of MeOH. The resulting suspension was heated and 2-AP was added slowly until the suspension became a solution. Colourless plate-shaped crystals that were suitable for X-ray diffraction studies formed overnight. Crystals of the salt **4.4** were found to be in a monoclinic cell and structure solution was performed in the space group $P2_1/n$. Details of the collection and structure refinement are given in Table 4.5 at the end of this chapter. The asymmetric unit consists of one molecule of (**47-4H**) (upper-rim CO₂H groups deprotonated), four 2-aminopyridinium cations and four water molecules (Figure 4.9). Three of the water molecules present in the asymmetric unit are disordered over two positions and were modelled at 50% occupancy in each.

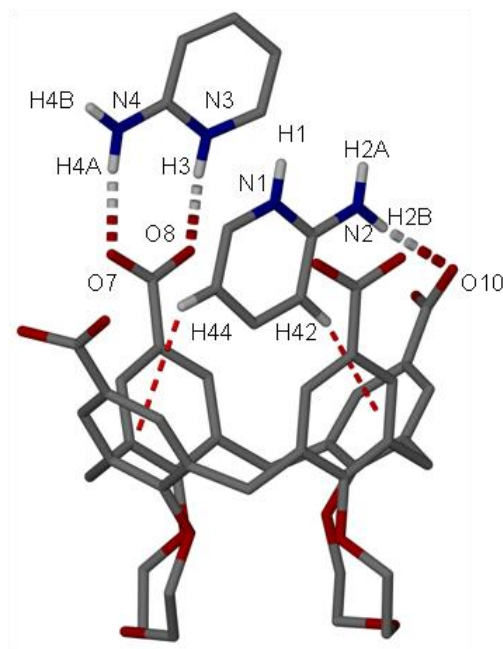


Figure 4.9. Part of the asymmetric unit found in the X-ray crystal structure of salt **4.4**. Hydrogen bonding and CH $\cdots\pi$ interactions are shown as split-colour and red dashed lines respectively. Hydrogen atoms (apart from those involved in hydrogen bonding and CH $\cdots\pi$ interactions) have been omitted for clarity. Selected atoms have been labelled according to discussion.

With compound (**47-4H**) locked in a cone conformation the cavity is now accessible to guest molecules. The cavity of (**47-4H**) is occupied by one (2-AP+H) cation and there are two CH $\cdots\pi$ interactions between the guest *meta* hydrogen atoms and the aromatic rings of the host. The two symmetry unique CH \cdots aromatic centroid distances associated with this (2-AP+H) cation guest molecule are observed between H[42] \cdots aromatic centroid and H[44] \cdots aromatic centroid with distances of 2.731 and 3.240 Å respectively. Additionally there is an HNH \cdots OCO hydrogen bonding interaction between the cation guest and an upper-rim CO₂⁻ group on the calixarene host. This symmetry unique HNH \cdots OCO hydrogen bonding interaction has an H[2B] \cdots O[10] distance of 2.193 Å. Symmetry expansion around the guest in **4.4** results in the formation of a hydrogen-bonded head-to-head dimer facilitated by both HNH \cdots OCO and NH \cdots OCO hydrogen bonding interactions as part of the expected salt formation between the (**47-4H**) anion and (2-AP+H) cation guests (Figure 4.10).^{24e}

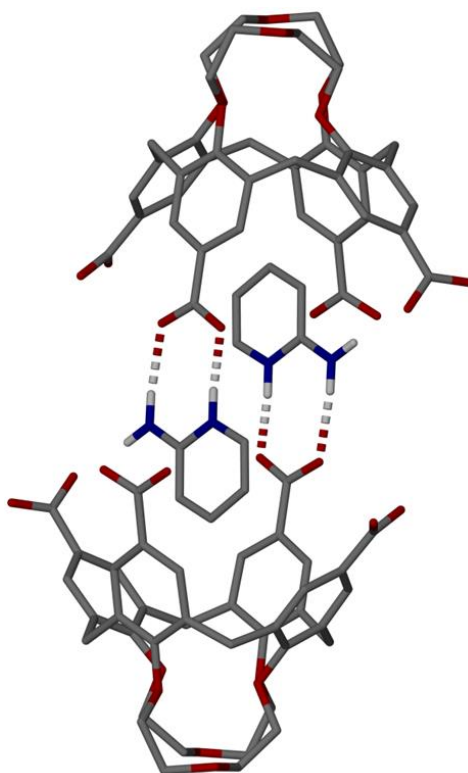


Figure 4.10. The hydrogen-bonded head-to-head dimer found in the crystal structure of **4.4**. Hydrogen bonding interactions are shown as split-colour dashed lines. Hydrogen atoms (apart from those involved in the hydrogen bonding interactions) are omitted for clarity.

In the hydrogen-bonded head-to-head dimer there is one $\text{NH}\cdots\text{OCO}$ and one $\text{HNH}\cdots\text{OCO}$ hydrogen bonding interaction with respective $\text{H}[1]\cdots\text{O}[11]$ and $\text{H}[2\text{A}]\cdots\text{O}[12]$ distances of 1.782 and 2.011 Å. The three remaining (2-AP+H) cations interact with the remaining upper-rim CO_2^- groups. This occurs *via* three $\text{HNH}\cdots\text{OCO}$ hydrogen bonding interactions with distances ranging from 1.905 – 2.009 Å, and three $\text{NH}\cdots\text{OCO}$ hydrogen bonding interactions with distances ranging from 1.762 – 1.779 Å (full details in Table 4.2).

$\text{H}[4\text{A}]\cdots\text{O}[7]$	1.905	$\text{H}[3]\cdots\text{O}[8]$	1.779
$\text{H}[6\text{A}]\cdots\text{O}[10]$	1.964	$\text{H}[5]\cdots\text{O}[9]$	1.762
$\text{H}[8\text{A}]\cdots\text{O}[5]$	2.009	$\text{H}[7]\cdots\text{O}[6]$	1.764

Table 4.2. Hydrogen bonding distances (in Å) between (2-AP+H) cations and the CO_2^- groups of compound **47**.

The hydrogen atoms were not added to the water molecules owing to three of them being disordered. They do however have the potential to hydrogen bond with the CO₂⁻ groups with O...O distances ranging from 2.806 – 3.058 Å. They were also found to bond with the (2-AP+H) cation guests with distances ranging from 1.930 – 2.646 Å.

4.4 Metal-organic assemblies of *p*-carboxylatocalix[4]arene-biscrown-3.

4.4.1 Structure of *p*-carboxylatocalix[4]arene-biscrown-3 metal-organic coordination polymer: [Cu^{II}PyC(47-2H)(Py)₂], **4.5**.

Crystals of the metal coordination polymer [Cu^{II}PyC(47-2H)(Py)₂] **4.5**, were obtained as a result of the addition of compound **47** to a methanolic solution of Cu(NO₃)₂. Pyridine was added drop-wise to the resulting suspension along with gentle heating until a blue solution was obtained. The solution was left to slowly evaporate over several weeks to yield small green/blue blocks which were suitable for X-ray diffraction studies by synchrotron radiation in order to obtain a complete structure solution. Crystals of **4.5** were found to be in an orthorhombic cell and structure solution was performed in the space group C222₁. Details of the collection and structure refinement are given in Table 4.5 at the end of this chapter. The asymmetric unit consists of one half molecule of **47** coordinated to one tetrahedral Cu centre, which itself is coordinated to one Py. Symmetry expansion reveals the formation of a metal-organic coordination polymer as shown in Figure 4.11. These interwoven pairs of 1-D chains assemble to form bi-layer type arrays frequently observed for C[4] building blocks.²⁵ One of the CO₂H groups is disordered over two positions and was modelled at 50% occupancy in each position. There was also found to be diffuse electron density associated with a disordered solvent molecule of pyridine that resides inside the cavity. As this could not be modelled appropriately the routine SQUEEZE was applied to the data.²⁶ This had the effect of dramatically improving the agreement indices during refinement for **4.5**. The Cu-O and Cu-N bond distances associated with the coordination sphere of Cu[1] are between Cu[1]...O[9] and Cu[1]...N[1] with distances of 1.970 Å and 1.978 Å respectively.

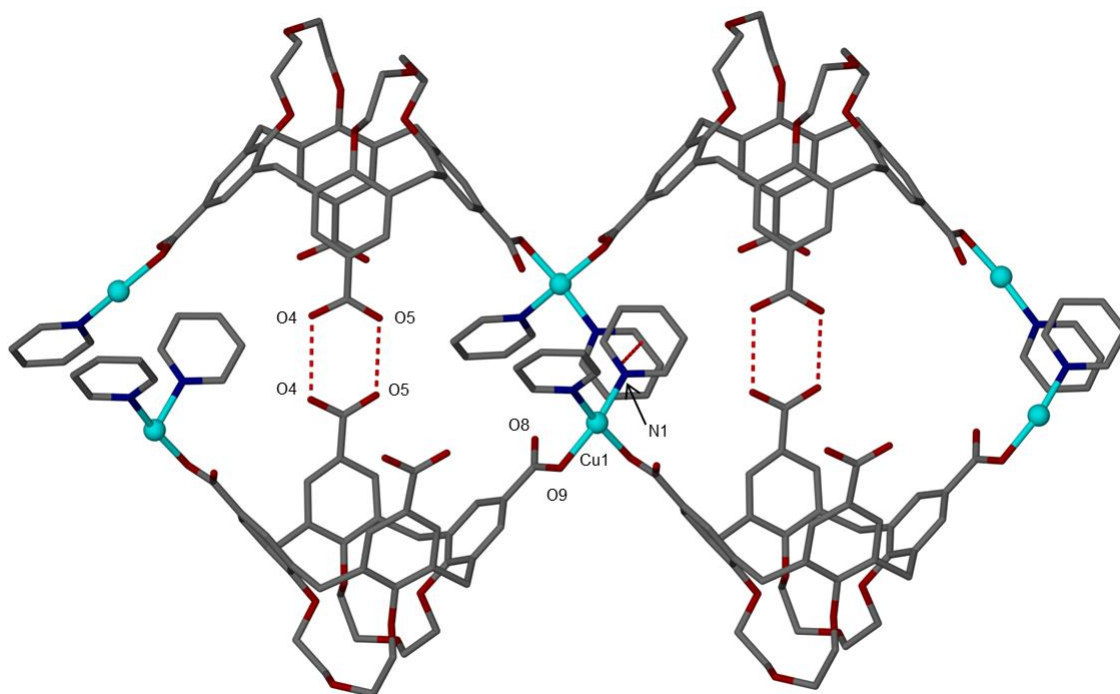


Figure 4.11. Partial extended structure of **4.5** showing neighbouring 1-D coordination polymer chains. O \cdots O bonding and $\pi\cdots\pi$ interactions are shown as red dashed lines. Selected atoms have been labelled according to discussion. The disordered upper-rim CO₂H group is shown in one of two positions. Hydrogen atoms and solvent molecules omitted for clarity.

Symmetry expansion of complex **4.5** reveals the presence of a π -stacking interaction present between two pyridine molecules that are ligated to the Cu metal centre with an aromatic centroid \cdots aromatic centroid distance of 3.506 Å. Hydrogen atoms were not placed on the upper-rim CO₂H groups due to disorder but homosynthon hydrogen bonding occurs in the off-set head-to-head arrangement with O \cdots O distances ranging from 2.626 – 3.074 Å.

4.4.2 Structure of *p*-carboxylatocalix[4]arene-biscrown-3 metal-organic coordination polymer: $[\text{Mn}^{\text{II}}(\mathbf{47}\text{-2H})(\text{Py})_2(\text{OMe})]\text{Py}(\text{H}_2\text{O})_2$, **4.6**.

Crystals of the metal coordination polymer $[\text{Mn}^{\text{II}}(\mathbf{47}\text{-2H})(\text{Py})_2(\text{OMe})]\text{Py}(\text{H}_2\text{O})_2$ **4.6**, were obtained as a result of the addition of compound **47** to a methanolic solution of $\text{Mn}(\text{NO}_3)_2$. Pyridine was added drop-wise to the resulting cloudy suspension along with gentle heating until a pale yellow solution was obtained. The solution was left to slowly evaporate over several weeks to yield small orange blocks which were suitable for X-ray diffraction studies by synchrotron radiation in order to obtain a complete structure solution. Crystals of **4.6** were found to be in a monoclinic cell and structure solution was performed in the space group *C2/c*. Details of the collection and structure refinement are given in Table 4.6 at the end of this chapter. The asymmetric unit consists of one half molecule of **47** coordinated to one octahedral Mn centre, which also has one ligated Py and a ligated disordered methanol (modelled at 50% occupancy). The asymmetric unit also contains a disordered pyridine molecule (modelled at 50% occupancy) and two water molecules, one of which is disordered over two positions and modelled at 50% accordingly in each. Symmetry expansion reveals the formation of a metal-organic coordination polymer as shown in Figure 4.12. Similarly to complex **4.5**, the 1-D chains assemble to build bi-layer type arrangements frequently exploited for C[4] building blocks. These interwoven pairs of 1-D chains assemble to form bi-layer type arrays frequently observed for C[4] building blocks.²⁵ The Mn-O and Mn-N bond distances associated with the coordination sphere of Mn[1] are given in Table 4.3.

Symmetry expansion shows that there is an interaction between one of the water molecules and one of the CO_2H groups with an $\text{H}[5\text{O}]\cdots\text{O}[10]$ distance of 1.788 Å. In addition to this there are several interactions between the other water molecules (disordered) and another CO_2H group with distances ranging from 2.589 – 2.826 Å. There is also a $\text{CH}\cdots\text{O}$ interaction between another CO_2H group and the disordered methanol group, with distances between 2.733 – 3.061 Å.

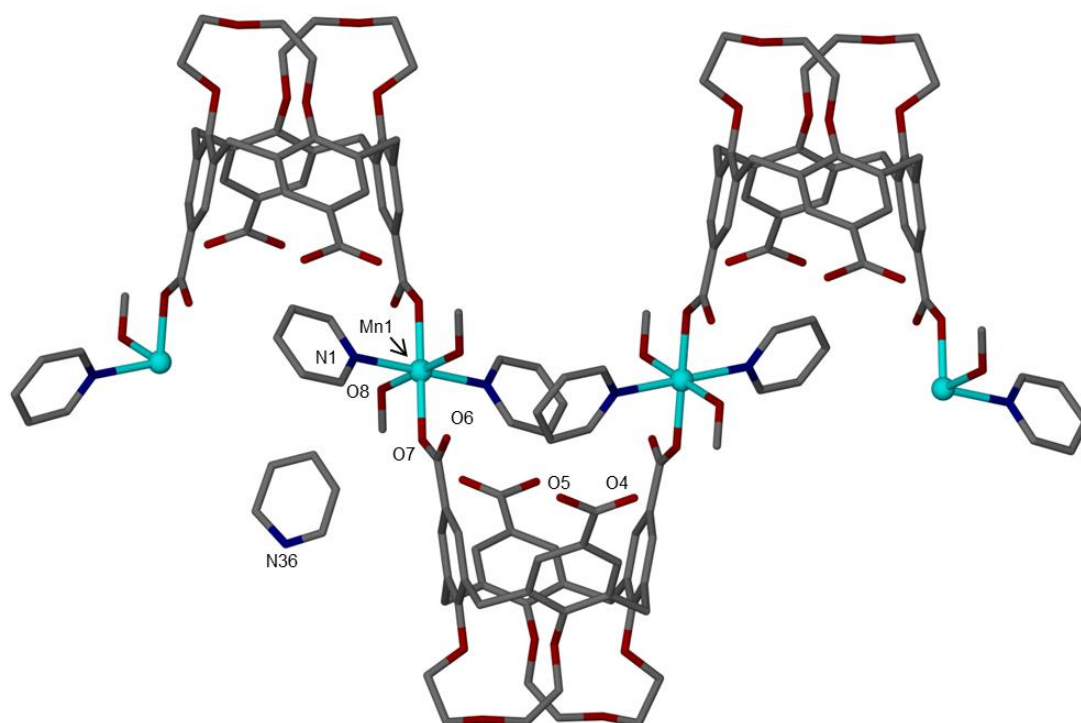


Figure 4.12. Partial extended structure of **4.6** showing neighbouring 1D coordination polymer chains. Selected atoms have been labelled according to discussion. The disordered methanol and pyridine group are shown in one of two positions. Hydrogen atoms omitted for clarity.

Mn[1]...O[7]	2.121
Mn[1]...O[8]	2.192
Mn[1]...N[1]	2.283

Table 4.3. Interatomic distances (in Å) relating to the coordination sphere of the manganese metal centre in the crystal structure of complex **4.6**.

An analogous synthetic procedure that was used to generate complex **4.6** was carried out, but using $\text{Co}(\text{NO}_3)_2$ as the metal salt in place of $\text{Mn}(\text{NO}_3)_2$. Slow evaporation over several weeks resulted in the formation of pale pink plates suitable for X-ray diffraction studies. Unit cell dimensions for **4.7** ($a = 12.4039$, $b = 27.9274$, $c = 15.9504$, $V = 5523.84 \text{ Å}^3$) were found to be very similar to those of **4.6**, suggesting that these are isostructural.

4.5. Conclusion.

The $p\text{CO}_2[4]\text{s}$ have been shown to be accomplished building blocks for use in supramolecular chemistry in the presence of pyridine (or pyridine-derivative) templates. This is achieved through exploitation of the $\text{Py}\cdots\text{CO}_2\text{H}$ heterosynthon and whether the cavity is able to occupy a guest molecule.^{16,24} The assembly of di-*O*-propoxy-di-*p*-carboxylatocalix[4]arene-crown-4 **43a** and *p*-carboxylatocalix[4]arene-biscrown-3 **47** in the presence of pyridine-templates has not been previously studied. It was found that compound **43a** adopted the pinched-cone conformation when crystallised from Py, as a result of there being only one ether bridge at the lower-rim of the macrocycle. This had the effect of blocking off the cavity to potential guest molecules. For the biscrown-C[4] **47** the introduction of two short diethylene glycol units restricts the residual flexibility, keeping the molecule locked in the cone conformation and the cavity accessible to guest molecules. The resulting structures show a tendency for the upper-rim CO_2H groups to hydrogen bond to the pyridine-containing template of choice (rather than CO_2H groups from symmetry equivalent calixarenes) through formation of the common $\text{Py}\cdots\text{CO}_2\text{H}$ heterosynthon. This template chemistry was expanded to include salt and related heterosynthon formation when 2-AP was used. This more basic template was found to fully deprotonate compound **47** which resulted in the formation of a hydrogen-bonded head-to-head dimer. This is formed through both $\text{HNH}\cdots\text{OCO}$ and $\text{NH}\cdots\text{OCO}$ hydrogen interactions, as part of the expected salt formation between the (**47**-4H) anion and (2-AP+H) cation guests as shown for complex **4.4**. Initial exploration of the coordination chemistry of the new $p\text{CO}_2[4]\text{s}$ presented in this chapter resulted in the formation of a small series of new 1-D coordination polymers (complexes **4.5** – **4.7**). These promising results suggest that these building blocks may find further utility in the assembly of higher-dimensionality CPs when a broader study of their supramolecular chemistry is undertaken.

4.6. Experimental.

4.6.1. General comments.

The majority of work that has been conducted so far has been ligand synthesis, with a view to exploring the self- and metal-directed assembly of all the compounds synthesised.

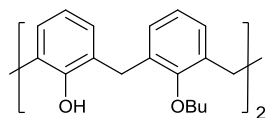
4.6.2. General experimental.

Unless stated, all reagents employed were purchased from chemical suppliers (Alfa Aesar, Fisher Scientific and Sigma Aldrich) and used as received. If required solvents were dried over molecular sieves (pore size 4 Å). Unless stated all experiments were carried out in air. When performed under a nitrogen atmosphere, this was dried over two columns of Drierite® gas purifier connected in series. Analytical thin layer chromatography was performed on precoated silica gel plates (Merck, 60 F254) and column chromatography was performed with silica gel (Merck, particle size 40-60 µm).

Electrospray ionisation and fourier transform mass spectra (ESI-FTMS) were obtained on a LTQ Orbitrap XL spectrometer at Swansea University. ¹H NMR and ¹³C NMR spectra were recorded on Bruker AC 300 and Bruker AC 400 spectrometers, with chemical shifts reported in ppm with respect to TMS as an internal standard. IR spectra were acquired on a Perkin Elmer Spectrum 100 FT-IR Spectrometer, with wavenumber (ν) of absorption reported in cm⁻¹. Single crystals were analysed on either a Bruker Apex II CCD diffractometer operating at 100(2) K with Mo-Kα radiation (λ = 0.71073 Å) with a graphite monochromator or a Bruker D8 diffractometer with PHOTON 100 detector operating at 100(2) K with synchrotron radiation (λ = 0.77490 Å). Microanalysis results were obtained using an Exeter Analytical CE440 Elemental Analyser.

4.6.3. Synthesis of compounds 39 - 47 and complexes 4.5 - 4.7.

25,27-Dibutoxy-26,28-dihydroxycalix[4]arene, **39**⁸



This was prepared by a route similar to compound **4** using 1-iodobutane (see Chapter 3 for details). Compound **39** was obtained as an off-white solid on recrystallisation from DCM/MeOH (6.53 g, 84%).

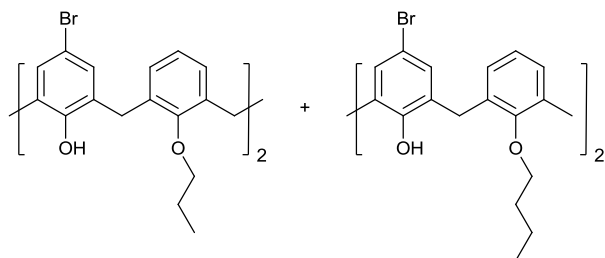
¹H NMR (300 MHz, 25 °C, CDCl₃): δ = 8.19 (s, 2H, OH), 6.97 (d, J = 7.5 Hz, 4H, ArH), 6.89 (d, J = 7.5 Hz, 4H, ArH), 6.66 (t, J = 7.5 Hz, 2H, ArH), 6.57 (t, J = 7.5 Hz, 2H, ArH), 4.25 (d, J = 12.9 Hz, 4H, ArCH₂Ar), 3.94 (t, J = 6.2 Hz, 4H, OCH₂CH₂CH₂CH₃), 3.30 (d, J = 12.9 Hz, 4H, ArCH₂Ar), 1.97 (m, 4H, OCH₂CH₂CH₂CH₃), 1.73 (m, 4H, OCH₂CH₂CH₂CH₃), 1.01 (t, J = 7.3 Hz, OCH₂CH₂CH₂CH₃).

¹³C NMR (300 MHz, 25 °C, CDCl₃): δ = 153.40, 152.02, 133.50, 128.94, 128.46, 128.21, 125.30, 119.00, 76.65, 32.31, 31.47, 19.46, 14.14.

IR (solid phase, ν cm⁻¹) = 3242m, 2957m, 2927m, 2871m, 15.91w, 1456s, 1428m, 1067s.

MS m/z observed 537.2991, 554.3252, theoretical 537.2999 [M + H]⁺, 554.3265 [M + NH₄]⁺.

Dibromo-dialkoxycalix[4]arenes, **40a-b**⁹



A solution of bromine (0.02 mol) in 40 mL dry DCM was added drop-wise to a stirred solution of either compound **4** or **39** (5.90 mmol) in 140 mL dry DCM. After 30 minutes the colourless precipitate formed was filtered off and washed with DCM to yield pure compounds **40a-b**.

5,17-Dibromo-25,27-dipropoxy-26,28-dihydroxycalix[4]arene, **40a**, (3.40 g, 86%);

¹H NMR (300 MHz, 25 °C, CDCl₃): δ = 8.40 (s, 2H, OH), 7.21 (s, 4H, ArH), 6.98 (d, *J* = 7.2 Hz, 4H, ArH), 6.85 (t, *J* = 7.2 Hz, 2H, ArH), 4.31 (d, *J* = 12.9 Hz, 4H, ArCH₂Ar), 4.00 (t, *J* = 6.8 Hz, 4H, OCH₂CH₂CH₃), 3.36 (d, *J* = 12.9 Hz, 4H, ArCH₂Ar), 2.12 (m, 4H, OCH₂CH₂CH₃), 1.32 (t, *J* = 7.4 Hz, OCH₂CH₂CH₃).

¹³C NMR (300 MHz, 25 °C, CDCl₃): δ = 132.76, 130.74, 130.06, 129.25, 78.49, 77.22, 31.17, 10.86.

IR (solid phase, ν cm⁻¹) = 3120m, 2958m, 2931m, 2875m, 1590w, 1456s, 1428s, 1219s, 1196s, 1072m, 766s.

MS *m/z* observed 684.1143, theoretical 684.1145 [M + NH₄]⁺.

5,17-Dibromo-25,27-dibutoxy-26,28-dihydroxycalix[4]arene, **40b**, (3.62 g, 88%);

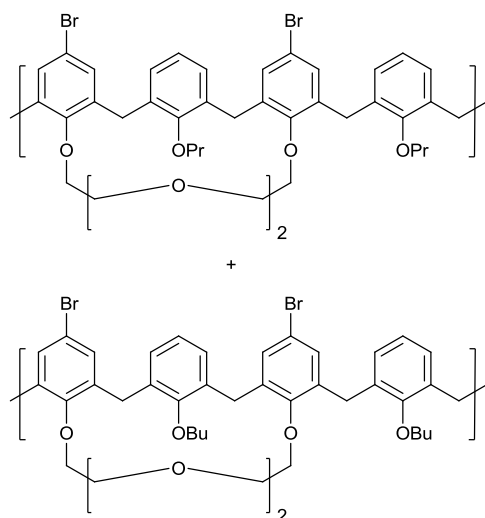
¹H NMR (300 MHz, 25 °C, CDCl₃): δ = 8.26 (s, 2H, OH), 7.10 (s, 4H, ArH), 6.88 (d, *J* = 7.4 Hz, 4H, ArH), 6.73 (t, *J* = 7.4 Hz, 2H, ArH), 4.19 (d, *J* = 13.0 Hz, 4H, ArCH₂Ar), 3.91 (t, *J* = 6.8 Hz, 4H, OCH₂CH₂CH₃), 3.26 (d, *J* = 13.0 Hz, 4H, ArCH₂Ar), 1.96 (m, 4H, OCH₂CH₂CH₃), 1.69 (m, 4H, OCH₂CH₂CH₃), 1.02 (t, *J* = 7.3 Hz, OCH₂CH₂CH₃).

¹³C NMR (300 MHz, 25 °C, CDCl₃): δ = 151.98, 132.74, 130.74, 130.08, 129.23, 125.47, 77.22, 32.21, 31.17, 19.38, 14.07.

IR (solid phase, ν cm⁻¹) = 3207m, 2956m, 2929m, 2871m, 1588w, 1461s, 1217s, 766s.

MS *m/z* observed 712.1455, theoretical 712.1458 [M + NH₄]⁺.

Dibromo-dialkoxycalix[4]arene-crown-4, **41a-b**¹⁰



To a suspension of NaH (60%, 0.01 mol) in 80 mL of DMF, were added the dibromo derivative **40a** or **40b** (3.75 mmol) and triethylene glycol ditosylate (3.75 mmol). The solution was heated at 70°C for one day. The solution was quenched with 1 M HCl (100 mL) once the solution was cooled. The precipitate formed was filtered and washed with water. The solid was triturated with MeOH to give compounds **41a-b** as off-white solids.

5,17-Dibromo-25,27-dipropoxycalix[4]arene-26,28-crown-4, **41a**, (2.59 g, 86%);

¹H NMR (300 MHz, 25 °C, CDCl₃): δ = 7.22 (s, 4H, ArH), 6.21 (t, *J* = 6.8 Hz, 2H, ArH), 6.08 (d, *J* = 7.2 Hz, 4H, ArH), 4.28 (d, *J* = 13.0 Hz, 4H, ArCH₂Ar), 4.03 (s, 8H, OCH₂CH₂O), 3.68 (s, 4H, OCH₂CH₂O), 3.57 (t, *J* = 7.0 Hz, 4H, CH₂CH₂), 3.08 (d, *J* = 13.0 Hz, 4H, ArCH₂Ar), 1.84 (m, 4H, CH₂CH₂), 1.03 (t, *J* = 7.0 Hz, 6H, CH₂CH₃).

¹³C NMR (300 MHz, 25 °C, CDCl₃): δ = 157.42, 154.71, 138.79, 132.23, 131.59, 127.68, 122.36, 114.74, 77.33, 77.22, 73.99, 71.87, 70.22, 30.30, 23.58, 10.92.

IR (solid phase, ν cm⁻¹) = 2958m, 2920m, 2872m, 1570w, 1455s, 1196s, 756s.

MS *m/z* observed 803.1356, theoretical 803.1381 [M + Na]⁺, 804.1925 [M + NH₄]⁺.

5,17-Dibromo-25,27-dibutoxycalix[4]arene-26,28-crown-4, **41b**, (2.66 g, 91%);

¹H NMR (300 MHz, 25 °C, CDCl₃): δ = 7.26 (s, 4H, ArH), 6.30 (t, *J* = 6.8 Hz, 2H, ArH), 6.18 (d, *J* = 7.2 Hz, 4H, ArH), 4.38 (d, *J* = 13.0 Hz, 4H, ArCH₂Ar), 4.09 (s, 8H, OCH₂CH₂O), 3.76 (s, 4H, OCH₂CH₂O), 3.70 (t, *J* = 6.8 Hz, 4H, CH₂CH₂), 3.13 (d, *J* = 13.0 Hz, 4H, ArCH₂Ar), 1.88 (m, 4H, CH₂CH₂), 1.54 (m, 8H, CH₂CH₂), 1.01 (t, *J* = 6.8 Hz, 6H, CH₂CH₃).

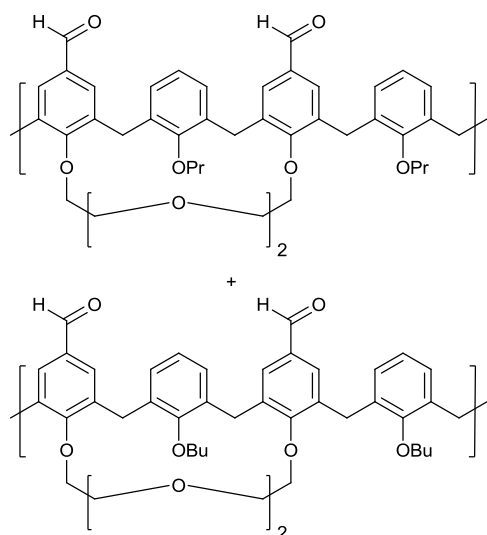
¹³C NMR (300 MHz, 25 °C, CDCl₃): δ = 157.43, 154.76, 138.79, 132.23, 131.58, 127.67, 122.35, 114.73, 77.23, 75.38, 73.99, 71.85, 70.22, 32.46, 30.30, 19.52, 14.02.

IR (solid phase, ν cm⁻¹) = 2956m, 2913m, 2863m, 1686w, 1588w, 1453s, 1196s, 754s.

Anal. Calcd. For C₄₂H₄₈Br₂O₆: C, 62.38; H, 5.98. **Found:** C, 63.29; H, 6.16.

MS *m/z* observed 831.1683, theoretical 831.1689 [M + Na]⁺, 832.2239 [M + NH₄]⁺.

Diformyl-dialkoxycalix[4]arene-crown-4, **42a-b**¹¹



A solution of **41a** or **41b** (2.56 mmol) in dry THF (100 mL) was stirred at -78°C for 15 mins. After this time *n*-BuLi (2.5 M, 25.14 mmol) was added and the solution was left to stir at this temperature for 30 mins. The mixture was quenched with DMF (0.08 mol) and stirred for an hour. The reaction mixture was poured into ice cold 1M HCl (100 mL) and extracted with CHCl₃. The organic layer was washed with

water (3 X 100 mL), dried (Na₂SO₄) and the solvent removed under reduced pressure to afford a crude yellow oil for both products. The yellow oil was recrystallised from acetone to yield compounds **42a-b** as colourless crystals.

5,17-Diformyl-25,27-dipropoxycalix[4]arene-26,28-crown-4, **42a**, (1.03 g, 59%);

¹H NMR (300 MHz, 25 °C, CDCl₃): δ = 10.00 (s, 2H, CHO), 7.61 (s, 4H, ArH), 6.15 (t, *J* = 7.0 Hz, 2H, ArH), 5.98 (d, *J* = 7.2 Hz, 4H, ArH), 4.38 (d, *J* = 13.0 Hz, 4H, ArCH₂Ar), 4.14 (t, *J* = 6.8 Hz, 4H, OCH₂CH₂O), 4.01 (t, *J* = 6.8 Hz, 4H, OCH₂CH₂O), 3.73 (s, 4H, OCH₂CH₂O), 3.61 (t, *J* = 7.0 Hz, 4H, CH₂CH₂), 3.21 (d, *J* = 13.0 Hz, 4H, ArCH₂Ar), 1.86 (m, 4H, CH₂CH₂), 1.04 (t, *J* = 7.0 Hz, 6H, CH₂CH₃).

¹³C NMR (300 MHz, 25 °C, CDCl₃): δ = 191.72, 164.05, 154.79, 137.68, 132.11, 131.17, 130.97, 127.75, 122.45, 77.23, 74.20, 71.96, 70.24, 30.94, 30.50, 23.61, 10.94.

IR (solid phase, ν cm⁻¹) = 2918m, 2871m, 2727w, 1684s, 1594m, 1291m, 1123s.

Anal. Calcd. For C₄₂H₄₆O₈: C, 74.31; H, 6.83. *Found*: C, 73.70; H, 6.98.

MS *m/z* observed 696.3526, 701.3072, theoretical 696.3531 [M + NH₄]⁺, 701.3085, [M + Na]⁺.

5,17-Diformyl-25,27-dibutoxycalix[4]arene-26,28-crown-4, **42b**, (1.11 g, 61%);

¹H NMR (300 MHz, 25 °C, CDCl₃): δ = 9.92 (s, 2H, CHO), 7.62 (s, 4H, ArH), 6.12 (t, *J* = 7.0 Hz, 2H, ArH), 5.98 (d, *J* = 7.2 Hz, 4H, ArH), 4.37 (d, *J* = 13.0 Hz, 4H, ArCH₂Ar), 4.16 (t, *J* = 6.6 Hz, 4H, OCH₂CH₂O), 4.03 (t, *J* = 6.6 Hz, 4H, OCH₂CH₂O), 3.64 (m, 8H, overlap of OCH₂CH₂O and CH₂CH₂), 3.21 (d, *J* = 13.0 Hz, 4H, ArCH₂Ar), 1.81 (m, 4H, CH₂CH₂), 1.52 (m, 4H, CH₂CH₂), 0.93 (t, *J* = 7.0 Hz, 6H, CH₂CH₃).

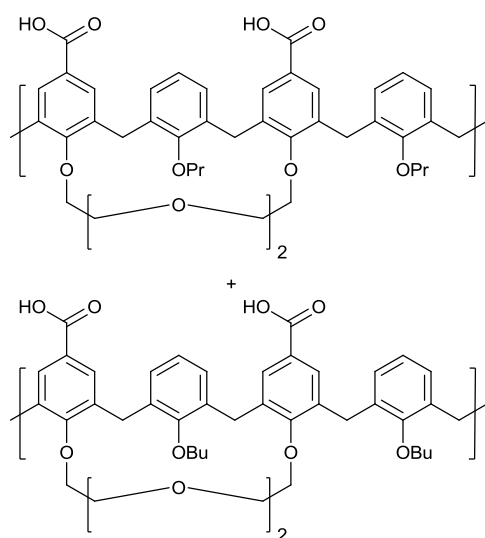
¹³C NMR (300 MHz, 25 °C, CDCl₃): δ = 190.68, 163.02, 153.81, 136.64, 131.07, 130.13, 129.94, 126.72, 121.41, 74.44, 73.16, 70.90, 69.21, 31.47, 29.47, 18.52, 13.01.

IR (solid phase, ν cm⁻¹) = 2930m, 2861m, 2723w, 1685s, 1592m, 1297m, 1129s.

Anal. Calcd. For C₄₄H₅₀O₈: C, 74.76; H, 7.13. *Found*: C, 74.13; H, 7.39.

MS *m/z* observed 706.9399, theoretical 706.9404 [M + NH₄]⁺.

Dicarboxylato-dialkoxycalix[4]arene-crown-4, **43a-b**



To a solution of either **42a** or **42b** (0.35 mmol) in DCM (5 mL) and acetone (15 mL) was added a solution of NaClO₂ (1.41 mmol) dissolved in water (3 mL) and a solution of sulfamic acid (1.41 mmol) dissolved in water (3 mL). The solution was left to stir at RT for one day. Organic solvents were removed under reduced pressure and the residue taken up with 1M HCl. The yellow solid was filtered, washed with water and left to air dry.

5,17-Dicarboxylato-25,27-dipropoxycalix[4]arene-26,28-crown-4, **43a**, (0.22 g, 88%);

¹H NMR (300 MHz, 25 °C, DMSO-d₆): δ = 12.71 (s, 2H, COOH), 7.88 (s, 4H, ArH), 6.27 (t, *J* = 6.8 Hz, 2H, ArH), 6.15 (d, *J* = 7.2 Hz, 4H, ArH), 4.36 (d, *J* = 13.0 Hz, 4H, ArCH₂Ar), 4.12 (s, 8H, OCH₂CH₂O), 3.74 (s, 4H, OCH₂CH₂O), 3.67 (t, *J* = 7.0 Hz, 4H, CH₂CH₂), 3.36 (d, *J* = 13.0 Hz, 4H, ArCH₂Ar), 1.92 (m, 4H, CH₂CH₂), 1.18 (t, *J* = 6.8 Hz, 6H, CH₂CH₃).

¹³C NMR (300 MHz, 25 °C, DMSO-d₆): δ = 167.53, 161.65, 154.44, 136.36, 132.17, 130.31, 127.20, 124.59, 121.82, 77.04, 73.66, 70.81, 69.34, 29.52, 22.97, 10.79.

IR (solid phase, ν cm⁻¹) = 2959m, 2925m, 2873m, 2360w, 1717s, 1659s, 1596m, 1453m, 1424m, 1189s.

Anal. Calcd. For C₄₂H₄₆O₁₀: C, 70.97; H, 6.52. *Found*: C, 69.61; H, 6.38.

MS *m/z* observed 728.3428, 733.2968, theoretical 728.3429 [M + NH₄]⁺, 733.2983 [M + Na]⁺.

5,17-Dicarboxylato-25,27-dibutoxycalix[4]arene-26,28-crown-4, **43b**, (0.23 g, 87%);

¹H NMR (300 MHz, 25 °C, DMSO-d₆): δ = 12.42 (s, 2H, COOH), 7.89 (s, 4H, ArH), 6.29 (t, *J* = 6.8 Hz, 2H, ArH), 6.16 (d, *J* = 7.2 Hz, 4H, ArH), 4.38 (d, *J* = 13.0 Hz, 4H, ArCH₂Ar), 4.12 (s, 6H, OCH₂CH₂O), 3.71 (m, 6H, OCH₂CH₂O), 3.31 (m, 8H, overlap of CH₂CH₂ and ArCH₂Ar), 1.89 (m, 4H, CH₂CH₂), 1.64 (m, 4H, CH₂CH₂), 1.07 (t, *J* = 6.8 Hz, 6H, CH₂CH₃).

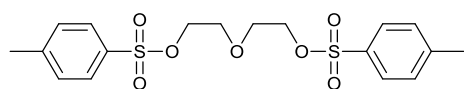
^{13}C NMR (300 MHz, 25 °C, DMSO- d_6): δ = 167.41, 161.66, 154.46, 136.31, 132.14, 130.34, 127.23, 124.68, 121.84, 75.00, 73.70, 70.86, 69.42, 31.90, 30.65, 29.54, 19.04, 13.85.

IR (solid phase, ν cm^{-1}) = 2957m, 2927m, 2868m, 2360w, 1714s, 1679s, 1597m, 1455m, 1424m, 1188s.

Anal. Calcd. For $\text{C}_{44}\text{H}_{50}\text{O}_{10}$: C, 71.53; H, 6.82. *Found*: C, 68.99; H, 6.80.

MS m/z observed 756.3742, theoretical 756.3742 $[\text{M} + \text{NH}_4]^+$.

Ethylene glycol di-*p*-toluene sulfonate, **44**¹³



Triethylamine (50.0 mL, 0.36 mol) was added to a solution of ethylene glycol (10.0 mL, 0.18 mol)

in THF (100 mL) under a nitrogen atmosphere. Tosyl chloride (71.8 g, 0.38 mol) was dissolved in THF (50 mL) and added drop-wise to the solution over 20 mins, and the reaction stirred at RT for 16 hours. The reaction was worked-up by extracting with water (300 mL) and DCM (300 mL) and the organic layer was separated, dried over MgSO_4 and the solvent evaporated. The product was recrystallised from ethyl acetate to yield compound **44** as a white crystalline solid (61.60 g, 91%).

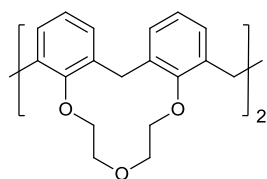
^1H NMR (300 MHz, 25 °C, CDCl_3): δ = 7.75 (d, J = 8.3 Hz, 4H, ArH), 7.38 (d, J = 8.5 Hz, 4H, ArH), 4.18 (s, 4H, $\text{OCH}_2\text{CH}_2\text{O}$), 2.42 (s, 6H, CH_3).

^{13}C NMR (300 MHz, 25 °C, CDCl_3): δ = 144.99, 132.85, 129.92, 127.94, 69.03, 68.74, 21.66.

IR (solid phase, ν cm^{-1}) = 3006w, 2962m, 2901m, 1597m, 1351s, 1167s.

MS m/z observed 415.0887, theoretical 415.0880 $[\text{M} + \text{H}]^+$.

Calix[4]arene-25,26,27,28-biscrown-3, **45**¹⁴



NaH (60%, 1.27 g, 0.03 mol) was added to a solution containing C[4] **2** (3.20 g, 7.54 mmol) dissolved in DMF (700 mL, high dilution) and the mixture was left to stir at RT for 30 mins.

Diethylene glycol ditosylate (7.82 g, 0.02 mol) dissolved in 50 mL DMF was added drop-wise to the reaction mixture. The solution was stirred at 50 °C for one day. Once cool, MeOH was added to kill the excess NaH before the solvent was removed under reduced pressure. The residue was taken up with 1M HCl (100 mL) and extracted with ethyl acetate (500 mL). The organic layer was washed with water, and

dried over Na₂SO₄, before being purified by column chromatography (hexane/ethyl acetate 3:2). The final product, after evaporation of eluent, yielded compound **45** as a fine white powder (1.34 g, 31%).

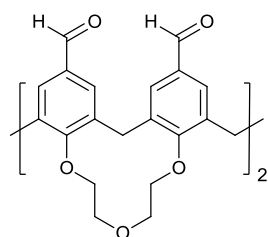
¹H NMR (300 MHz, 25 °C, CDCl₃): δ = 6.98 (m, 8H, ArH), 6.67 (t, *J* = 7.5 Hz, 4H, ArH), 4.98 (d, *J* = 12.10 Hz, 2H, ArCH₂Ar), 4.45 (d, *J* = 12.10 Hz, 2H, ArCH₂Ar), 4.15 (m, 12H, OCH₂CH₂O), 3.80 (m, 4H, OCH₂CH₂O), 3.15 (m, 4H, ArCH₂Ar).

¹³C NMR (300 MHz, 25 °C, CDCl₃): δ = 155.13, 135.61, 135.44, 128.94, 128.04, 123.70, 77.24, 76.30, 74.73, 30.70, 29.75.

IR (solid phase, ν cm⁻¹) = 2920m, 2873m, 2225s, 1605s, 1453s, 1176s.

MS *m/z* observed 565.2590, theoretical 565.2585 [M + H]⁺.

5,11,27,23-Tetraformylcalix[4]arene-25,26,27,28-biscrown-3, **46**



Compound **45** (1.00 g, 1.77 mmol) and HMTA (8.99 g, 0.06 mol) were dissolved in TFA (50 mL) and heated at reflux for 48 h. The hot reaction was poured onto ice water (50 mL) and stirred for 30 mins before the product was extracted into DCM (2 X 100 mL) and the organic layer was washed with water (2 X 100 mL),

dried (MgSO₄) and the solvents evaporated to give compound **46** as a pale yellow solid (1.00 g, 83%).

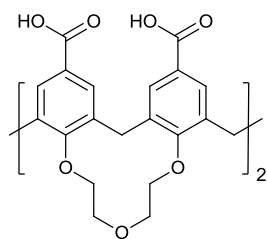
¹H NMR (300 MHz, 25 °C, CDCl₃): δ = 9.72 (s, 4H, CHO), 7.58 (d, *J* = 2.6 Hz, 4H, ArH), 7.52 (d, *J* = 2.6 Hz, 4H, ArH), 5.02 (d, *J* = 12.4 Hz, 2H, ArCH₂Ar), 4.50 (d, *J* = 12.4 Hz, 2H, ArCH₂Ar), 4.22 (m, 12H, OCH₂CH₂O), 3.88 (m, 4H, OCH₂CH₂O), 3.35 (m, 4H, ArCH₂Ar).

¹³C NMR (300 MHz, 25 °C, CDCl₃): δ = 191.29, 191.07, 160.59, 135.00, 135.79, 132.75, 131.20, 130.36, 77.24, 76.39, 74.12, 30.58, 29.71.

IR (solid phase, ν cm⁻¹) = 2920m, 2873m, 1605s, 1463s, 1286s, 1081m.

MS *m/z* observed 694.2639, theoretical 694.26347 [M + NH₄]⁺.

5,11,27,23-Tetracarboxylato-25,26,27,28-biscrown-3-calix[4]arene, **47**



In a 50 mL rbf containing a solution of compound **46** (0.27 g, 0.48 mmol) dissolved in DCM (5 mL) and acetone (15 mL) was added a solution of NaClO₂ (0.35 g, 3.87 mmol) in water (5 mL) and sulfamic acid (0.38 g, 3.87 mmol) in water (5 mL) and the mixture was left to stir at room temperature overnight. The organic solvents were removed under reduced pressure to afford compound **47** as a yellow solid that was filtered, washed with water and air dried (0.27 g, 88%).

¹H NMR (300 MHz, 25 °C, DMSO-d₆): δ = 12.51 (s, 4H, COOH), 7.73 (s, 8H, ArH), 5.00 (d, *J* = 12.0 Hz, 2H, ArCH₂Ar), 4.45 (d, *J* = 12.0 Hz, 2H, ArCH₂Ar), 4.19 (m, 12H, OCH₂CH₂O), 3.62 (m, 4H, OCH₂CH₂O), 3.45 (m, 4H, ArCH₂Ar).

¹³C NMR (300 MHz, 25 °C, DMSO-d₆): δ = 166.68, 159.19, 135.48, 135.46, 130.48, 129.70, 126.15, 76.55, 73.71, 29.44, 28.86.

IR (solid phase, ν cm⁻¹) = 2924m, 1682s, 1603m, 1423m, 1279s, 1196s.

MS *m/z* observed 758.2446, theoretical 758.2443 [M + NH₄]⁺.

Synthesis of 4.5: A mixture of compound **47** (0.10 g, 0.13 mmol) was suspended in methanol (2 mL), where a methanolic solution of Cu(NO₃)₂ (67.0 mg, 0.28 mmol) dissolved in 2 mL of methanol was added. Gentle heating followed by dropwise addition of Py resulted in a solution being obtained. Slow evaporation over several weeks resulted in the formation of green/blue blocks suitable for X-ray diffraction studies.

Synthesis of 4.6: An analogous procedure to **4.5** was carried out but using Mn(NO₃)₂ (0.10 g, 0.55 mmol) as the metal salt. Slow evaporation over several weeks resulted in the formation of orange blocks suitable for X-ray diffraction studies.

Synthesis of 4.7: An analogous procedure to **4.5** was carried out but using Co(NO₃)₂ (0.16 g, 0.55 mmol) as the metal salt. Slow evaporation over several weeks resulted in the formation of pale pink plates suitable for X-ray diffraction studies. Unit cell dimensions for **4.7**: *a* = 12.4039, *b* = 27.9274, *c* = 15.9504, *V* = 5523.84 Å³. These unit cell parameters were very similar to those of **4.6**, and we therefore assume that both **4.6**

and **4.7** are isostructural with the only difference being the presence of Co rather than Mn.

4.6.4. X-ray details of data collection/structure refinement of compounds 42b, 4.1 - 4.6.

Complex number	42b	4.1	4.2
Formula	C ₄₄ H ₅₀ O ₈	C ₄₅ H ₅₃ NO ₁₁	C ₅₂ H ₅₆ N ₂ O ₁₀
<i>Mr</i>	706.84	783.88	868.99
Crystal system	Orthorhombic	Triclinic	Monoclinic
Space group	<i>Pna</i> 2 ₁	<i>P</i> -1	<i>P</i> 2/ <i>c</i>
<i>T</i> /K	100(2)	100(2)	100(2)
<i>a</i> /Å	23.9030(10)	9.6365(4)	16.1196(6)
<i>b</i> /Å	11.3880(5)	12.4648(5)	14.7624(6)
<i>c</i> /Å	13.6262(5)	18.9601(7)	19.0456(7)
α /°	90	105.953(2)	90
β /°	90	93.615(2)	95.650(2)
γ /°	90	108.993(2)	90
<i>U</i> Å ³	3709.2(3)	2041.17(14)	4510.1(3)
<i>Z</i>	4	2	4
<i>F</i> (000)	1512	836	1848
<i>D_c</i> /g cm ⁻³	1.266	1.275	1.280
μ /mm ⁻¹	0.103	0.109	0.106
2 θ_{max} /°	69.5	72.1	62.3
Data collected	65693	62243	68514
Unique data	12312	14913	11243
<i>R_{int}</i>	0.0480	0.0489	0.0670
Obs data (<i>I</i> > 2 σ (<i>I</i>))	10466	11344	8296
Parameters	465	514	579
Restraints	1	6	0
<i>R</i> ₁ (observed data)	0.0535	0.0559	0.0433
ωR_2 (all data)	0.1297	0.1496	0.1003
<i>GooF</i>	1.026	1.037	1.015
Max/min residuals [e.Å ⁻³]	1.61/-1.13	1.01/-0.80	0.29/-0.28

Table 4.4. Details of data collection and structure refinement for complexes **42b**, **4.1** - **4.2**.

Complex number	4.3	4.4	4.5
Formula	C ₆₄ H ₆₄ N ₄ O ₁₄	C ₆₀ H ₆₈ N ₈ O ₁₈	C ₅₅ H ₄₉ CuN ₃ O ₁₄
<i>Mr</i>	1113.19	1189.22	1039.51
Crystal system	Orthorhombic	Monoclinic	Orthorhombic
Space group	<i>Pna</i> 2 ₁	<i>P</i> 2 ₁ / <i>n</i>	<i>C</i> 222 ₁
<i>T</i> /K	100(2)	100(2)	100(2)
<i>a</i> /Å	32.4701(18)	17.7720(18)	14.8977(4)
<i>b</i> /Å	16.2657(9)	11.6573(12)	29.2369(9)
<i>c</i> /Å	10.7306(6)	29.512(3)	12.7603(5)
α /°	90	90	90
β /°	90	101.183(3)	90
γ /°	90	90	90
<i>U</i> Å ³	5667.4(5)	5998.0(11)	5557.9(3)
<i>Z</i>	4	4	4
<i>F</i> (000)	2352	2512	2164
<i>D_c</i> /g cm ⁻³	1.305	1.317	1.242
μ /mm ⁻¹	0.111	0.098	0.574
2 θ_{max} /°	55.7	41.6	51.8
Data collected	71067	40470	31696
Unique data	10395	6251	4170
<i>R_{int}</i>	0.0598	0.1060	0.0499
Obs data (<i>I</i> >2 σ (<i>I</i>))	8996	3790	3763
Parameters	743	784	323
Restraints	1	0	46
<i>R</i> ₁ (observed data)	0.0406	0.0882	0.0637
ωR_2 (all data)	0.0966	0.2355	0.1769
<i>GooF</i>	1.018	1.017	1.065
Max/min residuals [e.Å ⁻³]	0.49/-0.27	1.30/-0.83	0.79/-0.36

Table 4.5. Details of data collection and structure refinement for complexes **4.3** - **4.5**.

Complex number	4.6
Formula	$C_{57}H_{65}MnN_3O_{20}$
<i>Mr</i>	1167.06
Crystal system	Monoclinic
Space group	<i>C2/c</i>
<i>T</i> /K	100(2)
<i>a</i> /Å	12.4398(5)
<i>b</i> /Å	27.9839(11)
<i>c</i> /Å	15.9403(6)
α /°	90
β /°	91.647(2)
γ /°	90
<i>U</i> Å ³	5546.8(4)
<i>Z</i>	4
<i>F</i> (000)	2452
<i>D_c</i> /g cm ⁻³	1.398
μ /mm ⁻¹	0.319
$2\theta_{max}$ /°	58.1
Data collected	35944
Unique data	5701
<i>R_{int}</i>	0.0440
Obs data (<i>I</i> > 2 $\sigma(I)$)	4310
Parameters	350
Restraints	41
<i>R</i> ₁ (observed data)	0.0852
ωR_2 (all data)	0.2477
<i>GooF</i>	1.040
Max/min residuals [e.Å ⁻³]	1.01/-1.81

Table 4.6. Details of data collection and structure refinement for complex **4.6**.

4.7. References.

1. A. Arduini, M. Fabbi, M. Mantovani, L. Mirone, A. Pochini, A. Secchi and R. Ungaro, *J. Org. Chem.*, 1995, **60**, 1454.
2. C. D. Gutsche, *Calixarenes Revisited*; J. F. Stoddart, Ed.; The Royal Society of Chemistry: Cambridge, 1998.
3. Z. Asfari, V. Böhmer, J. Harrowfield and J. Vicens, *Calixarenes 2001*, Kluwer Academic Publishers, 2001.
4. A. Pochini, and R. Ungaro, *Comprehensive Supramolecular Chemistry*; F. Vögtle, Ed.; Elsevier: New York, 1996.
5. W. Sliwa, and C. Kozłowski, *Calixarenes and Resorinarenes: Synthesis, Properties and Applications*; Wiley-VCH: Weinheim, 2009.
6. C. Alfieri, E. Dradi, A. Pochini, R. Ungaro and G. D. Andreotti, *J. Chem. Soc., Chem. Commun.*, 1983, 1075.
7. a) A. Arduini, A. Casnati, L. Dodi, A. Pochini and R. Ungaro, *J. Chem. Soc., Chem. Commun.*, 1990, 1597; b) A. Arduini, L. Domiano, A. Pochini, A. Secchi, R. Ungaro, F. Ugozzoli, O. Struck, W. Verboom and D. N. Reinhoudt, *Tetrahedron* 1997, **53**, 3767; c) S. Caccmese, A. Notti, S. Pappalardo, M. F. Parisi and G. Principato, *Tetrahedron* 1999, **55**, 5505.
8. A. Arduini, S. Fanni, G. Manfredi, A. Pochini, R. Ungaro, A. R. Sicuri and F. Ugozzoli, *J. Org. Chem.* 1995, **60**, 1448.
9. A. Casnati, M. Fochi, P. Minari, A. Pochini, M. Reggiani and R. Ungaro, *Gazz. Chim. Ital.* 1996, **126**, 99.
10. A. Casnati, A. Sartori, L. Pirondini, F. Bonetti, N. Pelizzi, F. Sansone, F. Ugozzoli and R. Ungaro, *Supramol. Chem.* 2006, **18**, 199.
11. T. Pierro, C. Gaeta, F. Troisi and P. Neri, *Tetrahedron Lett.* 2009, **50**, 350.
12. Q. Lin and A. D. Hamilton, *C. R. Chimie.*, 2002, **5**, 441.
13. M. Cui, X. Wang, P. Yu, J. Zhang, Z. Li, X. Zhang, Y. Yang, M. Ono, H. Jia, H. Saji and B. Liu, *J. Med. Chem.* 2012, **55**, 9283.
14. A. Arduini, W. M. McGregor, D. Paganuzzi, A. Pochini, A. Secchi, F. Ugozzoli and R. Ungaro, *J. Chem. Soc., Perkin Trans. 2*, 1996, 839.
15. V. Arora, H. M. Chawla and A. Santra, *Tetrahedron* 2002, **58**, 5591.
16. a) S. J. Dalgarno, J. E. Warren, J. Antesberger, T. E. Glass and J. L. Atwood, *New. J. Chem.* 2007, **31**, 1891. b) S. Kennedy and S. J. Dalgarno, *Chem. Commun.*, 2009, 5275. c) S. Kennedy, S. J. Teat and S. J. Dalgarno, *Dalton*

- Trans.*, 2010, **39**, 384. d) S. Kennedy, C. M. Beavers, S. J. Teat and S. J. Dalgarno, *New. J. Chem.* 2011, **35**, 28. e) S. Kennedy, C. M. Beavers, S. J. Teat and S. J. Dalgarno, *Cryst. Growth Des.* 2012, **12**, 679. f) S. Kennedy, I. E. Dodgson, C. M. Beavers, S. J. Teat and S. J. Dalgarno, *Cryst. Growth Des.* 2012, **12**, 688. g) S. Kennedy, P. Cholewa, R. D. McIntosh and S. J. Dalgarno, *CrystEngComm.*, 2013, **15**, 1520.
17. a) B. Linton and A. D. Hamilton, *Chem. Rev.* 1997, **97**, 1669. b) P. J. Stang and B. Olenyuk, *Acc. Chem. Res.* 1997, **30**, 502. c) L. R. MacGillivray and J. L. Atwood, *Angew. Chem. Int. Ed.* 1999, **38**, 1018. d) S. Leininger, B. Olenyuk and P. J. Stang, *Chem. Rev.* 2000, **100**, 853.
 18. S. Russel-Seidel and P. J. Stang, *Acc. Chem. Res.* 2002, **35**, 972.
 19. D. L. Caulder and K. N. Raymond, *Acc. Chem. Res.* 1999, **32**, 975.
 20. K. S. Hagen and R. Lachicotte, *J. Am. Chem. Soc.*, 1992, **114**, 8741.
 21. A. Karmakar, R. J. Sarma and J. B. Baruah, *Eur. J. Inorg. Chem.* 2006, 4673.
 22. M. E. Braun, C. D. Steffek, J. Kim, P. G. Rasmussen and O. M. Yaghi, *Chem. Commun.*, 2001, 2532.
 23. M. Eddaoudi, J. Kim, J. B. Wachter, H. K. Chae, M. O’Keeffe and O. M. Yaghi, *J. Am. Chem. Soc.*, 2001, **123**, 4368.
 24. a) S. Kennedy, G. Karotsis, C. M. Beavers, S. J. Teat, E. K. Brechin and S. J. Dalgarno, *Angew. Chem. Int. Ed.* 2010, **49**, 4205. b) P. P. Cholewa, C. M. Beavers, S. J. Teat and S. J. Dalgarno, *Cryst. Growth Des.* 2013, **13**, 2703. c) P. P. Cholewa, C. M. Beavers, S. J. Teat and S. J. Dalgarno, *Chem. Commun.*, 2013, **49**, 3203. d) P. P. Cholewa, C. M. Beavers, S. J. Teat and S. J. Dalgarno, *Cryst. Growth Des.* 2013, **13**, 5165; e) S. Kennedy, C. M. Beavers, S. J. Teat and S. J. Dalgarno, *CrystEngComm.*, 2014, **16**, 3712.
 25. For an example of a *p*-*tert*-butylcalix[4]arene bi-layer assembly see: J. L. Atwood, L. J. Barbour, A. Jerga and B. L. Schottel, *Science*, 2002, **298**, 1000.
 26. A. L. Spek, *Acta Crystallogr. A*, 1990, **46**, C34.

Chapter 5: Suzuki cross-coupling reactions of calix[4]arenes.

5.1. Introduction.

This chapter is concerned with extending the upper-rim of the calixarene skeleton in order to form a range of rigid aromatic systems as model compounds. The synthesis of elongated calix[4]arene precursors *via* C-C bond formation by palladium-catalysed Suzuki coupling reaction at the upper-rim was studied in order to achieve this. A number of novel cross-coupled *p*CO₂[4]s were generated and studied, with various substituents present at the lower-rim. Single crystal X-ray structures for some of the macrocycles synthesised have been obtained and are discussed below. The pyridine-templated assembly of these compounds was examined and structural studies of all single crystals obtained are presented.

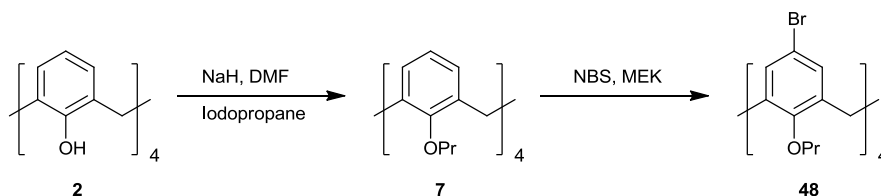
The palladium-catalysed Suzuki and Sonogashira cross-coupling reactions of halogenated calixarene precursors have become well established synthetic pathways for the preparation of deep cavity molecules. The Suzuki cross-coupling reaction will be implemented to synthesise a range of functionalised pinched cone or cone calixarene conformers with a relatively deep π -electron-rich cavity. To date the chemistry of deep cavity calixarenes has not been largely explored because the reaction pathways explored often lead to low yielding products.¹

5.2. Synthesis of cross-coupled calix[4]arenes.

C[4] **2** is commonly used as a molecular scaffold owing to its basket-like shape and ease of functionalisation. Given this, it is surprising that there are limited examples which recognise the importance of an extended preorganised rigid calixarene platform that can be used for the assembly of supramolecular systems.² Several extended calix[4]arene derivatives tetra-alkylated at the lower-rim and fully substituted at the upper-rim, utilising Suzuki cross-coupling were synthesised. However, before this work can be executed it was first necessary to synthesise tetra halogenated calix[4]arenes as starting materials in which to perform the cross-coupling on.

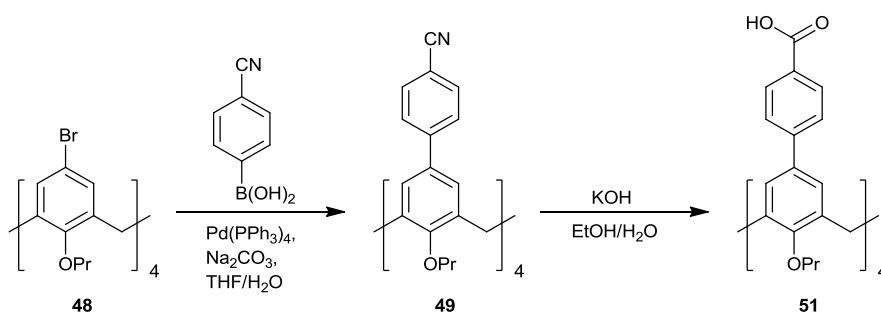
Compound **48** was prepared in two steps from C[4] **2** as shown in Scheme 5.1. Tetra-*O*-alkylated calix[4]arene **7** was obtained as previously discussed in Chapter 2³ and

subsequent bromination under the conditions developed by Gutsche *et al.*⁴ utilising *N*-bromosuccinimide (NBS) in methyl ethyl ketone yielded **48** in 91% yield. The introduction of *n*-propyl groups at the lower-rim of the C[4] framework inhibits rotation,⁵ and compound **48** was found to adopt the expected pinched-cone conformation with the distinctive set of doublets at 4.29 and 3.02 ppm in the ¹H NMR.



Scheme 5.1. Synthesis of tetrabromo-tetrapropoxycalix[4]arene, **48**.

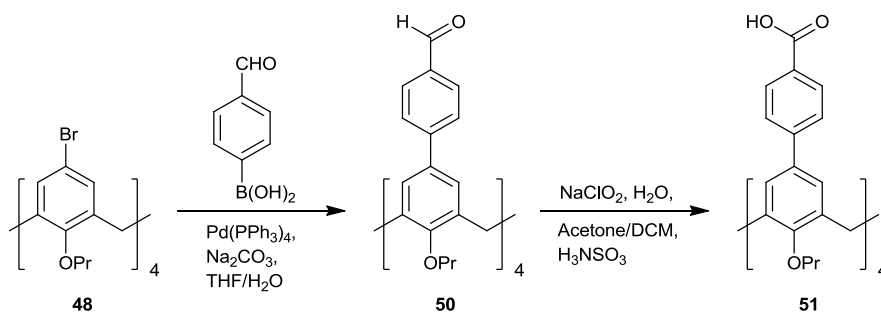
Two synthetic pathways were explored in order to obtain the desired carboxyphenylcalix[4]arene. Although both used the same principle Suzuki cross-coupling methodology, the boronic acids used were different. The first route that was explored prepared carboxyphenylcalix[4]arene **51** in two steps from compound **48** (Scheme 5.2).⁶ Suzuki coupling of compound **48** with *p*-cyanophenylboronic acid was achieved using palladium tetrakis(triphenylphosphine) and sodium carbonate in THF/water. Hydrolysis of the intermediate nitrophenylcalix[4]arene **49** with KOH in EtOH/water afforded compound **51** but only in low yield (< 15%).



Scheme 5.2. Synthesis of carboxyphenylcalix[4]arene **51** using *p*-cyanophenylboronic acid.

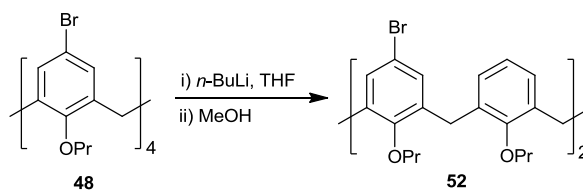
In an attempt to increase the yield of product **51** the boronic acid used in the same cross-coupling procedure was substituted. The synthesis of tetra(4-formylphenol)-tetrapropoxycalix[4]arene **50** is summarised in Scheme 5.3.⁶ The extended aryl calix[4]arene skeleton was constructed by a convergent approach using the palladium-catalysed Suzuki cross-coupling of 4-formylphenylboronic acid and compound **48**.

Oxidation of compound **50** using sodium chlorite in the presence of sulfamic acid⁷ yielded compound **51** in quantitative yield. It should be noted that the synthesis of compound **51** has also been reported using 4-formylphenylboronic acid with palladium(II) acetate ($\text{Pd}(\text{OAc})_2$) and tri(*o*-tolyl)phosphine ($\text{P}(\text{o-tol})_3$) used as a catalyst.⁸



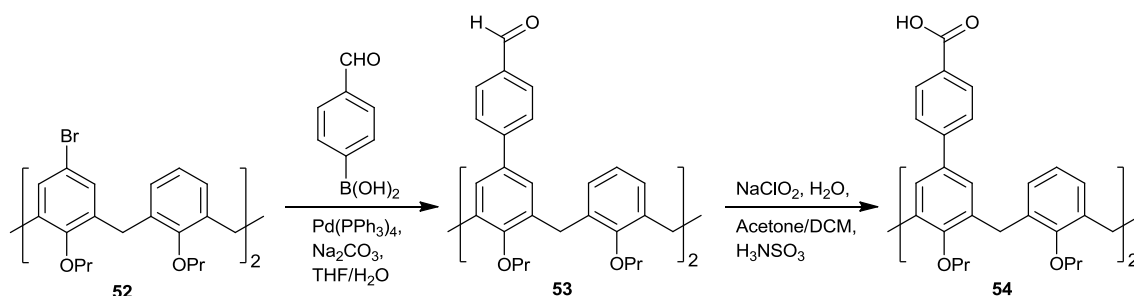
Scheme 5.3. Alternative synthetic pathway to give carboxyphenylcalix[4]arene, **51**.

With the successful isolation of compound **51** achieved, attention was turned towards the synthesis of the dicarboxyphenyl-tetrapropoxycalix[4]arene analogue. To accomplish the synthesis of this desired product, compound **48** was subject to selective bromine-lithium exchange⁹ with excess *n*-BuLi in THF at -78°C to yield the dibromo-tetrapropoxycalix[4]arene **52** (Scheme 5.4).



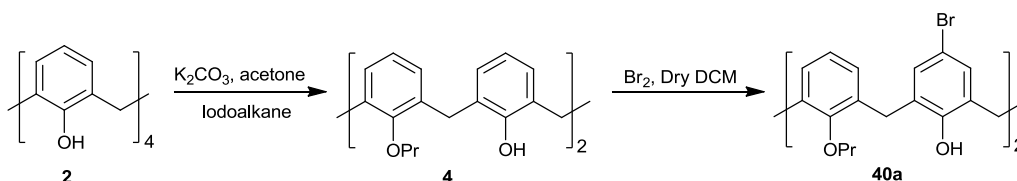
Scheme 5.4. Synthesis of dibromo-tetrapropoxycalix[4]arene, **52**.

The same synthetic approach to prepare the diacid cross-coupled C[4] (compound **54**, Scheme 5.5) relies upon the Suzuki cross-coupling reaction of 4-formylphenyl boronic acid at the upper-rim of compound **52**, followed by the oxidation of the diformylphenyl intermediate compound **53** with sodium chlorite in the presence of sulfamic acid.^{6,7}



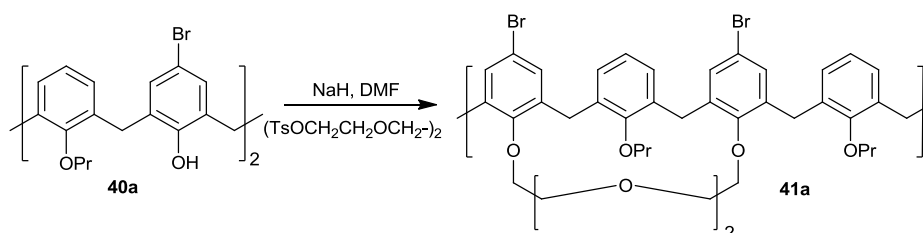
Scheme 5.5. Suzuki cross-coupling with 4-formylphenylboronic acid, followed by oxidation to give compound **54**.

Another approach to obtain a derived calix[4]arene deep cavity was to suppress the mobility of the cone conformer, followed by Suzuki cross-coupling at the upper-rim of the macrocycle. To begin, a polyether bridge at the lower-rim was introduced, linking two distal phenolic rings¹⁰ as previously discussed and synthesised in Chapter 4. The other alternative avenue was to protect the two hydroxyl groups on the lower-rim with benzyl groups in the hope of cleaving them following cross-coupling at the upper-rim. Selective 1,3-dipropylation of C[4] **2** was carried out with an excess of 1-iodopropane and K_2CO_3 in acetone¹¹ to give compound **4** as discussed in Chapter 2 (Scheme 5.6). Subsequent reaction of compound **4** with bromine solution gave the halogenated calixarene **40a**.¹²



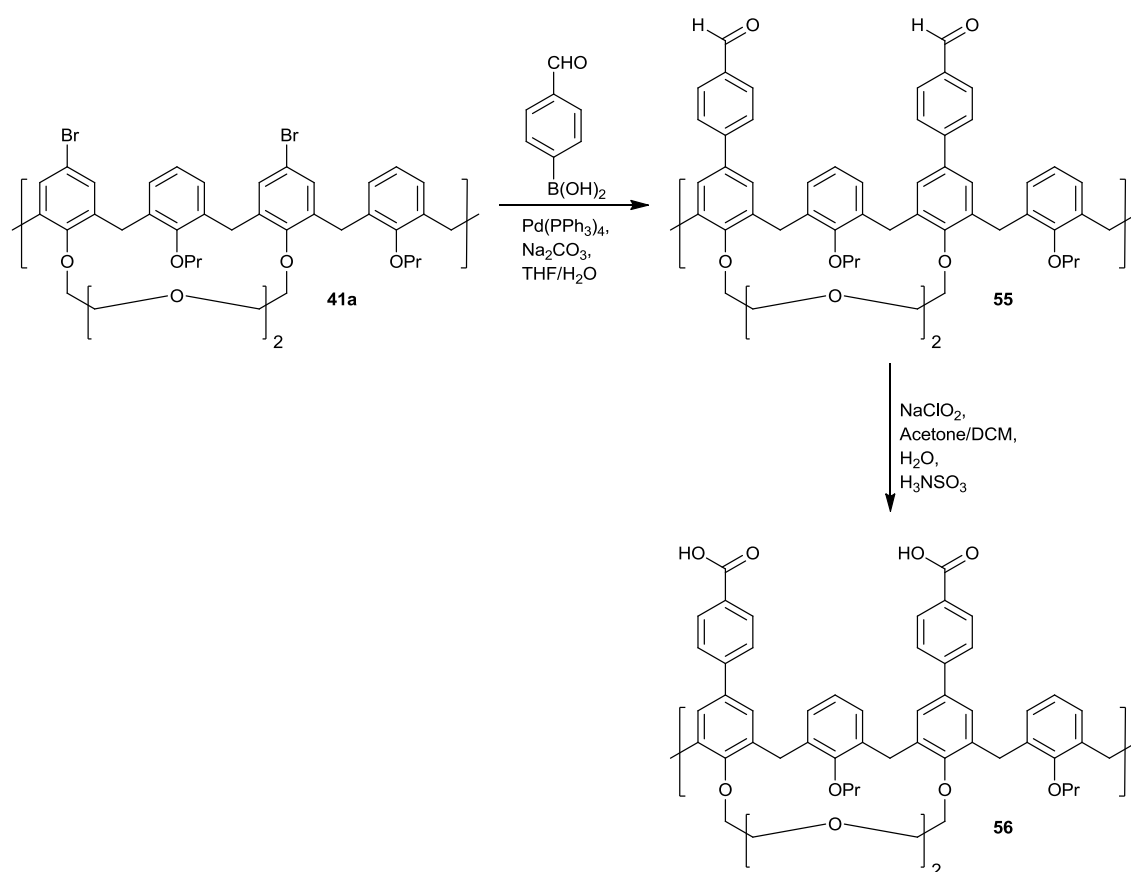
Scheme 5.6. Synthesis of di-*O*-propoxycalix[4]arene and subsequent dibromination.

Reaction of compound **40a** with triethylene glycol ditosylate with an excess of NaH as a base in DMF afforded the desired product **41a** in 86% yield as shown in Scheme 5.7.¹⁰



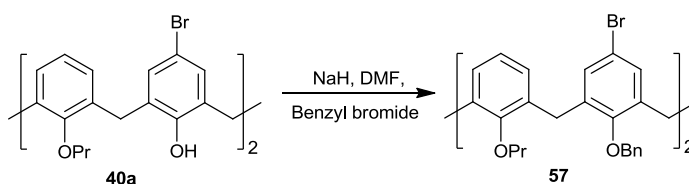
Scheme 5.7. Synthesis of dibromocalix[4]arene-crown-4 derivative **41a**.

In order to extend the framework with 4-formyl phenyl units, a previously established palladium-catalysed Suzuki cross-coupling reaction was employed.⁶ Suzuki coupling of compound **41a** with 4-formylphenylboronic acid was achieved *via* the same procedure used to give compound **55**. Oxidation of compound **55** using sodium chlorite in the presence of sulfamic acid⁷ yielded the corresponding diacid **56** in quantitative yield (Scheme 5.8).



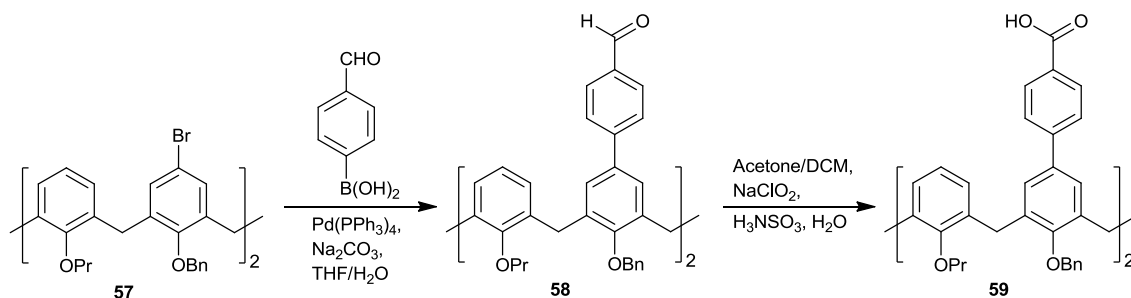
Scheme 5.8. Synthesis of di(*p*-benzoic acid)dipropoxycalix[4]arene-crown-4, **56**.

The same synthetic procedure was followed for the addition of benzyl groups to the lower-rim of compound **40a**. Reaction of compound **40a** with benzyl bromide in DMF with an excess of NaH as a base afforded compound **57** in 87% yield (Scheme 5.9).¹³



Scheme 5.9. Synthesis of dibromo-dibenzyloxy-dipropoxycalix[4]arene, **57**.

The aforementioned palladium-catalysed Suzuki cross-coupling reaction⁶ was applied once again to compound **57**, affording the extended diformyl compound **58** in 60% yield. Oxidation using sodium chlorite in addition with sulfamic acid afforded compound **59** in almost quantitative yield (Scheme 5.10).⁷



Scheme 5.10. Suzuki cross-coupling reaction to afford compound **59**.

As eluded to above, it was thought that the benzyl protecting groups could be readily removed using AlCl_3 , thereby giving the cross-coupled lower-rim di-propoxy C[4]. This would have allowed the C[4] to adopt a cone conformation due to hydrogen bonding present at the lower-rim. However, these conditions were found to be too harsh and rather than remove the benzyl group as expected, the cross-coupled sections of the molecule were cleaved. An alternative synthetic route for lower-rim de-protection is required but this was not explored due to time constraints.

With the optimised Suzuki cross-coupling proving successful, the self-assembly of compounds **51**, **54**, **56**, **58** and **59** was explored by their crystallisation from a series of commercially available pyridine derivative solvents; these were pyridine (Py), 2-picoline (2-Pic), 3-picoline (3-Pic) and 4-picoline (4-Pic). Acetone and DMF were also used in an attempt to obtain single crystals that could be studied using single crystal X-ray diffraction. In addition to this, an investigation into the use of 2-aminopyridine (2-AP) for salt formation and templation was executed. Nine sets of single crystals were acquired from these five compounds, all of which are discussed in detail below.

5.3. X-ray crystal structures of compounds **51**, **54**, **56**, **58** and **59**.

Calix[4]arene derivatives **51** and **54** were synthesised according to literature procedures and fully characterised, along with the synthesis of novel *p*CO₂[4]s **56** and **59**. The ¹H NMR spectra that were recorded for each compound indicated that the dominant conformer is pinched cone in all cases.

5.3.1. Structure of tetra(*p*-benzoic acid)tetrapropoxycalix[4]arene pyridine, **5.1**.

Crystals of tetra(*p*-benzoic acid)tetrapropoxycalix[4]arene Py, **5.1**, were obtained as a result of the addition of 2 mL of Py to a sample of compound **51**. Slow evaporation of the solvent over the period of a week yielded small colourless blocks which were suitable for X-ray diffraction studies by synchrotron radiation in order to obtain satisfactory structure solution. Single crystals of **5.1** were found to be in a monoclinic cell and the structure solution was performed in the space group *P*2₁/*c*. Details of the collection and structure refinement are given in Table 5.3 at the end of this chapter. The asymmetric unit consists of one molecule of **51** and six Py molecules (Figure 5.1). Compound **51** was found to adopt the pinched cone conformation, with the proximal carbon atoms in the pinched upper-rim CO₂H groups being separated by a C[42]...C[56] distance of 3.573 Å. Four of the six Py molecules in the asymmetric unit interact with the upper-rim CO₂H groups *via* the common Py...CO₂H synthon. There are four symmetry unique N...HOCO hydrogen bonding interactions with distances ranging from 1.760 – 1.873 Å, and four CH...OCOH interactions with distances ranging from 2.593 – 3.056 Å (full details in Table 5.1).

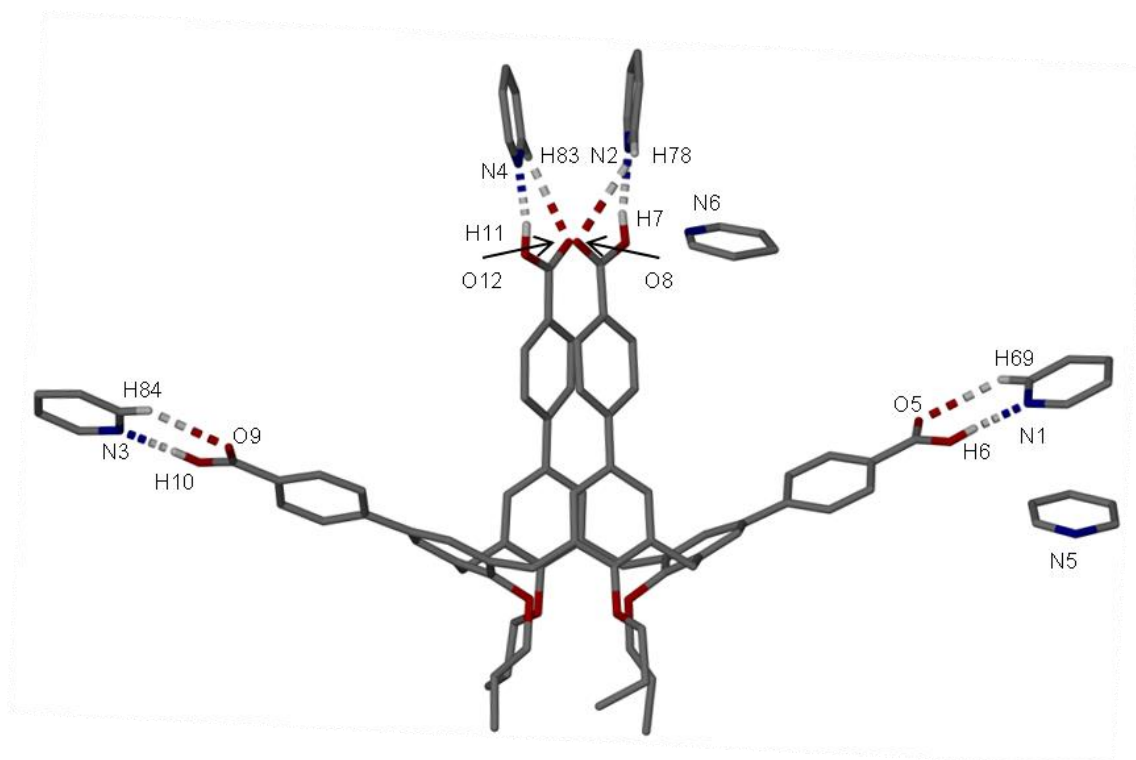


Figure 5.1. The asymmetric unit in the X-ray crystal structure of **5.1**. Hydrogen bonding interactions are shown as split-colour dashed lines. Hydrogen atoms (apart from those involved in hydrogen bonding interactions) have been omitted for clarity. Selected atoms have been labelled according to discussion.

H[6]···N[1]	1.767	H[69]···O[5]	2.692
H[7]···N[2]	1.873	H[78]···O[8]	3.056
H[10]···N[3]	1.770	H[84]···O[9]	2.593
H[11]···N[4]	1.760	H[83]···O[12]	2.694

Table 5.1. Hydrogen bonding distances (in Å) between Py molecules and the upper-rim CO₂H groups of compound **5.1**.

Four of the six Py molecules in the asymmetric unit interact with each other *via* π -stacking interactions, with aromatic centroid···aromatic centroid distances of 3.778 Å and 3.906 Å. There is an additional π -stacking interaction present between the two pinched upper-rim CO₂H groups, and this occurs with an aromatic centroid···aromatic centroid distance of 4.047 Å (Figure 5.2).

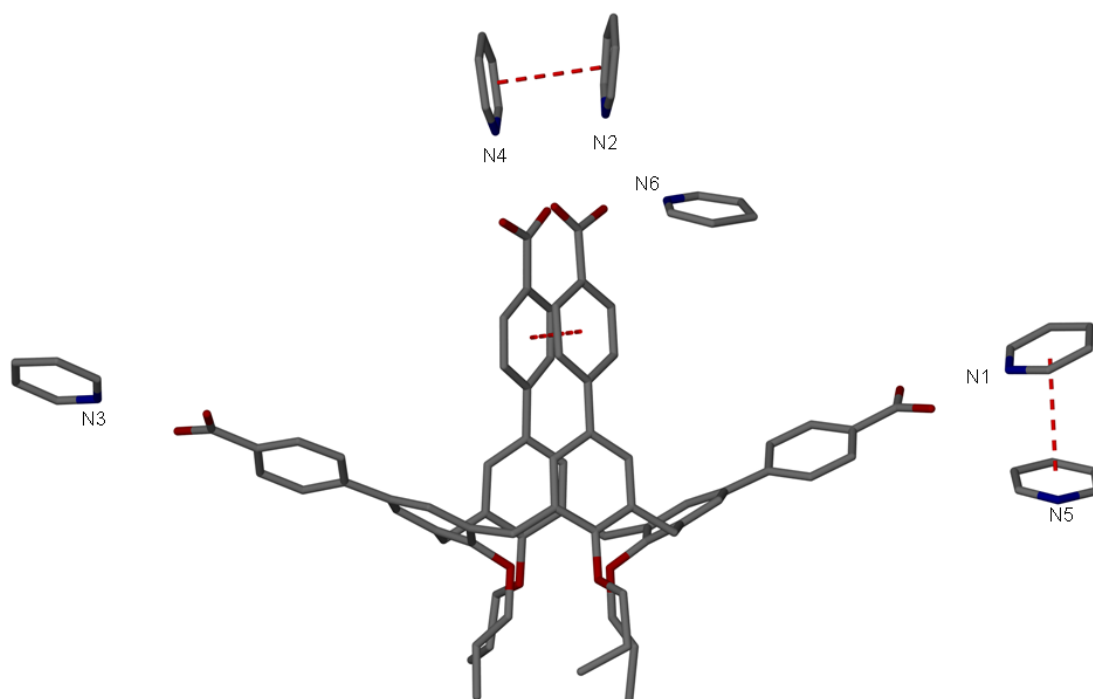


Figure 5.2. The asymmetric unit observed in the X-ray crystal structure of **5.1**. $\pi \cdots \pi$ stacking interactions are shown as red dashed lines. Hydrogen atoms have been omitted for clarity. Selected atoms have been labelled according to discussion.

5.3.2. Structure of tetra(*p*-benzoic acid)tetrapropoxycalix[4]arene-4-picoline, **5.2**.

Crystals of tetra(*p*-benzoic acid)tetrapropoxycalix[4]arene-4-Pic, **5.2**, were obtained as a result of the addition of 2 mL of 4-Pic to a sample of compound **5.1**. Slow evaporation of the solvent over the period of a week yielded small colourless plates which were suitable for X-ray diffraction studies. Single crystals of **5.2** were found to be in a monoclinic cell and the structure solution was performed in the space group $P2_1/n$. Details of the collection and structure refinement are given in Table 5.3 at the end of this chapter. The asymmetric unit consists of one molecule of **5.1** and six 4-Pic molecules. Compound **5.1** was found to adopt the pinched cone conformer, with the proximal carbon atoms in the pinched upper-rim CO_2H groups separated by a $\text{C}[65] \cdots \text{C}[67]$ distance of 3.446 Å. Four of the six 4-Pic molecules in the asymmetric unit interact with the upper-rim CO_2H groups *via* the common $\text{Py} \cdots \text{CO}_2\text{H}$ synthon (Figure 5.3). There are four symmetry unique $\text{N} \cdots \text{HOCO}$ hydrogen bonding interactions with distances ranging from 1.788 – 1.815 Å, and four $\text{CH} \cdots \text{OCOH}$ interactions with distances ranging from 2.516 – 3.580 Å (full details in Table 5.2).

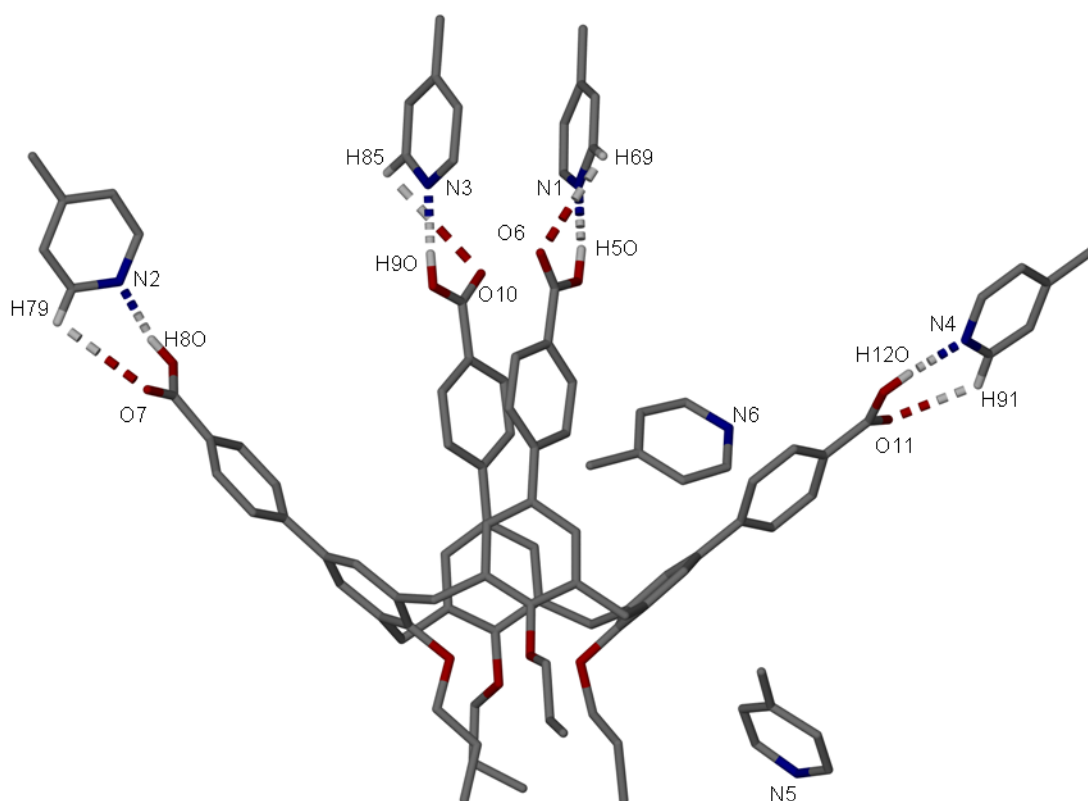


Figure 5.3. The asymmetric unit in the X-ray crystal structure of **5.2**. Hydrogen bonding interactions are shown as split-colour dashed lines. Hydrogen atoms (apart from those involved in hydrogen bonding interactions) have been omitted for clarity. Selected atoms have been labelled according to discussion.

H[50]...N[1]	1.788	H[69]...O[6]	3.154
H[80]...N[2]	1.815	H[79]...O[7]	3.052
H[90]...N[3]	1.805	H[85]...O[10]	3.580
H[120]...N[4]	1.797	H[91]...O[11]	2.516

Table 5.2 Hydrogen bonding distances (in Å) between 4-Pic molecules and the upper-rim CO₂H groups of compound **51**.

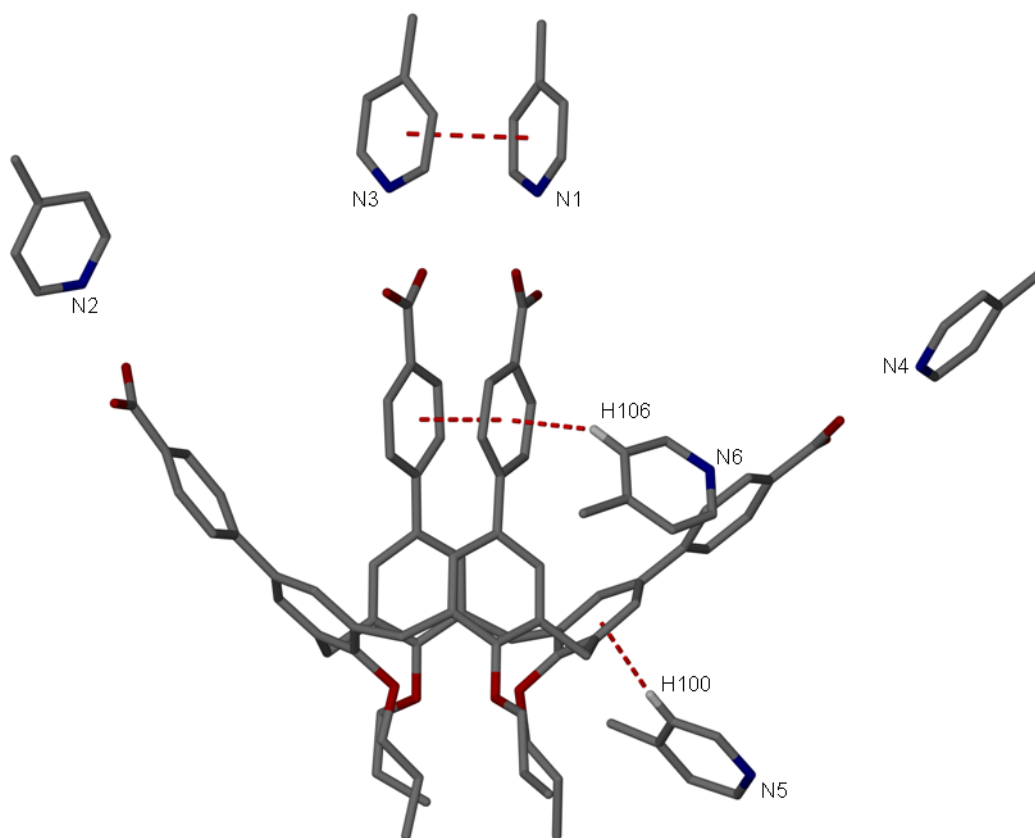


Figure 5.4. The asymmetric unit observed in complex **5.2**. CH $\cdots\pi$ and $\pi\cdots\pi$ stacking interactions are shown as red dashed lines. Hydrogen atoms (apart from those involved in CH $\cdots\pi$ interactions) have been omitted for clarity. Selected atoms have been labelled according to discussion.

Two of the four 4-Pic molecules in the asymmetric unit interact with each other *via* a π -stacking interaction with an aromatic centroid \cdots aromatic centroid distance of 3.976 Å. There is an additional π -stacking interaction present between the two pinched upper-rim CO₂H groups (Figure 5.4). This occurs with an aromatic centroid \cdots aromatic centroid distance of 3.675 Å. There are also two CH $\cdots\pi$ interactions located between a *meta* hydrogen atom on the two 4-Pic molecules that are not involved in upper-rim hydrogen bonding interactions. The two symmetry unique interactions are located with H[100] \cdots aromatic centroid and H[106] \cdots aromatic centroid distances of 2.936 and 2.714 Å. Examination of the extended structure in **5.2** reveals that molecules of **5.1** pack in an anti-parallel bi-layer array. This reveals the presence of a π -stacking interaction between one of the aromatic rings that are splayed out with the extended splayed ring of a symmetry equivalent molecule of **5.1** with an aromatic centroid \cdots aromatic centroid distance of 3.787 Å (Figure 5.5).

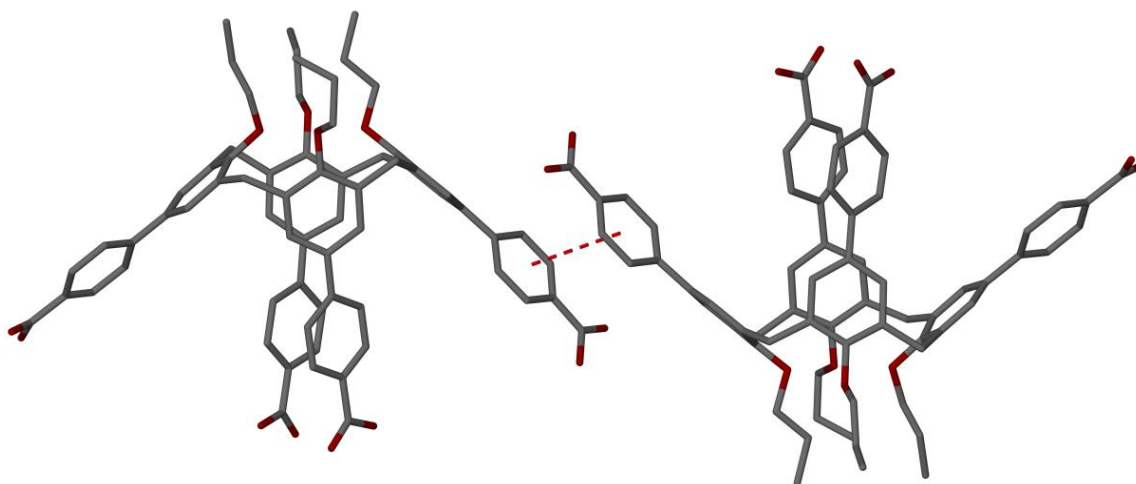


Figure 5.5. Part of the extended structure observed in **5.2**. $\pi \cdots \pi$ stacking interactions are shown as red dashed lines. Hydrogen atoms and solvent molecules have been omitted for clarity.

5.3.3. Structure of $[(\mathbf{51-2H})(2\text{-AP+H})_2](\text{MeOH})_2(\text{H}_2\text{O})_2$, **5.3**.

Single crystals of the salt $[(\mathbf{51-2H})(2\text{-AP+H})_2](\text{MeOH})_2(\text{H}_2\text{O})_2$, **5.3**, were obtained as the result of the addition of compound **51** to 3 mL of MeOH. The resulting suspension was heated and 2-AP was added slowly until the suspension became a solution. Colourless block-shaped crystals were formed overnight that were suitable for X-ray diffraction studies. Crystals of the salt **5.3** were found to be in a triclinic cell and structure solution was performed in the space group $P-1$. Details of the collection and structure refinement are given in Table 5.3 at the end of this chapter. The asymmetric unit consists of one molecule of (**51-2H**) (with two upper-rim CO_2H groups deprotonated), two 2-aminopyridinium cations, two methanol molecules and two water molecules (Figure 5.6). Two of the *O*-propyl chains attached to the lower-rim are disordered over two positions and were modelled at 50% occupancy in each position. One of the extended upper-rim aromatic rings was also found to be disordered over two positions and modelled at 50% occupancy in each position.

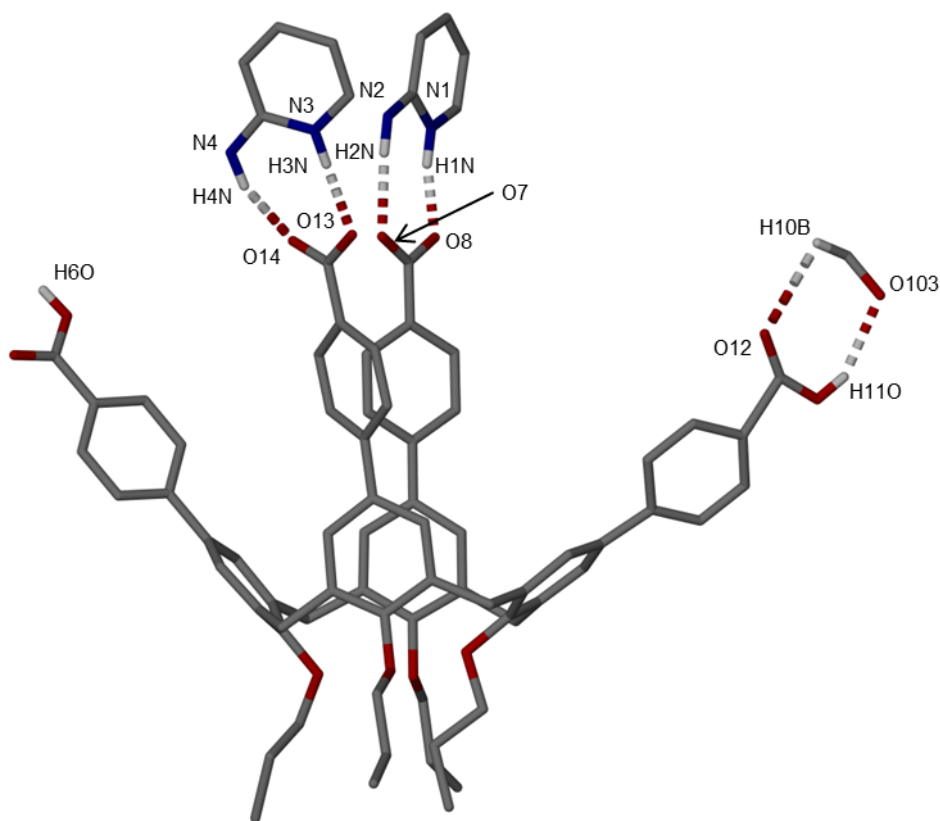


Figure 5.6. The asymmetric unit in the X-ray crystal structure of salt **5.3**. Hydrogen bonding interactions are shown as split-colour dashed lines. Hydrogen atoms (apart from those involved in hydrogen bonding interactions) have been omitted for clarity. Selected atoms have been labelled according to discussion.

Two of the cross-coupled aromatic ring CO_2^- groups interact with the (2-AP+H) cations *via* two $\text{HNH}\cdots\text{OCO}$ hydrogen bonding interactions with distances between $\text{H}[2\text{N}]\cdots\text{O}[7]$ and $\text{H}[4\text{N}]\cdots\text{O}[14]$ of 2.025 and 2.072 Å respectively. In addition, there are also two $\text{NH}\cdots\text{OCO}$ interactions between $\text{H}[1\text{N}]\cdots\text{O}[8]$ and $\text{H}[3\text{N}]\cdots\text{O}[13]$ with distances of 1.781 and 1.842 Å. There is also a $\text{COH}\cdots\text{O}$ interaction between one CO_2^- group and a water molecule with an $\text{H}[6\text{O}]\cdots\text{O}[16]$ distance of 1.767 Å. The other CO_2^- group interacts with a methanol molecule with $\text{H}[11\text{O}]\cdots\text{O}[103]$ and $\text{H}[12]\cdots\text{O}[10\text{B}]$ corresponding distances of 2.152 and 2.824 Å (Figure 5.6).

Examination of the extended structure in **5.3** reveals that anions of (**51-2H**) pack in a bi-layer array. This reveals the presence of a number of $\text{CH}\cdots\pi$ interactions between a symmetry equivalent (2-AP+H) cationic guest and the aromatic rings of the (**51-2H**) anion. There are two $\text{CH}\cdots\pi$ interactions between one of the *meta* hydrogen atoms of the (2-AP+H) cation and two aromatic centroids of the extended upper-rim with distances between $\text{H}[84]\cdots$ aromatic centroids of 2.745 and 3.537 Å. Furthermore, the *para*

hydrogen atom of (2-AP+H) cationic guest interacts with another aromatic ring with a H[83] \cdots aromatic centroid distance of 4.283 Å. The *meta* hydrogen of this aromatic ring forms a CH \cdots π interaction with the upper-rim extended aromatic ring of a symmetry equivalent (**51-2H**) anion with an H[18] \cdots aromatic centroid distance of 3.345 Å (Figure 5.7).

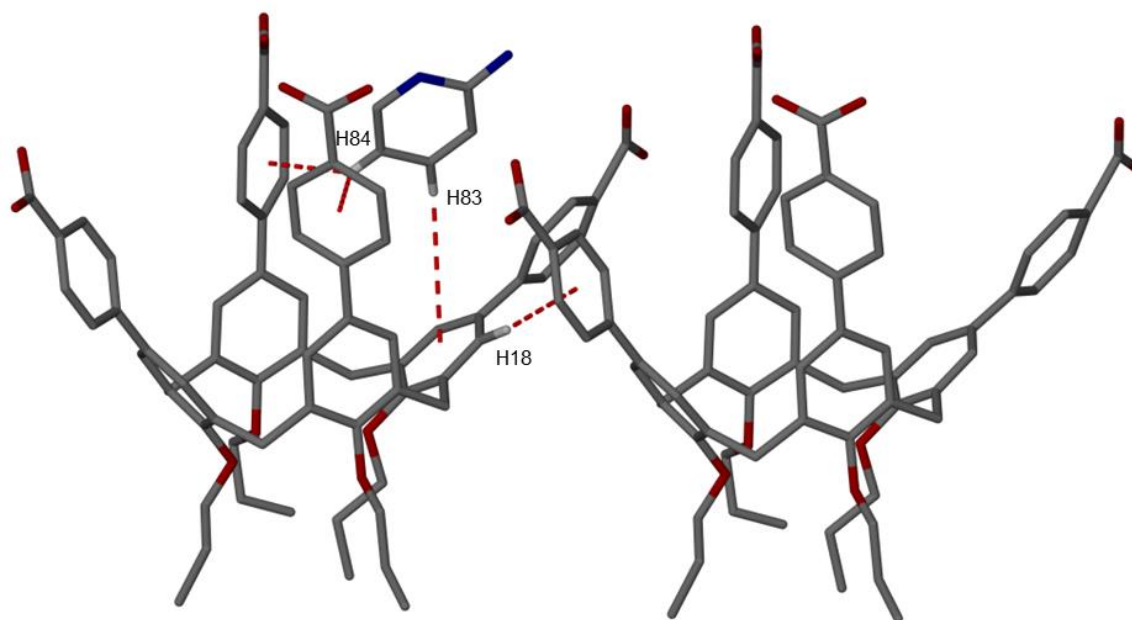


Figure 5.7. Part of the extended structure observed in **5.3**. CH \cdots π interactions are shown as red dashed lines. Hydrogen atoms (apart from those involved in CH \cdots π interactions) have been omitted for clarity. Selected atoms have been labelled according to discussion.

5.3.4. Structure of di(*p*-benzoic acid)tetrapropoxycalix[4]arene-3-picoline, **5.4**.

Crystals of di(*p*-benzoic acid)tetrapropoxycalix[4]arene-3-Pic, **5.4**, were obtained as a result of the addition of 2 mL of 3-Pic to a sample of compound **54**. Slow evaporation of the solvent over several days yielded colourless plates which were suitable for X-ray diffraction studies by synchrotron radiation in order to obtain a complete structure solution. Single crystals of **5.4** were found to be in a monoclinic cell and the structure solution was performed in the space group *P2/c*. Details of data collection and structure refinement are given in Table 5.4 at the end of this chapter. The asymmetric unit of **5.4** consists of one half molecule of **54**, one molecule of 3-Pic and a water molecule disordered over two positions that was modelled at 50% occupancy in each position

(Figure 5.8). It was seen that compound **54** was found to adopt the pinched cone conformer, owing to the propyl chains present on the lower-rim of the macrocycle. The proximal carbon atoms in the pinched upper-rim groups are separated by a C[10]...C[10] distance of 4.495 Å.

The CO₂H groups on the molecule were found to interact with both the 3-Pic molecule and the disordered water molecule. There is one CH...OCOH interaction between H[28]...O[3] with a distance of 2.682 Å. In addition there is an O...HOCO interaction between the disordered oxygen of the water molecule and the hydrogen atom of the CO₂H group with a H[4O]...O[5] distance of 1.765 Å. There should also be a N...H interactions (from the water molecule) but the hydrogen atoms are not present on the molecule so there is an N[1]...O[5] interaction with a distance of 2.716 Å (Figure 5.8).

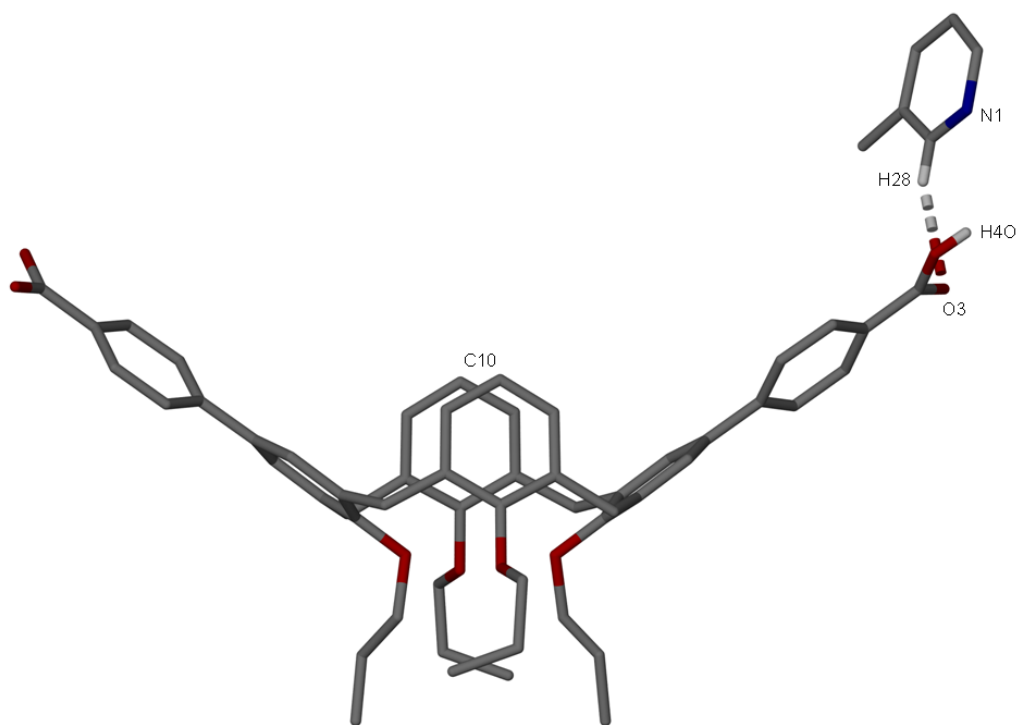


Figure 5.8. Part of the asymmetric unit in the X-ray crystal structure of **54**. Hydrogen bonding interactions are shown as split-colour dashed lines. Hydrogen atoms (apart from those involved in hydrogen bonding interactions) have been omitted for clarity. Selected atoms have been labelled according to discussion.

Symmetry expansion around molecule **54** reveals the presence of a CH... π interaction between one of the extended CO₂H groups and an aromatic ring of a symmetry

equivalent molecule with a distance of 2.659 Å between H[19]⋯aromatic centroid and another between a 3-Pic *meta* hydrogen and the aromatic ring of the extended CO₂H group with an H[30]⋯aromatic centroid distance of 2.575 Å (Figure 5.9).

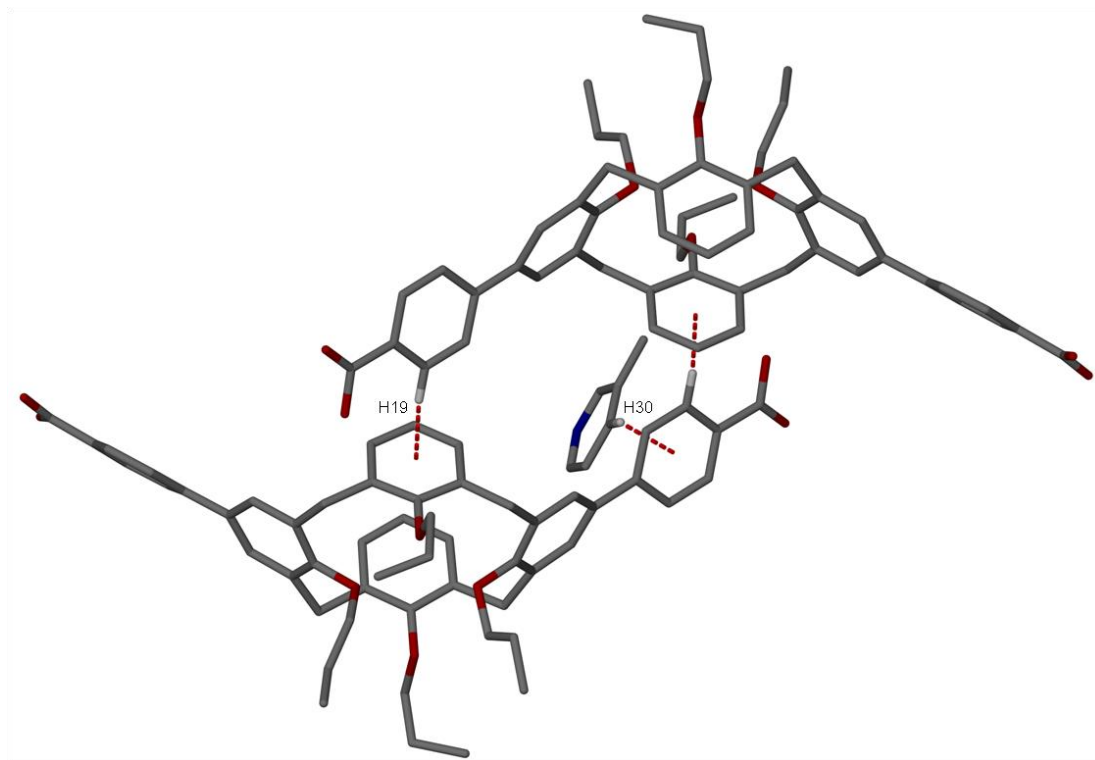


Figure 5.9. Symmetry expansion around molecule **5.4**. CH⋯π interactions are shown as red dashed lines. Hydrogen atoms (apart from those involved in CH⋯π interactions) have been omitted for clarity. Selected atoms have been labelled according to discussion.

5.3.5. Structure of di(*p*-benzoic acid)tetrapropoxycalix[4]arene·4-picoline, **5.5**.

Crystals of di(*p*-benzoic acid)tetrapropoxycalix[4]arene·4-Pic, **5.5**, were obtained as a result of the addition of 2 mL of 4-Pic to a sample of compound **5.4**. Slow evaporation of the solvent over several days yielded colourless blocks which were suitable for X-ray diffraction studies by synchrotron radiation in order to obtain an adequate structure solution. Single crystals of **5.5** were found to be in a tetragonal cell and the structure solution was performed in the space group $P4_32_12$. Details of data collection and structure refinement are given in Table 5.4 at the end of this chapter. The asymmetric unit of **5.5** consists of one half molecule of **5.4** and one 4-Pic molecule (Figure 5.10). It was seen that compound **5.4** was found to adopt the pinched cone conformer, owing to

the propyl chains present on the lower-rim of the macrocycle. The proximal carbon atoms in the pinched upper-rim groups are separated by a C[10]...C[10] distance of 4.286 Å.

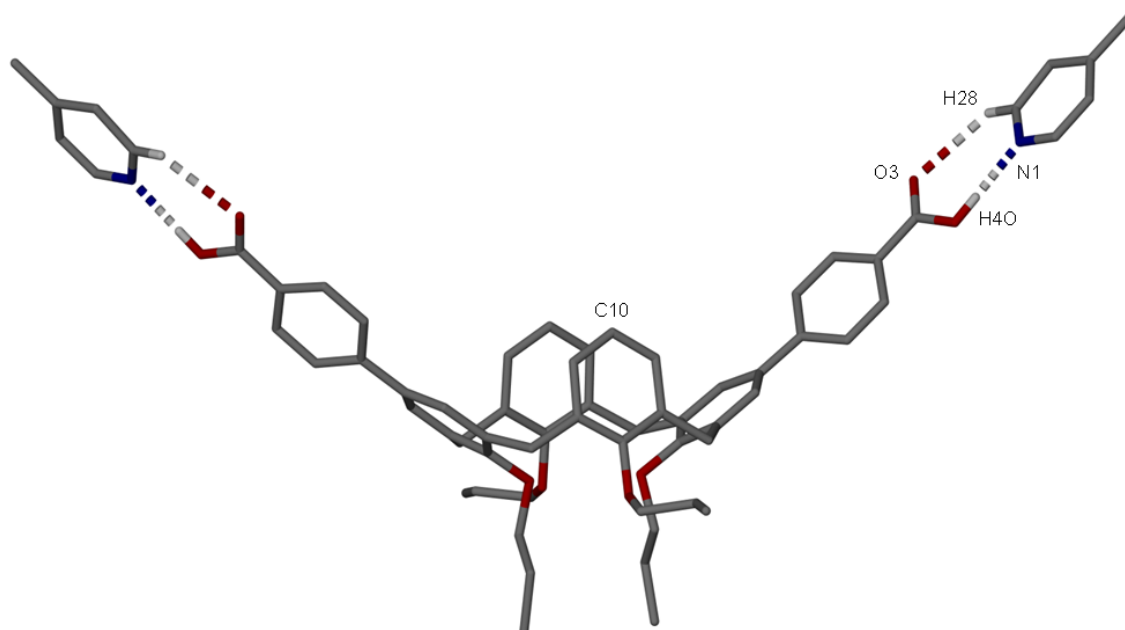


Figure 5.10. Part of the asymmetric unit in the X-ray crystal structure of **5.5**. Hydrogen bonding interactions are shown as split-colour dashed lines. Hydrogen atoms (apart from those involved in hydrogen bonding interactions) have been omitted for clarity. Selected atoms have been labelled according to discussion.

The 4-Pic molecule in the asymmetric unit interacts with the upper-rim CO₂H group *via* the common Py...CO₂H synthon. There is one N...HOCO hydrogen bonding interaction with a N[1]...H[4O] distance of 1.834 Å, and one CH...OCOH interaction with a H[28]...O[3] distance of 2.629 Å. There are also a few CH... π interactions between H[17A]...aromatic centroid, H[31]...aromatic centroid and H[33C]...aromatic centroid with distances of 3.121, 3.221 and 3.136 Å respectively (Figure 5.11).

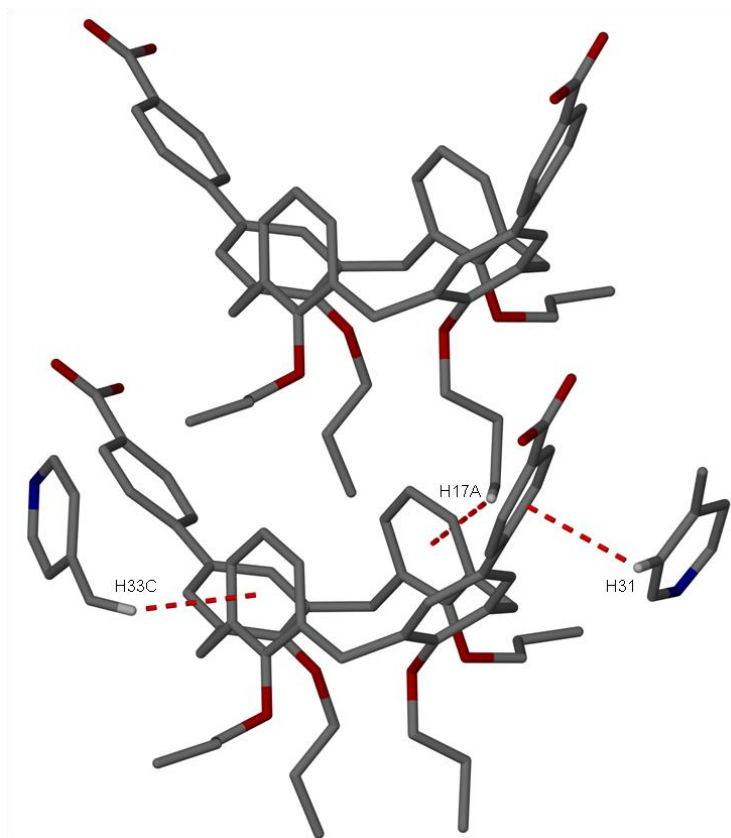


Figure 5.11. Part of the extended structure observed in **5.5**. CH $\cdots\pi$ interactions are shown as red dashed lines. Hydrogen atoms (apart from those involved in CH $\cdots\pi$ interactions) have been omitted for clarity. Selected atoms have been labelled according to discussion.

5.3.6. Structure of di(*p*-benzoic acid)dipropoxycalix[4]arene-crown-4·DMF, **5.6**.

Crystals of di(*p*-benzoic acid)dipropoxycalix[4]arene-crown-4·DMF, **5.6**, were obtained from the recrystallisation of compound **56** from DMF. Slow evaporation of the solvent overnight yielded small colourless tablet-shaped crystals which were suitable for X-ray diffraction studies. These crystals were also found to be weakly diffracting, so were studied using synchrotron radiation in order to obtain data of sufficient quality for structure solution. Single crystals of **5.6** were found to be in a monoclinic cell and the structure solution was performed in the space group *C2/c*. Details of the collection and structure refinement are given in Table 5.4 at the end of this chapter. The asymmetric unit consists of one molecule of **56** and two molecules of DMF (one is disordered over two positions). It shows that the CO₂H groups on the upper-rim of the molecule hydrogen bond to the DMF solvent molecules (Figure 5.12). One of the CO₂H groups is disordered over two positions and was modelled at 50% occupancy in each position.

This disorder of the molecule was found to show diffuse electron density associated with it. As this could not be modelled appropriately the routine SQUEEZE was applied to the data.¹⁴ This had the effect of dramatically improving the agreement indices during refinement for **5.6**.

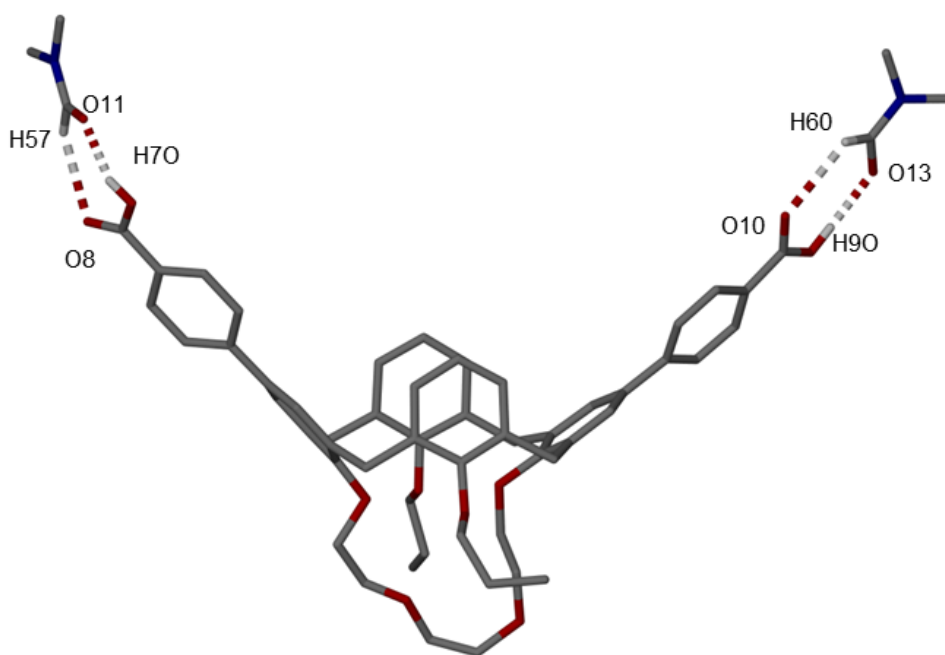


Figure 5.12. The asymmetric unit in the X-ray crystal structure of **5.6**. Hydrogen bonding interactions are shown as split-colour dashed lines. Hydrogen atoms (apart from those involved in hydrogen bonding interactions) have been omitted for clarity. Selected atoms have been labelled according to discussion.

The DMF molecules in the asymmetric unit form hydrogen bonding interactions with the two CO₂H groups in the molecule. For the first DMF molecule (not disordered) there are O[8]...H[57] and O[11]...H[70] interactions with distances of 2.471 and 1.791 Å respectively. As stated previously both the second DMF solvent molecule and one of the CO₂H groups are disordered and have been modelled at 50% occupancy in each position. Only one position is shown in Figure 5.12 with an O[10]...H[60] distance of 2.550 Å and an O[13]...H[90] distance of 1.880 Å. Due to the disorder this leads to other O...H interactions that could be possible with distances ranging from 1.652 - 3.014 Å.

Symmetry expansion around molecule **5.6** confirms the presence of a number of CH... π interactions. Two of these are between hydrogen atoms on the propyl chains and the

aromatic rings of another symmetry equivalent molecule with H[39A]...aromatic centroid and H[36B]...aromatic centroid distances of 3.187 and 2.889 Å as shown in Figure 5.13. There is also a CH... π interaction located between a meta hydrogen atom of an aromatic ring with the aromatic ring of another with an H[2]...aromatic centroid distance of 3.941 Å (Figure 5.13).

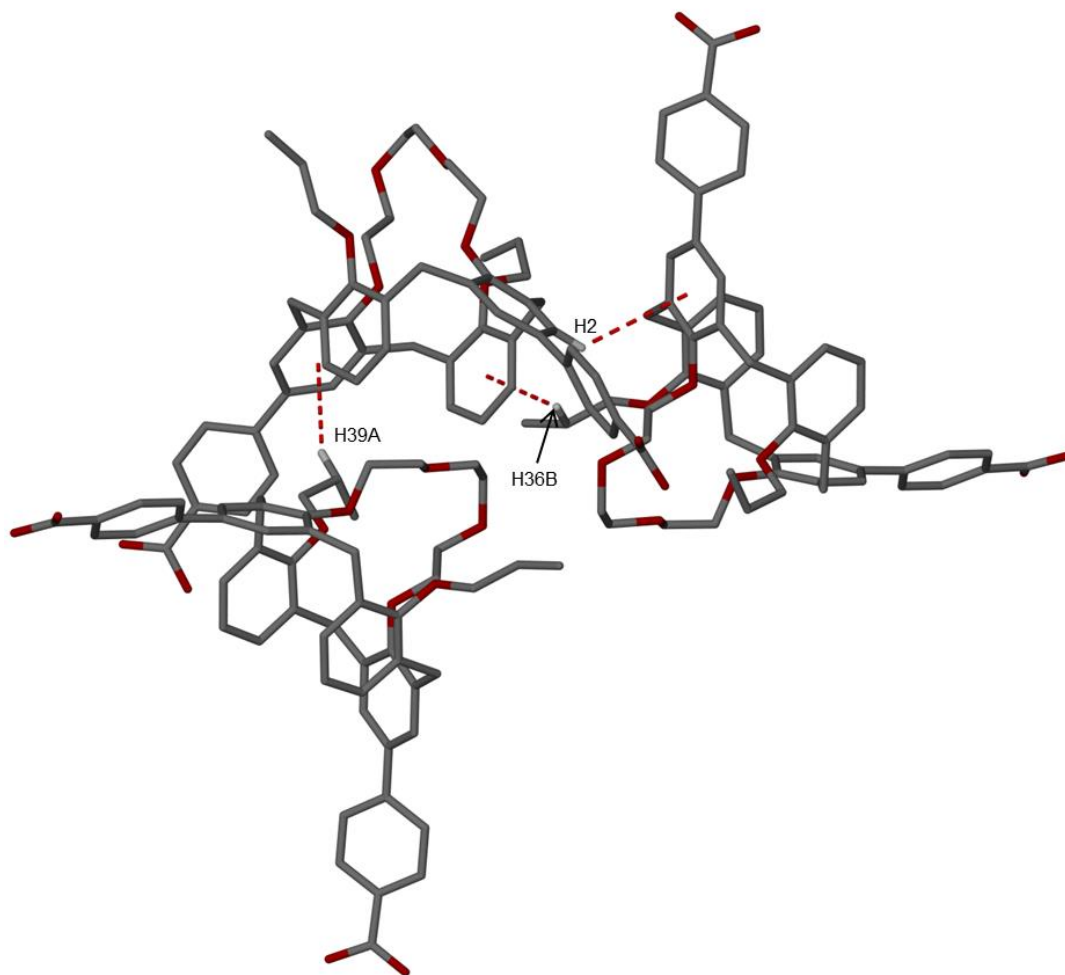


Figure 5.13. Symmetry expansion around molecule **5.6**. CH... π interactions are shown as red dashed lines. Hydrogen atoms (apart from those involved in CH... π interactions) have been omitted for clarity. Selected atoms have been labelled according to discussion.

5.3.7. Structure of di(4-formylphenyl)-dibenzyloxy-dipropoxycalix[4]arene, **58**.

Crystals of di(4-formylphenyl)-dibenzyloxy-dipropoxycalix[4]arene, compound **58**, were obtained as a result of crystallisation from acetone. Slow evaporation of the solvent overnight yielded small colourless plates which were suitable for X-ray diffraction studies by synchrotron radiation in order to obtain satisfactory structure solution. Single crystals of compound **58** were found to be in an orthorhombic cell and the structure solution was performed in the space group *Pbcn*. Details of the collection and structure refinement are given in Table 5.5 at the end of this chapter. The asymmetric unit consists of one half molecule of **58** with no solvent present in the crystal structure. Expansion of the asymmetric unit shows that compound **58** was found to adopt the pinched cone conformation. The proximal carbon atoms in the pinched upper-rim CO₂H groups are separated by a C[18]...C[18] distance of 3.713 Å. There is one OCOH...OCO hydrogen bonding interaction present between H[21]...O[3] with a distance of 3.159 Å. In addition there is a π ... π interaction between the two upper-rim cross-coupled aromatic rings with an aromatic centroid...aromatic centroid distance of 3.784 Å (Figure 5.14).

There is also one CH... π interaction located between the hydrogen atom on the formyl group with the centre of an aromatic ring on the symmetry equivalent generated molecule with a H[21]...aromatic centroid distance of 2.820 Å. Furthermore, the aldehyde oxygen interacts with another two hydrogen atoms from another symmetry equivalent molecule with distances of 2.550 and 2.819 Å for O[3]...H[7B] and O[3]...H[9] respectively. There is one final O...H interaction with the aldehyde oxygen and the *para* hydrogen from one of the benzyl groups with a O[3]...H[26] distance of 3.159 Å (Figure 5.15).

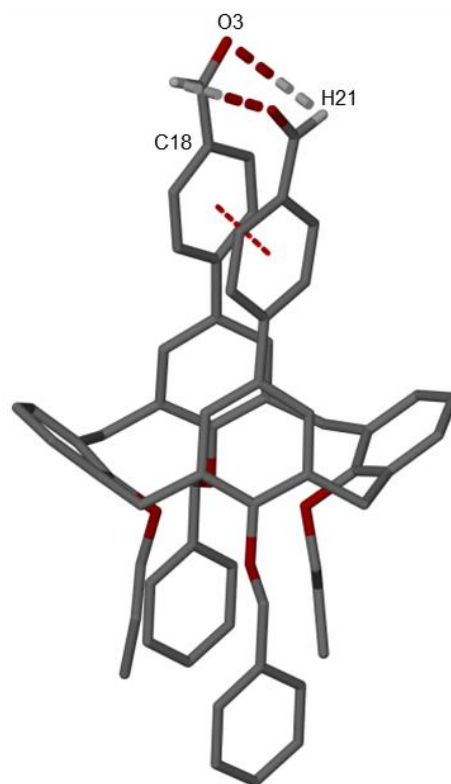


Figure 5.14. X-ray crystal structure of compound **58**. Hydrogen bonding and $\pi \cdots \pi$ interactions are shown as split-colour and red dashed lines respectively. Hydrogen atoms (apart from those involved in hydrogen bonding and $\pi \cdots \pi$ interactions) have been omitted for clarity. Selected atoms have been labelled according to discussion.

There is also one $\text{CH} \cdots \pi$ interaction located between the hydrogen atom on the formyl group with the centre of an aromatic ring on a symmetry equivalent molecule with a $\text{H}[21] \cdots \text{aromatic centroid}$ distance of 2.820 Å. Furthermore, the aldehyde oxygen interacts with another two hydrogen atoms from another symmetry equivalent molecule with distances of 2.550 and 2.819 Å for $\text{O}[3] \cdots \text{H}[7\text{B}]$ and $\text{O}[3] \cdots \text{H}[9]$ respectively. There is one final $\text{O} \cdots \text{H}$ interaction with the aldehyde oxygen and the *para* hydrogen from one of the benzyl groups with a $\text{O}[3] \cdots \text{H}[26]$ distance of 3.159 Å (Figure 5.15).

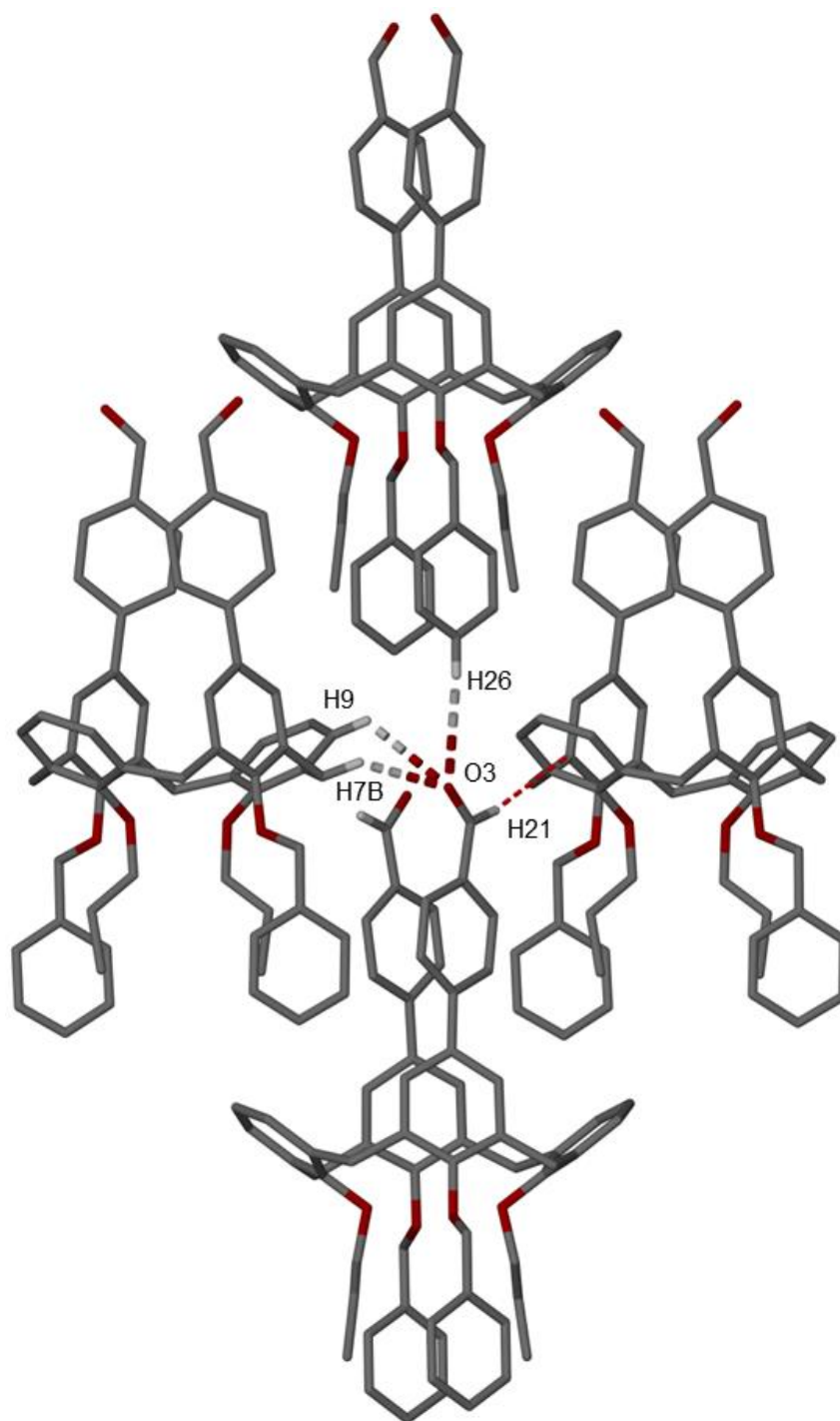


Figure 5.15. Symmetry expansion around compound **58**. Hydrogen bonding interactions and $\text{CH}\cdots\pi$ interactions are shown as split-colour and red dashed lines respectively. Hydrogen atoms (apart from those involved in hydrogen bonding and $\text{CH}\cdots\pi$ interactions) have been omitted for clarity. Selected atoms have been labelled according to discussion.

5.3.8. Structure of di(*p*-benzoic acid)-dibenzyloxy-dipropoxycalix[4]arene-2-picoline, **5.7**.

Crystals of di(*p*-benzoic acid)-dibenzyloxy-dipropoxycalix[4]arene-2-Pic, **5.7**, were obtained as a result of the addition of 2 mL of 2-Pic to a sample of compound **58**. Slow evaporation of the solvent over the period of a week yielded colourless irregular hexagonal blocks which were suitable for X-ray diffraction studies by synchrotron radiation in order to obtain a satisfactory structure solution. Single crystals of **5.7** were found to be in a monoclinic cell and the structure solution was performed in the space group *C2/c*. Details of data collection and structure refinement are given in Table 5.5 at the end of this chapter. The asymmetric unit of **5.7** consists of one molecule of **59** and two molecules of 2-Pic (Figure 5.16). It was seen that compound **59** was found to adopt the pinched cone conformer, owing to the propyl chains present on the lower-rim of the macrocycle. The proximal carbon atoms in the pinched upper-rim groups are separated by a C[55]...C[62] distance of 3.868 Å. This prevents a guest molecule from residing in the cavity. The two propyl chains attached to the lower-rim of the calixarene are disordered over two positions. There was also found to be diffuse electron density associated with a disordered solvent molecule of 2-Pic that interacts with one of the CO₂H groups, which is disordered over two positions and was modelled at 50% occupancy in each position. In order to dramatically improve the agreement indices during the refinement for **5.7**, the routine SQUEEZE was applied to the data.¹⁴

The two 2-Pic molecules in the asymmetric unit interact with the upper-rim CO₂H groups *via* the common Py...CO₂H synthon as seen in Figure 5.16. There are two symmetry unique N...HOCO hydrogen bonding interactions with an N[1]...H[7O] distance of 1.822 Å and an N[2]...H[6O] distance of 1.771 Å. There was found to be two CH...OCOH interactions due to the disorder with H[69]...O[5] and H[63]...O[8] distances of 3.070 and 3.421 Å respectively.

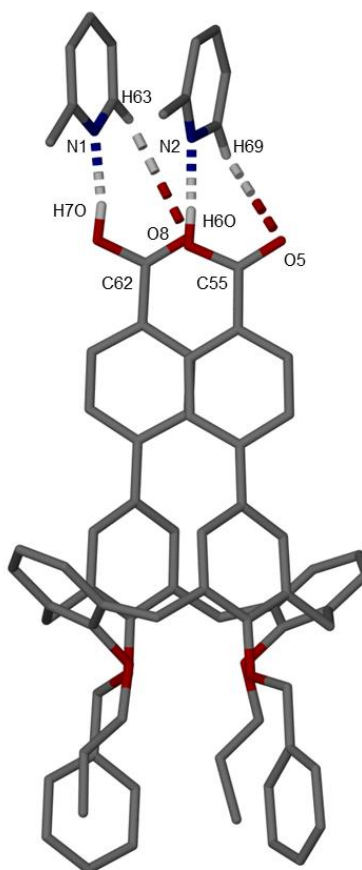


Figure 5.16. The asymmetric unit in the *X*-ray crystal structure of **5.7**. Hydrogen bonding interactions are shown as split-colour dashed lines. Hydrogen atoms (apart from those involved in hydrogen bonding interactions) have been omitted for clarity. Selected atoms have been labelled according to discussion.

The upper-rim cross-coupled aromatic rings are slightly twisted but there is still found to be a $\pi\cdots\pi$ interaction with an aromatic centroid \cdots aromatic centroid distance of 4.203 Å. There are also $\pi\cdots\pi$ interactions between the 2-Pic molecules, one of which is shown in Figure 5.17 with a distance of 3.567 Å between them (or 4.048 Å due to the disorder). In comparison to the previous example of compound **58**, it was found that rather than the two lower-rim benzyl groups being parallel with each other, one of the benzyl groups is rotated round by 90°.

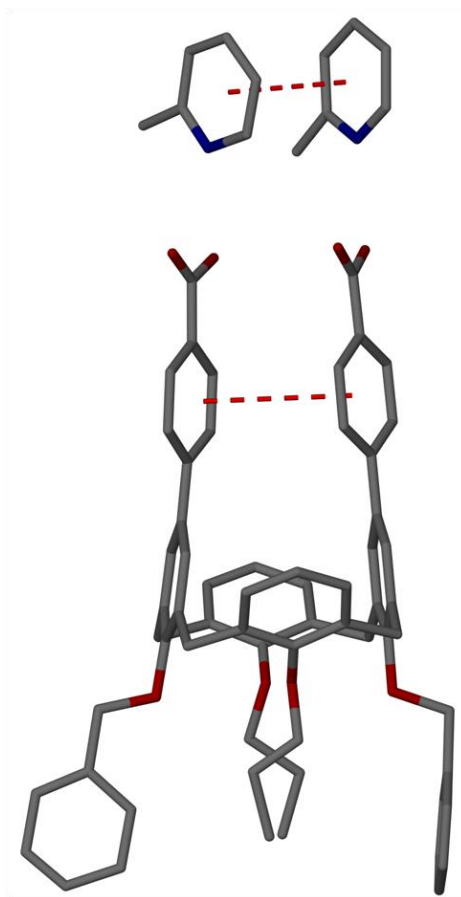


Figure 5.17. The asymmetric unit in the X-ray crystal structure of **5.7**. $\pi \cdots \pi$ interactions are shown as red dashed lines. Hydrogen atoms have been omitted for clarity.

Expansion of the asymmetric unit around **5.7** showed a $\text{CH} \cdots \text{O}$ hydrogen bonding interaction between one of the CO_2H groups and a *meta* hydrogen of an aromatic ring of a symmetry equivalent molecule with an $\text{O}[5] \cdots \text{H}[25]$ distance of 2.657 Å. In addition, there is also a $\text{CH} \cdots \pi$ interaction between one of the propyl chains attached to the lower-rim and the same aromatic ring described previously (Figure 5.18). This has a $\text{H}[48\text{B}] \cdots$ aromatic centroid distance of 2.906 Å.

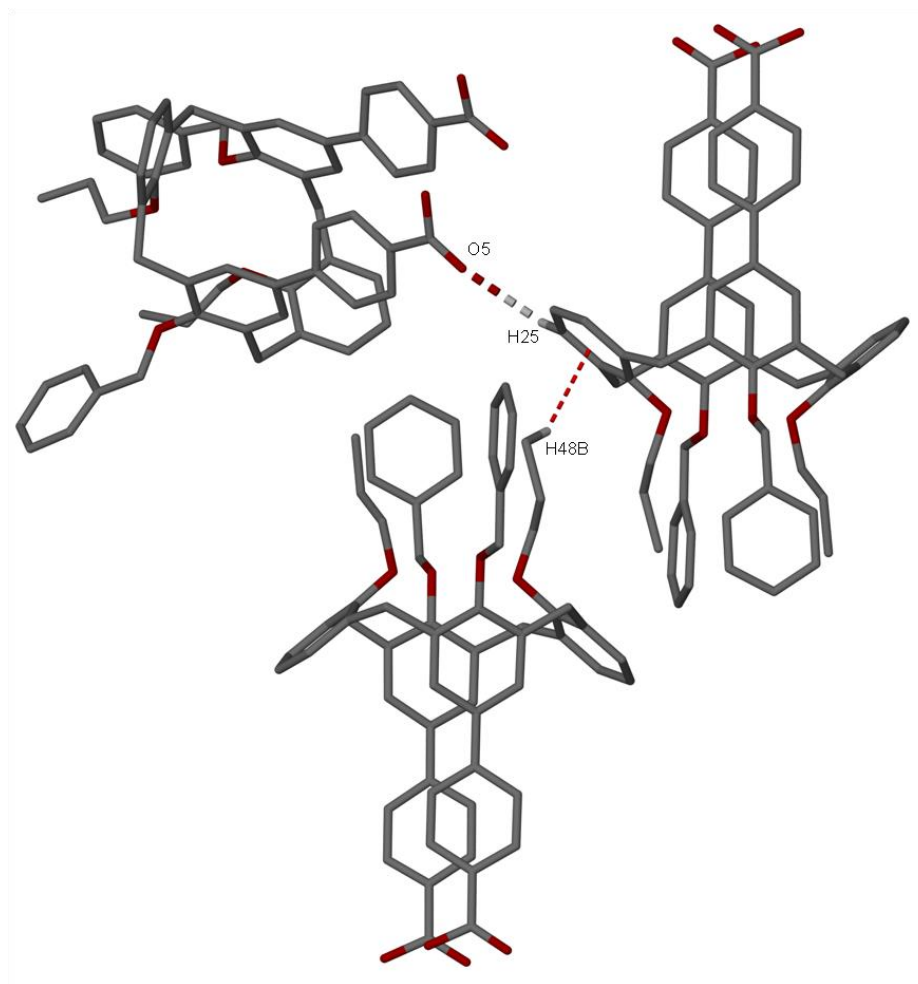


Figure 5.18. Symmetry expansion around molecule **5.7**. Hydrogen bonding interactions and $\text{CH}\cdots\pi$ interactions are shown as split-colour and red dashed lines respectively. Hydrogen atoms (apart from those involved in hydrogen bonding and $\text{CH}\cdots\pi$ interactions) have been omitted for clarity. Selected atoms have been labelled according to discussion.

5.3.9. Structure of di(*p*-benzoic acid)-dibenzyloxy-dipropoxycalix[4]arene-4-picoline, **5.8**.

Crystals of di(*p*-benzoic acid)-dibenzyloxy-dipropoxycalix[4]arene-4-Pic, **5.8**, were obtained as a result of the addition of 2 mL of 4-Pic to a sample of compound **59**. Slow evaporation of the solvent over the period of a week yielded colourless needles that were suitable for X-ray diffraction studies by synchrotron radiation in order to obtain an adequate structure solution. Single crystals of **5.8** were found to be in a monoclinic cell and the structure solution was performed in the space group $P2_1/c$. Details of the collection and structure refinement are given in Table 5.5 at the end of this chapter. The

asymmetric unit consists of one molecule of **59** and three molecules of 4-Pic (Figure 5.19). As before compound **59** was found to adopt the pinched cone conformation with the proximal carbon atoms in the pinched upper-rim CO₂H groups separated by a C[55]...C[62] distance of 3.737 Å. The two propoxy chains attached to the lower-rim are disordered over two positions.

Two of the 4-Pic molecules in the asymmetric unit interact with the upper-rim CO₂H group *via* the commonly seen Py...CO₂H synthon. There are two N...HOCO hydrogen bonding interactions with respective N[1]...H[5] and N[2]...H[8] distances of 1.741 and 1.748 Å. There are also two CH...OCOH interactions with respective O[6]...H[63] and O[7]...H[69] distances of 2.468 and 2.832 Å. The remaining 4-Pic molecule in the asymmetric unit interacts with an aromatic ring of compound **59** through a CH... π interaction with a distance of 3.090 Å between H[75]...aromatic centroid. Moreover, there are two π ... π interactions present in the asymmetric unit. The first one is between two of the 4-Pic molecules with an aromatic centroid...aromatic centroid distance of 3.953 Å. The other is located between the two extended aromatic rings on the upper-rim with an aromatic centroid...aromatic centroid distance of 4.073 Å (Figure 5.19).

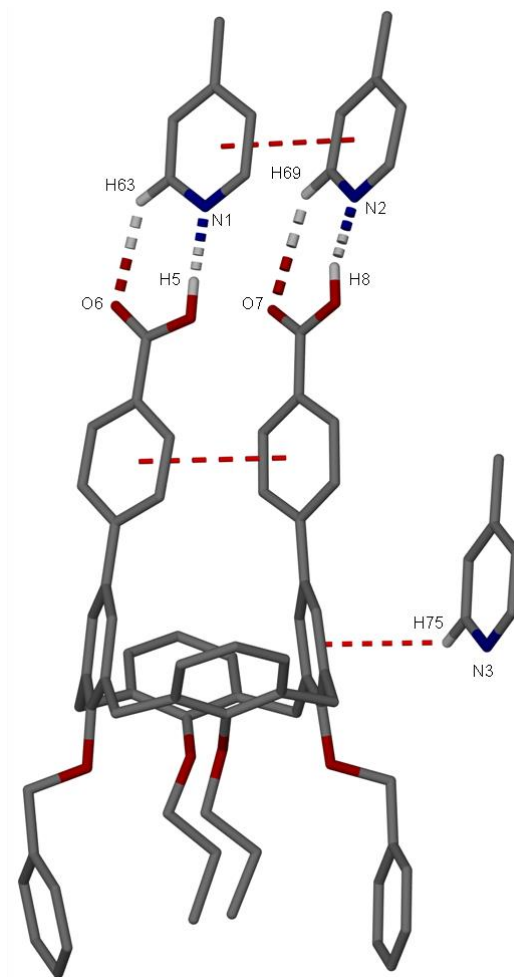


Figure 5.19. The asymmetric unit in the X-ray crystal structure of **5.8**. Hydrogen bonding and $\text{CH}\cdots\pi$ interactions/ $\pi\cdots\pi$ interactions are shown as split-colour and red dashed lines respectively. Hydrogen atoms (apart from those involved in hydrogen bonding and $\text{CH}\cdots\pi$ interactions) have been omitted for clarity. Selected atoms have been labelled according to discussion.

Expansion of the asymmetric unit around **5.8** showed there is $\text{CH}\cdots\pi$ interactions located within the molecule. There is one between a hydrogen atom on one of the lower-rim benzyl groups that interacts with an upper-rim aromatic ring of a symmetry generated molecule with a $\text{H}[35]\cdots\text{aromatic centroid}$ distance of 3.496 Å. The other two involve an aromatic ring of a 4-Pic molecule with respective $\text{H}[10]\cdots\text{aromatic centroid}$ and $\text{H}[68\text{C}]\cdots\text{aromatic centroid}$ distances of 2.816 and 3.411 Å (Figure 5.20).

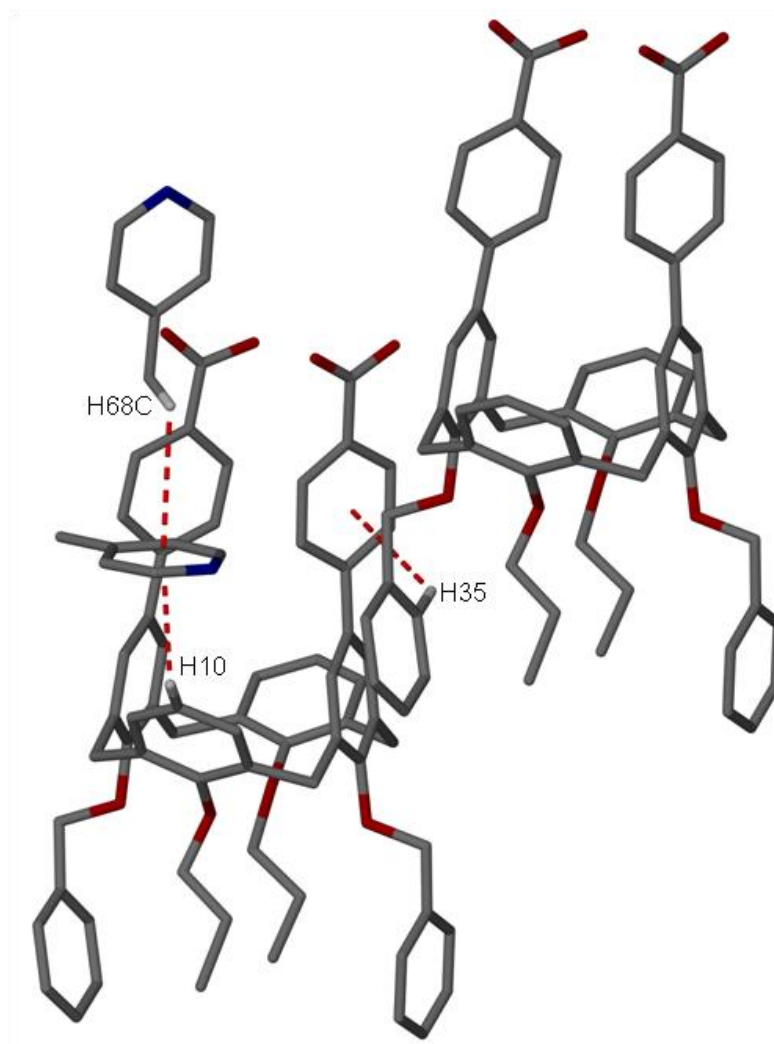


Figure 5.20. Symmetry expansion around molecule **5.8**. $\text{CH}\cdots\pi$ interactions are shown as red dashed lines. Hydrogen atoms (apart from those involved in $\text{CH}\cdots\pi$ interactions) have been omitted for clarity. Selected atoms have been labelled according to discussion.

5.4. Conclusion.

To conclude, the synthesis of a range of new deep cavity $p\text{CO}_2[4]\text{s}$ has been achieved in this chapter. The assembly of Suzuki cross-coupled $p\text{CO}_2[4]\text{s}$ **51**, **54**, **56** and **59** in the presence of pyridine-templates has not been previously studied. When all four positions on the lower-rim are alkylated a variety of different conformations can arise depending on the length of the alkyl chain attached during synthesis. Unlike in the series of di-*O*-alkoxy-di-*p*-carboxylatocalix[4]arenes discussed previously in Chapter 2, where lower-rim hydrogen bonding interactions gave rise to the calix[4]arenes adopting the common cone conformation, tetra-alkylation gives rise to different conformers due to the loss of this conformational rigidity. The addition of propyl chains to the lower-rim of the macrocycle prevents this rotation and resulted in compounds **51**, **54**, **58** and **59** adopting the pinched-cone conformation; which resulted in the cavity of the macrocycle being blocked to guest molecules.

The aforementioned compounds **51**, **54** and **59** when crystallised from various pyridine-containing templates were observed in the pinched-cone conformation. The majority of the resulting structures show a tendency for the upper-rim CO_2H groups to hydrogen bond to the pyridine-containing template of choice through the expected and common $\text{Py}\cdots\text{CO}_2\text{H}$ synthon. It was found that compound **56** also adopts the pinched-cone conformation when crystallised from DMF, as a result of there being a distal ether tether present at the lower-rim of the macrocycle. Again this template chemistry was expanded to include salt and related heterosynthon formation when 2-AP was employed. The addition of the more basic 2-AP was found to partially deprotonate compound **51**, resulting in the interaction between two of the cross-coupled aromatic ring CO_2^- groups with the (2-AP+H) cationic *via* two $\text{HNH}\cdots\text{OCO}$ and two $\text{NH}\cdots\text{OCO}$ hydrogen interactions as part of the expected salt formation as shown in complex **5.3**.

5.5. Experimental.

5.5.1. General comments.

The majority of work that has been conducted so far has been ligand synthesis, with a view to exploring the self- and metal-directed assembly of all the compounds synthesised.

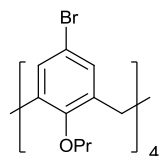
5.5.2. General experimental.

Unless stated, all reagents employed were purchased from chemical suppliers (Alfa Aesar, Fisher Scientific and Sigma Aldrich) and used as received. If required solvents were dried over molecular sieves (pore size 4 Å). Unless stated all experiments were carried out in air. When performed under a nitrogen atmosphere, this was dried over two columns of Drierite® gas purifier connected in series. Analytical thin layer chromatography was performed on precoated silica gel plates (Merck, 60 F254) and column chromatography was performed with silica gel (Merck, particle size 40-60 µm).

Electrospray ionisation and fourier transform mass spectra (ESI-FTMS) were obtained on a LTQ Orbitrap XL spectrometer at Swansea University. ¹H NMR and ¹³C NMR spectra were recorded on Bruker AC 300 and Bruker AC 400 spectrometers, with chemical shifts reported in ppm with respect to TMS as an internal standard. IR spectra were acquired on a Perkin Elmer Spectrum 100 FT-IR Spectrometer, with wavenumber (ν) of absorption reported in cm⁻¹. Single crystals were analysed on either a Bruker Apex II CCD diffractometer operating at 100(2) K with Mo-K α radiation (λ = 0.71073 Å) with a graphite monochromator or a Bruker D8 diffractometer with PHOTON 100 detector operating at 100(2) K with synchrotron radiation (λ = 0.77490 Å). Microanalysis results were obtained using an Exeter Analytical CE440 Elemental Analyser.

5.5.3. Synthesis of compounds 48 - 59.

5,11,27,23-Tetrabromo-25,26,27,28-tetrapropoxycalix[4]arene, **48**⁴



To a solution of compound **7** (0.02 mol) in 500 mL of 2-butanone was added *N*-bromosuccinimide (NBS) (0.15 mol) and the yellow solution was stirred at RT for one day. The mixture was then stirred with 100 mL of 10% NaHSO₃ and the product extracted into CHCl₃ and dried over MgSO₄ before the solvent was removed under reduced pressure. The product was recrystallised from CHCl₃/MeOH to yield product **48** as colourless crystals (13.92 g, 91%).

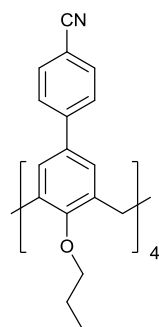
¹H NMR (300 MHz, 25 °C, CDCl₃): δ = 6.84 (s, 8H, ArH), 4.29 (d, J = 13.5 Hz, 4H, ArCH₂Ar), 3.76 (t, J = 7.4 Hz, 8H, OCH₂CH₂CH₃), 3.02 (d, J = 13.5 Hz, 4H, ArCH₂Ar), 1.78 (m, 8H, OCH₂CH₂CH₃), 0.90 (t, J = 7.5 Hz, 12H, OCH₂CH₂CH₃).

¹³C NMR (300 MHz, 25 °C, CDCl₃): δ = 155.58, 136.46, 131.02, 115.17, 30.76, 23.10, 10.23.

IR (solid phase, ν cm⁻¹) = 2962m, 2930m, 2874m, 1570w, 1454s, 1195s, 758s.

MS m/z observed 908.4401, theoretical 908.4404 [M + NH₄]⁺.

Tetra(*p*-cyanophenyl)-25,26,27,28-tetrapropoxycalix[4]arene, **49**⁶



Compound **48** (1.00 g, 1.11 mmol), Pd(PPh₃)₄ (770.0 mg, 0.67 mmol), 4-cyanophenylboronic acid (1.06 g, 6.67 mmol) and sodium carbonate (706.0 mg, 6.67 mmol) were combined in a flame-dried 250 mL 3-necked flask that had been flushed with nitrogen. Freshly distilled THF (50 mL) and degassed water (25 mL) were added to the flask and the mixture was heated at reflux under nitrogen for one week. The cooled reaction mixture was poured into a saturated NH₄Cl solution and EtOAc was added. The organic layer was washed with water (2 X 100 mL) and brine (2 X 100 mL) before being dried over MgSO₄ and filtered through a silica plug (rinsed with lots of EtOAc). Evaporation of the solvents left a brown oil that was recrystallised from DCM/MeOH to afford colourless crystals of compound **49** (0.79 g, 72%).

¹H NMR (300 MHz, 25 °C, CDCl₃): δ = 7.42 (d, J = 8.0 Hz, 8H, ArH), 7.19 (d, J = 8.0 Hz, 8H, ArH), 6.95 (s, 8H, ArH), 4.60 (d, J = 13.1 Hz, 4H, ArCH₂Ar), 3.90 (t, J = 7.3

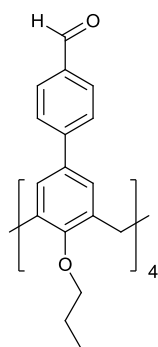
Hz, 8H, OCH₂CH₂CH₃), 3.35 (d, J = 13.1 Hz, 4H, ArCH₂Ar), 1.98 (m, 8H, OCH₂CH₂CH₃), 0.98 (t, J = 7.3 Hz, 12H, OCH₂CH₂CH₃).

¹³C NMR (300 MHz, 25 °C, CDCl₃): δ = 157.43, 145.03, 135.64, 133.01, 132.19, 127.04, 126.81, 118.67, 110.17, 77.20, 31.34, 23.29, 10.33.

IR (solid phase, ν cm⁻¹) = 2961m, 2934m, 2874m, 2225s, 1605s, 1462s, 1228m, 1175s, 1002s.

MS m/z observed 1014.4951, theoretical 1014.4953 [M + NH₄]⁺.

Tetrakis(4-formylphenyl)-25,26,27,28-tetrapropoxycalix[4]arene, **50**⁶



Compound **48** (1.00 g, 1.11 mmol), Pd(PPh₃)₄ (765.0 mg, 0.66 mmol), 4-formylphenylboronic acid (1.07 g, 7.15 mmol) and sodium carbonate (700.0 mg, 6.60 mmol) were combined in a flame-dried 250 mL 3-necked flask that had been flushed with nitrogen. Freshly distilled THF (50 mL) and degassed water (25 mL) were added to the flask and the mixture was heated at reflux under nitrogen for one week. The cooled reaction mixture was poured into a saturated NH₄Cl solution and EtOAc was added. The organic layer was washed with water (2 X 100 mL) and brine (2 X 100 mL) before being dried over MgSO₄ and filtered through a silica plug (rinsed with lots of EtOAc). Evaporation of the solvents left a yellow oil that was recrystallised from DCM/MeOH to afford white crystals of compound **50** (0.61 g, 55%).

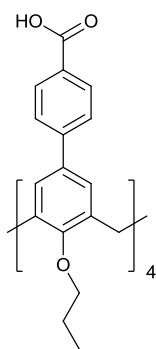
¹H NMR (300 MHz, 25 °C, CDCl₃): δ = 9.79 (s, 4H, CHO), 7.48 (d, J = 7.8 Hz, 8H, ArH), 7.18 (d, J = 7.8 Hz, 8H, ArH), 6.92 (s, 8H, ArH), 4.54 (d, J = 13.0 Hz, 4H, ArCH₂Ar), 3.90 (t, J = 7.4 Hz, 8H, OCH₂CH₂CH₃), 3.24 (d, J = 13.0 Hz, 4H, ArCH₂Ar), 1.96 (m, 8H, OCH₂CH₂CH₃), 0.98 (t, J = 7.4 Hz, 12H, OCH₂CH₂CH₃).

¹³C NMR (300 MHz, 25 °C, CDCl₃): δ = 191.72, 157.32, 146.72, 135.55, 134.48, 133.58, 129.92, 127.27, 126.74, 77.24, 77.17, 31.33, 23.33, 10.37.

IR (solid phase, ν cm⁻¹) = 2961m, 2932m, 2874m, 2728w, 1692s, 1601s, 1564m, 1462m, 1228m, 1169s.

MS m/z observed 1009.4671, 1026.4937, theoretical 1009.4674 [M + H]⁺, 1026.4937 [M + NH₄]⁺.

Tetra(*p*-benzoic acid)-25,26,27,28-tetrapropoxycalix[4]arene, **51**^{6,7}



To a solution of compound **50** (0.55 g, 0.54 mmol) in DCM (10 mL) and acetone (30 mL) was added a solution of sodium chlorite (0.39 g, 4.33 mmol) dissolved in water (3 mL) and a solution of sulfamic acid (0.42 g, 4.33 mmol) dissolved in water (3 mL). The solution was left to stir at RT for one day. Organic solvents were removed under reduced pressure and the residue taken up with 1M HCl. The yellow solid was filtered, washed with water and left to air dry (0.53 g, 91%).

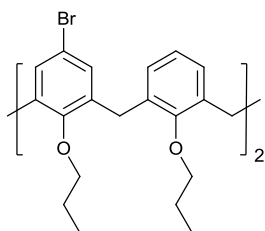
¹H NMR (300 MHz, 25 °C, DMSO-*d*⁶): δ = 12.60 (bs, 4H, OH), 7.61 (d, J = 8.4 Hz, 8H, ArH), 7.20 (d, J = 8.1 Hz, 8H, ArH), 7.05 (s, 8H, ArH), 4.45 (d, J = 12.8 Hz, 4H, ArCH₂Ar), 3.89 (t, J = 7.2 Hz, 8H, OCH₂CH₂CH₃), 3.37 (d, J = 12.4 Hz, 4H, ArCH₂Ar), 1.98 (m, 8H, OCH₂CH₂CH₃), 1.01 (t, J = 6.8 Hz, 12H, OCH₂CH₂CH₃).

¹³C NMR (300 MHz, 25 °C, DMSO-*d*⁶): δ = 166.89, 156.48, 144.37, 134.94, 132.93, 129.44, 128.46, 126.77, 126.24, 125.89, 22.81, 10.18.

IR (solid phase, ν cm⁻¹) = 2962m, 2933m, 2875m, 2658w, 2544w, 1688s, 1607s, 1463m, 1231s, 1178s, 1002m.

MS m/z observed 1090.4742, theoretical 1090.4736 [M + NH₄]⁺.

5,17-Dibromo-25,26,27,28-tetrapropoxycalix[4]arene, **52**⁹



To a stirred solution of compound **48** (4.84 g, 5.33 mmol) in dry THF (200 mL) at -78 °C was added *n*-BuLi/hexane (5.60 mL, 2.5 M, 14.0 mmol). The yellow solution was stirred at -78 °C for 15 mins, then quenched with MeOH (3 mL) and stirred for a further 10 mins. The reaction was poured over cold 2M HCl (200 mL) and extracted with CHCl₃. The organic layer was washed with water (2 X 100 mL), dried (Na₂SO₄) and the solvents removed under reduced pressure to give a pink crude product. The crude was recrystallised from hot EtOAc to give compound **52** as a white solid (3.42 g, 86%).

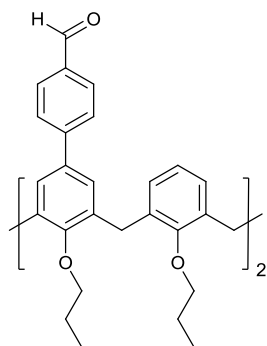
¹H NMR (300 MHz, 25 °C, CDCl₃): δ = 6.71 (s, 4H, ArH), 6.52 (s, 6H, ArH), 4.40 (d, J = 13.4 Hz, 4H, ArCH₂Ar), 3.71 (t, J = 7.5 Hz, 8H, OCH₂CH₂CH₃), 3.05 (d, J = 13.4 Hz, 4H, ArCH₂Ar), 1.78 (m, 8H, OCH₂CH₂CH₃), 0.87 (m, 12H, OCH₂CH₂CH₃).

^{13}C NMR (300 MHz, 25 °C, CDCl_3): δ = 156.38, 155.71, 137.23, 134.38, 130.77, 128.42, 122.49, 114.71, 76.92, 76.82, 30.86, 23.27, 23.20, 10.32, 10.28.

IR (solid phase, $\nu \text{ cm}^{-1}$) = 2959m, 2930m, 2873m, 1571w, 1455s, 1196s, 760s.

MS m/z observed 751.1818, theoretical 751.1815 $[\text{M} + \text{H}]^+$.

Di(4-formylphenyl)-25,26,27,28-tetrapropoxycalix[4]arene, **53**⁶



Dibromocalix[4]arene **52** (2.00 g, 2.66 mmol), $\text{Pd}(\text{PPh}_3)_4$ (925.0 mg, 0.80 mmol), 4-formylphenylboronic acid (1.30 g, 8.66 mmol) and sodium carbonate (0.85 g, 7.99 mmol) were combined in a flame-dried 250 mL 3-necked flask that had been flushed with nitrogen. Freshly distilled THF (50 mL) and degassed water (25 mL) were added to the flask and the mixture was heated at reflux under nitrogen for one week. The cooled reaction mixture was poured into a saturated NH_4Cl solution and EtOAc was added. The organic layer was washed with water (2 X 100 mL) and brine (2 X 100 mL) before being dried over MgSO_4 and filtered through a silica plug (rinsed with lots of EtOAc). Evaporation of the solvents left an orange solid that was recrystallised from DCM/MeOH to yield compound **53** as a yellow solid (1.11 g, 52%).

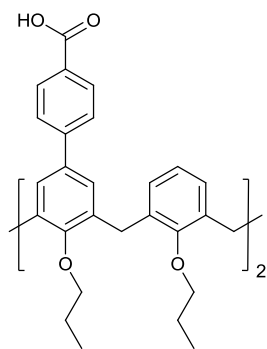
^1H NMR (300 MHz, 25 °C, CDCl_3): δ = 9.71 (s, 2H, CHO), 7.35 (d, J = 8.2 Hz, 4H, ArH), 6.92 (d, J = 8.0 Hz, 4H, ArH), 6.83 (d, J = 8.0 Hz, 4H, ArH), 6.69 (t, J = 7.2 Hz, 2H, ArH), 6.60 (s, 4H, ArH), 4.45 (d, J = 12.8 Hz, 4H, ArCH_2Ar), 3.91 (t, J = 7.4 Hz, 4H, CH_2CH_2), 3.76 (t, J = 7.4 Hz, 4H, CH_2CH_2), 3.18 (d, J = 12.8 Hz, 4H, ArCH_2Ar), 1.90 (m, 8H, CH_2CH_2), 0.98 (t, J = 7.3 Hz, 6H, CH_2CH_3), 0.91 (t, J = 7.3 Hz, 6H, CH_2CH_3).

^{13}C NMR (300 MHz, 25 °C, CDCl_3): δ = 191.82, 157.02, 146.76, 135.64, 135.14, 135.06, 135.04, 134.15, 133.05, 130.52, 129.64, 128.68, 128.15, 128.08, 127.98, 126.77, 126.49, 122.28, 77.23, 76.76, 31.12, 23.43, 23.16, 10.55, 10.14.

IR (solid phase, $\nu \text{ cm}^{-1}$) = 2958m, 2932m, 2873m, 2829w, 1697s, 1601s, 1455s, 1246m, 1185s.

MS m/z observed 801.1003, theoretical 801.1006 $[\text{M} + \text{H}]^+$.

Di(*p*-benzoic acid)-25,26,27,28-tetrapropoxycalix[4]arene, **54**⁷



To a solution of compound **53** (0.23 g, 0.29 mmol) in DCM (10 mL) and acetone (30 mL) was added a solution of sodium chlorite (0.11 g, 1.16 mmol) dissolved in water (3 mL) and a solution of sulfamic acid (0.12 g, 1.16 mmol) dissolved in water (3 mL). The solution was left to stir at RT for one day. Organic solvents were removed under reduced pressure and the residue taken up with 1M HCl. The yellow solid was filtered, washed with water and left to air dry to give compound **54** (0.18 g, 74%).

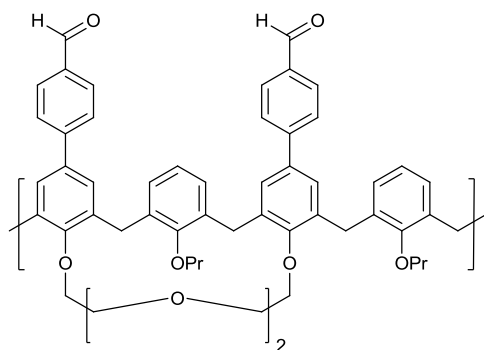
¹H NMR (300 MHz, 25 °C, DMSO-*d*⁶): δ = 12.83 (bs, 2H, COOH), 7.91 (d, J = 7.8 Hz, 4H, ArH), 7.62 (d, J = 8.2 Hz, 4H, ArH), 7.30 (s, 4H, ArH), 6.56 (d, J = 8.2 Hz, 4H, ArH), 6.48 (m, 2H, ArH), 4.47 (d, J = 13.0 Hz, 4H, ArCH₂Ar), 4.02 (t, J = 8.0 Hz, 4H, CH₂CH₂), 3.81 (t, J = 8.0 Hz, 4H, CH₂CH₂), 3.36 (d, J = 13.0 Hz, 4H, ArCH₂Ar), 1.95 (m, 8H, CH₂CH₂), 1.11 (t, J = 7.4 Hz, 6H, CH₂CH₃), 1.01 (t, J = 7.4 Hz, 6H, CH₂CH₃).

¹³C NMR (300 MHz, 25 °C, DMSO-*d*⁶): δ = 191.55, 169.54, 161.35, 154.86, 135.96, 134.34, 133.43, 131.51, 131.38, 129.60, 128.81, 128.65, 106.15, 78.86, 75.43, 31.03, 25.92, 23.47, 10.43, 9.98.

IR (solid phase, ν cm⁻¹) = 2962m, 2931m, 2873m, 2359w, 1733s, 1689s, 1605s, 1462s, 1259s, 1186s, 1086s.

MS m/z observed 850.4313, theoretical 850.4313 [M + NH₄]⁺.

Di(4-formylphenyl)-25,27-dipropoxycalix[4]arene-26,28-crown-4, **55**



Dibromocalix[4]arene **41a** (1.00 g, 1.28 mmol), Pd(PPh₃)₄ (445.0 mg, 0.38 mmol), 4-formylphenylboronic acid (0.63 g, 4.16 mmol) and sodium carbonate (0.41 g, 3.85 mmol) were combined in a flame-dried 250 mL 3-necked flask that had been flushed with nitrogen. Freshly distilled THF (50 mL) and degassed

water (25 mL) were added to the flask and the mixture was heated at reflux under nitrogen for one week. The cooled reaction mixture was poured into a saturated NH₄Cl solution and EtOAc was added. The organic layer was washed with water (2 X 100 mL)

and brine (2 X 100 mL) before being dried over MgSO_4 and filtered through a silica plug (rinsed with lots of EtOAc). Evaporation of the solvents left a yellow oil that was recrystallised from EtOAc to yield compound **55** as a white solid (0.45 g, 42%).

^1H NMR (300 MHz, 25 °C, CDCl_3): δ = 9.98 (s, 2H, CHO), 7.91 (d, J = 7.2 Hz, 4H, ArH), 7.76 (d, J = 7.2 Hz, 4H, ArH), 7.48 (s, 4H, ArH), 6.16 (d, J = 7.0 Hz, 2H, ArH), 6.07 (d, J = 7.2 Hz, 4H, ArH), 4.42 (d, J = 13.2 Hz, 4H, ArCH_2Ar), 4.08 (m, 8H, $\text{OCH}_2\text{CH}_2\text{O}$), 3.71 (s, 4H, $\text{OCH}_2\text{CH}_2\text{O}$), 3.63 (t, J = 6.8 Hz, 4H, CH_2CH_2), 3.20 (d, J = 13.2 Hz, 4H, ArCH_2Ar), 1.89 (m, 4H, CH_2CH_2), 1.08 (t, J = 7.0 Hz, 6H, CH_2CH_3).

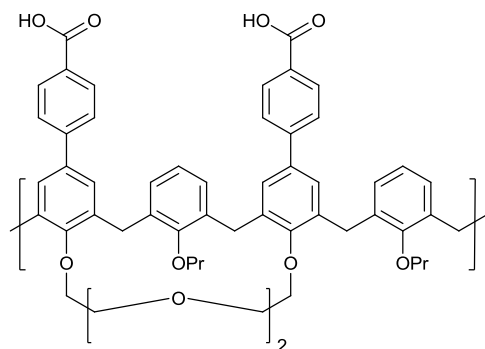
^{13}C NMR (300 MHz, 25 °C, CDCl_3): δ = 191.98, 137.43, 132.62, 130.30, 127.98, 127.62, 127.39, 77.23, 30.73, 23.65, 10.99.

IR (solid phase, ν cm^{-1}) = 2954w, 2903w, 2874w, 2733w, 1742m, 1688s, 1598s, 1456m, 1173s, 1007s.

Anal. Calcd. For $\text{C}_{54}\text{H}_{54}\text{O}_8$: C, 78.05; H, 6.55. *Found*: C, 75.93; H, 6.60.

MS m/z observed 848.4155, theoretical 848.4157 $[\text{M} + \text{NH}_4]^+$.

Di(*p*-benzoic acid)-25,27-dipropoxycalix[4]arene-26,28-crown-4, **56**



To a solution of compound **55** (0.30 g, 0.36 mmol) in DCM (10 mL) and acetone (30 mL) was added a solution of sodium chlorite (0.13 g, 1.44 mmol) dissolved in water (3 mL) and a solution of sulfamic acid (0.14 g, 1.44 mmol) dissolved in water (3 mL). The solution was left to stir at RT for one day. Organic solvents were

removed under reduced pressure and the residue taken up with 1M HCl. The yellow solid was filtered, washed with water and left to air dry to give compound **56** (0.27 g, 88%).

^1H NMR (300 MHz, 25 °C, $\text{DMSO}-d_6$): δ = 12.98 (bs, 2H, COOH), 8.07 (d, J = 7.3 Hz, 4H, ArH), 7.92 (d, J = 7.3 Hz, 4H, ArH), 7.68 (s, 4H, ArH), 6.34 (m, 6H, ArH), 4.45 (d, J = 13.0 Hz, 4H, ArCH_2Ar), 4.22 (m, 4H, $\text{OCH}_2\text{CH}_2\text{O}$), 4.11 (m, 4H, $\text{OCH}_2\text{CH}_2\text{O}$), 3.80 (s, 4H, $\text{OCH}_2\text{CH}_2\text{O}$), 3.72 (t, J = 7.2 Hz, 4H, CH_2CH_2), 3.38 (d, J = 13.0 Hz, 4H, ArCH_2Ar), 1.97 (m, 4H, CH_2CH_2), 1.18 (t, J = 6.8 Hz, 6H, CH_2CH_3).

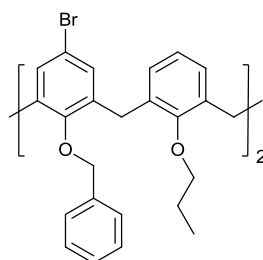
^{13}C NMR (300 MHz, 25 °C, DMSO- d_6): δ = 167.27, 157.95, 154.52, 136.75, 132.41, 129.86, 128.81, 127.46, 126.52, 73.63, 54.79, 23.00, 10.83.

IR (solid phase, ν cm^{-1}) = 2959w, 2924w, 2874w, 2360w, 1717s, 1681m, 1606s, 1457s, 1245s, 1187s, 1087s, 1006s.

Anal. Calcd. For $\text{C}_{54}\text{H}_{54}\text{O}_{10}$: C, 75.15; H, 6.31. **Found:** C, 69.47; H, 5.90.

MS m/z observed 880.4050, theoretical 880.4055 $[\text{M} + \text{NH}_4]^+$.

5,17-Dibromo-25,27-dipropoxy-26,28-dibenzoyloxycalix[4]arene, **57**¹³



NaH (60%, 0.48 g, 0.01 mol) was added to a mixture of compound **40a** (2.00 g, 3.00 mmol) dissolved in THF (100 mL) and DMF (20 mL). After one hour stirring at RT, benzylbromide (1.44 mL, 0.01 mol) dissolved in THF (10 mL) was added dropwise. The mixture was stirred for a further two hours at RT and then one hour heated at reflux. After cooling, HCl (1M, 50 mL) was added and the product extracted into DCM. The separated organic phase was washed with water (2 X 100 mL), dried over MgSO_4 and the solvent evaporated *in vacuo*. The remaining residue was dissolved in DCM and MeOH was added to crystallise out the desired product **57** as colourless crystals (2.20 g, 87%).

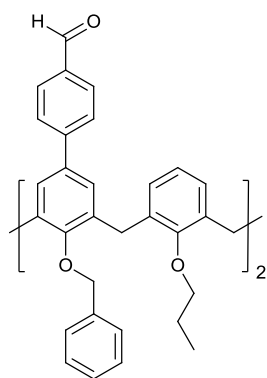
^1H NMR (300 MHz, 25 °C, CDCl_3): δ = 7.36 (m, 4H, OBn), 7.28 (m, 6H, OBn), 6.80 (d, J = 7.6 Hz, 4H, ArH), 6.71 (t, J = 7.4 Hz, 2H, ArH), 6.51 (s, 4H, ArH), 4.78 (s, 4H, OCH_2), 4.29 (d, J = 12.9 Hz, 4H, ArCH_2Ar), 3.68 (t, J = 6.4 Hz, 4H, $\text{OCH}_2\text{CH}_2\text{CH}_3$), 3.00 (d, J = 12.9 Hz, 4H, ArCH_2Ar), 1.59 (m, 4H, $\text{OCH}_2\text{CH}_2\text{CH}_3$), 0.57 (t, J = 7.2 Hz, $\text{OCH}_2\text{CH}_2\text{CH}_3$).

^{13}C NMR (300 MHz, 25 °C, CDCl_3): δ = 157.04, 154.08, 137.23, 136.64, 135.20, 130.61, 129.37, 128.78, 128.24, 128.15, 122.58, 115.36, 77.24, 77.19, 76.71, 31.04, 22.86, 9.68.

IR (solid phase, ν cm^{-1}) = 2959w, 2928w, 2869w, 1574w, 1453s, 1196s, 1078m, 758s.

MS m/z observed 864.2088, theoretical 864.2087 $[\text{M} + \text{NH}_4]^+$.

Di(4-formylphenyl)-25,27-dipropoxy-26,28-dibenzyloxycalix[4]arene, **58**



Dibromocalix[4]arene **57** (1.00 g, 1.18 mmol), Pd(PPh₃)₄ (410.0 mg, 0.35 mmol), 4-formylphenylboronic acid (0.58 g, 3.84 mmol) and sodium carbonate (0.38 g, 3.54 mmol) were combined in a flame-dried 250 mL 3-necked flask that had been flushed with nitrogen. Freshly distilled THF (50 mL) and degassed water (25 mL) were added to the flask and the mixture was heated to reflux under nitrogen for one week. The cooled reaction mixture was poured into a saturated NH₄Cl solution and EtOAc was added. The organic layer was washed with water (2 X 100 mL) and brine (2 X 100 mL) before being dried over MgSO₄ and filtered through a silica plug (rinsed with lots of EtOAc). Evaporation of the solvents left an off-white solid that was recrystallised from DCM/MeOH to yield compound **58** as yellow crystals (0.64 g, 60%).

¹H NMR (300 MHz, 25 °C, CDCl₃): δ = 9.65 (s, 2H, CHO), 7.41 (m, 4H, ArH), 7.28 (m, 6H, ArH), 7.22 (d, *J* = 7.2 Hz, 4H, ArH), 7.01 (d, *J* = 7.2 Hz, 4H, ArH), 6.87 (t, *J* = 7.0 Hz, 2H, ArH), 6.73 (d, *J* = 6.8 Hz, 4H, ArH), 6.46 (s, 4H, ArH), 4.78 (s, 4H, OCH₂), 4.42 (d, *J* = 13.4 Hz, 4H, ArCH₂Ar), 3.78 (t, *J* = 7.0 Hz, 4H, CH₂CH₂), 3.11 (d, *J* = 13.4 Hz, 4H, ArCH₂Ar), 1.62 (m, 4H, CH₂CH₂), 0.53 (t, *J* = 7.0 Hz, 6H, CH₂CH₃).

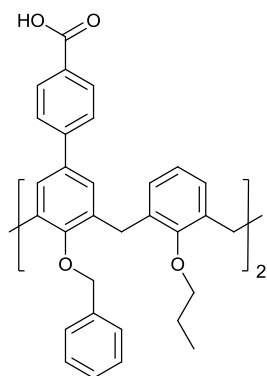
¹³C NMR (300 MHz, 25 °C, CDCl₃): δ = 191.77, 157.52, 155.58, 146.59, 137.37, 136.27, 134.57, 134.10, 133.50, 129.52, 129.13, 128.94, 128.31, 128.13, 126.62, 126.34, 122.32, 77.23, 76.69, 31.21, 22.86, 9.52.

IR (solid phase, ν cm⁻¹) = 2963w, 2922w, 2868w, 2835w, 2737w, 1695s, 1599s, 1450m, 1207m, 1151s.

Anal. Calcd. For C₆₂H₅₆O₆: C, 83.01; H, 6.29. *Found*: C, 80.72; H, 6.13.

MS *m/z* observed 897.4142, theoretical 897.4150 [M + H]⁺.

Di(*p*-benzoic acid)-25,27-dipropoxy-26,28-dibenzyloxycalix[4]arene, **59**



To a solution of compound **58** (0.91 g, 1.02 mmol) in DCM (10 mL) and acetone (30 mL) was added a solution of sodium chlorite (0.37 g, 4.06 mmol) dissolved in water (3 mL) and a solution of sulfamic acid (0.39 g, 4.06 mmol) dissolved in water (3 mL). The solution was left to stir at RT for one day. Organic solvents were removed under reduced pressure and the residue taken up with 1M HCl. The off-white solid was filtered, washed with water and left to air dry to give compound **59** (0.83 g, 88%).

¹H NMR (300 MHz, 25 °C, DMSO-*d*⁶): δ = 12.68 (bs, 2H, COOH), 7.68 (d, J = 7.2 Hz, 4H, ArH), 7.59 (m, 6H, ArH), 7.41 (m, 6H, ArH), 7.12 (d, J = 7.2 Hz, 4H, ArH), 7.01 (d, J = 7.3 Hz, 4H, ArH), 6.80 (s, 4H, ArH), 4.94 (s, 4H, OCH₂), 4.46 (d, J = 13.2 Hz, 4H, ArCH₂Ar), 3.81 (t, J = 7.0 Hz, 4H, CH₂CH₂), 3.31 (d, J = 13.2 Hz, 4H, ArCH₂Ar), 1.69 (m, 4H, CH₂CH₂), 0.68 (t, J = 7.2 Hz, 6H, CH₂CH₃).

¹³C NMR (300 MHz, 25 °C, DMSO-*d*⁶): δ = 166.79, 156.69, 155.11, 144.20, 137.20, 135.15, 134.54, 132.95, 129.29, 129.20, 128.48, 128.41, 128.08, 128.02, 126.26, 125.67, 122.07, 76.68, 76.19, 30.48, 22.35, 9.51.

IR (solid phase, ν cm⁻¹) = 2961w, 2914w, 2870w, 2545w, 1690s, 1607m, 1454m, 1288s, 1180s.

Anal. Calcd. For C₆₂H₅₆O₈: C, 80.15; H, 6.08. *Found*: C, 76.54; H, 6.01.

MS m/z observed 946.4321, theoretical 946.4313 [M + NH₄]⁺.

5.5.4. X-ray details of data collection/structure refinement of compounds 5.1 - 5.8, 58.

Complex number	5.1	5.2	5.3
Formula	C ₉₈ H ₉₅ N ₆ O _{12.5}	C ₁₀₄ H ₁₀₄ N ₆ O ₁₂	C ₈₀ H ₈₈ N ₄ O ₁₆
<i>Mr</i>	1556.80	1629.93	1361.54
Crystal system	Monoclinic	Monoclinic	Triclinic
Space group	<i>P</i> 2 ₁ / <i>c</i>	<i>P</i> 2 ₁ / <i>n</i>	<i>P</i> -1
<i>T</i> /K	100(2)	100(2)	100(2)
<i>a</i> /Å	15.7321(6)	20.5736(7)	12.5227(5)
<i>b</i> /Å	32.6146(13)	13.6636(5)	17.0230(8)
<i>c</i> /Å	16.8431(7)	32.3659(11)	19.3491(9)
α /°	90	90	94.324(3)
β /°	108.004(2)	98.980(2)	108.394(3)
γ /°	90	90	107.620(3)
<i>U</i> Å ³	8219.0(6)	8986.8(5)	3663.1(3)
<i>Z</i>	4	4	2
<i>F</i> (000)	3300	3464	1448
<i>D_c</i> /g cm ⁻³	1.258	1.205	1.234
μ /mm ⁻¹	0.099	0.079	0.086
2 θ_{max} /°	52.4	49.5	58.0
Data collected	62045	105286	49107
Unique data	12645	15306	14951
<i>R_{int}</i>	0.0608	0.0764	0.0886
Obs data (<i>I</i> >2 σ (<i>I</i>))	9181	10692	8833
Parameters	1028	1099	872
Restraints	9	44	72
<i>R</i> ₁ (observed data)	0.0687	0.0624	0.0869
ωR_2 (all data)	0.1752	0.1718	0.2077
<i>GooF</i>	1.016	1.003	1.014
Max/min residuals [e.Å ⁻³]	1.34/-1.36	0.81/-0.46	1.49/-1.44

Table 5.3. Details of data collection and structure refinement for complexes **5.1 - 5.3.**

Complex number	5.4	5.5	5.6
Formula	C ₆₆ H ₇₁ N ₂ O ₉	C ₆₆ H ₇₀ N ₂ O ₈	C ₆₃ H ₇₅ N ₃ O ₁₃
<i>Mr</i>	1036.25	1019.24	1082.26
Crystal system	Monoclinic	Tetragonal	Monoclinic
Space group	<i>P2/c</i>	<i>P4₃2₁2</i>	<i>C2/c</i>
<i>T</i> /K	100(2)	100(2)	100(2)
<i>a</i> /Å	14.8751(8)	9.4556(3)	36.4660(15)
<i>b</i> /Å	9.2537(5)	9.4556(3)	18.3657(8)
<i>c</i> /Å	20.7882(10)	60.504(2)	18.4342(8)
α /°	90	90	90
β /°	97.786(3)	90	110.793(2)
γ /°	90	90	90
<i>U</i> Å ³	2835.1(3)	5409.6(3)	11541.7(9)
<i>Z</i>	2	4	8
<i>F</i> (000)	1106	2176	4624
<i>D_c</i> /g cm ⁻³	1.214	1.251	1.246
μ /mm ⁻¹	0.096	0.097	0.104
<i>2</i> θ_{max} /°	63.3	56.4	54.4
Data collected	34918	45643	70405
Unique data	7363	5159	9901
<i>R_{int}</i>	0.0601	0.0541	0.0536
Obs data (<i>I</i> > 2 σ (<i>I</i>))	5348	4784	7767
Parameters	351	346	640
Restraints	0	48	7
<i>R</i> ₁ (observed data)	0.0544	0.0604	0.0742
ωR_2 (all data)	0.1343	0.1353	0.1979
<i>GooF</i>	1.017	1.120	1.055
Max/min residuals [e.Å ⁻³]	0.71/-0.42	0.48/-0.34	1.19/-0.79

Table 5.4. Details of data collection and structure refinement for complexes **5.4** - **5.6**.

Complex number	5.7	5.8	58
Formula	C ₈₀ H ₇₇ N ₃ O ₈	C ₈₀ H ₇₇ N ₃ O ₈	C ₆₂ H ₅₆ O ₆
<i>Mr</i>	1208.45	1208.45	897.07
Crystal system	Monoclinic	Monoclinic	Orthorhombic
Space group	<i>C2/c</i>	<i>P2₁/c</i>	<i>Pbcn</i>
<i>T</i> /K	100(2)	100(2)	100(2)
<i>a</i> /Å	29.2211(14)	26.0844(13)	14.1518(5)
<i>b</i> /Å	13.8821(6)	12.2230(6)	19.0569(7)
<i>c</i> /Å	33.417(2)	20.8147(9)	17.9599(7)
α /°	90	90	90
β /°	112.367(2)	98.561(3)	90
γ /°	90	90	90
<i>U</i> Å ³	12535.8(12)	6562.4(5)	4843.6(3)
<i>Z</i>	8	4	4
<i>F</i> (000)	5136	2568	1904
<i>D_c</i> /g cm ⁻³	1.281	1.223	1.230
μ /mm ⁻¹	0.134	0.093	0.093
<i>2</i> θ_{max} /°	64.3	52.4	45.7
Data collected	75350	48520	16133
Unique data	16966	10115	2550
<i>R_{int}</i>	0.0519	0.0534	0.0684
Obs data (<i>I</i> >2 σ (<i>I</i>))	13351	7680	1855
Parameters	698	811	308
Restraints	8	17	0
<i>R</i> ₁ (observed data)	0.1013	0.0544	0.0439
ωR_2 (all data)	0.2774	0.1338	0.1034
<i>GooF</i>	1.095	1.016	1.013
Max/min residuals [e.Å ⁻³]	2.13/-1.69	1.09/-0.67	0.38/-0.18

Table 5.5. Details of data collection and structure refinement for complexes **5.7**, **5.8** and compound **58**.

5.6 References.

1. a) R. K. Juneja, K. D. Robinson, C. P. Johnson and J. L. Atwood, *J. Am. Chem. Soc.* 1993, **115**, 3818; b) X. Cao, L. Luo, F. Zhang, F. Miao, D. Tian and H. Li, *Tetrahedron Lett.* 2014, **55**, 2029.
2. Y. L. Cho, D. M. Rudkevich and J. Rebek Jr, *J. Am. Chem. Soc.* 2000, **122**, 9868.
3. A. Arduini, S. Fanni, G. Manfredi, A. Pochini, R. Ungaro, A. R. Sicuri and F. Ugozzoli, *J. Org. Chem.* 1995, **60**, 1448.
4. C. D. Gutsche and P. F. Pagoria, *J. Org. Chem.* 1985, **50**, 5795.
5. T. Gu, P. Ceroni, G. Marconi, N. Armaroli and J-F. Nierengarten, *J. Org. Chem.* 2001, **66**, 6432.
6. J. S. Sasine, R. E. Brewster, K. L. Caran, A. M. Bentley and S. B. Shuker, *Org. Lett.* 2006, **8**, 2913.
7. Q. Lin and A. D. Hamilton, *C. R. Chimie.*, **5**, 2002 441.
8. a) X. H. Sun, W. Li, P. F. Xia, H-B. Luo, Y. Wei, M. S. Wong, Y-K. Cheng and S. Shuang, *J. Org. Chem.* 2007, **72**, 2419; b) W. T. An, Y. Jiao, X. H. Sun, X. L. Zhang, C. Dong, S. M. Shuang, P. F. Xia and M. S. Wong, *Talanta* 2009, **79**, 54.
9. M. Larsen and M. Jørgensen, *J. Org. Chem.* 1996, **61**, 6651.
10. A. Casnati, A. Sartori, L. Pirondini, F. Bonetti, N. Pelizzi, F. Sansone, F. Ugozzoli and R. Ungaro, *Supramol. Chem.* 2006, **18**, 199.
11. A. Arduini, S. Fanni, G. Manfredi, A. Pochini, R. Ungaro, A. R. Sicuri and F. Ugozzoli, *J. Org. Chem.* 1995, **60**, 1448.
12. A. Casnati, M. Fochi, P. Minari, A. Pochini, M. Reggiani and R. Ungaro, *Gazz. Chim. Ital.* 1996, **126**, 99.
13. L. Grubert and W. Abraham, *Tetrahedron* 2007, **63**, 10778.
14. A. L. Spek, *Acta Crystallogr. A*, 1990, **46**, C34.